NEDO-21864
79NED73
CLASS I
JUNE 1979

MARK I CONTAINMENT PROGRAM FINAL REPORT MONTICELLO T-QUENCHER TEST

TASK NUMBER 5.1.2

50-263
Ltr 8-13-79
7908310441

7908310446

GENERAL ELECTRIC

NEDO-21864
79NED73
CLASS I
June 1979

MARK I CONTAINMENT PROGRAM

FINAL REPORT

MONTICELLO T-QUENCHER TEST

Task Number 5.1.2

Contributors

R.A. Asai
L.E. Benes
R.F. Brodrick*
E.A. Buzek
J.D. Byron
O.M. Fawal
J.F. Hosler
H.H. Hwang
R.N. Lutman
R.A. Sanchez
J.W. Wheaton*

Reviewed: M.E. Tanner
M.E. Tanner, Manager
Safety/Relief Valve Programs

Approved: P.W. Ianni
P.W. Ianni, Manager
Containment Design

S.J. Stark
S.J. Stark, Manager
Mark I Containment Engineering

P.W. Marriott
P.W. Marriott, Manager
Containment Engineering

E.O. Swain
E.O. Swain, Manager
BWR Piping Design

*Teledyne Engineering Services

NUCLEAR ENERGY PROJECTS DIVISION • GENERAL ELECTRIC COMPANY
SAN JOSE, CALIFORNIA 95125

GENERAL ELECTRIC

DISCLAIMER OF RESPONSIBILITY

TABLE OF CONTENTS

TABLE OF CONTENTS (Continued)

TABLE OF CONTENTS (Continued)

APPENDICES

LIST OF ILLUSTRATIONS

LIST OF ILLUSTRATIONS (Continued)

LIST OF ILLUSTRATIONS (Continued)

LIST OF ILLUSTRATIONS (Continued)

LIST OF TABLES

ABSTRACT

This document presents results of the in-plant Monticello Safety/ Relief Valve (SRV) Discharge T-Quencher Test performed in December 1977 and February 1978. Hydrodynamic, structural, and T-Quencher/ piping data recorded during the test are summarized.

The primary objective of this test was to obtain containment loads resulting from discharges through a T-Quencher device in support of the Mark I Containment Load Definition Report. Additional objectives included determination of pool thermal mixing characteristics and acquisition of torus stresses, column loads, T-Quencher/ piping and support stresses.

1.0 INTRODUCTION

1.1 BACKGROUND

At the request of the Mark I Owners, General Electric Company undertook an effort to develop and test a device that would result in reduced safety/relief valve (SRV) discharge loads in the containment when compared with the ramshead device. To meet this request, a T-Quencher device was developed. It incorporated data from testing by an overseas licensee of quencher-type discharge devices and could be readily installed in Mark I containments.

To evaluate the loads resulting from an SRV discharge through the T-Quencher device, a full scale test with three T-Quenchers installed was performed in December 1977 at the Monticello Plant. Another test to obtain additional pool thermal mixing data was performed at the Monticello Plant in February 1978. This report presents the results of these tests.*

During an outage that preceded the December test, T-Quenchers were installed on the discharge lines of safety relief valves 71A, 71E, and 71G (see Figure 3-1). The T-Quenchers, shown in Figures 1-1 and 1-2, consist of perforated arms attached to the discharge of a ramshead, which is similar to the ramshead device previously installed on the SRVDL. The T-Quencher is designed to effect a gradual discharge of air into the torus water during the air clearing transient associated with SRV actuation, thereby reducing the hydrodynamic pressure transient. To accomplish this, the density of holes in the quencher increases with the distance from the ramshead fitting. The quencher is supported at the ramshead fitting and at the mid-span of the quencher arms as shown in Figure 1-3. The supports are connected to a beam (14-in. schedule 120 pipe), which is attached to the ring girders. Figure 1-4 illustrates the Monticello Plant configuration. General data for the safety/relief valve and the vacuum breaker are presented in Table 1-1.

---

*No SRV discharges through a ramshead device are addressed in this report. Refer to In-Plant Safety/Relief Valve Discharge Load Test-Monticello Plant, August 1977 (NEDC-21581-P).

Plant configuration. General data for the safety/relief valve and the vacuum breaker are presented in Table 1-1.

1.2 TEST OBJECTIVES

The overall objective of the Monticello T-Quencher test was to obtain containment loads resulting from discharges through a T-Quencher device in support of Mark I Containment Load Definition Report. Specific objectives included:

- Obtaining the data base necessary to verify analytical models to be used for prediction of SRV pipe and torus shell pressures, safety relief valve discharge line water reflood characteristics, and also thrust loads in SRVDL piping. This includes obtaining consecutive valve actuation (CVA-hot pipe) and multiple valve actuation (MVA) data.

- Determining the pool thermal mixing characteristics of a T-Quencher device.

- Obtaining torus column loads and torus shell stresses.

- Obtaining SRV piping, T-Quencher, and quencher support stresses for comparison with analytical predictions.

Table 1-1

GENERAL DATA - SRV AND VACUUM BREAKER

Safety/Relief Valve

Manufacturer:	Target Rock
Model Number:	67F
Valve Type:	Pilot Operated Safety/Relief Valve
Size - Inlet: Outlet:	6-in.-1500 lb Flange 10-in.-300 lb Flange
Design Pressure:	1250 psi
Design Temperature	575°F
Set Pressure Range:	1025 to 1155 psi (Monticello - 1080 psi)
Capacity:	734,000 to 900,000 lb/hr saturated steam (for Monticello seat bore and set pressure)

Vacuum Breaker

Manufacturer:	Crosby
Set Pressure:	0.2 psig
Flow Area:	28.375 in.^{2}, valve full open
Service Limits (steam):	135 psig - 475°F

*

Figure 1-2. Quencher Arm

*Proprietary information deleted.

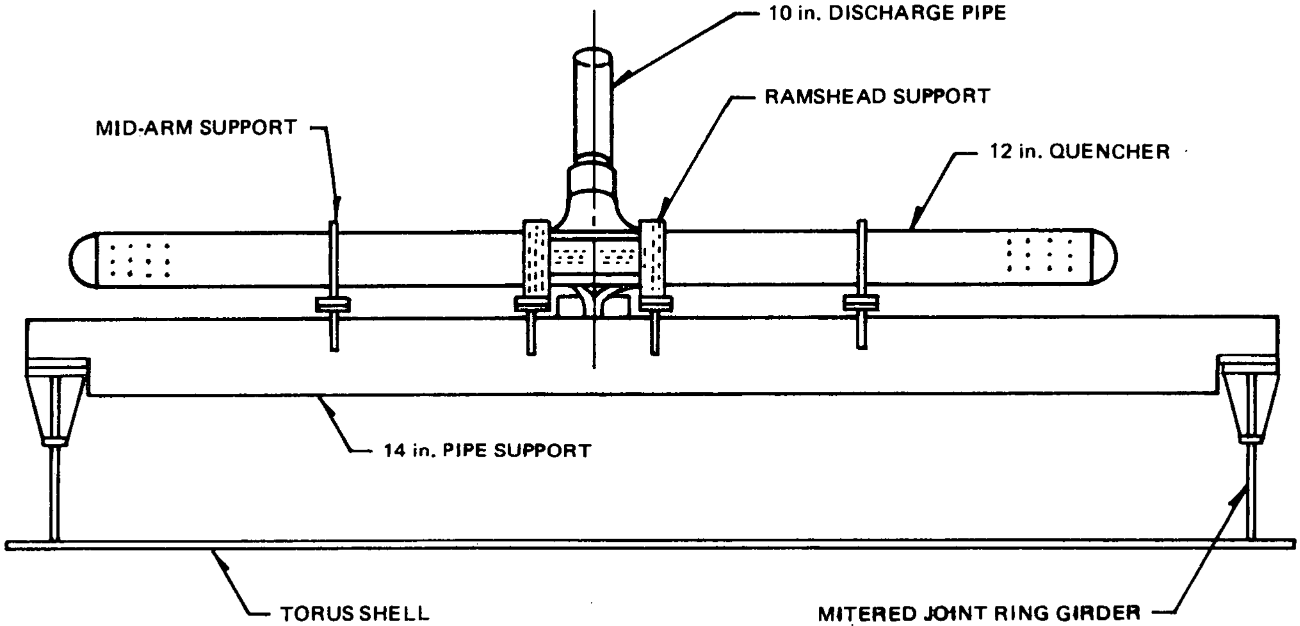

Figure 1-3. Quencher Installation

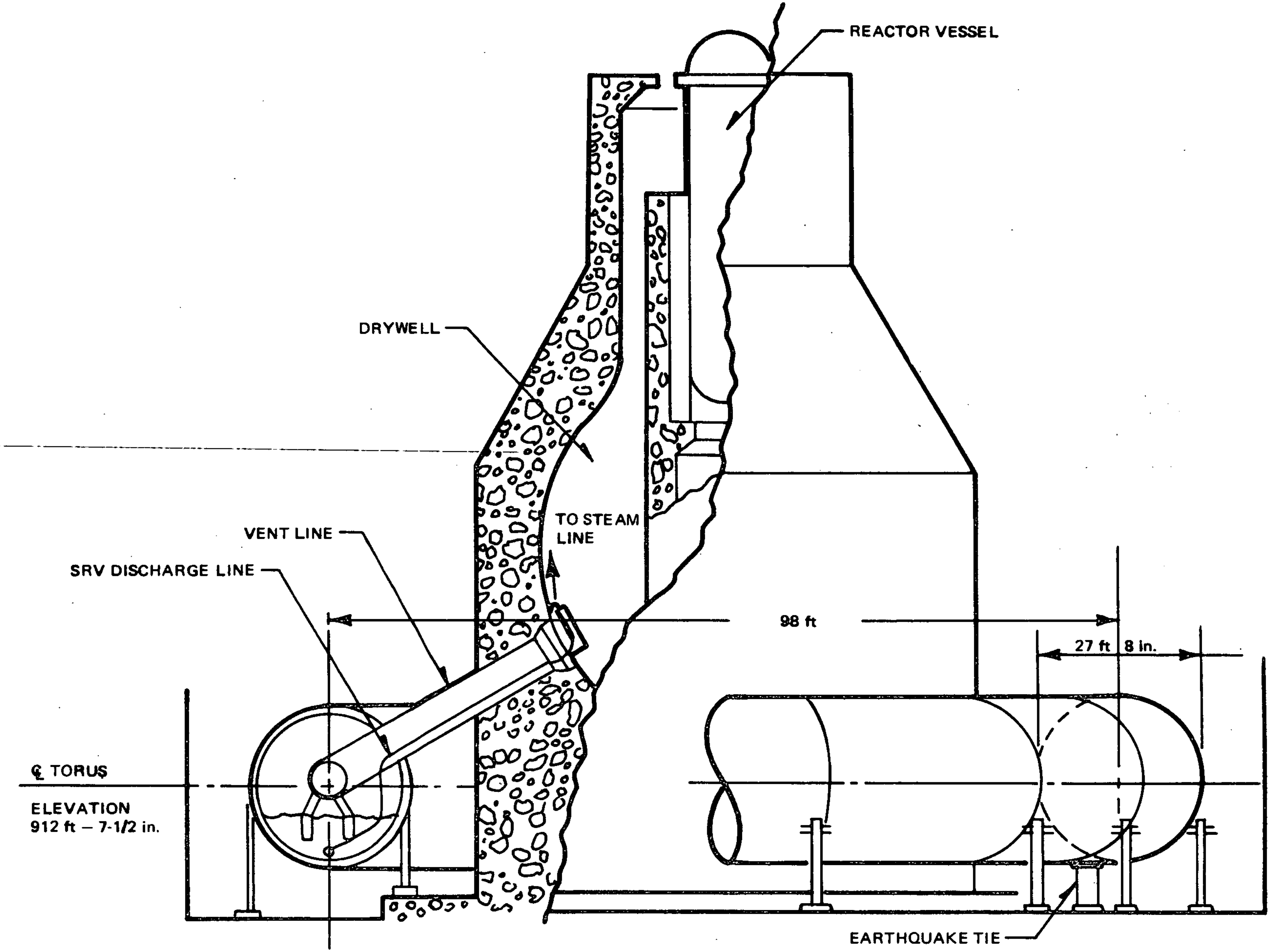

Figure 1-4. Monticello Plant Configuration

2.0 SUMMARY OF PRINCIPAL OBSERVATIONS

2.1 HYDRODYNAMIC

- Highest measured torus shell pressures were psid, resulting from a cold pipe (CP), normal water leg (NWL), single valve actuation (SVA).

- Torus shell pressures resulting from all hot pipe, single valve actuations were lower than those from cold pipe, normal water leg, single valve actuations. The hot pipe tests were performed with depressed, normal, and slightly elevated initial water legs in the SRV discharge line.

- Frequencies of measured shell pressures resulting from SRV air bubble oscillation ranged from Hz for cold pipe tests and from to Hz for hot pipe consecutive actuation tests. Shell pressure frequencies for single and multiple valve actuations (cold pipe) were approximately equal.

- Highest measured steam condensation pressures on the torus shell were 1.1 psid, peak to peak. The magnitude of these pressure oscillations increased from psid peak to peak over the pool temperature range of

- Multiple valve actuations (three adjacent valves) resulted in maximum shell pressures no greater than single valve actuations under similar conditions (CP, NWL).

- SRV discharge line refloods of approximately ten feet beyond the normal water leg were measured. After the initial reflood, the air-water interface in the discharge line stabilized at a point approximately feet lower than the initial water leg (just above the T-Quencher entrance). These tests were performed with an 8-in. SRV discharge line vacuum breaker. In all cases the water slug had returned to the initial water level within seconds of valve closure.

- Maximum pressure in the SRV discharge line was psig, measured nine feet downstream of the SRV. This pressure resulted from a hot pipe test when the initial water leg in the line was just above NWL and had an upward velocity of approximately /sec.

- Maximum pressure in the T-Quencher arms was psig, measured just upstream of the first column of quencher holes during a test similar to that which resulted in the maximum SRV discharge line pressure. This pressure spike had an extremely short duration; i.e., the pressure magnitude was greater than psig for less than milliseconds.

- Steady state pressures recorded just downstream of the SRV psig) and within the T-Quencher arms psid) were both less than half of the pressures occurring just upstream of their choke points, which were the SRV throat and the entrance to the reducer upstream of the ramshead, respectively. This indicates that the presence of the T-Quencher device did not result in unchoking at the SRV and, therefore, had no adverse effect on SRV flow.

- Following each SRV initiation signal and before movement of the main disk of the SRV, a small amount of steam was bled from the valve into the discharge line.* This steam flow resulted in a prepressurization of the discharge line of approximately psig, which pushed the water leg in the line down approximately 2 feet before each SRV opening.

- Air bubbles formed by the same T-Quencher were approximately in phase during all tests. In general, the bubbles that formed on the reactor side of the T-Quencher arms had maximum pressures approximately twice those of the bubbles on the far side of the quencher arms. This asymmetry in bubble pressures resulted in maximum differential pressures across the T-Quencher arms psid, where the positive sign means that the force is directed away from the reactor (see Figure 8-9).

---

*This is a normal characteristic of the SRV tested.

**During one test (test 2306, HP, EWL), a peak differential pressure of psid was recorded; however, this pressure spike had a magnitude greater than psid for only milliseconds.

***The maximum and minimum pressure differentials did not occur in the same test.

- Extended SRV discharges were performed both with and without a Residual Heat Removal (RHR) loop in operation.* The maximum differences between measured local and calculated bulk pool temperature were (with RHR) and (without RHR).

- Thirty minutes after SRV closure (extended discharge test without RHR), the maximum measured vertical pool temperature difference from the pool surface to torus bottom was approximately For the extended blowdown with RHR, the maximum measured vertical pool temperature difference from surface to torus bottom was thirty minutes after SRV closures.

2.2 STRUCTURAL

- With two exceptions, the measured stress intensities were less than ksi.

  The tie bars between downcomers exhibited higher stresses, the maximum absolute value being ksi.

  The strain gages in the region of the ECCS suction nozzle exhibited a maximum stress intensity of ksi.

- The largest single downward dynamic load on a torus support outer column was kips and the largest single upward load was kips. These loads occurred during a multiple-valve discharge.

- The largest single downward dynamic load on an inner column was kips and the corresponding largest upward load was kips. These also occurred during MVA discharge.

- The average maximum stress among shell locations in the vicinity of the single-valve discharge was reduced by 17% for hot pipe discharge, relative to cold pipe discharge.

*One RHR loop was operated in the recirculation mode (no cooling) throughout one of the extended discharge tests.

- The depressed water level resulted in a 27% decrease in shell stress and the elevated water level resulted in a 23% increase in shell stress for that region of the shell in the discharge bay relative to normal water level, hot pipe discharge.

- Column loads from hot pipe discharges were about one-half as great as those from cold pipe discharges.

- Under hot pipe conditions, the column loads from depressed water level tests were essentially the same as those from normal water level tests.

- Under hot pipe conditions, the column loads from elevated water tests averaged about 50% greater than those from normal water level tetss.

- The largest structural responses occurred during the MVA test. The Bay D midbay shell stress response averaged 37% greater during MVA than during a single Bay D discharge. The Bay D column loads averaged 7% greater during MVA than during a single Bay D discharge.

2.3 T-QUENCHER AND SRV DISCHARGE PIPING

- All stresses measured on the SRV piping in the torus, T-Quencher, and T-Quencher supports were less than 5600 psi, which was a factor of three to four below ASME code allowables. The highest stress on SRV support beams was 6160 psi which was also below code allowable. The highest stress on SRV vent pipe penetration was 1960 psi.

- There was little variation in the stresses measured for all normal water leg tests.

- Depressed water leg tests resulted in 5% lower stresses than did not pipe normal water leg tests.

- Elevated water level tests generally resulted in 4.5% higher stresses than did hot pipe normal water leg tests.
- Cold pipe normal water leg tests resulted in 7% higher stresses than hot pipe normal water leg tests.
- The effect of air/water clearing on the main steam piping and branch piping was negligible (no evidence of stresses caused by air/water clearing).

3.0 TEST PLAN AND PROCEDURE

3.1 TEST PLAN

Table 3-1 presents the Monticello T-Quencher Test Matrix as performed in December 1977. Thirty-eight tests were performed; a summary of the conditions tested is given below.

Test Condition	Number of Tests Performed
Cold Pipe, Normal Water Leg, Single Valve Actuation (CP, NWL, SVA) Valve A	7
Cold Pipe, Normal Water Leg, Multiple (3 adjacent) Valve Actuation (CP, NWL, MVA) Valves A, E, G	4
Cold Pipe, Normal Water Leg, Single Valve (Distant Bay) 4 Valve E Actuations, 4 Valve G Actuations	8
Hot Pipe, Normal Water Leg, Single Valve Actuation (HP, NWL, SVA) Valve A	5
Hot Pipe, Normal Water Leg, Single Valve (Distant Bay) Valve E	4
Hot Pipe, Depressed Water Leg, Single Valve Actuation (HP, DWL, SVA) Valve A	5
Hot Pipe, Elevated Water Leg, Single Valve Actuation (HP, EWL, SVA) Valve A	4
Warm Pipe, Normal Water Level, Single Valve Actuation (WP, NWL, SVA) Valve A	1

The single warm pipe test was performed as a safety measure to insure that performance of later tests under hot pipe conditions would not result in excessive loadings. Since only one test was performed, this case is not considered as a separate Test Condition in the data evaluations made with the report.

The initial pipe temperature (averaged along the pipe length) was approximately 100°F for the cold pipe tests, 230°F for the warm pipe tests, and 320°F to 365°F for the hot pipe tests.

One of the CP, NWL, SVA tests (Test 24) was an extended discharge that lasted approximately 6.5 minutes. This test was performed to determine the pool thermal mixing characteristics of the T-Quencher device without the Residual Heat Removal (RHR) system in operation. An additional test was performed in February 1978 (not shown in test matrix). This test was similar to Test 24 except that one RHR loop was in operation (recirculation mode only) and only pool temperature data were recorded during the additional test, which lasted for approximately eight minutes.

Four elevated water level tests were attempted. The timing between actuations was specified (based on measured water reflood data) so the valve would actuate at the moment of maximum reflood (approximately 10 ft of overshoot was observed). Evaluation of the reflood data indicates that for tests 1302 and 2307 the reflood had not yet reached the normal water level when the valve actuated, so these tests could not be included in the evaluation of results in Section 8.3 or Table 8-1. On tests 2305 and 2306 the reflood had just reached normal water level at a high upward (∿30 ft/sec) velocity when valve actuation occurred. Before conducting the test, two shakedown tests were performed to evaluate the data acquisition system. One test was performed at a reactor pressure of 155 psia and one at 1000 psia.

Before each SRV opening (movement of the SRV main disc), a small amount of steam was bled from the SRV into the SRV discharge line — a normal operating characteristic of the valve tested. This steam bleed resulted in a pressurization of the discharge line and movement of the water leg in the pipe before valve opening. Table 3-2 presents detailed test initial conditions, which existed just before SRV handswitch activation. Table 3-3 presents new values for any initial conditions in Table 3-2 that changed due to the pressurization described above before SRV main disk opening. The values presented in Table 3-3 correspond in time to the arrival of the primary pressure wave (due to SRV main disc opening) at the air/water interface in the discharge line. A description of the methods used to estimate those initial conditions presented in Tables 3-2 and 3-3, which were not directly measured, is provided in Appendix I.

Figure 3-1 presents a plan view of the Monticello torus showing locations of the T-Quenchers actuated. Figure 3-2 shows the T-Quencher configuration in the bays where they were installed.

3.2 TEST PROCEDURE

All valves were actuated manually by one or two men. Dry runs were conducted to develop a uniform procedure, particularly for the consecutive and multiple valve actuations. During each test run, on-line real-time data from approximately 48 of the 290 data channels were monitored and were evaluated during the test.

Control of SRVDL Water Level

Upon evaluation of the data obtained from the 1000 psia shakedown test, it was determined that during the reflood transient, the air-water interface rose about ten feet above normal water level, dropping to and oscillating about a point one foot above the T-Quencher centerline. Thus, in order to relieve the excess pressure contained in the lines A, E or G so that the water leg could return to its normal value, special discharge line vent valves were installed as shown in Figure 4-31. These valves were opened for at least five minutes before the normal water level tests to equalize the pressures in the lines and the drywell, allowing the return of the water leg to its normal value.

3.2.1 Single Valve Actuations

After verification that all initial condition requirements were satisfied and proper communication existed between the control room and the recording stations, steady state data were collected. The actual test started with a 15-sec countdown. All recording equipment was started before the count of 10 and the valve was actuated at time zero. It was closed after the predetermined time.

Recording of reactor/plant data continued for at least 60 sec following closure of the valve; recording of structural and hydrodynamic data continued for at least 80 sec after closure.

Brush recorder and reactor/plant data were reviewed after each test run for acceptability and initial conditions were changed when necessary.

3.2.2 Consecutive Valve Actuations

Consecutive valve actuation tests were conducted in the same manner as the single valve actuations except the valve was reopened after initial closure after various time intervals (to attain depressed, normal, and elevated water legs). The reactor/plant data, and structural and hydrodynamic data were recorded for 60 sec after the final actuation.

3.2.3 Multiple Valve Actuations

Multiple valve actuation tests were conducted in the same manner as the single valve actuations; however, two men operated the valves. For the three-valve tests, one man operated two valves. Since synchronization was dependent upon operator skill and timing, dry runs were made to develop skills. The valves were actuated within two-thirds of a second between the earliest and the latest. Valves were closed individually at approximately 10-sec intervals. Recording of reactor/plant data was continued for at least 60 sec following closure of the last valve. Recording of structural and hydrodynamic data was continued for at least 80 sec after the last valve closure.

3.2.4 Extended SRV Blowdown Tests

The procedure for the extended SRV discharge tests was to first cool the pool to approximately 50°F using both loops of the RHR system. The extended discharge test performed without RHR operation was initiated 50 min after both loops of the RHR system had been turned off. The extended discharge test performed with one RHR loop (pumps A and C, FIgure 8-21) in operation (recirculation mode only - no cooling) was initiated 50 min after the other RHR loop (pumps B and D, Figure 8-21) was turned off and RHR loop containing pumps A and C was switched to the recirculation mode rather than the cooling mode.

The SRV remained open in both extended discharge tests until the average Bay D temperature exceeded 110°F as measured by temperature sensors T17, T25, and T28.

Recording of reactor/plant data continued for at least 60 sec following closure of the valve for both tests. Recording of torus and phenomena data was continued for 60 sec after the valve opening and again for approximately 90 sec toward the end of the extended discharge performed without RHR operation. Pool temperature measurements, including those recorded by plant instrumentation, were made throughout both tests and for 30 minutes following SRV closure. Only pool temperature data were recorded during the extended discharge performed with one loop of the RHR system in the recirculation mode.

Table 3-1

MONTICELLO T-QUENCHER TEST MATRIX

Run Number	Test Number	Test Type(1)	Valve	Bay	Initial Conditions: Pipe Temp Water Leg(1)	Initial Conditions: Power Level(2) (%)	Discharge Time-Approx(3) (Sec)	Valve On: Date	Valve On: Time Valve On(3) (Hr:Min:Sec)	Time Between Valve Off and Valve On(3) (Hr:Min:Sec)
2	2	SVA	A	D	CP,NWL	65-85	8	12/19/77	8:46:06	2:50:00
3	501	SVA	A	D	CP,NWL	"	17	"	11:36:08	:30:00
4	502	CVA	A	D	WP,NWL	"	17	"	12:06:08	2:24:00
5	801	SVA	A	D	CP,NWL	"	18	"	14:30:07	:06:00
6	802	CVA	A	D	HP,NWL	"	15	"	14:36:07	2:25:00
7	901	SVA	A	D	CP,NWL	"	17	"	17:01:09	:06:00
8	902	CVA	A	D	HP,NWL	"	13	"	17:07:08	:06:00
9	903	CVA	A	D	HP,NWL	"	14	"	17:13:07	:06:00
10	904	CVA	A	D	HP,NWL	"	14	"	17:19:08	:06:00
11	905	CVA	A	D	HP,NWL	"	14	"	17:25:08	:50:00
12	1101	SVA	E	C	CP,NWL	"	17	"	18:15:07	:06:00
13	1102	CVA	E	C	HP,NWL	"	14	"	18:21:08	:06:00
14	1103	CVA	E	C	HP,NWL	"	14	"	18:27:08	:06:00
15	1104	CVA	E	C	HP,NWL	"	15	"	18:33:08	:06:00
16	1105	CVA	E	C	HP,NWL	"	14	"	18:39:09	1:56:00
17	12	SVA	G	E	CP,NWL	"	18	"	20:35:07	2:40:00
18	1301	SVA	A	D	CP,NWL	"	18	"	23:15:07	00:00.56
18	1302	CVA	A	0	HP,EWL	"	18	"	23:15:26	00:56.7
18	1303	CVA	A	D	HP,DWL	"	18	"	23:16:42	1:18:24
19	14	SVA	E	C	CP,NWL	"	15	12/20/77	00:35:06	25:00
20	15	SVA	G	E	CP,NWL	"	15	"	01:00:06	1:14:00
21	1601	SVA	A	D	CP,NWL	"	18	"	02:14:05	01:00
21	1602	CVA	A	D	HP,DWL	"	15	"	02:15:17	01:00
21	1603	CVA	A	D	HP,DWL	"	14	"	02:16:33	01:00

Table 3-1 (Continued)

MONTICELLO T-QUENCHER TEST MATRIX

					Initial Conditions			Valve On		
Run Number	Test Number	Test Type (1)	Valve	Bay	Pipe Temp Water Leg	Power (2) Level (%)	Discharge Time-Approx (3) (Sec)	Date	Time Valve On (4) (Hr:Min:Sec)	Time Between Valve Off and Valve On (3) (Hr:Min:Sec)
21	1604	CVA	A	D	HP,DWL	65-85	15	12/20/77	02:17:45	
21	1605	CVA	A	D	HP,DWL	"	14	"	02:18:56	01:00
22	18	SVA	E	C	CP,NWL	"	15	"	03:30:05	1:11:00
23	19	SVA	G	E	CP,NWL	"	14	"	03:56:05	22:00
24	21	SVA	E	C	CP,NWL	"	15	"	05:40:06	1:46:00
25	22	SVA	G	E	CP,NWL	"	15	"	06:10:06	30:00
26	2301	MVA	E,A,G	C,D,E	CP,NWL	"	17-E 28-A 38-G	"	08:56:07	2:46:00 2:15:00
28	2302	MVA	E,A,G	C,D,E	CP,NWL	"	38-E 28-A 17-G	"	11:21:09	2:15:00
30	2303	MVA	E,A,G	C,D,E	CP,NWL	"	17-E 29-A 31-G	"	13:46:56	2:20:00
31	2304	MVA	E,A,G	C,D,E	CP,NWL	"	18-E 38-A 30-G	"	16:05:56	:00:1.32
31	2305	CVA	A	D	HP,EWL	"	18	"	16:06:42	:00:1.0
31	2306	CVA	A	D	HP,EWL	"	18	"	16:07:07	:00:0.84
31	2307	CVA	A	D	HP,EWL	"	19	"	16:07:26	
32	24	Extended Blowdown	A	D	CP,NWL	"	6 min 42 sec	"	20:56:12	4:49:00

(1) Legend:
- SVA - Single Valve Actuation
- CVA - Consecutive Valve Actuation
- MVA - Multiple Valve Actuation
- CP - Cold Pipe
- WP - Warm Pipe
- HP - Hot Pipe
- NWL - Normal Water Leg in the S/RV Line. Note: NWL obtained by opening S/RV discharge line solenoid - bleed valve opening valves E, A and G
- DWL - Depressed Water Leg in the S/RV Line
- EWL - Elevated Water Leg in the S/FV Line or intended to be.

(2) Reactor Dome pressure for all tests was 1000 $\pm$ 10 psia. Estimates for SRV flow rate range between 200 and 227 lbm/sec. See Appendix J.

(3) Discharge time estimated from the SRVDL pressure transient as recorded by P1. The time between valve off and valve on is also estimated with P1

(4) Based on Hand Switch.

Table 3-2

TEST INITIAL CONDITIONS BEFORE PREPRESSURIZATION(1)

Run	Test	Average Pipe Temperature (°F)	Air Mass (lbm)	Steam Partial Pressure (psia)	Water(5) Leg Length (ft)	Pool Temperature at T-Quencher Elevation (°F)	Drywell* Pressure (psia)	Drywell/* Wetwell Pressure Difference (psid)	Total Pipe Pressure (psia)	Estimated Water Leg Velocity(7) (ft/sec)
2	2	101	3.04	0.98	13.3	76*	14.4	-0.01	14.4	0
3	501	113	2.89	1.39	13.3	76*	14.4	-0.01	14.4	0
4	502	229	(2)	(2)	13.5	76*	14.4	-0.01	14.3	0
5	801	122	2.78	1.79	13.3	77*	14.5	-0.01	14.5	0
6	802	321	(2)	(2)	12.4	81*	14.5	-0.01	14.9	0
7	901	125	2.86	1.94	13.4	75*	15.1	-0.01	15.1	0
8	902	324	(2)	(2)	12.3	79*	15.1	-0.01	15.5	0
9	903	335	(2)	(2)	11.6	79*	15.1	-0.01	15.8	0
10	904	337	(2)	(2)	12.1	81*	15.1	-0.01	15.6	0
11	905	337	(2)	(2)	12.3	81*	15.1	-0.01	15.6	0
12	1101	116	3.10	1.51	13.3	83*	14.6	-0.01	(3)	0
13	1102	(3)	(3)	(3)	(3)	84	14.6	-0.01	(3)	0
14	1103	(3)	(3)	(3)	(3)	84	14.6	-0.01	(3)	0
15	1104	(3)	(3)	(3)	(3)	84	14.6	-0.01	(3)	0
16	1105	(3)	(3)	(3)	(3)	84	14.6	-0.01	(3)	0
17	12	(3)	(3)	(3)	(3)	70*	14.6	-0.01	(3)	0
18	1301	107	3.03	1.17	13.3	72*	14.7	-0.01	14.7	0
18	1302	361	0.03	17.20	(4)	80*	14.7	-0.01	17.4	30
18	1303	359	1.02	10.20	6.9	72	14.7	-0.01	16.4	0
19	14	116	3.10	1.51	13.3	79*	14.75	-0.01	(3)	0
20	15	116	2.7	1.51	13.3	71*	14.75	-0.01	(3)	0
21	1601	119	2.87	1.65	13.3	72*	14.7	0.00	14.7	0
21	1602	323	0.98	10.64	7.2	72	14.7	0.00	16.3	0
21	1603	321	1.09	9.65	8.8	72	14.7	0.00	16.0	0
21	1604	365	1.08	9.16	9.6	72	14.7	0.00	15.9	0
21	1605	363	1.12	8.96	9.5	72	14.7	0.00	15.9	0

Table 3-2 (Continued)

TEST INITIAL CONDITIONS BEFORE PREPRESSURIZATION(1)

Run	Test	Average Pipe Temperature (°F)	Air Mass (lbm)	Steam Partial Pressure (psia)	Water Leg Length (ft)(5)	Pool Temperature at T-Quencher Elevation (°F)	Drywell* Pressure (psia)	Drywell/* Wetwell Pressure Difference (psid)	Total Pipe Pressure (psia)	Estimated Water Leg Velocity (ft/sec)(7)
22	18	116	3.1	1.51	13.3	80*	14.8	-0.01	(3)	0
23	19	116	2.7	1.51	13.3	71*	14.8	-0.01	(3)	0
24	21	116	3.1	1.51	13.3	78*	14.8	-0.01	(3)	0
25	22	116	2.70	1.51	13.3	71*	14.8	-0.01	(3)	0
26	2301	106	3.07	1.13	13.4	69,76,68(6)*	14.75	-0.01	14.7	0
28	2302	125	2.77	1.94	13.5	70,77,69(6)*	14.82	-0.01	14.7	0
30	2303	125	2.79	1.94	13.5	70,77,69(6)*	14.88	-0.01	14.8	0
31	2304	127	2.76	2.05	13.5	70,77,69(6)*	14.92	-0.01	14.8	0
31	2305	359	1.11	8.54	10.6	89	14.92	-0.01	15.5	30
31	2306	359	0.85	4.05	8.8	95	14.92	-0.01	9.3	25
31	2307	359	0.89	9.44	(4)	99	14.92	-0.01	14.5	25
32	24	107	3.06	1.17	13.3	51*	14.8	+0.03	14.8	0

*Entries to this table that have asterisks represent data which were measured directly. All other entries were calculated in the methods summarized in Appendix I.

(1) Values reported correspond to the arrival of the primary pressure wave (due to SRV steam bleed) at the air-water interface.

(2) Values cannot be provided due to insufficient data.

(3) No available data

(4) For these tests, the air-water interface was still within the T-Quencher arms.

(5) Measured from the center of the T-Quencher arms.

(6) Temperatures in Bay D, C and E, respectively.

(7) A positive value indicates that the water is moving toward the SRV.

Table 3-3

TEST INITIAL CONDITIONS[1] (AT THE START OF SRV MAIN DISC MOTION)

Run	Test	Estimated[2] Water Leg Velocity (ft/sec)	Estimated[3] Water Leg Length (ft)	Total Pipe[4] Pressure (psia)
2	2	-9.1	11.2	18.2
3	501	-9.1	11.2	18.4
4	502	-9.1	11.4	21.1
5	801	-9.1	11.2	18.5
6	802	-9.1	11.1	21.7
7	901	-9.1	11.3	19.5
8	902	-9.1	11.0	22.1
9	903	-9.1	10.3	22.0
10	904	-9.1	10.8	21.0
11	905	-9.1	11.0	20.6
12	1101	(5)	(5)	(5)
13	1102	(5)	(5)	(5)
14	1103	(5)	(5)	(5)
15	1104	(5)	(5)	(5)
16	1105	(5)	(5)	(5)
17	12	(5)	(5)	(5)
18	1301	-9.1	11.2	18.1
18	1302	30	0.0	12.7
18	1303	-4.3	6.5	19.9
19	14	(5)	(5)	(5)
20	15	(5)	(5)	(5)
21	1601	-9.1	11.2	19.2
21	1602	-4.3	6.8	19.7
21	1603	-4.3	8.4	18.7
21	1604	-4.3	9.2	18.7
21	1605	-4.3	9.1	18.6
22	18	(5)	(5)	(5)
23	19	(5)	(5)	(5)

Table 3-3 (Continued)

TEST INITIAL CONDITIONS[1] (AT THE START OF SRV MAIN DISC MOTION)

Run	Test	Estimated[2] Water Leg Velocity (ft/sec)	Estimated[3] Water Leg Length (ft)	Total Pipe[4] Pressure (psia)
24	21	(5)	(5)	(5)
25	22	(5)	(5)	(5)
26	2301	-9.1	11.3	19.0
28	2302	-9.1	11.4	19.4
30	2303	-9.1	11.4	19.5
31	2304	-9.1	11.4	19.7
31	2305	30	14.3	22.1
31	2306	25	12.4	20.6
31	2307	25	3.4	17.1
32	24	-9.1	11.2	19.2

Note: The parameters not shown here are assumed to be the same as those in Table 3-2 except for the steam pressure.

(1) Values reported correspond in time approximately to the arrival of the primary pressure wave (due to SRV main disk opening) at the air-water interface.

(2) A positive value indicates that the water is moving toward the SRV.

(3) Measured from the center of the T-Quencher arms

(4) Values reported were obtained from P49 (P49 is located 11 ft above NWL) and the drywell pressure.

(5) Data were not available.

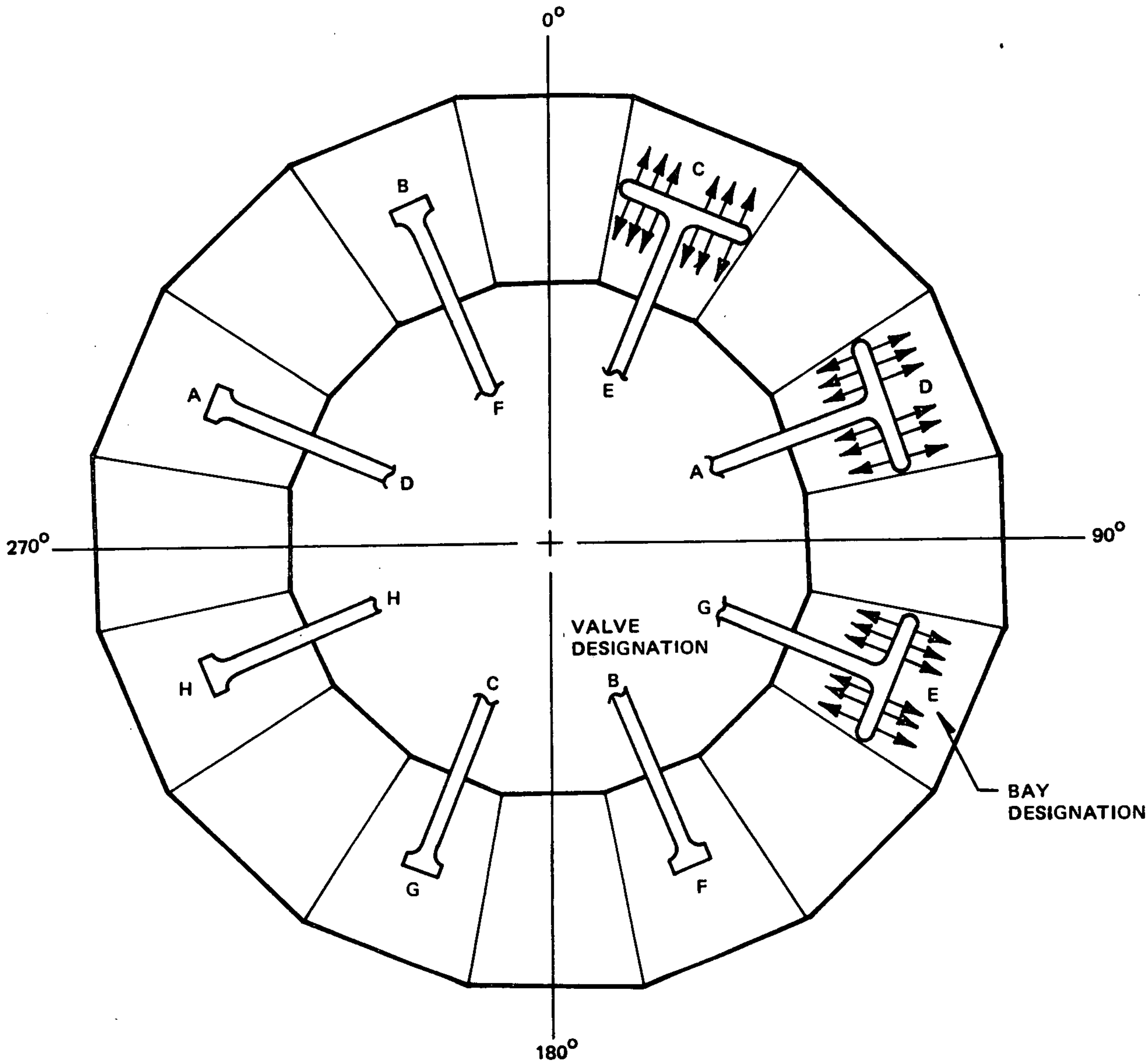

BAY	SR VALVE DESIGNATION	CATEGORY	AZIMUTH (DEGREES)	ACCESS LOCATION
A	RV2-71D		292-1/2	
B	RV2-71F		337-1/2	
C	RV2-71E		22-1/2	
D	RV2-71A	ADS*	67-1/2	48-in. MANWAY
E	RV2-71G		112-1/2	
F	RV2-71B	ADS	157-1/2	
G	RV2-71C	ADS	202-1/2	
H	RV2-71H		247-1/2	48-in. MANWAY

*ADS = AUTOMATIC DEPRESSURIZATION SYSTEM

Figure 3-1. Orientation of Safety Relief Valve Discharges Within Monticello Torus

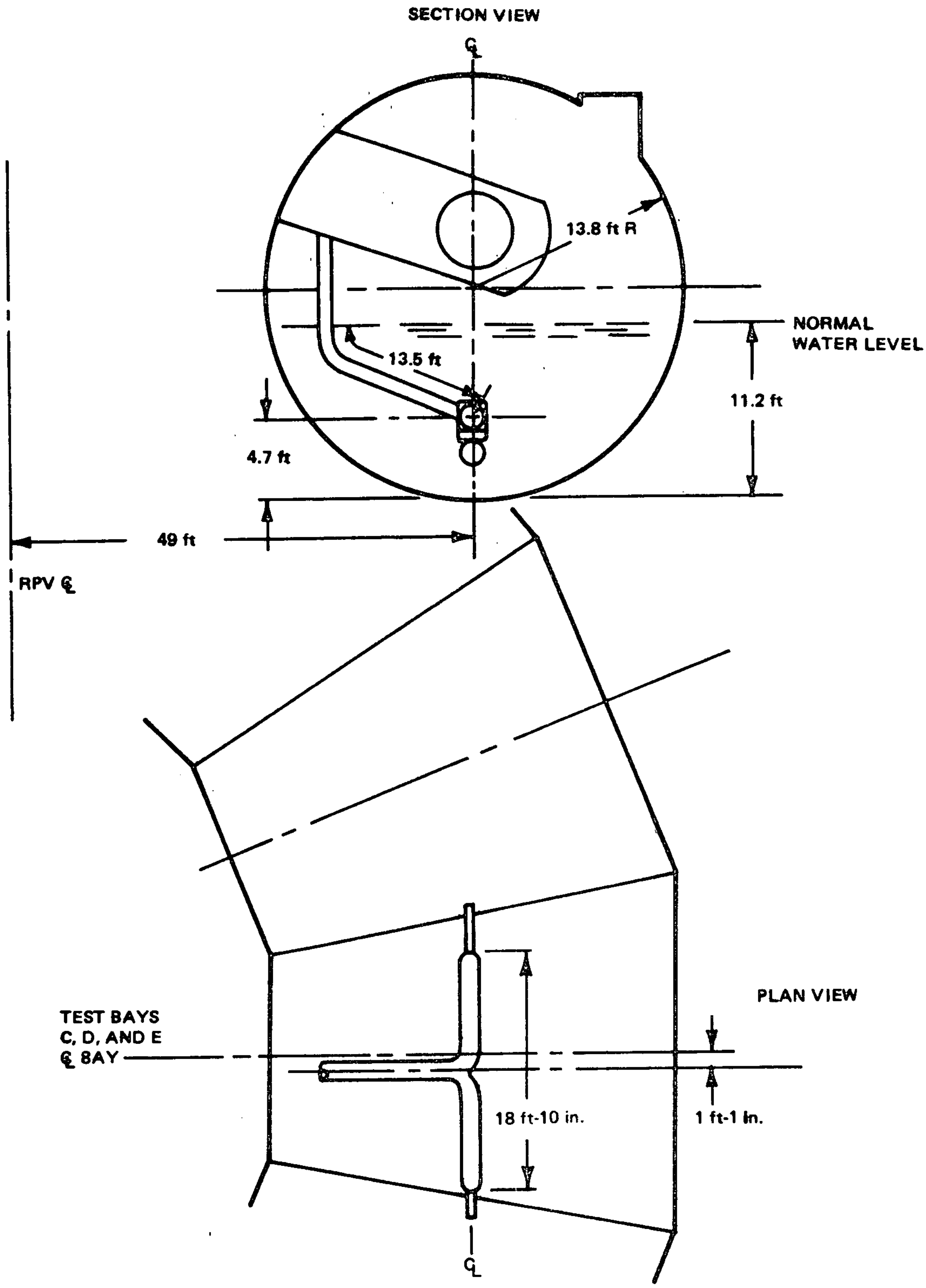

Figure 3-2. Quencher Configuration

4. INSTRUMENTATION

4.1 INTRODUCTION

In order to match various requirements for frequency response and numbers of sensors with the timely availability of both data acquisition hardware and data reduction software, three separate instrumentation systems were used for the Monticello T-Quencher Test. The largest and most complex was the Pulse Code Modulation (PCM) system (Figure 4-1). This system sampled the analog signals from 252 transducers at a rate of 1,000 samples per second per channel. At this rate there are 5 samples per cycle at the design upper frequency limit of 200 Hz.

Because the temperature of the torus water cannot change rapidly, such rapid scanning of torus water temperature sensors is unnecessary. Therefore, the 39 resistance temperature detectors installed in the pool were connected to the DS-83 temperature data scan system. Temperature data were printed on paper tape in real time, with an interval of approximately 2 minutes between successive readings of the same sensor. The details of this system are shown in Figure 4-2.

When additional strain gage information from remote torus bays was desired, but all possible inputs to the PCM system were already committed, it was decided to use a separate FM tape recording system. The block diagram of Figure 4-3 shows this system. Data from 7 strain gage rosettes, 1 single gage, and 4 4-arm axial load bridges on 4 columns were recorded on two 14-track tape recorders.

4.2 SUMMARY OF SENSOR TYPES

Sensors for the PCM system consisted of 20 single and 46 rosette weldable strain gauges (158 channels), 4 rosette foil gauges (12 channels), 8 bending bridges composed of 4 foil gauges each (8 channels), 4 axial bridges composed of 8 foil gauges each (4 channels), 9 accelerometer locations (11 channels), 46 pressure transducers (46 channels), 4 water level probes (4 channels), 1 vacuum breaker flow-indicating transducer (1 channel), 7 temperature sensors (7 channels), and one hand switch to indicate SRV open/close status (1 channel) for a total of 252 channels. Detailed sensor characteristics of these sensors are provided in Appendix A. Figures 4-4 through 4-18 show sensor location.

The torus support column bending bridges and axial bridges were wired such that their output, multiplied by constants based upon the column section properties, produced axial load and components of bending in two orthogonal directions. The method of installation is shown in Figure 4-10.

Sensors for the DS-83 temperature sensor scanning system consisted of 39 RTDs (39 channels). Detailed sensor characteristics are presented in Appendix A. Figures 4-19 through 4-26 show the sensor locations.

The FM tape system recording sensors consisted of 22 single foil gauges (22 channels) and 4 axial bridges composed of 8 foil gauges each (4 channels), for a total of 26 channels. Detailed sensor characteristics are listed in Appendix A. Figures 4-27 through 4-30 show sensor locations.

4.3 SRV DISCHARGE LINE BLEED VALVES

Because water leg height in the SRV discharge line could return to normal slowly, or key sensor failure might not allow accurate tracking of the water leg, special discharge line vent valves were installed to relieve any excess pressure contained in lines A, E, or G before all normal water leg tests. A schematic piping diagram of these valves is presented in Figure 4-31.

4.4 SENSOR CALIBRATION PROCEDURES

The sensors recorded on the PCM system were calibrated as follows: strain gauges were calibrated by the shunt calibration resistor method; the Entran accelerometers and pressure transducers were calibrated by the ratio transformer method; the Endevco accelerometers and in-line temperature sensors were calibrated by the manufacturer; and the water level sensors were calibrated by jumper wire.

In addition to the pretest calibrations described above, a shunt calibration was performed before each test to record the calibration throughout the entire series of tests. This applies to the PCM strain gauge, pressure transducer, Entran accelerometer, axial and bending bridges, water level signals and in-line temperature sensors.

The DS-83 temperature signals were calibrated by a decade resistor. The FM recorded signals were calibrated by the shunt calibration method. Further appplicable calibration details are given in Appendix B.

4.5 FAILED OR SUSPECTED SENSORS

4.5.1 Hydrodynamic

4.5.1.1 Failed Sensors

The following sensors failed:

P44 - failed after the 1000 psi shakedown test

T6 - failed during test 501

T8 - failed during test 2301

T1 - failed during test 2304

4.5.1.2 Erratic Performance

The following sensors performed erratically:

P43 - yielded no data for tests 1301, 1302, and 1303

T7 - response during tests 2301, 2302, and 2303 had a high frequency oscillation.

4.5.1.3 Pool Temperature Sensors

During the extended discharge tests, these pool temperature sensors deviated from expected performance as follows:

T47 - readings from this sensor during the test with the RHR system in operation, were ∿102°F, 30 min after SRV discharge ended. This may be seen in Appendix E, Figure E4-19. Other sensors at the same height, such as T41 (Figure E4-17) and T44 (Figure E4-18), read below 79°F. Since other sensors in the same bay (T48 and T49 in Figure E4-19) read temperatures in the eighties (degrees Fahrenheit), there is a possibility of a local hot spot. The data for sensor T47 have therefore been included in the report.

T29 - The initial bulk pool temperature for the long discharge tests was 50°F. Before the test with the RHR system in operation, most sensors read ∿50°F, while T29 read below the freezing point. Thus, the data obtained in the test with RHR for this sensor have been deleted in this report.

T31 and T33 - For the two long discharge tests, T31 and T33 initially read ∿60°F, while the other sensors read ∿50°F. After stratification occurred following SRV discharge, T31 and T33 read ∿87°F. Other sensors at the same height read ∿110°F. For these reasons, it is believed that T31 and T33 were outside of the water. Data from these sensors have been deleted in this report.

4.5.1.4 Calibration Change

All sensors were calibrated before the test program was started (see Section 4.4). Before each test, the calibration reading of each sensor was recorded. Calibration readings recorded for tests 2 and 24 were compared to determine drift. Pressure sensors P25, P28, and P32 showed a calibration drift greater than 5% from tests 2 and 24; hence, data from these sensors are not included in this report.

4.5.2 Structural

There were no instances of complete failure of a strain gauge used for torus structure measurements. There were many instances of spurious signals (wildpoints) which, although rather widely dispersed throughout the data, were more prevalent in certain data channels. Where possible, these spurious signals were removed during the data processing operation. In cases where the signals were too numerous to remove without biasing the data, the data channels were omitted. In the case of strain gauge rosettes, the remaining channels were treated as single element gauges and processed accordingly. The criteria used for identifying wild points are discussed in Section 6.

4.5.3 T-Quencher and SRV Piping

4.5.3.1 Intermittent Data

No data were recorded for the following strain gauges:

SG 45 - Tests 2306, 2307, 1303, 1602, 1603, 1604, 1605, and 14.

SG 51C - Tests 24, 2301, 2302, 2303, 21, 15, and 22.

4.5.3.2 Erroneous Data

Accelerometers A8H, A8V, and A9V yielded data with unrealistic wave forms and amplitudes (see Figure 10-20); hence the data are not included in the report. This is discussed in subsection 10.3.1. A8 is located on the ramshead portion of the quencher and A9 is located on the quencher support.

4.5.3.3 Impossible Phenomena

Accelerometer A9H yielded a good wave form plot, but double integration indicated impossible displacements (on the order of 50 inches displacement at the quencher support). The data did indicate a higher peak force for elevated water level tests.

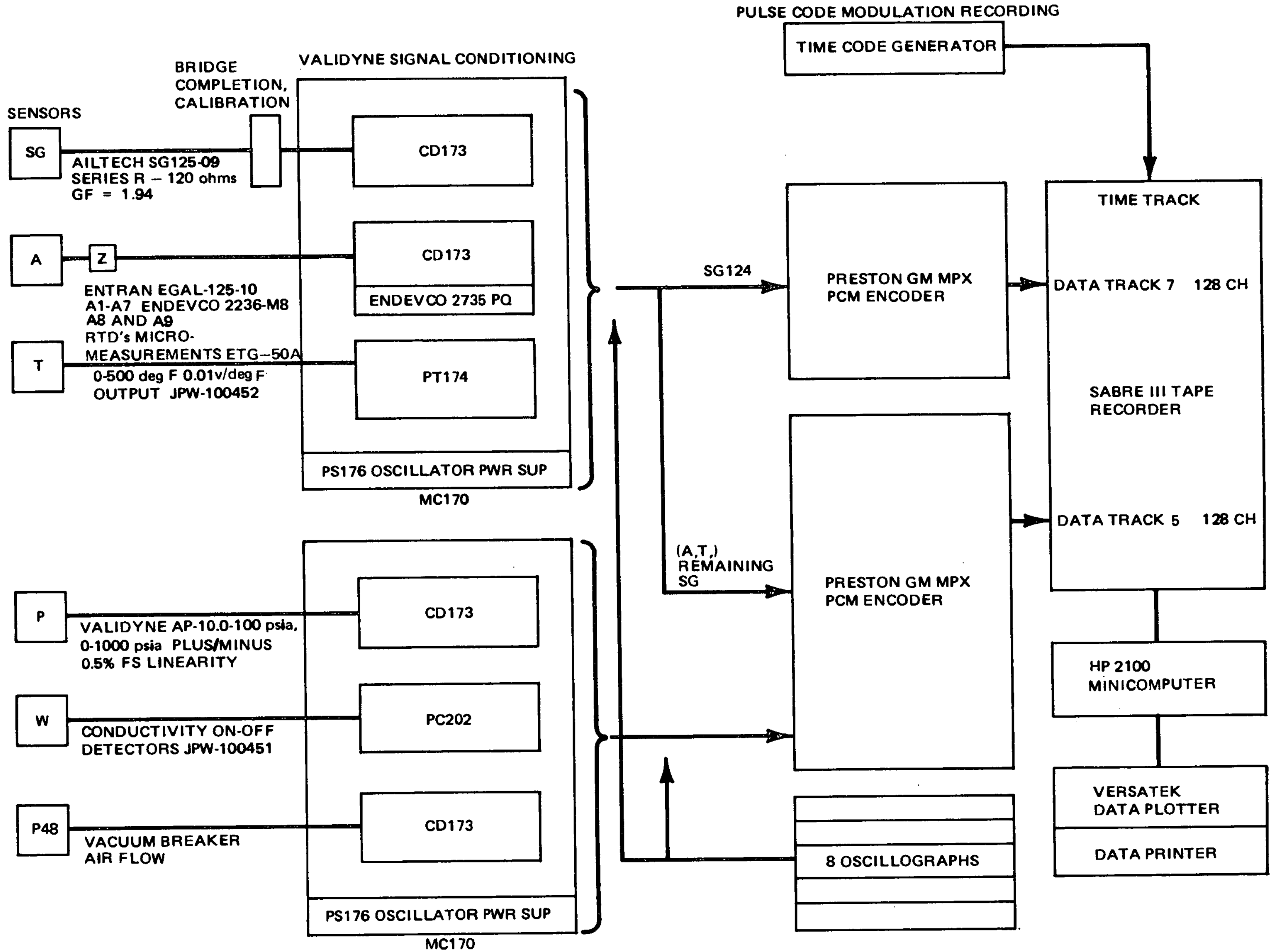

Figure 4-1. Block Diagram of Instrumentation System With Pulse Code Modulated System

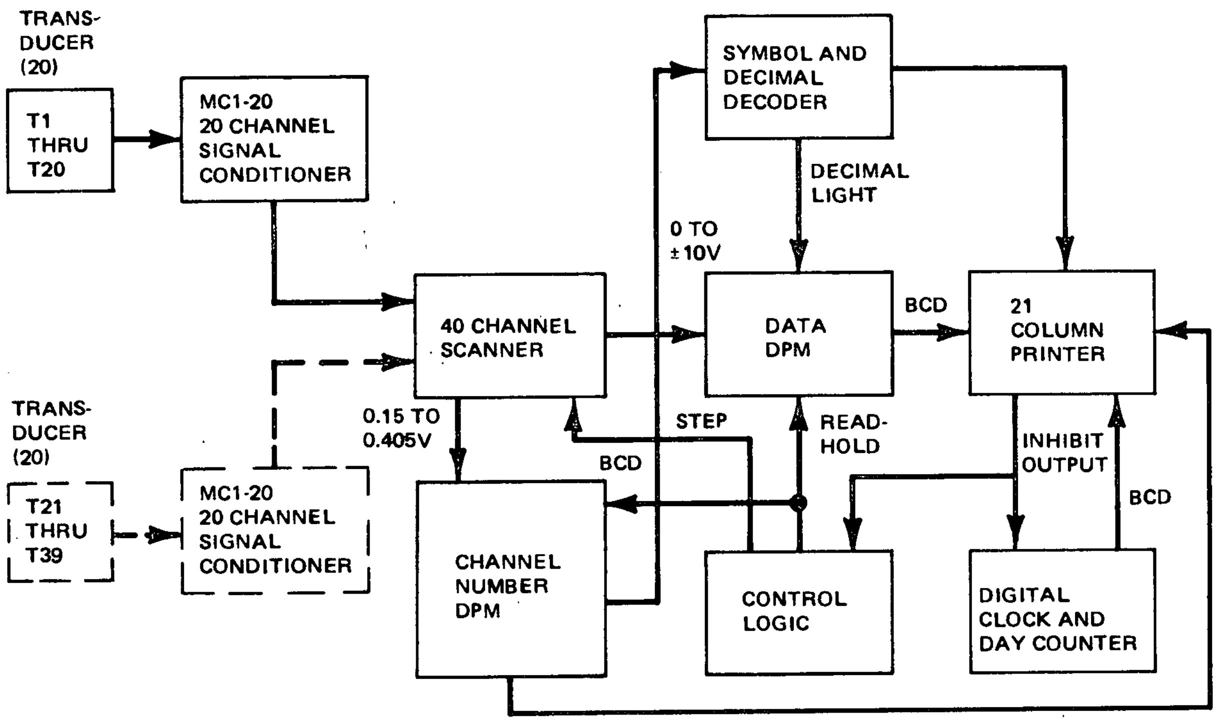

Figure 4-2. 40-Channel Data System Block Diagram DS-83 Scanner

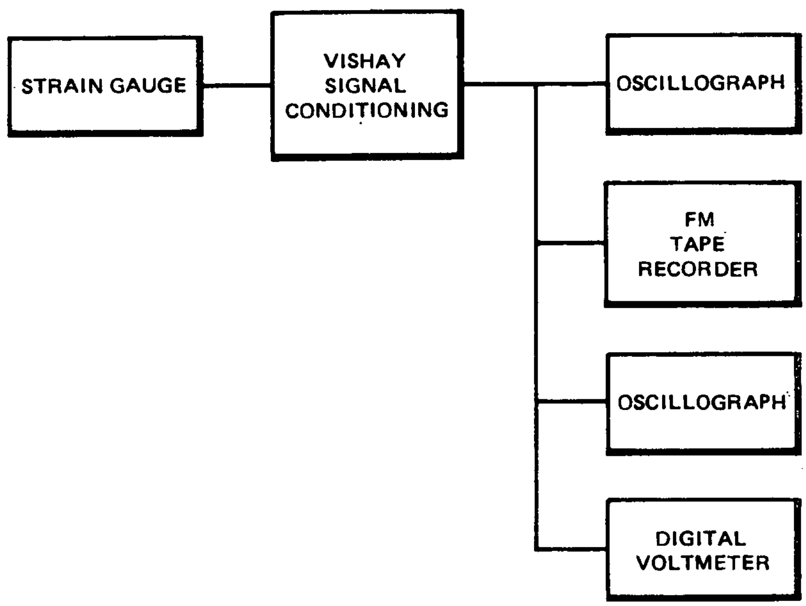

Figure 4-3. Block Diagram of the FM Tape Recording System

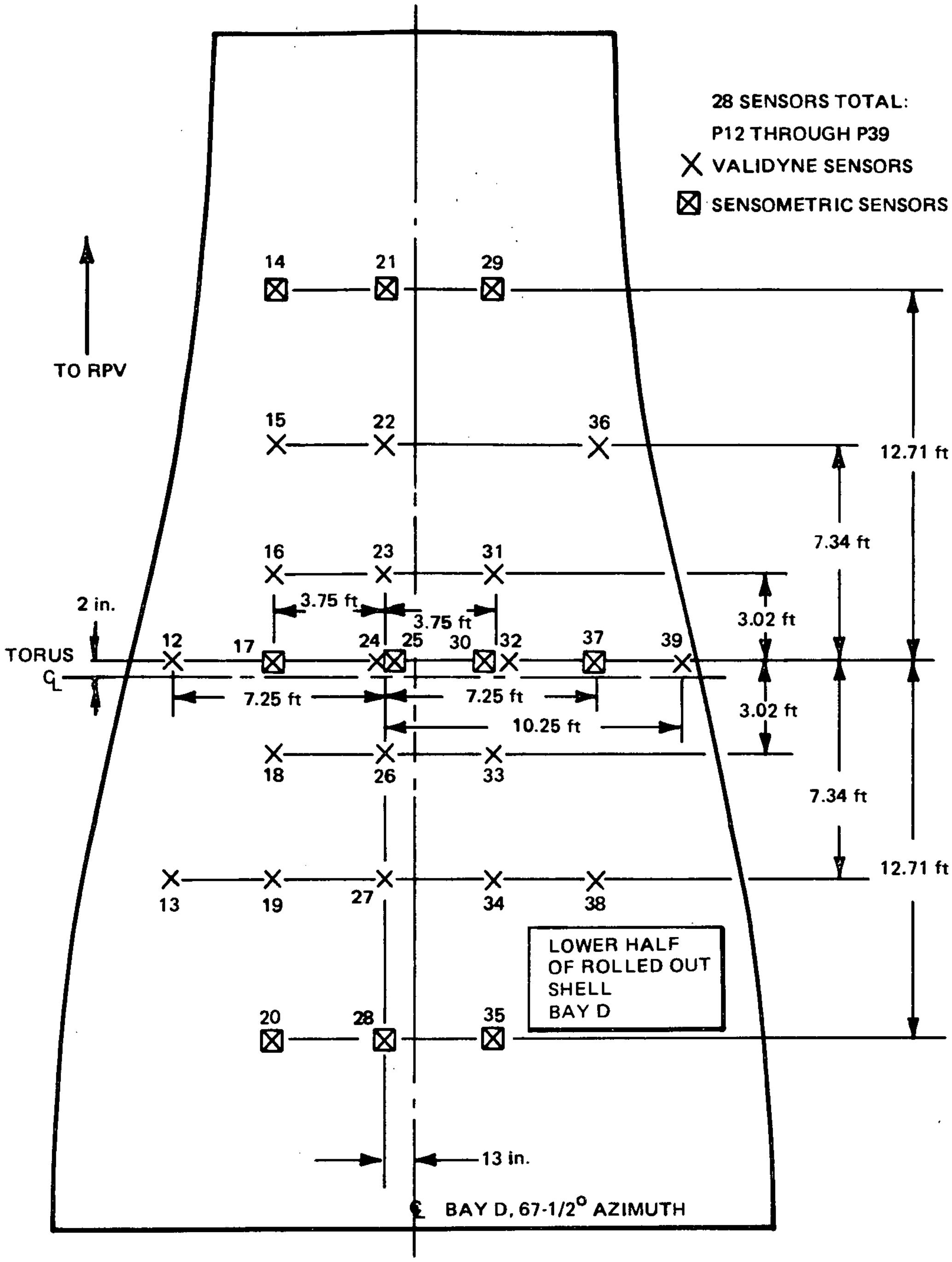

Figure 4-4. Pressure Transducer-Location - Half-Shell Layout of Bay D (view from inside torus looking out)

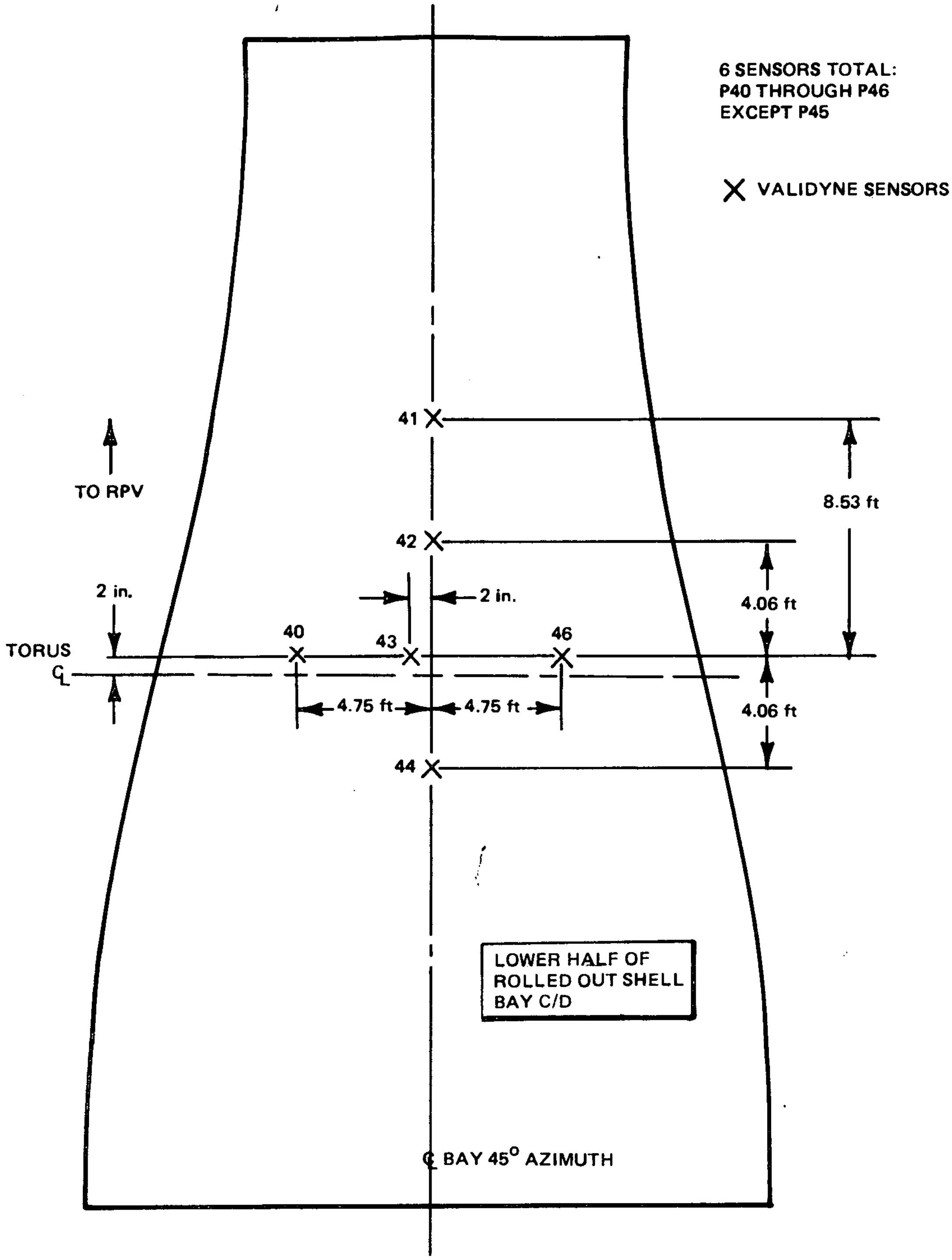

Figure 4-5. Pressure Transducer - Half Shell Layout of Bay C/D
(View from inside torus looking out)

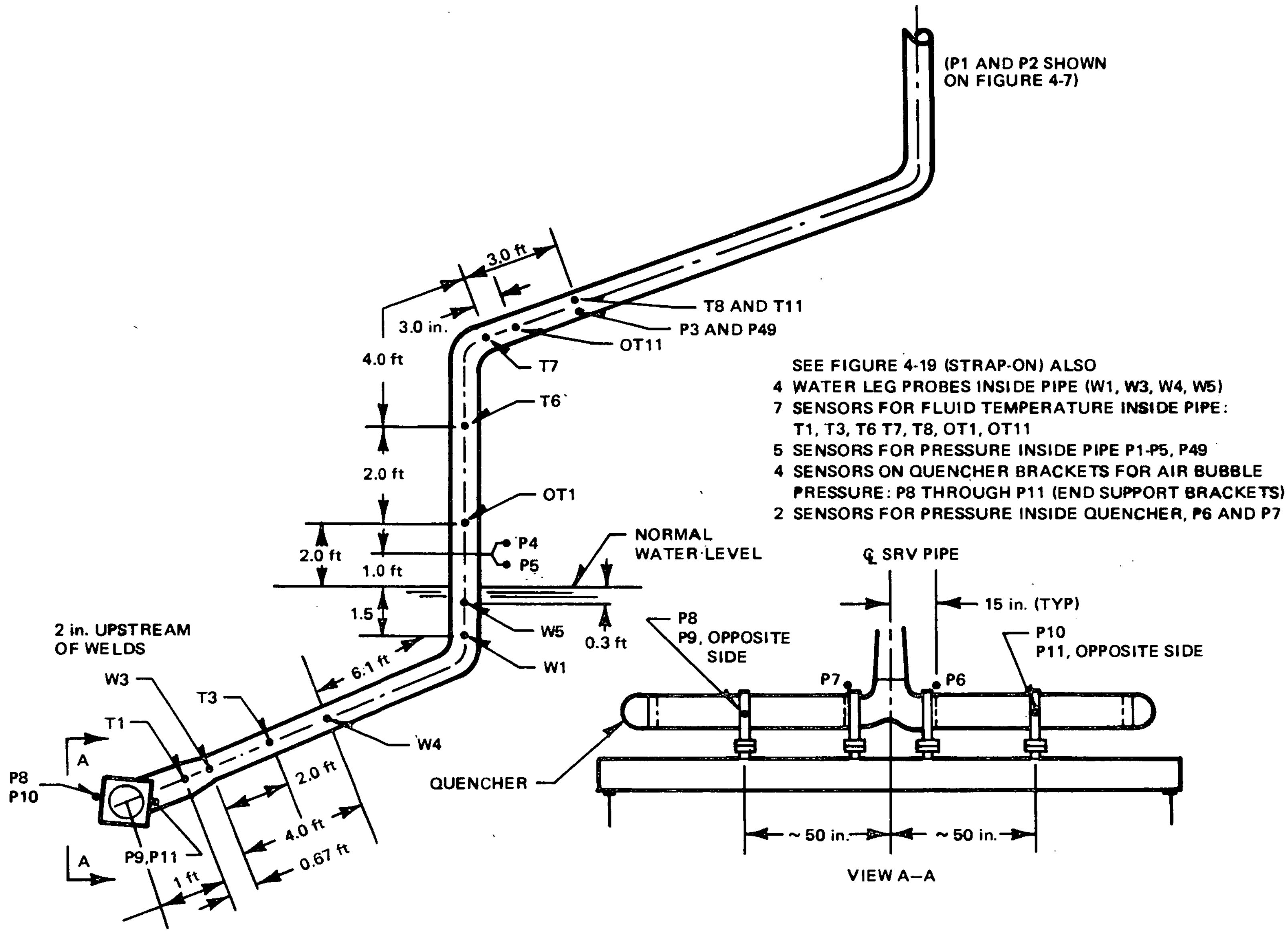

Figure 4-6. Pressure Transducer, Temperature Sensor, and Water Leg Probe Location on SRV Piping and Quencher

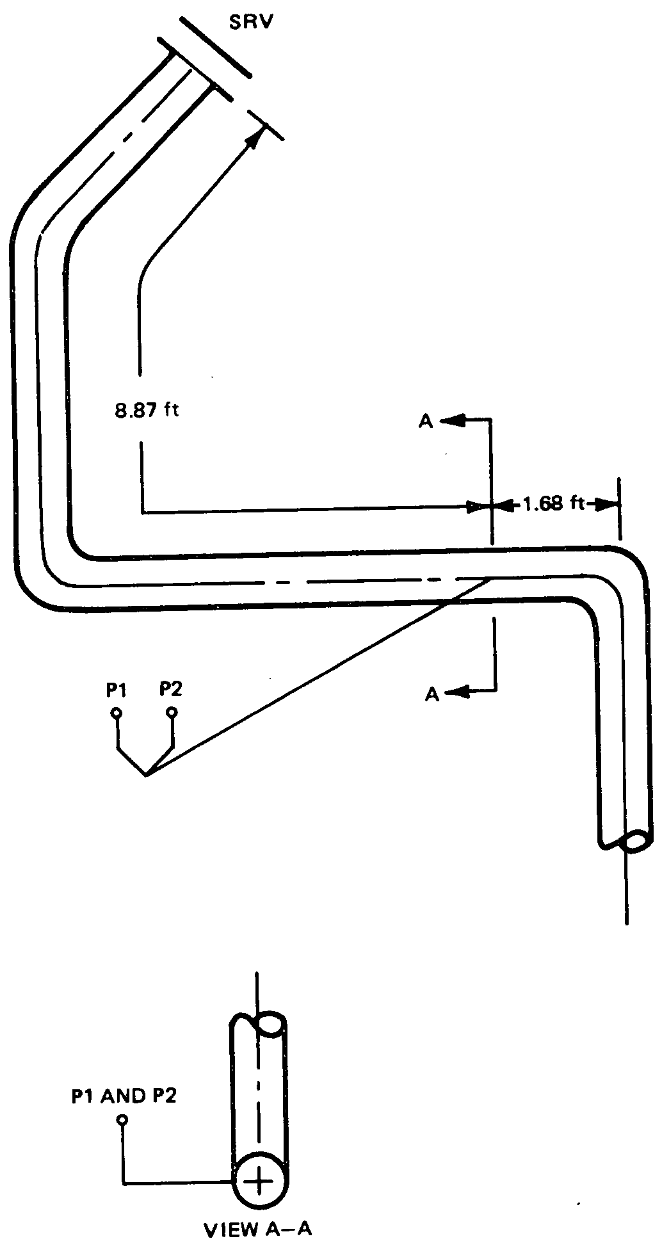

Figure 4-7. Location of Sensors P1 and P2

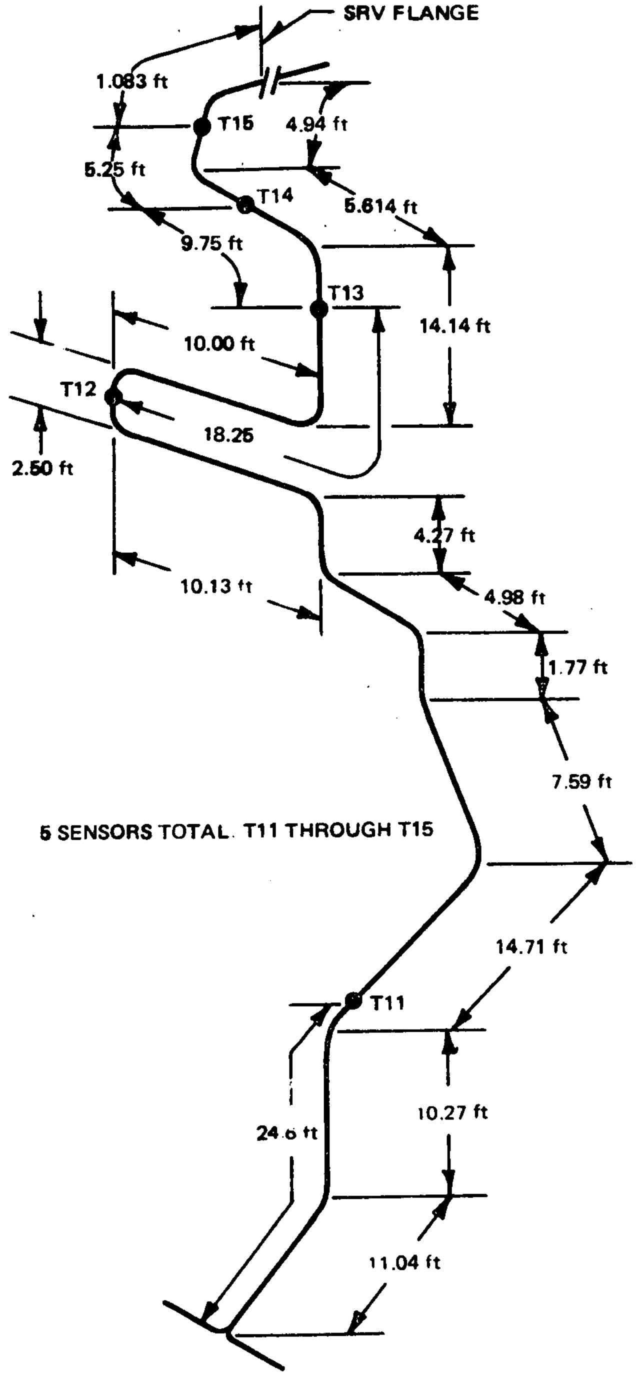

Figure 4-8. Temperature Sensor Locations - Strap-on SRV Pipe for Skin Temperature Measurement

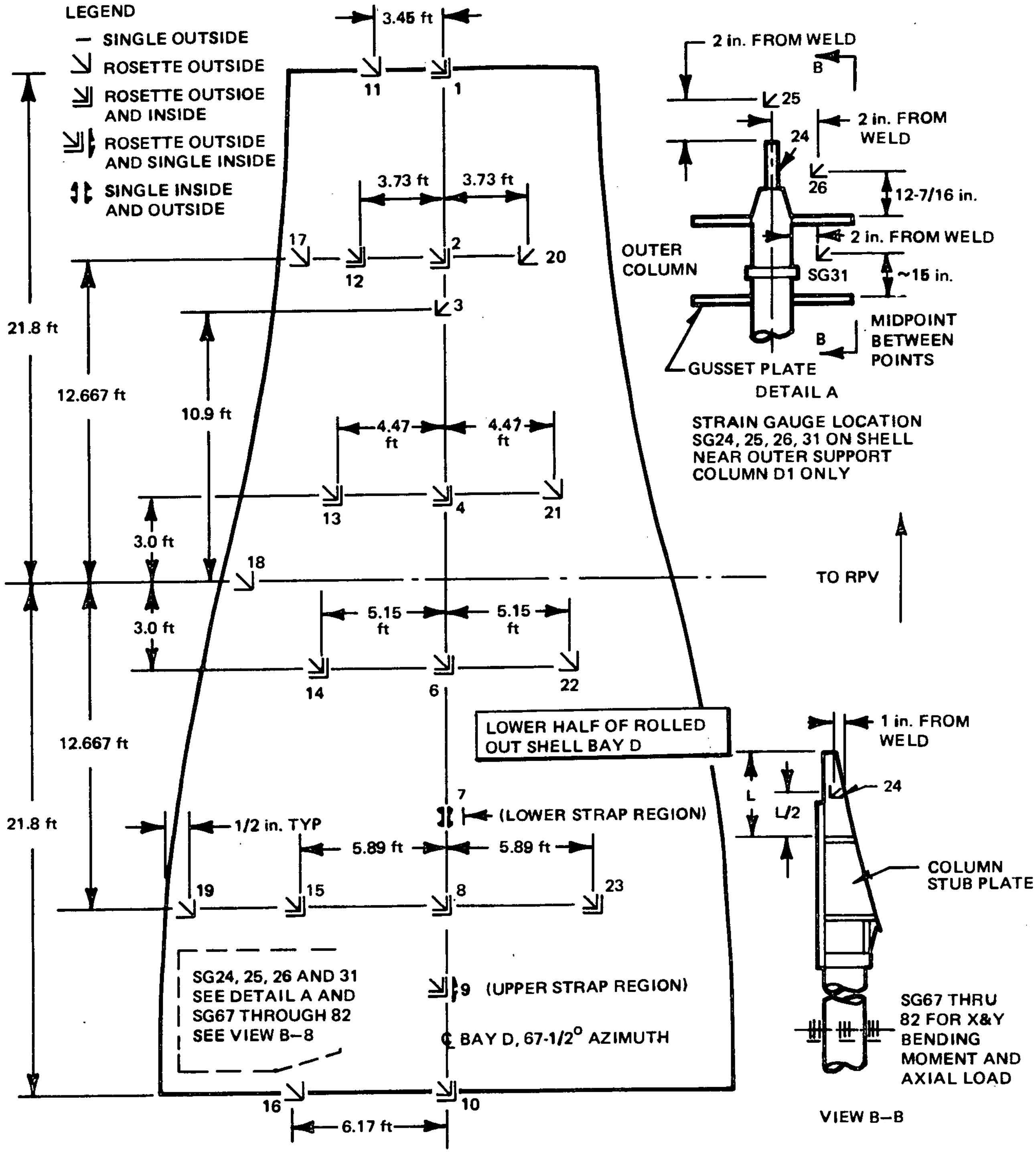

Figure 4-9. Strain Gauge Location - Shell & Column of Half-Shell Layout of Bay D (view from inside torus looking out)

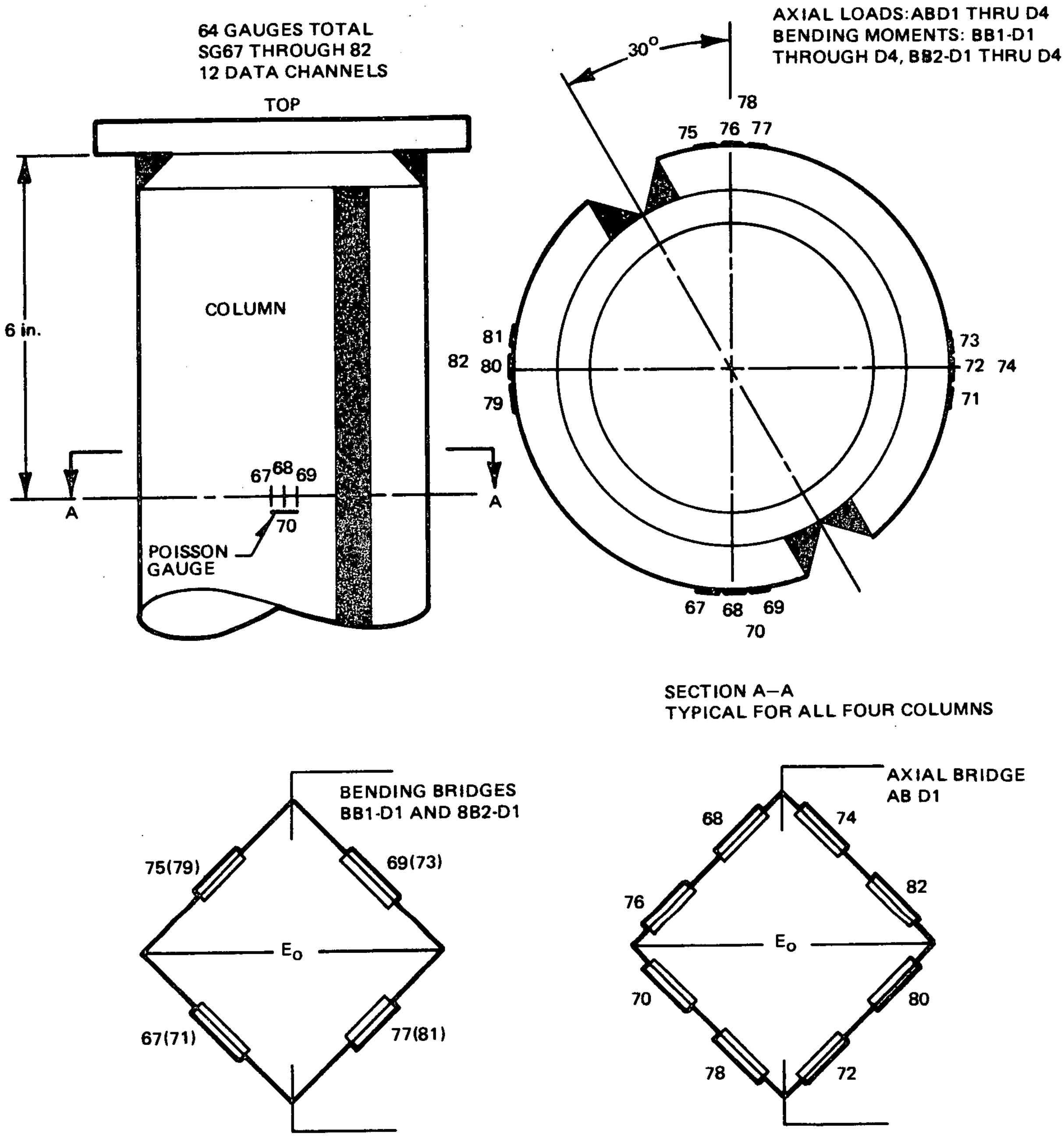

Figure 4-10. Strain Gauge Location on Four Support Columns - Bay D

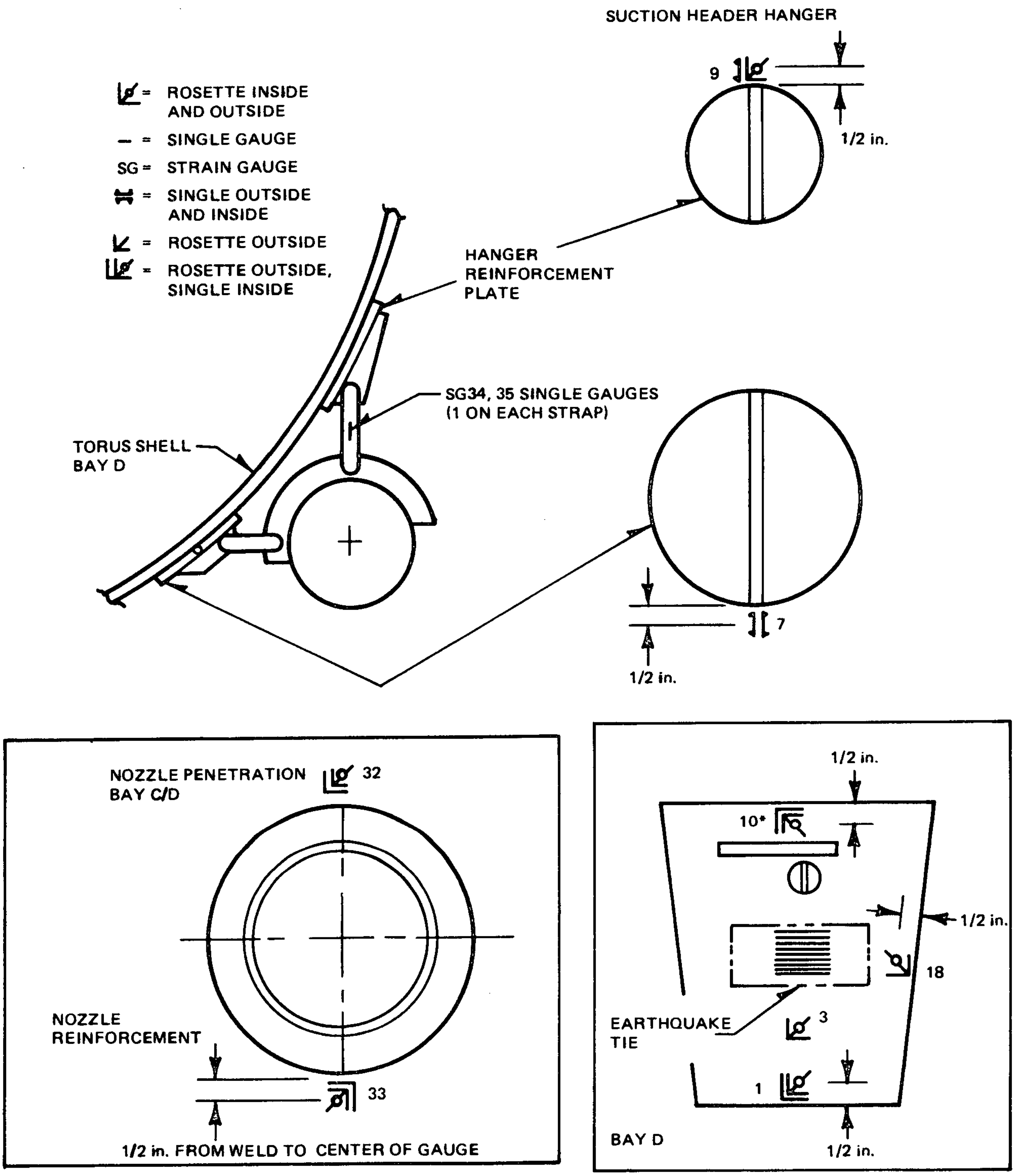

Figure 4-11. Location of Strain Gauges on Torus Wall and Suction Header

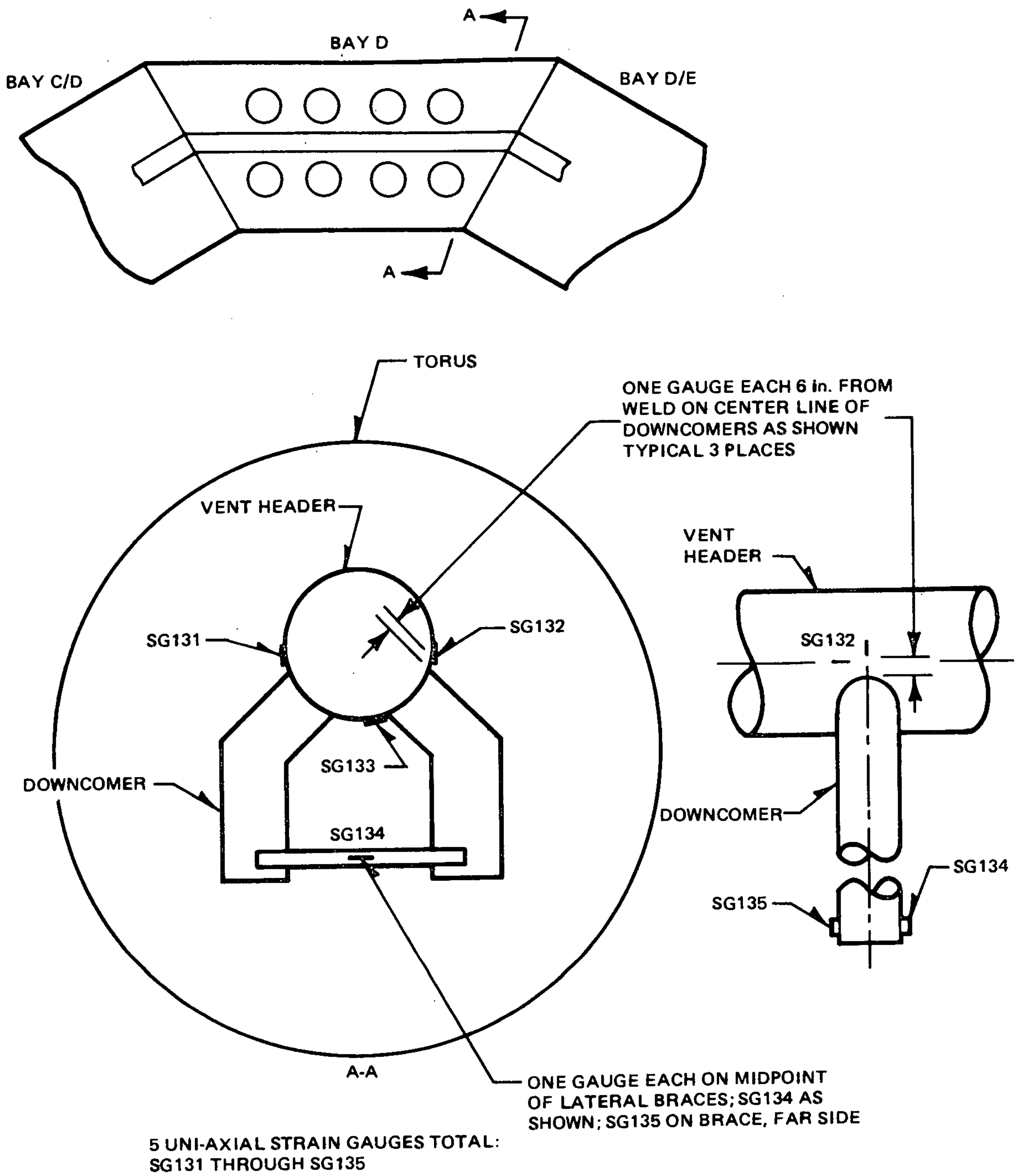

Figure 4-12. Strain Gauge Location on Vent Header and Downcomer Braces - Bay D

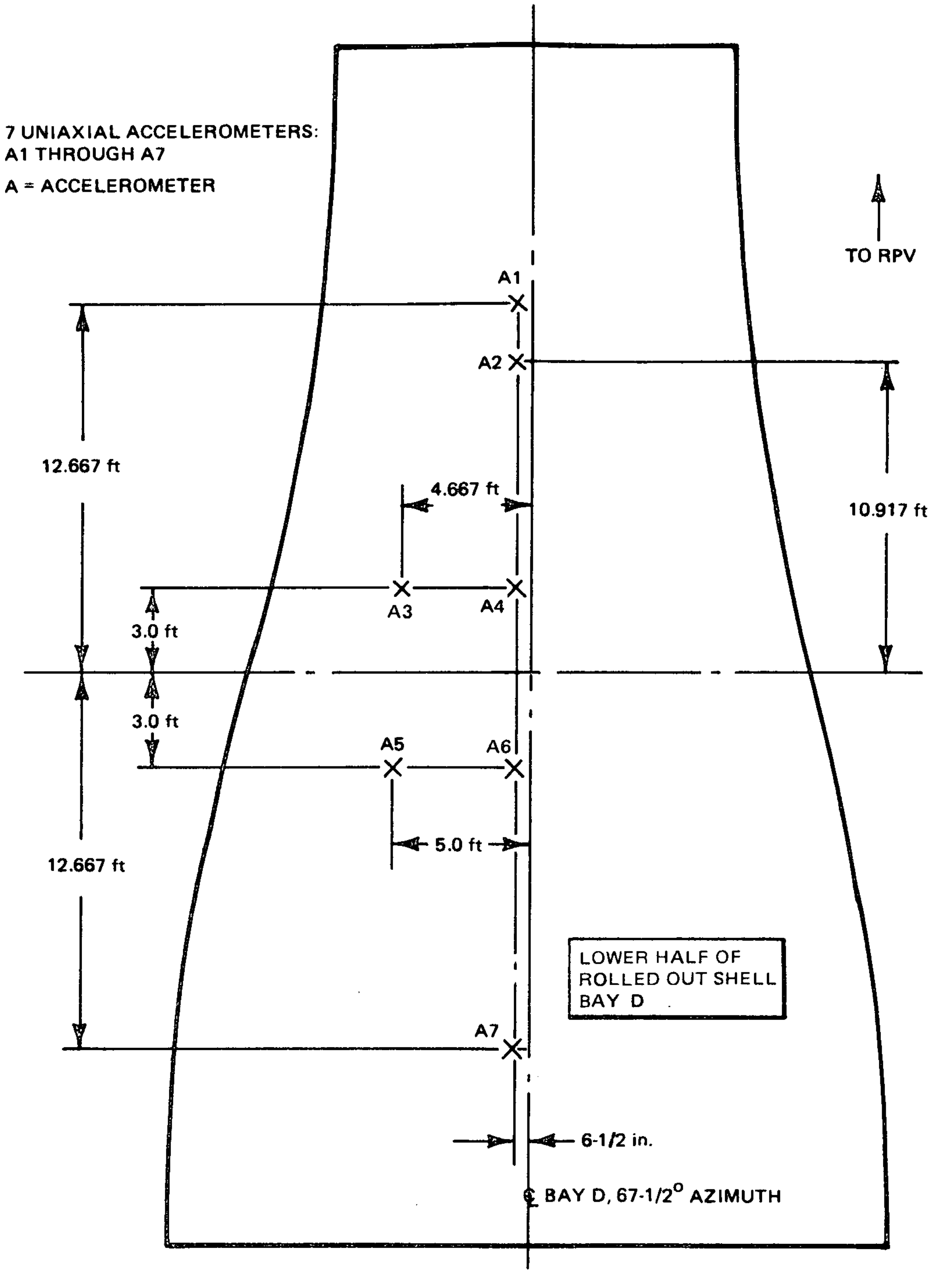

Figure 4-13. Accelerometer Location on Outside Shell - Half-Shell Layout of Bay D (view from inside torus looking out)

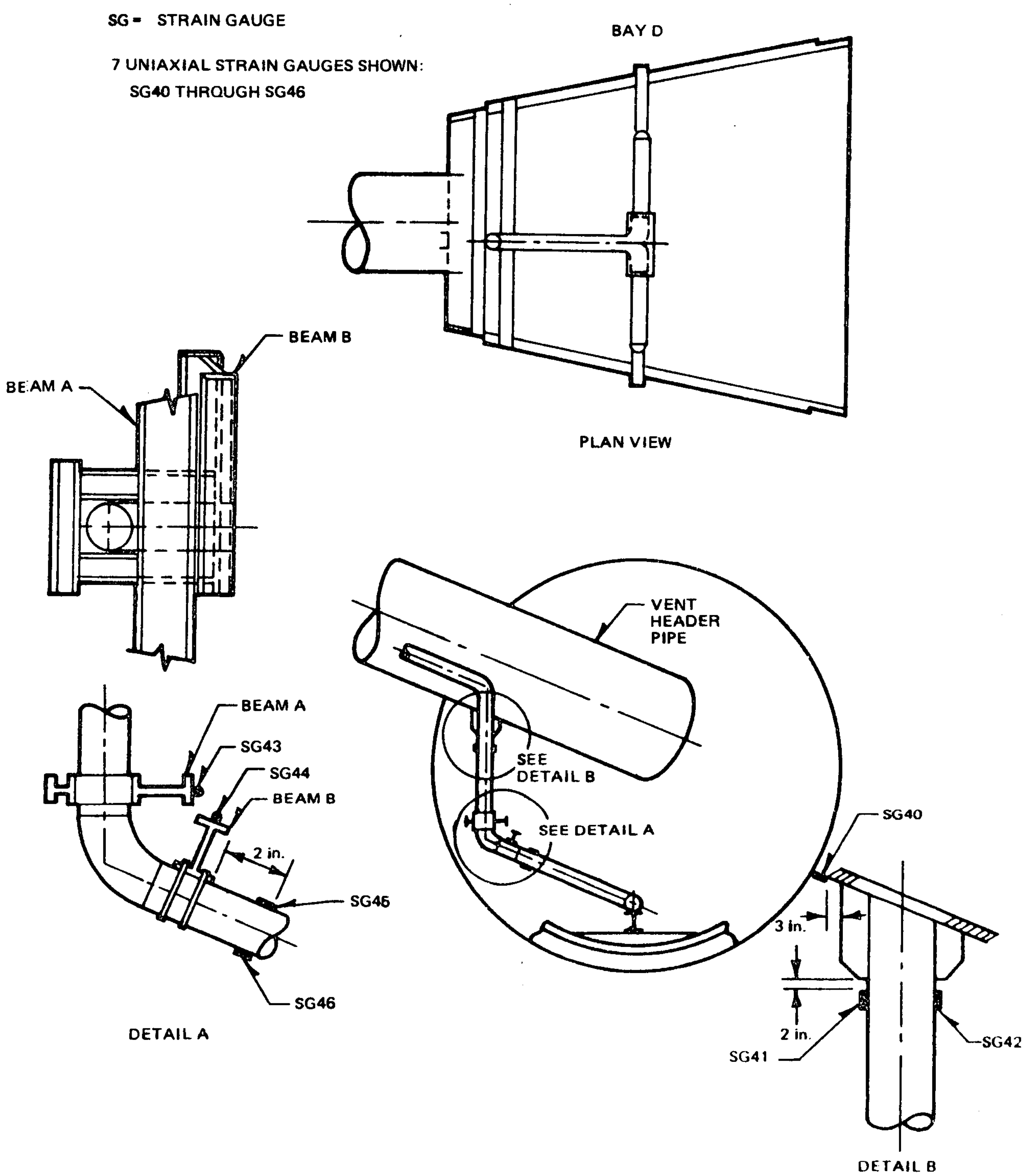

Figure 4-14. Strain Gauge Locations - SRV Pipe and Support - Bay D

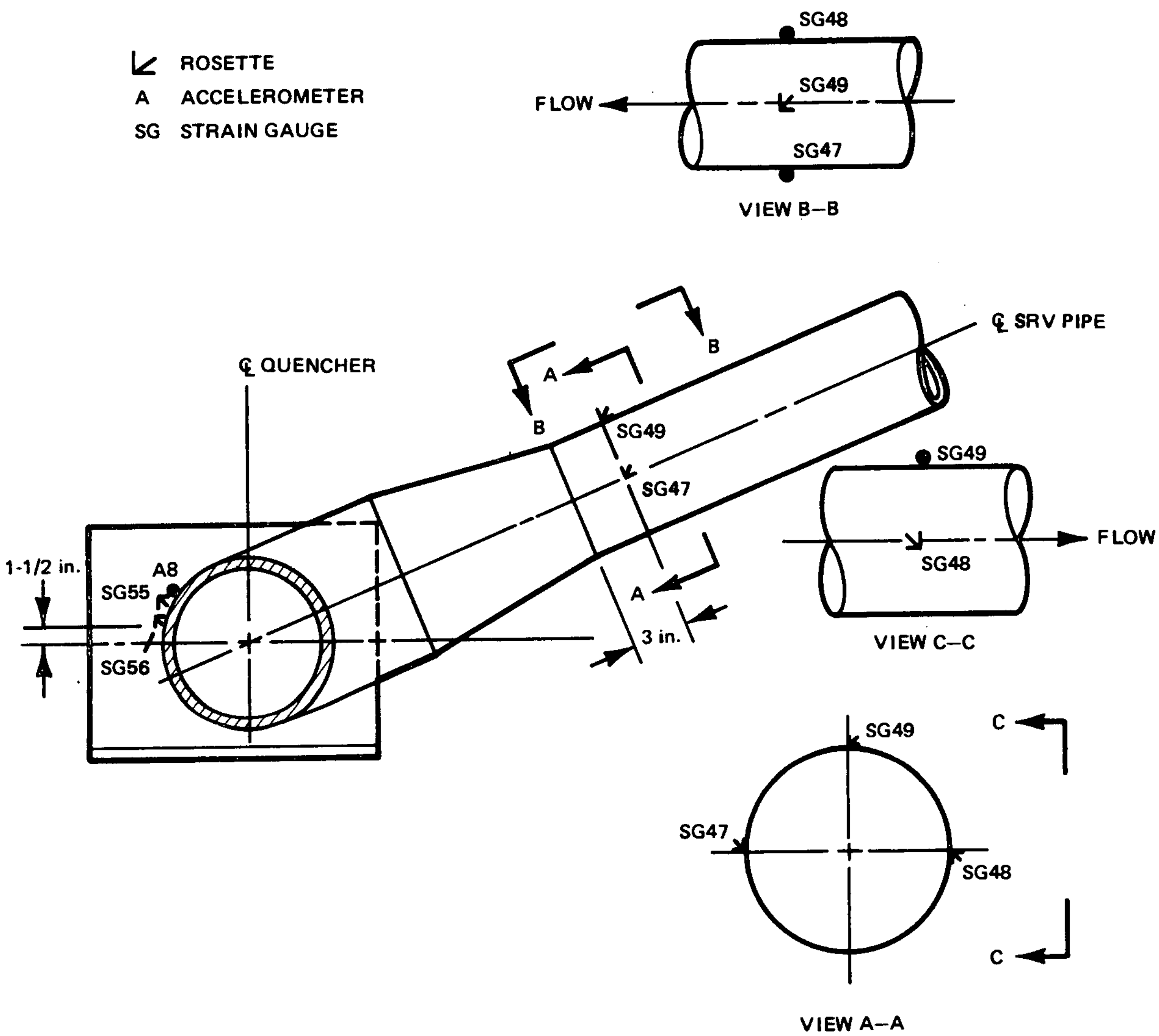

Figure 4-15. Strain Gauge and Accelerometer Location SRV Pipe and Quencher - Bay D

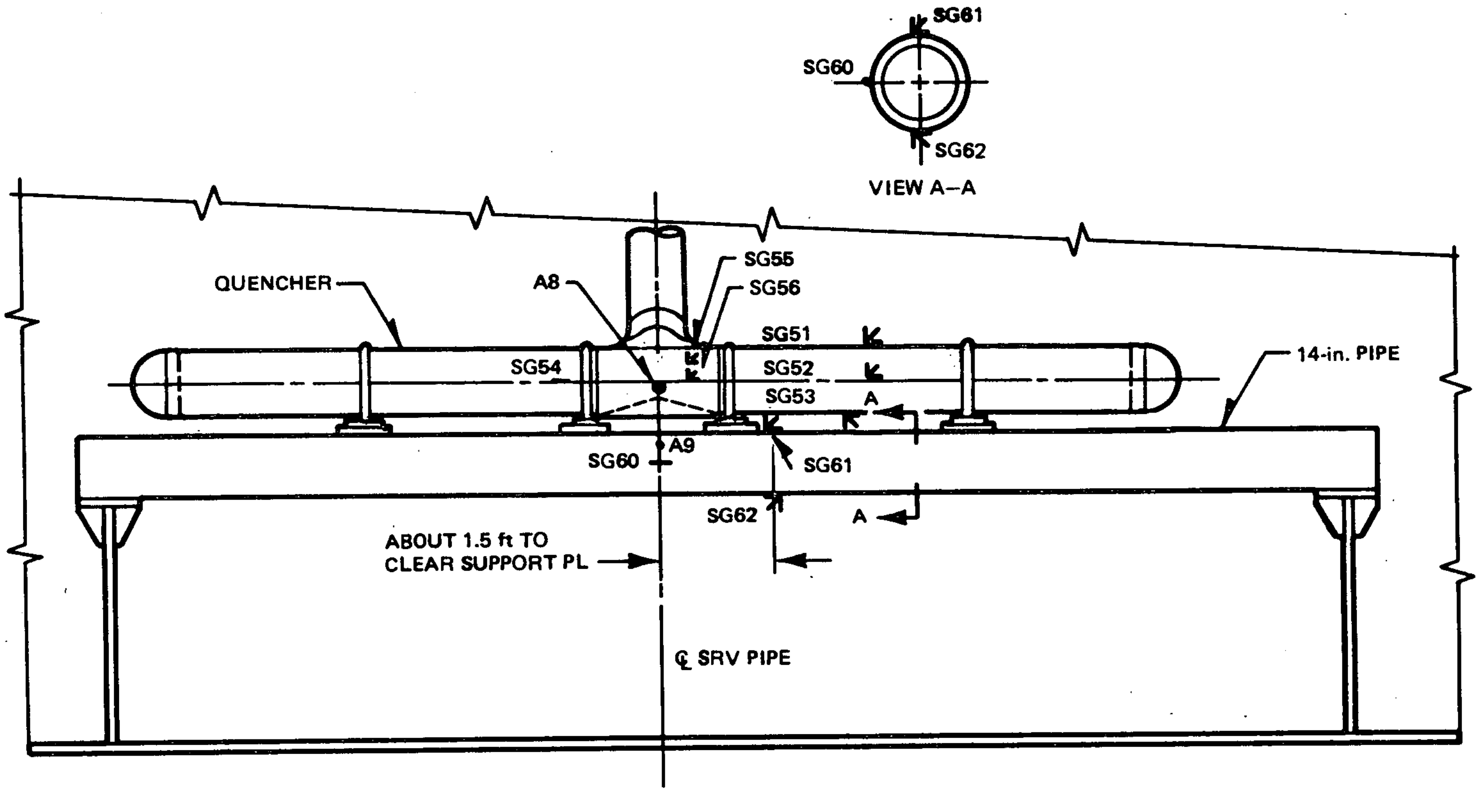

Figure 4-16. Strain Gauge and Accelerometer Location - Quencher and Support - Bay D

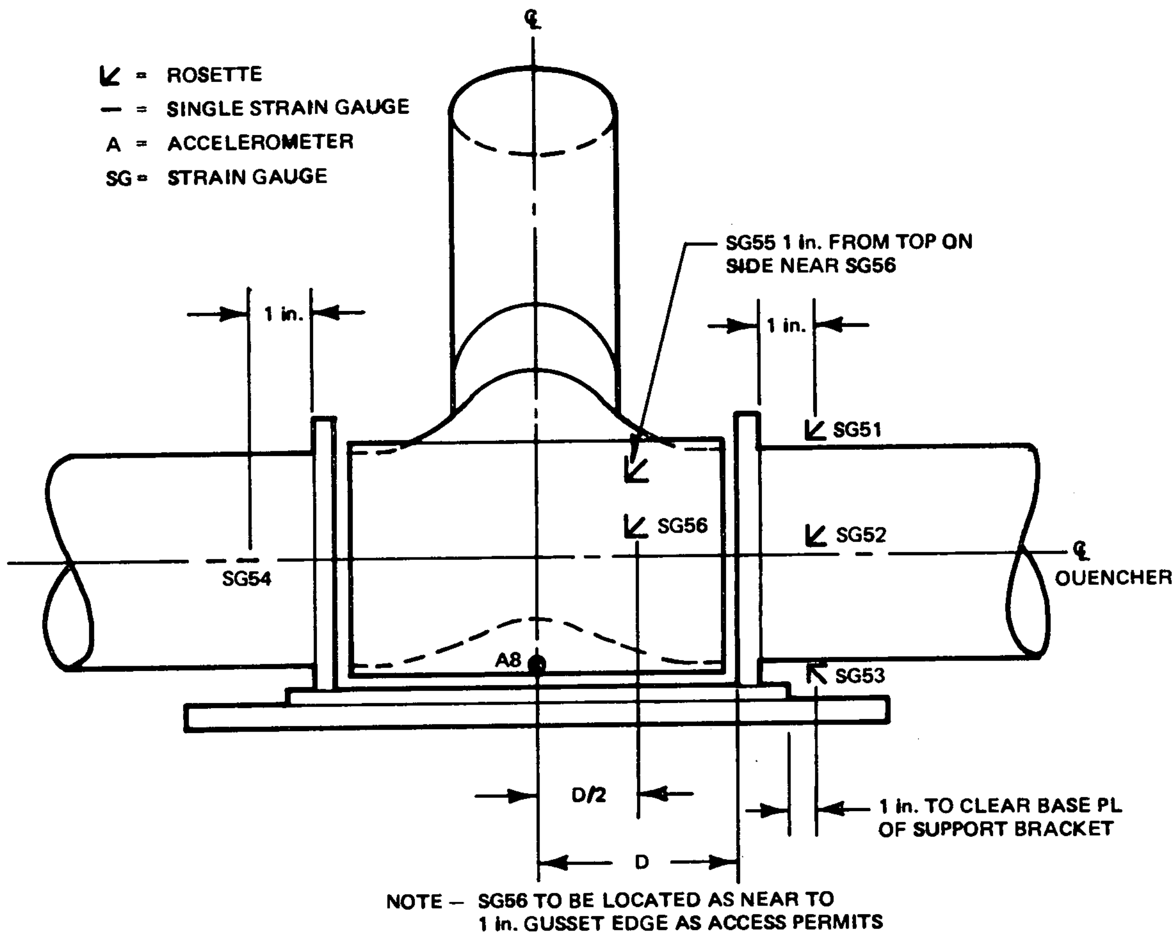

Figure 4-17. Strain Gauge Location - Quencher - Bay D

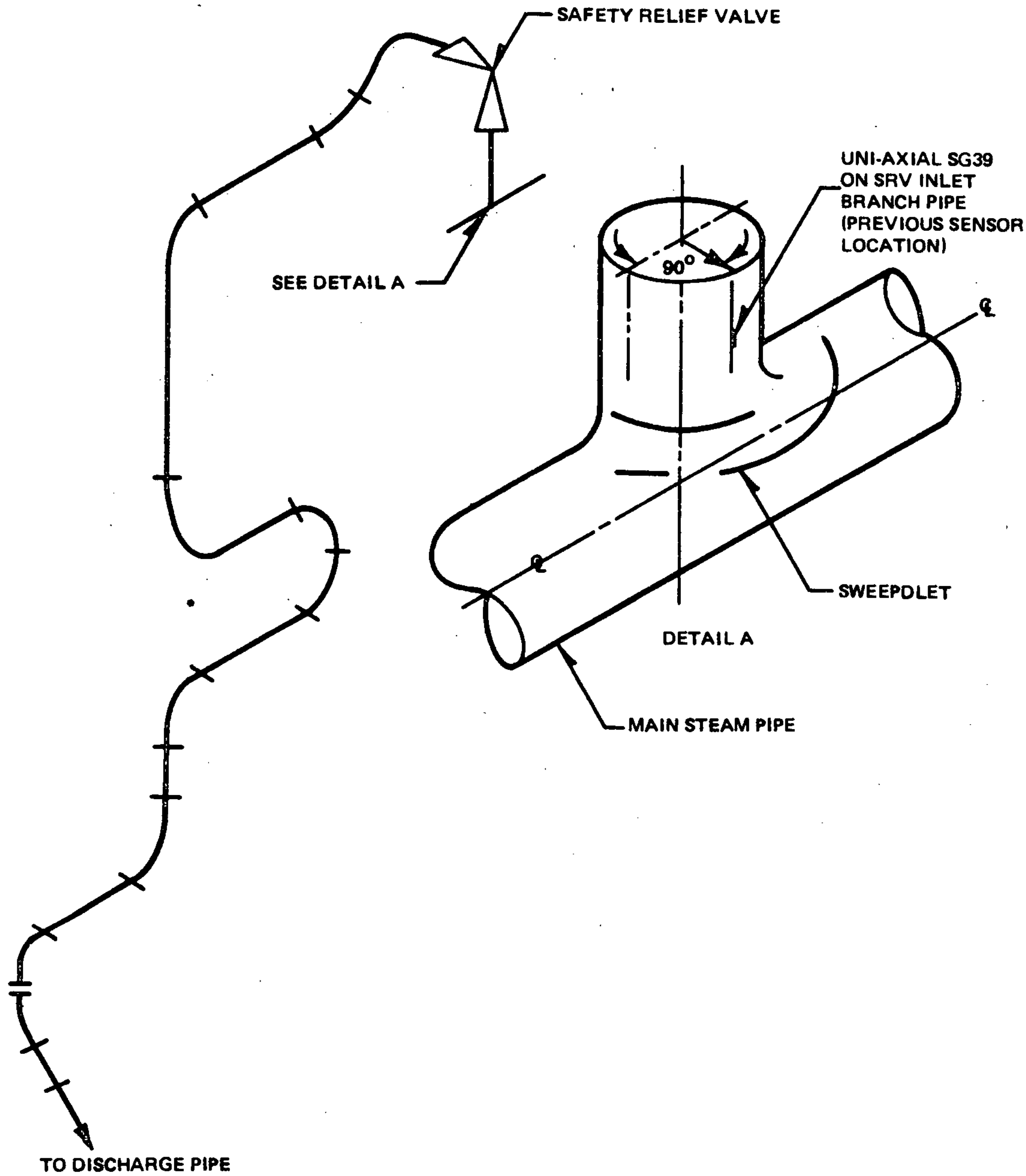

Figure 4-18. Strain Gauge Location on Upstream SRV Pipe - SRV Line A

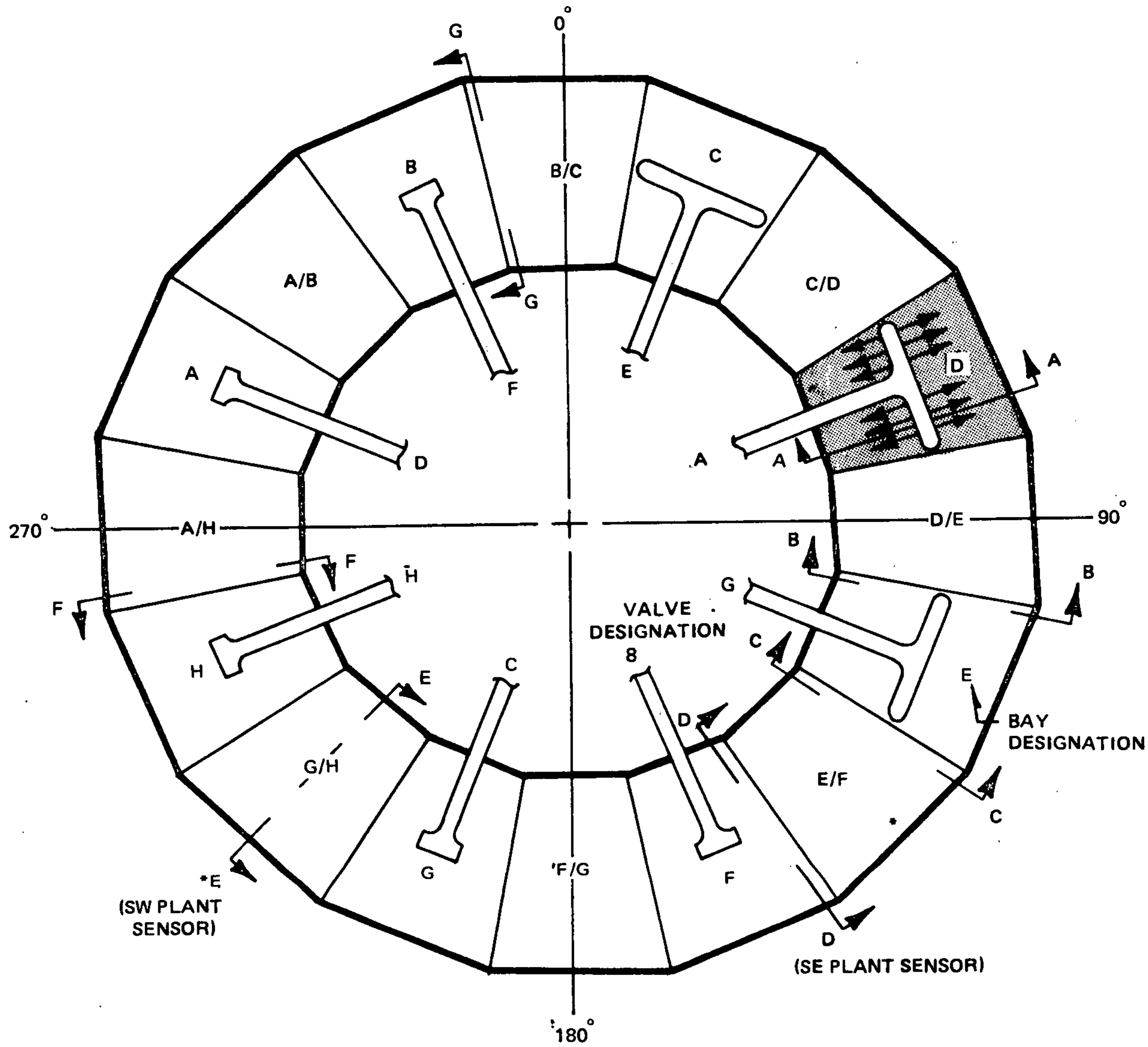

SECTIONS A-A THROUGH G-G SHOWN IN FIGURES 4-20 THROUGH 4-26.

*AZIMUTHAL LOCATIONS OF THE PLANT TEMPERATURE SENSORS

Figure 4-19. Plan View of Torus Showing Cross-Sectional Locations of Pool Temperature Instrumentation

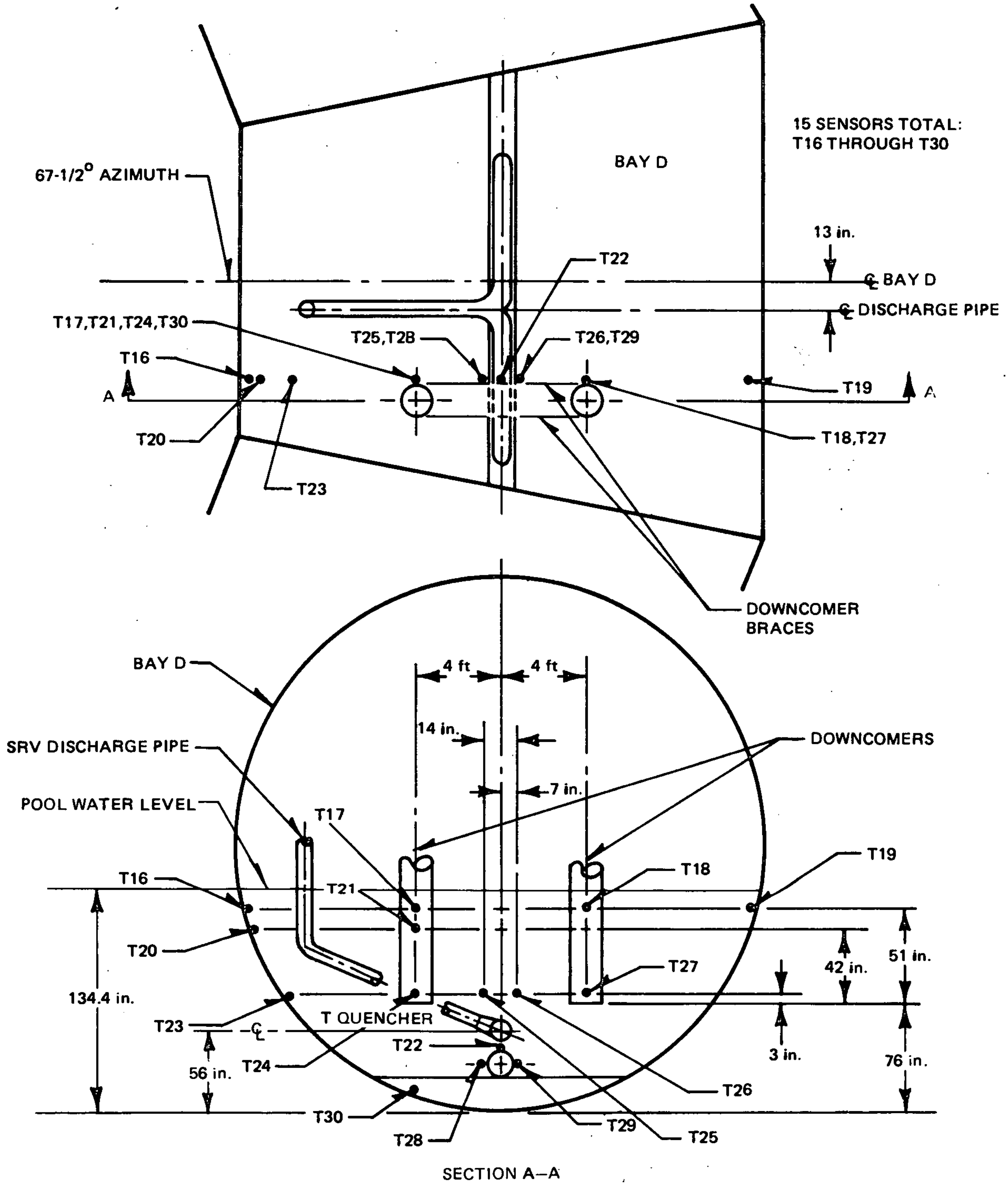

Figure 4-20. Pool Water Temperature Sensor Location - Bay D

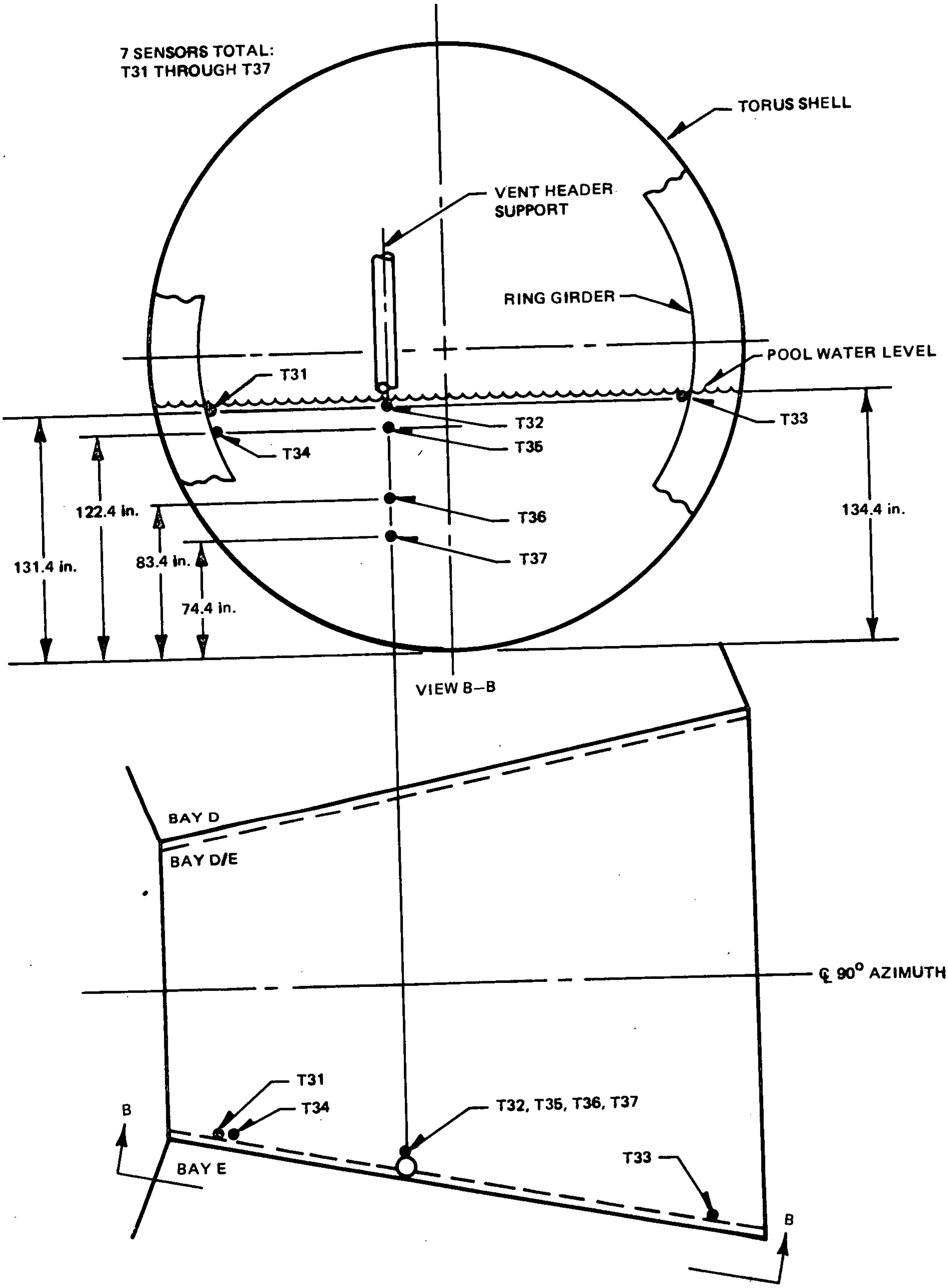

Figure 4-21. Pool Water Temperature Sensor Location - Bay D/E

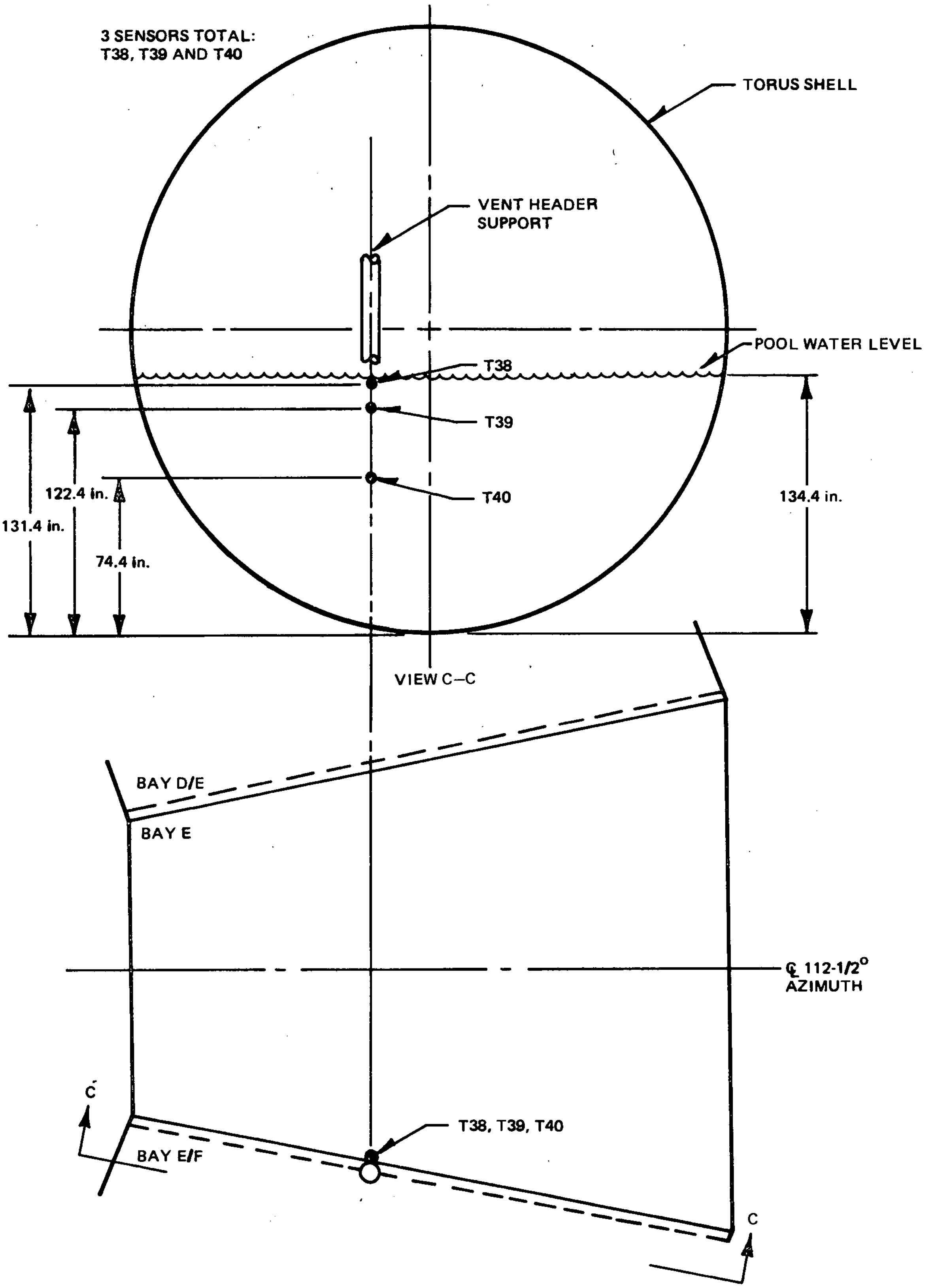

Figure 4-22. Pool Water Temperature Sensor Location - Bay E

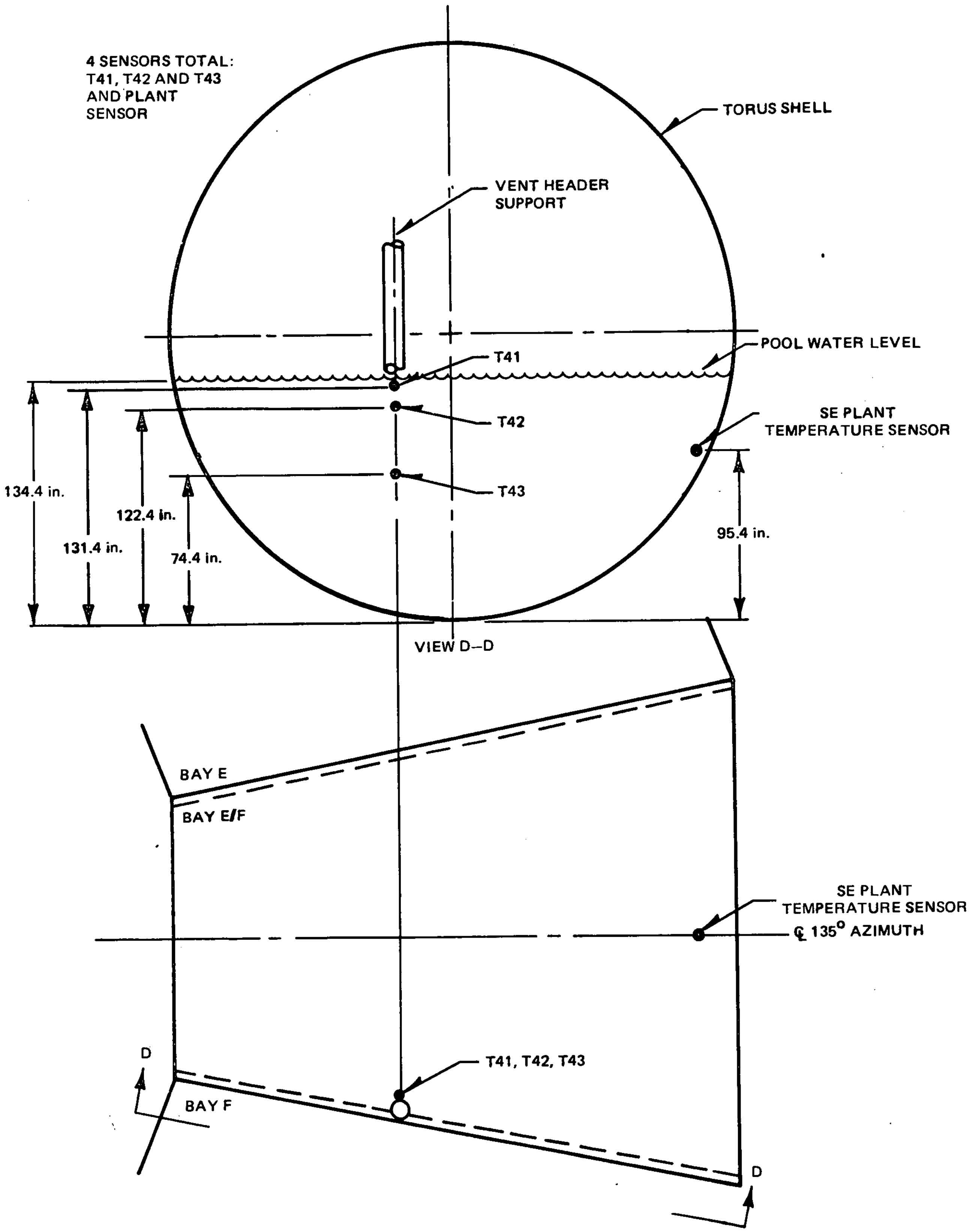

Figure 4-23. Pool Water Temperature Sensor Location - Bay E/F

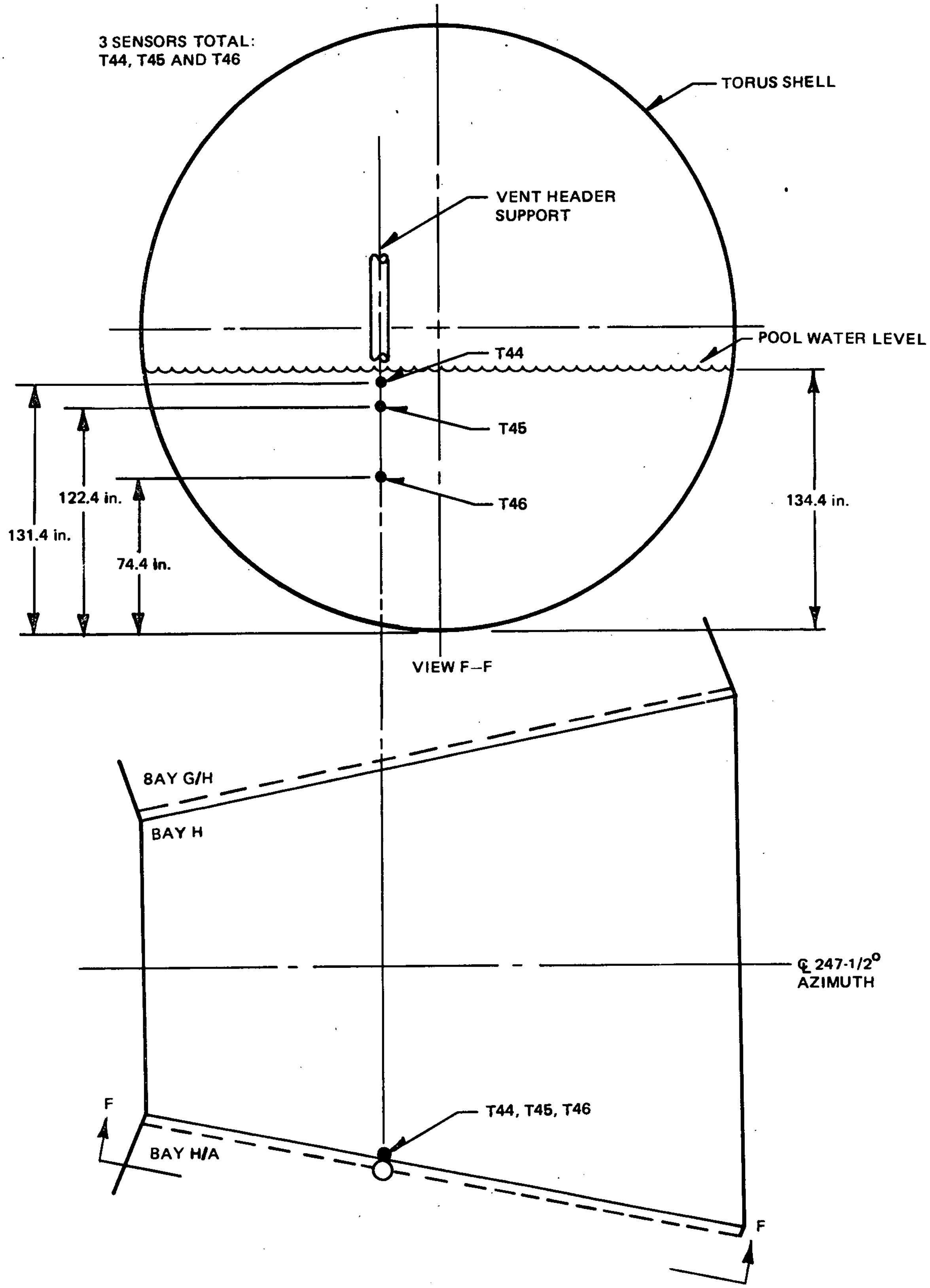

Figure 4-24. Pool Water Temperature Sensor Location - Bay H

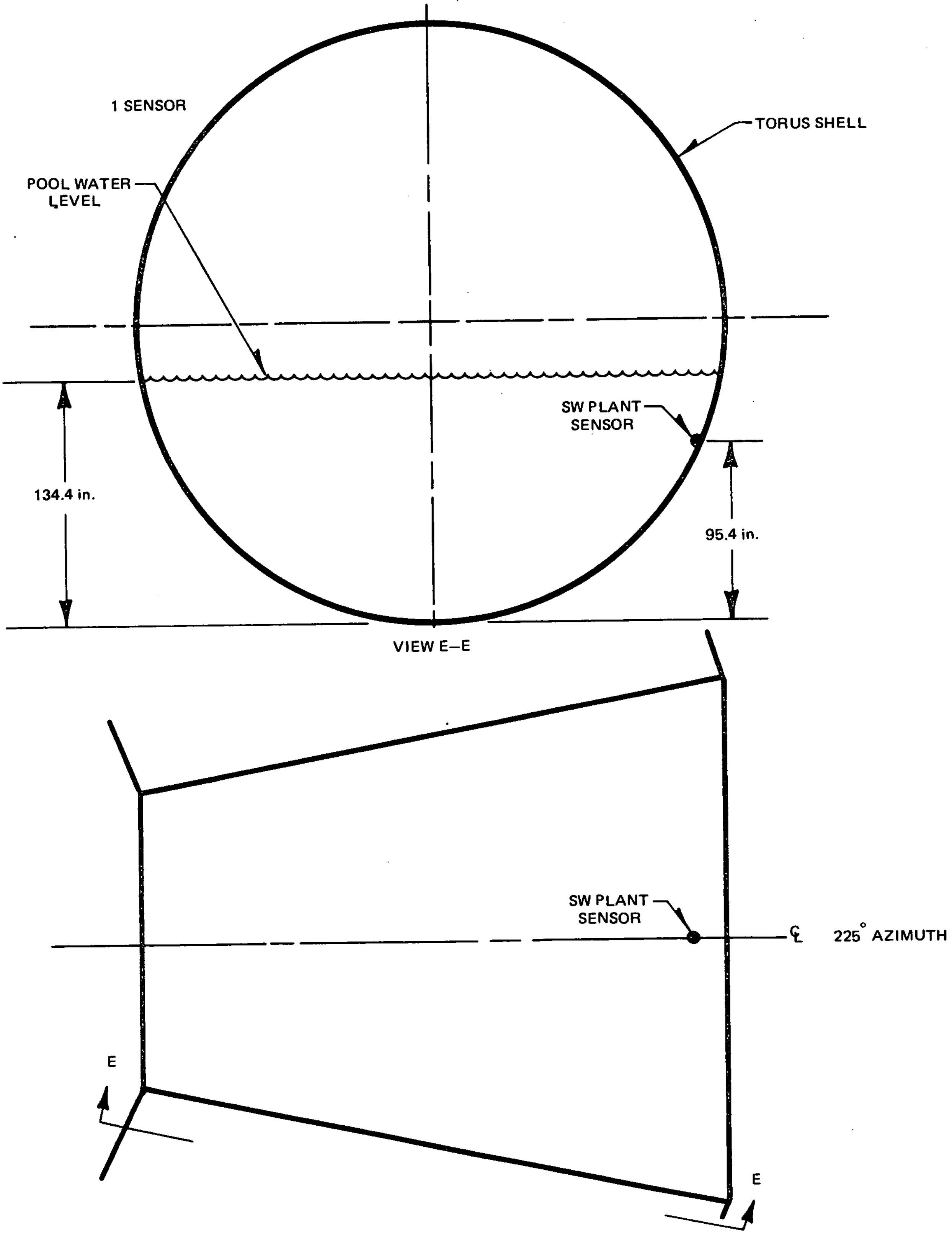

Figure 4-25. Pool Water Plant-Temperature-Sensor Location-Bay G/H

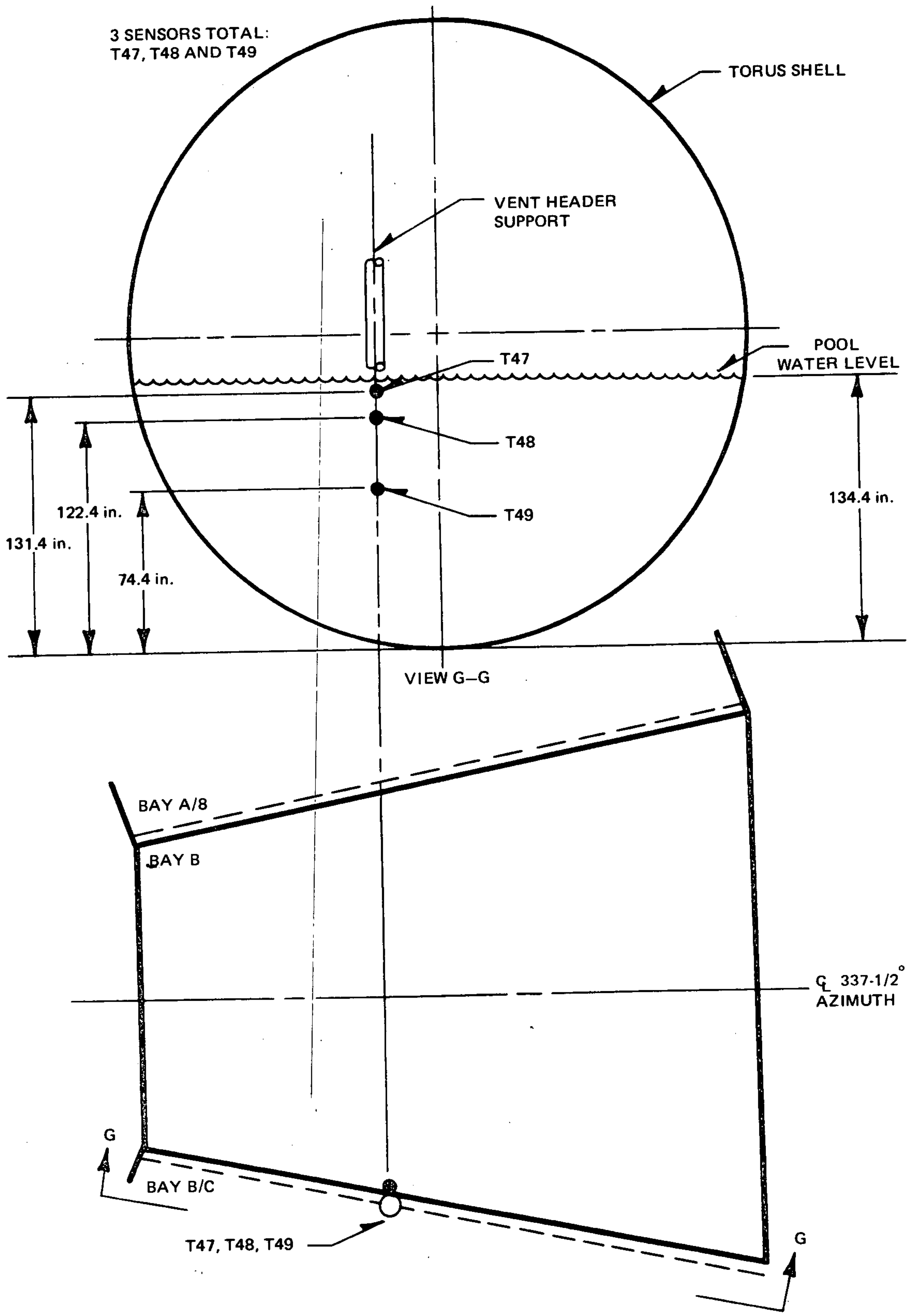

Figure 4-26. Pool Water Temperature Sensor Location - Bay B

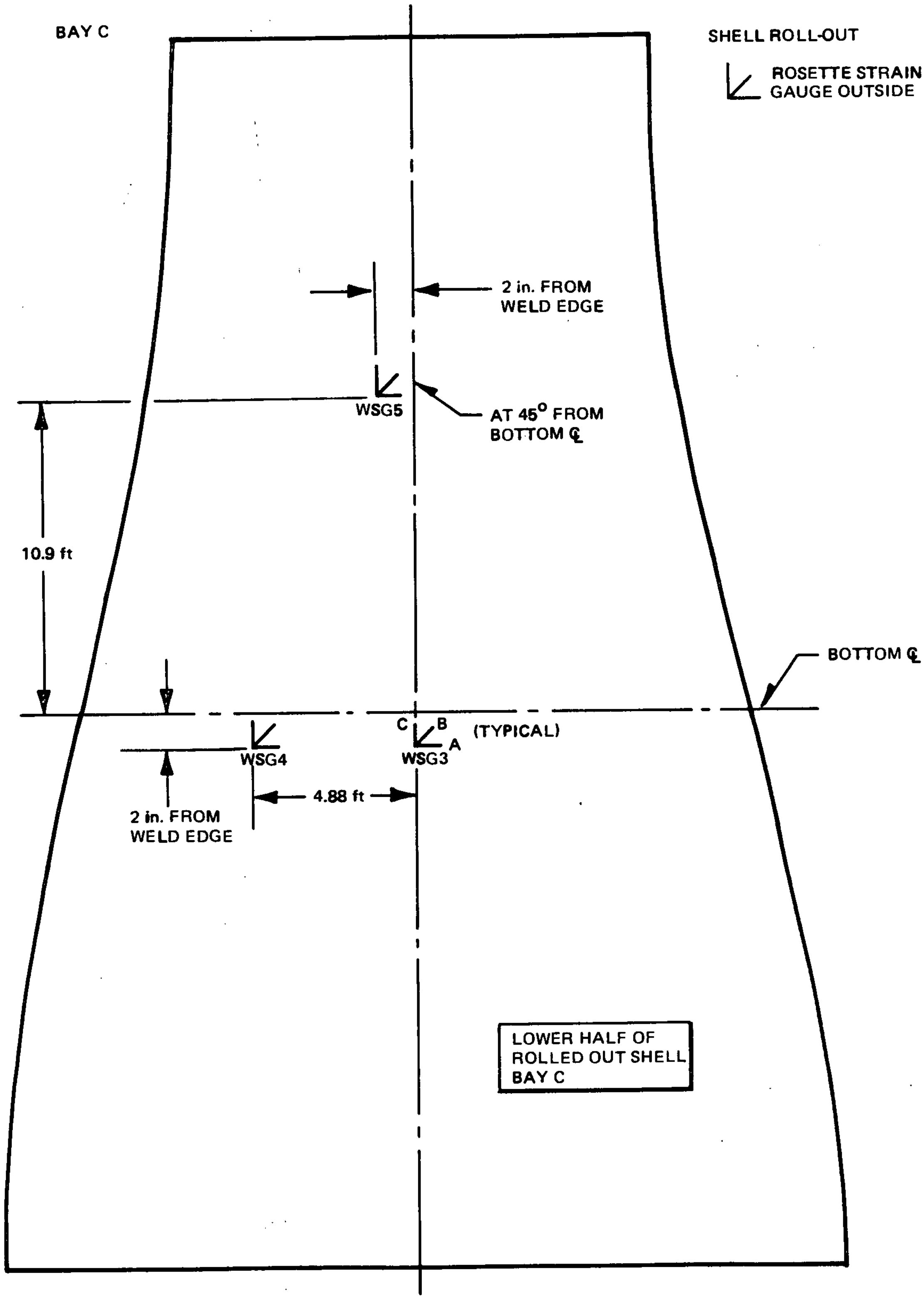

Figure 4-27. FM Tape Systems Gauge Locations - Bay C (view from inside torus looking out)

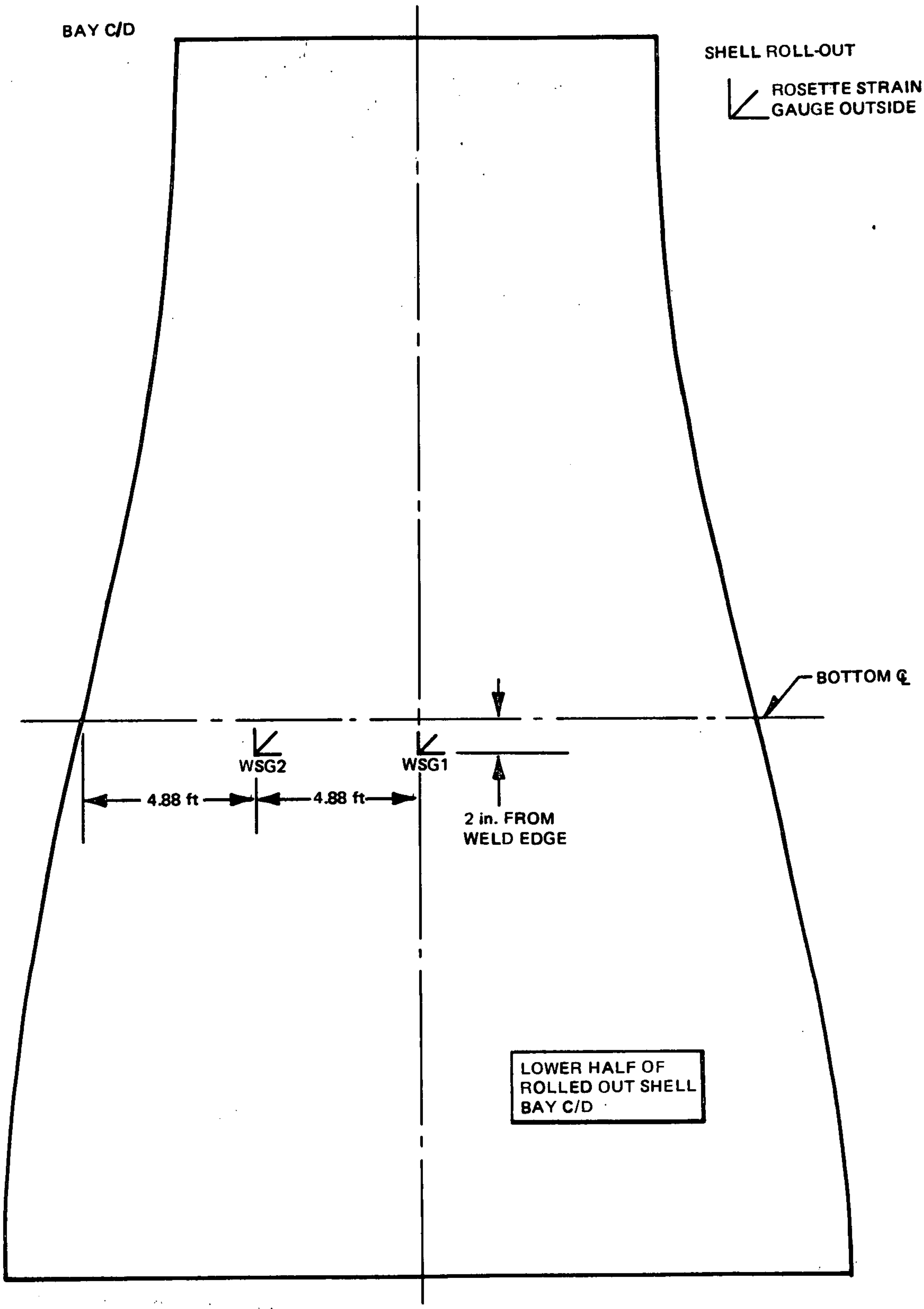

Figure 4-28. FM Tape System Gauge Locations - Bay C/D (view from inside torus looking out)

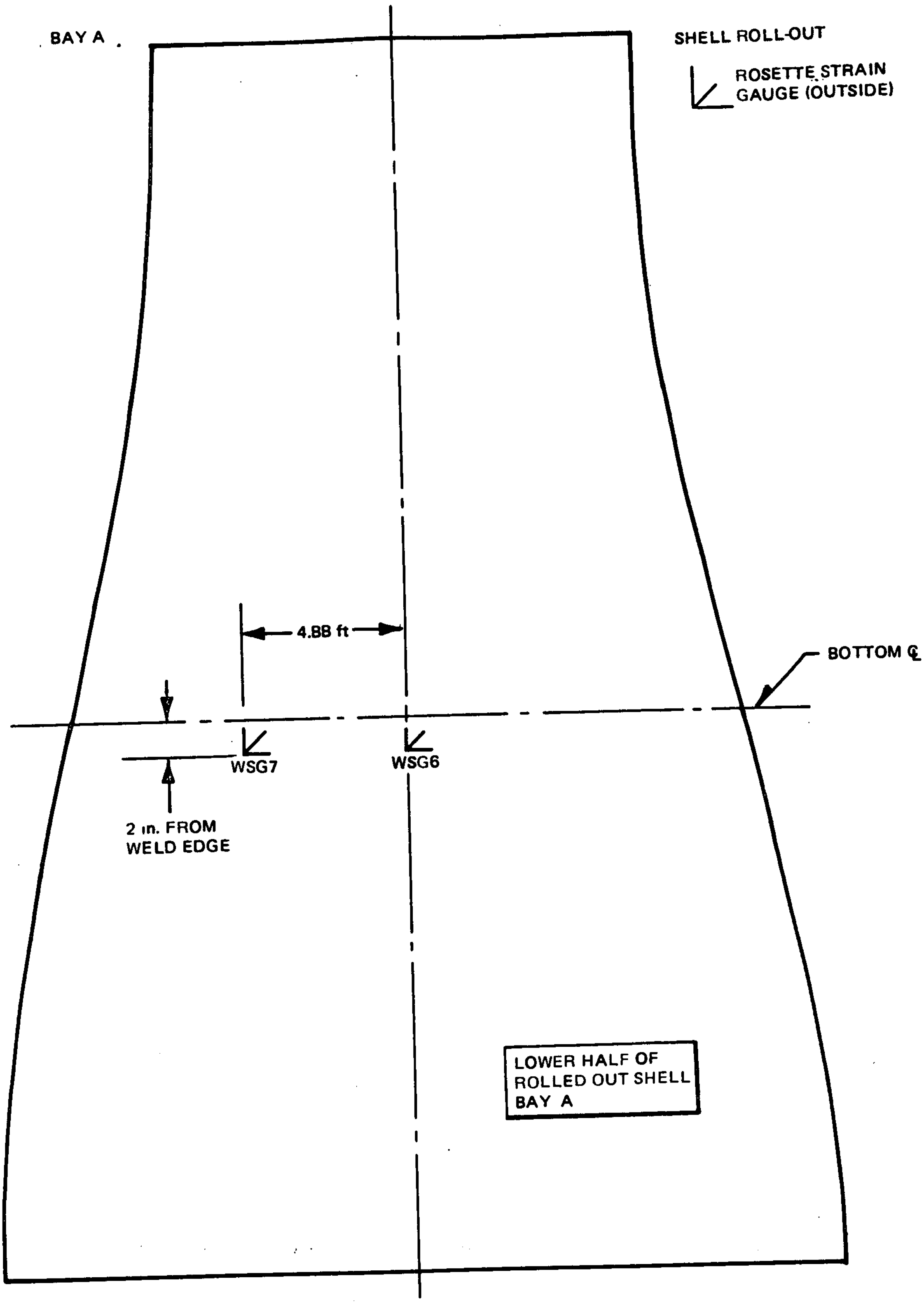

Figure 4-29. FM Tape System Gauge Locations - Bay A (view from inside torus looking out)

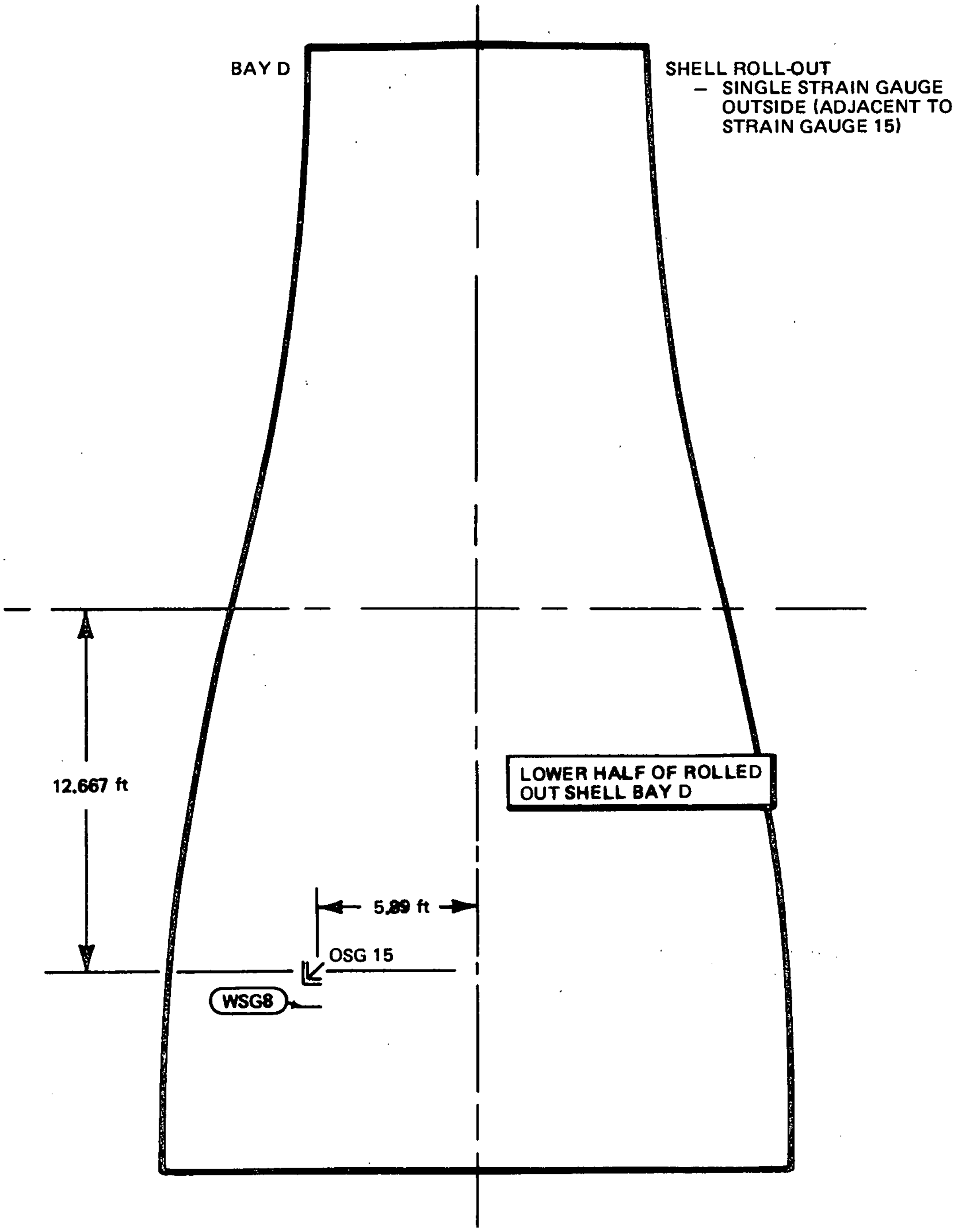

Figure 4-30. FM Tape System Gauge Location - Bay D (view from inside torus looking out)

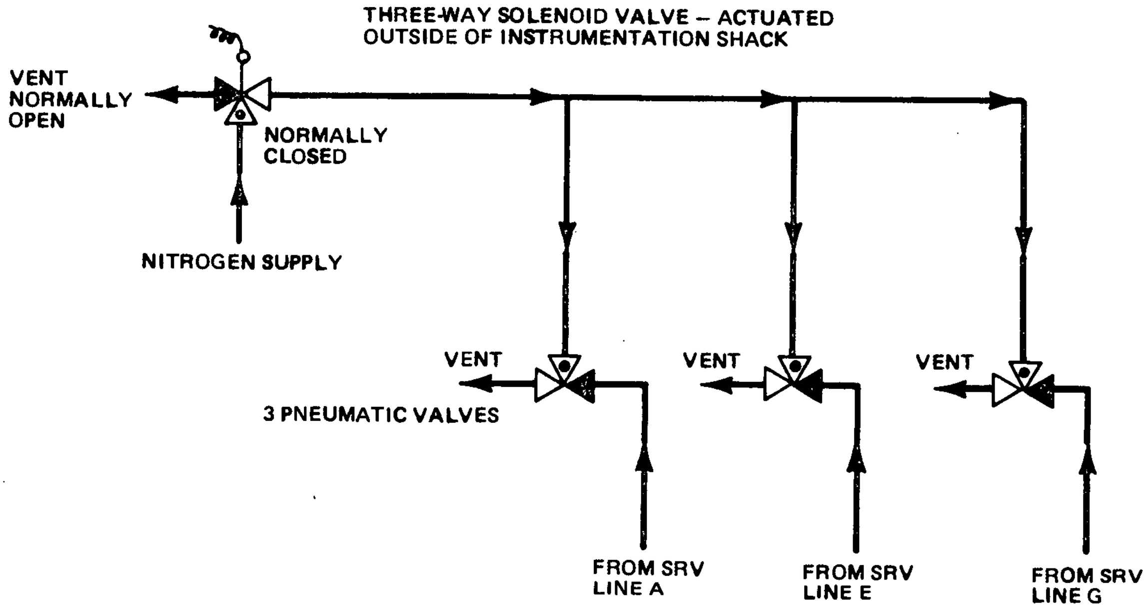

NOTES: 1. CONNECTIONS TO SRV DISCHARGE LINE ARE AT EXISTING PLANT DISCHARGE LINE THERMOCOUPLE PIPE PENETRATIONS
2. ALL DEPICTED VALVES ARE IN DRYWELL

Figure 4-31. Schematic of Vent Valves for SRV Discharge Lines A, E, and G

5. DATA ACQUISITION SYSTEMS

Three separate data acquisition systems were used for the Monticello tests (described in Section 4).

The pulse code modulation (PCM) system recorded 252 channels. A block diagram is shown in Figure 4-1; detailed specifications are given in Table 5-1.

The DS-83 temperature scanning system recorded 39 RTDs. A block diagram is given in Figure 4-2; detailed specifications are given in Table 5-2.

The FM tape system recorded 26 strain gauge channels. A block diagram is shown in Figure 4-3; detailed specifications are given in Table 5-3.

For immediate on-site decisions and for criteria comparison, 8 Brush Recorders with 48 PCM channels were provided for real-time monitoring. Table 5-4 lists these channels.

Table 5-1

PCM SYSTEM CHARACTERISTICS

1. Overall System:	Validyne MC 170 High Density Multi-Channel Modular Transducer Control System
2. Power Supply:	PS 176 Modular Oscillator
Input:	90 to 275 Vac continuous
Outputs:	AC carrier 5V rms at 3 kHz, phase-locked to 60 Hz AC input power, regulation 0.1%, 10% to 100% rated load (5 VA) ± 15 Vdc (tracking), 0.1% regulation, 10 to 100% rated load (± 500 mA)
3. Carrier Demodulator for Strain and Pressure Transducers:	
Validyne CD 173.	
Input range:	1 to 50 mV/V
Output:	± 10 Vdc
Frequency Response:	0 to 200 Hz
Non-linearity:	$\leq$±0.05% full scale
4. Temperature Sensor Model:	Validyne PT 174 constant current supply, amplifier, and filter (0 to 200 Hz)
Linearity:	Better than ±0.1% using standard RTD curves
5. Acceleration:	
Validyne PA 175	
6. Water Leg Probes:	
Validyne BA 172	
7. Multiplexer and A/D Converter:	
Preston Scientific Type GM	
Input:	0 (-10 volts produced 0 count) to +10 volts = 2048 to 4096 counts
Scan Rate:	127,000 samples per second
Output:	12-bits unipolar per sample
Format:	NRZL with zero degree clock output
8. PCM Encoder:	EMR, Inc.
9. Tape Recorder:	Sangamo Sabre III 3600

Table 5-2

DS-83 SYSTEM CHARACTERISTICS

Digital Recorder:	Validyne DS-83 (for pipe skin and pool temperature)
Input:	±10 volts for 10,000 counts
Scan Rate:	Intervals of 1, 2, 4, 10, or 20 minutes (or 1, 2, 4, 10 or 24 hrs.) Automatic 40-channel mechanical scanner
Signal Conditioning:	PT-174
Output:	On Newport Labs, Model 2000 DPM and 200B DPM
Format:	21 columns for 11 headings

Table 5-3

FM SYSTEM CHARACTERISTICS

1. Overall System:	Vishay Series 2100 Multi-Channel Modular Strain Gauge Signal Conditioning System
2. Power Supply:	Vishay 2110
Input:	107, 115, 214, 230 VAC +10% (selected internally); 50-60 Hz.
Output:	±15V at 1.2A and +17.5 V at 1.1A, all regulators current limited against overload
3. Strain Gauge Signal Conditioner:	Vishay 2120
Input:	Quarter (120 ohm and 350 ohm), half and full bridge. Dummy resistors provided for quarter bridge.
Output:	±10V (min) at 30mA; ±50 mA (min) into 150 ohm load; ±100 mA (min) into 15 ohm load. Current limit - 120 mA.
4. Tape Recorder:	Honeywell 5600, 14-channel, FM.

Table 5-4

BRUSH RECORDER CHANNELS

Recorder	Channel	Sensor	Recorder	Channel	Sensor
1	1	OSG 8C	5	1	SG 48A
	2	OSG 8B		2	SG 48C
	3	OSG 8A		3	SG 52A
	4	ISG 8C		4	SG 55A
	5	ISG 8B		5	SG 56A
	6	ISG 8A		6	SG 40
2	1	OSG 32C	6	1	SG 60
	2	ISG 32C		2	P-16
	3	OSG 33C		3	P-12
	4	ISG 33C		4	P-7
	5	SG 131		5	Hand switches RV2 - 71A
	6	SG 134		6	P2
3	1	AB-D3	7	1	T-8
	2	AB-D4		2	OT-11
	3	BB1-D4		3	OT-1
	4	BB2-D4		4	W-1
	5	A8H		5	W-4
	6	A9H		6	W-3
4	1	SG 39	8	1	P-1
	2	SG 41		2	P-49
	3	SG 43		3	P-8
	4	SG 45		4	P-9
	5	SG 47A		5	P-10
	6	SG 47C		6	P-11

6. DATA REDUCTION

Two systems were used to reduce data for the three Monticello SRV data acquisition systems. The major data reduction system was the pulse code modulation (PCM) system, which is described in Section 6.1; the other system was the FM analog system as outlined in Section 6.2. The DS-83 temperature data scan system required no reduction as it directly output tabular time history edits to an on-line printer.

6.1 PCM SYSTEM

This system processed 252 data channels recorded on the PCM tapes. The computer software programs that comprise the PCM data reduction system are described in the following subsections and a flow chart is presented in Figure 6-1.

6.1.1 PCMDC

This software program, implemented on the HP 2100 minicomputer, stores data in a formatted medium acceptable for data reduction on the H-6000 computer. The program reads the pulse coded modulation (PCM) recorded data, combines it with time information, and produces a formatted nine-track field digital magnetic tape. The PCMDC program processes one data track of the PCM tape (126 channels of data) at a time, so two passes are necessary to process all 252 channels.

6.1.2 UTILITY

This is a general software program, available on the H-6000 computer, that copies tapes. UTILITY is specifically used to generate two copies (one for backup) of the field digital magnetic tapes, the purpose of which is to save and use only tapes generated on the H-6000 computer system where the tapes can be generated and maintained in an environment suitable for magnetic tapes.

6.1.3 PPBD

This software program, implemented on the H-6000 computer, converts the data into a usable form and allows for time correlation of all 252 data channels (merge) for a given test run. Channel data are converted from HP 2100 counts to H-6000 engineering units. Two 126 data channels are merged with respect to time so that any one time frame of 252 data channels will have a common time element. This conversion and merging generates an Engineering Units (E.U.) tape which becomes the common storage medium of the test data.

6.1.4 WILDPT

This software program, implemented on the H-6000 computer, removes, identifies or defines wild points from an Engineering Units tape. It can perform a band pass removal of data points in addition to removal of specific (identified by input time and channel) data points. Data values removed by either technique will have the value of the succeeding data point. The insertion of a particular input value for the latter case is also possible. The band pass method allows input of specific band values for each channel. In particular, a band was selected arbitrarily higher than observed maxima for each and every channel. This program, in conjunction with output from the CRNCH program, can generate a "clean" modified Engineering Units tape.

Wild point identification and removal is a subjective matter. Care was taken with the specific procedures that were followed in order to maintain data integrity.

6.1.5 CRNCH

This software program, implemented on the H-6000 computer, edits and plots user-specified data channels and also provides specific calculations for editing and plotting. CRNCH also has the additional capabilities of filtering or decimating data before editing, plotting or performing specified calculations. The user specifies the time interval and the sample rate which is to be processed. CRNCH also identifies or defines potential wild points and displays calibration signals.

6.2 FM ANALOG SYSTEM

This data reduction system processes 26 channels originally recorded on FM analog tape. System components are described in the following subsections and a flow chart is presented in Figure 6-2.

6.2.1 FM Analog

This component is a 14-channel frequency modulated analog tape that records strain gauge data.

6.2.2 A/D Subsystem

This component is a 128-channel capability multiplexer for the conversion and input of analog data to XDS.

6.2.3 XDS

This is the central processing unit of the data reduction system called the "XDS Sigma 5 CPU" for the conversion of analog data to digital data. This conversion system also allows for the merging of the two analog tape recorders used in the test to synchronous digital data. The digital tapes are the product of the analog to digital conversion.

6.2.4 Software Program

This software data reduction and analysis program, implemented on the Varian Y-73 computer, edits and plots user-specified data channels and also provides defined calculations for editing and plotting.

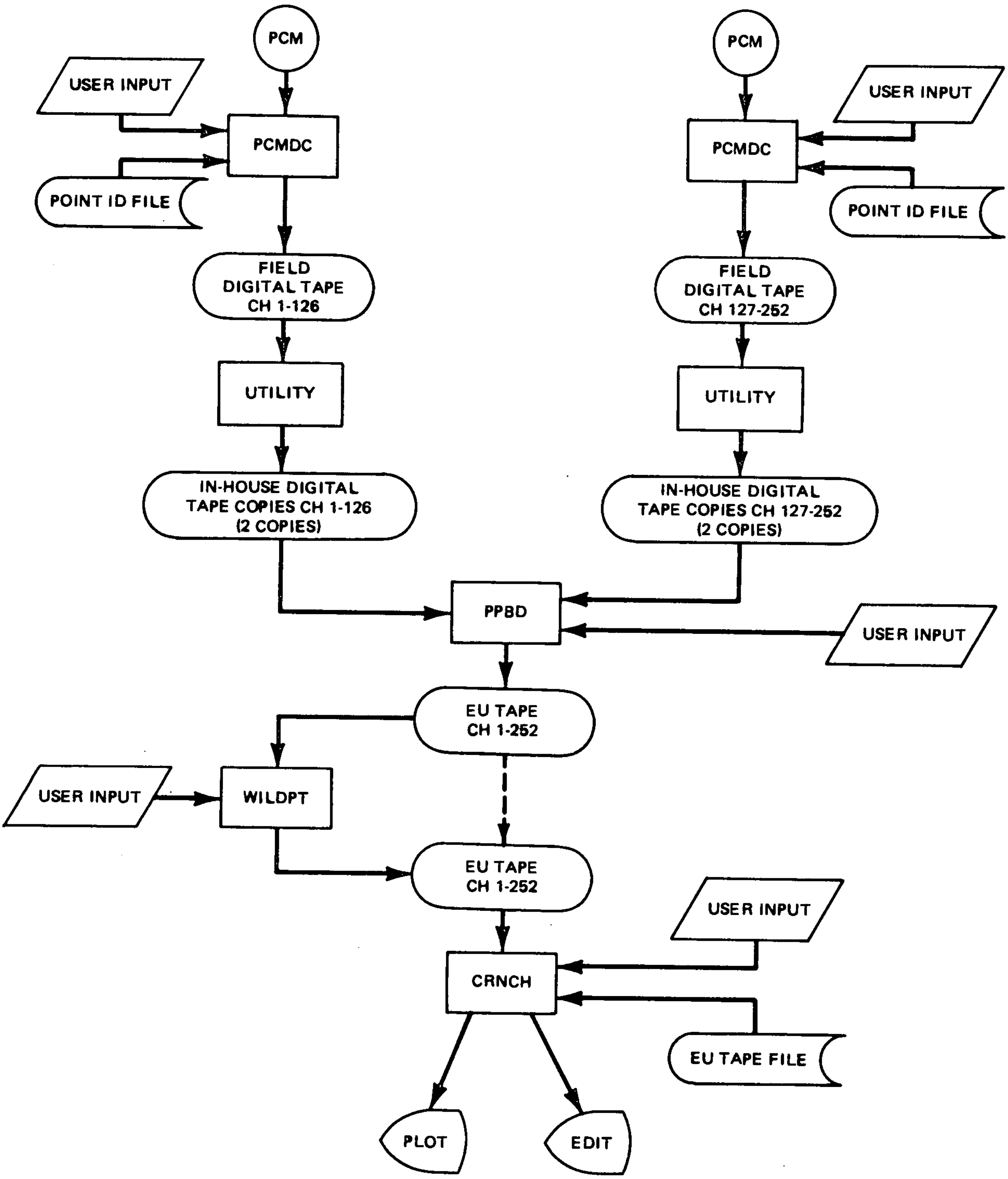

Figure 6-1. PCM Data Reduction System Block Diagram

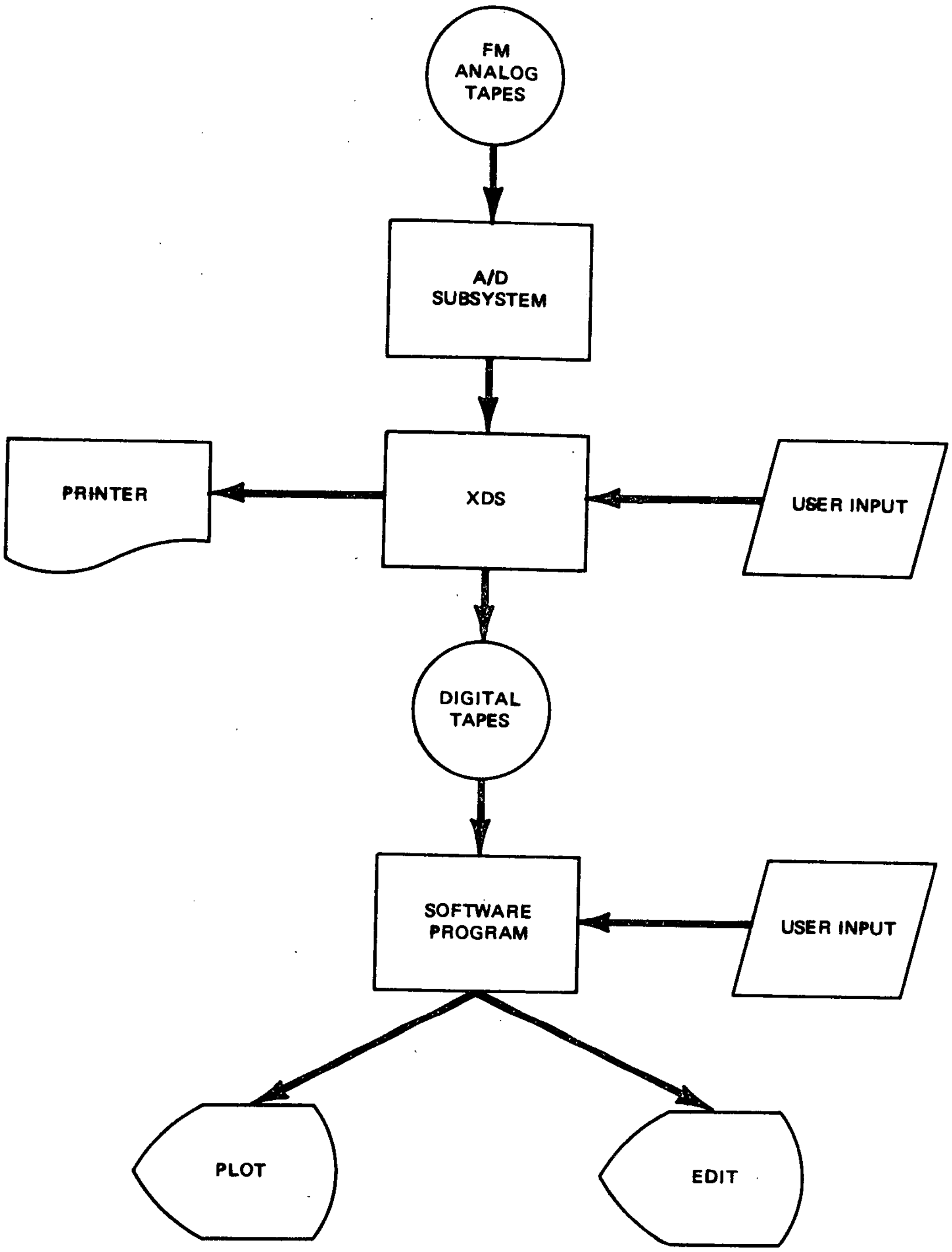

Figure 6-2. FM Analog Data Reduction System Block Diagram

7. DATA ACQUISITION AND REDUCTION SYSTEM ACCURACY EVALUATION

7.1 INTRODUCTION AND SUMMARY

This accuracy evaluation considers the various physical elements of the system and makes an estimate of the accuracy with which the final data represent the physical phenomena being measured. The evaluation is confined to the predictable tolerances based on known uncertainties. It cannot assure that every data point is within these tolerances, however. True confidence in the accuracy of the data must result from a combination of this analysis with a detailed examination of the data in context. This is especially true because of the appearance of some spurious ("wild") data points in the raw plots and edits. Both computer and manual techniques have been used to eliminate these points in the structural data, because it was desired to use the computer to list maximum values. Hydrodynamic data, however, have been scaled manually from plots, and wild points, when they occur, have been ignored through the engineering judgement of the data analyst. Examination of the data in context is necessary also to reveal unpredictable zero shifts which may affect the apparent absolute data amplitudes.

A summary of the predictable accuracy of the various transducers and systems follows. It is subdivided because of the sensitivity of the tolerances to the absolute signal levels.

System	Transducer	Conditions	Probable Maximum Variation from True Value
PCM	Weldable strain gauges	data = 2.8 KSI	±6%
	Column loads	data = 90 KIPS	±11%
	Temperatures	all	±2°F
	Pressures	See section 7.5	
	Accelerations	See section 7.5	
DS-83	RTD	All	±2°F
FM	Foil strain gauges	All	±2%

The tolerances assigned in this table to the weldable strain gage data result primarily from the digitizing resolution of approximately 5 microstrain per count. For data less than the values given in the table, the resolution, and thus the accuracy, will degrade.

The discussions which follow present an overview of the information presented in Appendix B.

7.2 SINGLE GAUGE STRAIN DATA

The following elements contribute to uncertainty in the Monticello strain gauge data:

a. Gauge factor
b. Gauge resistance
c. Signal conditioning accuracy
d. PCM conversion resolution

The first two elements contributed errors applicable to data of any magnitude, but the effects of the second two varied with magnitude. For example, a raw strain signal presented in the data as 50 microstrain was derived from an electrical signal whose relationship to true strain depended on gauge factor, known only to ±3 percent according to the strain gauge manufacturer. Another 1 percent uncertainty lay in the gauge, completion resistor, and calibration resistor tolerances. These uncertainties can be applied to all strain data. Signal conditioning accuracy becomes important for small signals, however, because the accuracy is normally quoted as a percentage of a full-scale signal. Thus, an output accurate to ±0.1 percent of full scale is known only to ±1 percent at 10 percent of full scale. The last contribution to strain data inaccuracy is the resolution of the PCM conversion, which is about 5 microstrain per count. A signal given as 50 microstrain in the output table or plot may be between 50 and 55 microstrain, a 10 percent uncertainty.

For single-gauge data (including rosettes, since each element was recorded separately), the ±5 microstrain tolerance is the most important uncertainty up to a strain level of about 160 microstrain, at which level the gauge factor uncertainty becomes controlling for weldable gauges. The gauge factor of the foil gauges is known more accurately, so the digitizing resolution is controlling for all foil gauge data.

In summary, weldable strain data is known at best to ±6 percent, and this tolerance broadens as the signal level decreases.

7.3 STRAIN DATA (COLUMN AXIAL LOAD AND BENDING BRIDGES)

The initial calculation of calibration strain value of the column axial and bending bridges did not account for the resistance of the wire connecting the signal conditioning equipment to the bridges. The test was run, therefore, with scale factors known to need adjustment. The correction was made in the data reduction process by modifying the appropriate slope and intercept values in the Engineering Unit Channel Description.

The PCM digitizing resolution was a source of uncertainty in the column data because of the low strain signals. For example, in Test 2, the largest axial strain reported (AB-D2) was -43.7 microstrain. With a conversion factor of 1.418 per microstrain to KIPS of axial load, and a least step of 6.3352 microstrain per count for this transducer, the resulting least step was 8.89 KIPS per digitizing step, or an uncertainty of about 20 percent in the answer. In Test 2304, transducer AB-D4 had a reported maximum value of 59 KIPS, which may, in fact, have been as high as about 68 KIPS or 15 percent higher. For this column, the conversion was 1.624 KIPS per microstrain, and the microstrain/count slope was 6.0329.

The reason for this coarse resolution on small strains is a decision concerning the voltage-to-microstrain conversion factor early in the system design process. Because the strains which would be generated at each strain gage location by each test in the matrix could not be calculated accurately in advance, the conservative approach required an allowance for possible high strains at the risk of poor resolution on low strains. The conversion factor was established, therefore, at 1.0 volt output (or one-tenth of digitizer full scale) per 1,000 microstrain (about 30,000 psi).

To estimate the accuracy of the column data, therefore, the absolute level of the data must be examined with respect to the resolution. For load data of 90 KIPS, for example, the digitizing resolution accounts for a tolerance of ±11 percent.

7.4 WELDABLE VS FOIL GAUGES

Weldable gauges are different from foil gauges in their lengths and tolerances on gauge factor. Gauge lengths are 3/4 inch and 1/4 inch, and the tolerances on gauge factor are 3 percent and 0.5 percent, respectively. The difference in gauge length is important in a region of stress gradient, such as a transition to a nozzle, for example. The strain gauges used in the T-Quencher test were generally not in such regions, except for SG32 and 33. The only place where a foil gauge was placed next to a weldable gauge was WSG-8 next to OSG-15C. The low levels of strain, however, made it difficult to compare their relative performances, because for this case the resolution tolerance on the PCM data is about 20 percent.

7.5 OTHER TRANSDUCERS

7.5.1 Accelerometers

Data from the accelerometer on the quencher support could not be reconciled with other data on a physical basis, and is considered not to be an accurate measurement (see section 10.6 for further discussion). The accelerometers on the torus shell (A1 - A7) provided data consistent with local strain data, and at a reasonable proportion of their full-scale ranges. Their basic accuracy is stated as ±1% of reading.

7.5.2 Pressure Transducers

Some zero shifts were noted on the SRV air bubble pressure data, and their consequences are noted in Section 8.2.2. Maximum dynamic pressures can be determined from the data by ignoring the zero shift. The relatively low pressures measured compared with the full-scale range of the transducers (100 psi) magnify inaccuracies as a percentage of the actual measurement. That is, the basic linearity of the transducer (± 0.5% full-scale) is 0.5 psi. Measurements below 5 psi, therefore, have an absolute value uncertainty of at least 10 percent plus any uncorrected zero shift. Pulse heights relative to initial readings are substantially more accurate since zero drift errors are essentially eliminated.

SRV pipe pressures were measured by transducers having full-scale ranges of 1,000 psi. Applying the same linearity figure, a tolerance of ± 5 psi must be assigned. Since the significant measurements were over 100 psi, these data are accurate to better than 5 percent.

7.5.3 Temperature Sensors

The basic limitation on the absolute accuracy of data from RTDs is the ±2°F tolerance on the basic temperature/resistance characteristic plus limits on the system signal conditioning calibration.

7.6 OTHER SYSTEM ELEMENTS

Appendix B presents a detailed discussion of the signal conditioning, digitizing, recording, and computer systems, and also the calibration methods used. The various equipment elements are capable of excellent performance by themselves. Degradation of potential overall system performance is the result of the digitizing resolution (mentioned above), and constraints on the playback speed of the PCM tape. This latter factor is believed to be the main contributor of spurious ("wild") data points, which were eliminated (or ignored) through a combination of computer analysis and manual techniques.

8. DISCUSSION OF HYDRODYNAMIC AND THERMODYNAMIC RESULTS

8.1 INTRODUCTION

Hydrodynamic and thermodynamic data from the Monticello Safety/Relief Valve (SRV) Discharge Test (T-Quencher) Program are presented in this section. These data include pressure loading measured within the torus pool, on the torus shell, and within the SRV discharge line and T-Quencher arms. Also measured were SRV pipe temperature, torus pool temperature, air flow through the SRV discharge line vacuum breaker valve, and water reflood into the SRV line following SRV closure. Locations of instrumentation used to record these parameters are presented in Figures 4-4 through 4-8 and 4-19 through 4-26. Information on specific instrumentation characteristics is presented in Section 4 and Appendix A. The signal conditioning and data acquisition system characteristics are described in Section 5. A detailed test matrix and a table of test initial conditions are presented in Section 3.

8.2 DATA REDUCTION AND EVALUATION METHODS

8.2.1 Data Sampling Rates

The data acquisition system used to record the hydrodynamic data taken during the test sampled and recorded data at 1-millisecond intervals.* Most hydrodynamic data (e.g., SRV pipe and torus shell pressures) were reduced at this rate. Data that did not require such high resolution (e.g., some pipe temperature and water level sensor measurements) were reduced at greater time intervals.

* Some pool and pipe temperature measurements were made by a separate data acquisition system which sampled at 1- or 2-min intervals.

8.2.2 Zero Shifts in Pressure Measurements

On some pressure sensor data, a zero shift occurred between the initial and final values of the base line or zero signal (i.e., before and after each SRV discharge). Such zero shifts are not the result of the phenomenon being measured but rather can be attributed to possible ground potential changes and/or thermal effects on pressure sensor measurements.

In general, the torus shell pressure measurements were free of zero shifts. The maximum zero shift recorded for a torus shell sensor was 0.6 psid. No zero shifts were noted in the SRV discharge line and T-Quencher pressure data. The SRV air bubble pressure data had zero shifts no greater than 1.6 psid.

Torus shell and pool pressures due to SRV air bubble oscillation have been tabulated in the appendices. These values were read from data plots assuming that the initial zero or base line was valid throughout the SRV air bubble oscillation phase of the transient. Therefore, the torus shell data as tabulated have a possible zero shift error of ±0.6 psid and the SRV air bubble pressures have errors of ± 1.6 psid, at most.

Steam condensation pressures in the pool and on the torus shell were read from data plots as peak to peak values without regard to the value of the base line. Therefore, the steam condensation pressures reported should include no zero shift error.

8.2.3 Manual Filtering of SRV Pipe Pressure Data

The pressure data recorded near the SRV in the SRV discharge line contained high frequency (approx. 200 Hz) oscillations superimposed on the primary pressure transient. These oscillations are attributed to vibration of the SRV line in this region and perturbations in the flow as it passed the pressure sensor. The peak and steady state pressures reported for these sensors were read from data plots as the mean value of this oscillation to obtain the bulk pressurization of the line. This method is considered accurate to ± 15 psi.

Reading the SRV pipe pressure data directly; i.e., including the high frequency oscillations, would result in measurements as much as 5 percent higher than those reported.

8.2.4 Superposition of Steam Condensation and Air Bubble Oscillation Pressures

After the SRV air bubble has been expelled into the torus pool, steam from the SRV is discharged through the T-Quencher device. As the steam is discharged, low magnitude (±0.5 psid), high frequency (∿ 150 Hz), pressures are produced on the torus shell. Therefore, during the SRV air bubble oscillation phase these high frequency pressure oscillations are superimposed on the torus shell and pool pressures resulting from air bubble oscillation. Magnitudes of torus pool and shell pressures due to SRV air bubble oscillation reported here include both the steam condensation and air bubble oscillation components of the pressure loading.

8.3 SRV PIPE AND T-QUENCHER PRESSURE

8.3.1 Description of the Phenomena

SRV Operation

Figures 8-1A and 8-1B present cross-sectional schematics of the safety/relief valve tested in the closed and open conditions, respectively. This valve can be actuated by two methods. The first is by an electrical signal to a solenoid which admits plant air to the region above the remote air actuator (A in Figure 8-1A). The air actuator is then stroked downward, depressing the second stage piston and likewise the second stage disk. The downward motion of the second stage disk allows the initial high pressure (approximately 1000 psia) steam in region B, Figure 8-1A, to bleed through the "pilot valve and main piston discharge line", "C" in Figure 8-1B, into the SRV discharge line. As the steam is bled from region "B" this volume depressurizes, allowing the 1000 psia pressure below the main valve piston, "D" in Figure 8-1A, to overcome the downward force exerted by the main valve preload spring as well as that exerted by pressure in the SRV inlet on the top of the main valve disk, "E" in Figure 8-1A. This results in the upward stroke of the main valve disk, and the SRV is opened, (see Figure 8-1B). This was the method used to open the SRV during the test program.

The second method is to actuate the SRV on set pressure. When an overpressure occurs in the main steam line (at inlet to the SRV), it is sensed in the pilot sensing port, "F" in Figure 8-1A, and results in a movement of the pilot stage disc, "G" in Figure 8-1A, to the left. This allows steam in the pilot sensing port to enter the region above the second stage piston, "H" in Figure 8-1A, resulting of a downward stroke of the second stage piston and likewise the second stage disc. The remaining steps in the opening process are identical to the first method.

When the SRV opening sequence is initiated by either method described above, the steam in region "B" plus any that flows through the main valve piston orifice, "I" in Figure 8-1A, and any that flows past the main valve piston rings, is bled into the SRV discharge line prior to main disc opening. This bleeding of steam before valve opening results in a prepressurization of the SRV line to a low pressure (approximately 4 psig). As a result of this prepressurization, the water slug in the SRV line is pushed downward (approximately 2 ft) and accelerated to a velocity of approximately 7 ft/sec before the SRV opens.

<u>Pressure Loading in the SRVDL and T-Quencher</u>

When the SRV main disk opens, the pressure within the SRV line undergoes an additional pressure transient before reaching a steady state value. Transient pressure waves travel back and forth in the line as the pressure continues to increase until the inertia of the water initially in the submerged portion of piping is overcome. During the water clearing transient, the pressure within the T-Quencher arms also reaches a maximum value. Following expulsion of the water slug, the peak pressure in the SRV discharge line decreases to a steady state value which is a function of SRV steam flowrate and friction along the pipe wall upstream of the entrance to the T-Quencher. The T-Quencher pressure likewise decreases to a steady state value which is a function of steam flowrate and pressure losses through the holes in the T-Quencher arms.

8.3.2 Instrumentation and Test Data Summary

Eight pressure transducers were mounted along the SRV discharge line (SRVDL) and within the T-Quencher (SRV line RV2-71A) to record the pipe and T-Quencher pressure transients, (sensors P1-P7 and P49, Figure 4-6). Table 8-1 presents peak SRV pipe and T-Quencher pressures for various test conditions. In addition, this table presents the means and standard deviations of these pressures for each condition tested.

A tabulation of peak and steady state pressures measured in the SRV pipe and T-Quencher arms for all tests is presented in Appendix C. Representative plots of SRV pipe and T-Quencher pressure are presented in Appendix E.

8.3.3 Results

As discussed in subsection 8.3.1, a small amount of steam was bled into the SRV line before each SRV opening. This resulted in a prepressurization of the line and a depression of the water leg before each test. Evidence of this discharge line prepressurization and the resulting depression of the water leg is presented in Figure 8-2. Note that sensor P49 (11 ft upstream of the initial air/water interface) measured approximately 4 psig before the primary pressure wave (indicating opening of the SRV main disc) reached this sensor. Note also that water leg sensors W5 (3 in.

below the normal water level) and W1 (1.5 ft below NWL) showed step changes before the primary pressure wave reached the air/water interface; i.e., before sensor P5 recorded a step increase in pressure. This indicates that for the test shown in the figure, the water leg had been depressed at least 1.5 ft before there was any indication at the air/water interface that the SRV had opened. Estimates of the position and downward velocity of the air/water interface following prepressurization (before the arrival of the primary pressure wave) have been made using water level and SRV line pressure data in combination with an analytical line clearing model.* These estimates are provided in Table 3-2, which presents detailed test initial conditions.

The highest measured SRV discharge line pressure during the test program was 300 psig, recorded nine ft downstream of the SRV during a hot pipe, elevated water leg test (test 2305). For the elevated water level tests, an attempt was made to time the consecutive SRV actuations so the valve would open during the initial reflood (following the previous actuation) and while the water leg was above its normal value. When the primary pressure wave (resulting from SRV main disc opening) reached the air/water interface in test 2305, the water leg was approximately above the normal water level and had an upward velocity of approximately /sec.

The maximum pressure measured within the T-Quencher was psid, recorded during a test similar to that described above (test 2306). In general, the peak pressure recorded in the T-Quencher was characterized by a short duration spike which occurred during the water clearing transient. Specifically, the psid pressure spike had a magnitude greater than psid for less than milliseconds. Figure 8-3 presents an example of the pressures measured in the SRV discharge line and T-Quencher during test 2306.

The steady state pressure measured just downstream of the SRV was approximately psig for all tests. Since this is well below 53 percent of the driving pressure (1000 psia), the SRV was choked during all discharges.

* This model is documented in the General Electric Company report NEDE-23739.

In addition, the steady state pressure within the T-Quencher was between psid. Since this is well below 53 percent of the steady pressure occurring just upstream of the entrance to the T-Quencher (120 psig),* the SRV flow was choked at the entrance to the T-Quencher also.

Therefore, the replacement of the ramshead with the T-Quencher device had no adverse effect on either SRV flow or steady state backpressure at the valve.

8.4 SRV DISCHARGE LINE WATER REFLOOD

8.4.1 Description of the Phenomena

Following SRV closure, steam within the line condenses on the interface of the water slug as it reenters the line through the T-Quencher. This condensation lowers the pressure in the line rapidly, causing the water to reflood into the T-Quencher and piping and the SRV line vacuum breaker valve (VB) to open, allowing air to enter the line. The inflowing air, together with residual steam and/or steam produced at the air/water interface caused by contact with the hot pipe, repressurizes the SRV line. The line will repressurize to a value somewhat above drywell pressure for the 8-in. vacuum breaker used. For the 8-in. vacuum breaker, the line may overfill with air during the initial reflood transient and stabilize at a water leg significantly below its normal value.

*No measurement of steady pressure just upstream of the T-Quencher was made; however, a value of 120 psig was recorded during the Monticello Ramshead Test (NEDC-21581) just upstream of the ramshead. No change in this pressure would be expected with a T-Quencher unless the flow resistance through the quencher holes was excessive. In such a case this pressure would be greater than 120 psig, and the T-Quencher pressure would still be less than 53% of this value.

8.4.2 Instrumentation and Test Data Summary

Four conductivity probes were mounted in the SRV discharge line RV2-71A to record the water reflood transient (sensors W1, W3, W4, and W5, Figure 4-6). In addition to these sensors, seven temperature sensors (T1, T3, OT1, T6, T7, OT11, and T8, Figure 4-6) were mounted within the SRV line and acted as water position sensing devices. Two pressure sensors (P3 and P49, Figure 4-6) were also mounted in the line to provide information on the reflood transient. Sensor P3 accurately measured the absolute pressure in the line in the range of 0 - 25 psia. Sensor P49 accurately measured the difference in pressure between the SRVDL and the drywell in the range of 2 to psid. This information, combined with measurements from plant instrumentation of drywell to wetwell pressure difference and drywell pressure, allowed determination of the position of the air/water interface in the SRV line after the initial reflood transient.

Figure 8-4 presents a sample data plot for the conductivity and pipe temperature sensors during the initial reflood following test 2. As shown in this figure, the slopes of the temperature sensor traces change as the air/water interface rises above the temperature sensors. Likewise, there is a step conductivity change in the water level sensor measurements as the interface rises above or falls below these probes. These traces and knowledge of the location of each sensor were used to determine the approximate water level in the pipe during the initial reflood transient. After the initial reflood and following the first downward oscillation of the water leg, the approximate location of the air/water interface was determined by evaluation of data from sensor P49. Figure 8-5 presents the data from this sensor for test 2. Note that after the initial reflood the pressure in the SRV line oscillated about a value above that of the drywell.* This indicates the water level in the line was oscillating about a point below its normal value. The pressure in the line, as measured by P49, was used with the ideal gas law to estimate the water leg position as a function of time after the initial reflood and after the vacuum breaker valve had closed.

---

*The drywell to wetwell pressure differential was never more than 0.03 psid.

8.4.3 Results

Water level sensing instrumentation (temperature and conductivity probes) were located at various points along the SRV discharge line. These devices recorded only whether they were in contact with water or air. Therefore, for a given initial reflood transient, the only definitive statement that can be made is that the maximum reflood occurred between two sensor locations. Table 8-2 presents the regions along the line in which the maximum refloods were known to occur. These regions are bounded below by a sensor that recorded water contact and above by a sensor that did not. In addition, Table 8-2 presents estimates of the time at which the peak reflood occurred referenced to the closure of the SRV main disc.

Figures 8-6 and 8-7 present representative plots of water reflood versus time. Figure 8-7 also shows the timing of vacuum breaker opening during the transient.

In general, the water reflood transient was characterized by an initial reflood from beyond the normal water leg* followed by a drop to a position approximately below the normal water leg with oscillations about that point of approximately plus or minus This secondary oscillation damped out quickly and was negligible within sec after the SRV was closed.

The maximum reflood measured was between and ft beyond NWL and occurred approximately sec after the closure of the SRV main disc. The reflood had dropped below NWL within sec of valve closure for all tests.

*The normal water leg during this test was 13.3 feet.

8.5 SRV PIPE HEATING/COOLING

8.5.1 Description of the Phenomena

When an SRV actuates, high pressure and temperature steam enters the line. The SRV pipe will then be heated to some maximum temperature which is dependent on the duration of discharge and the maximum steady state steam pressure in the line. Following valve closure, the SRV pipe will begin to cool by natural convection and radiation to the drywell and wetwell air space and will eventually reach its initial steady state temperature.

8.5.2 Instrumentation and Test Data Summary

Five temperature sensors were mounted on the outside of the SRV discharge line (T11 - T15, Figure 4-8). The data for these sensors were recorded in a printed paper tape format by a data acquisition system which recorded data at one or two minute intervals.

8.5.3 Results

The maximum pipe temperature recorded during the test program was , reached following a series of discharges with a total discharge time of seconds. Figure 8-8 presents the pipe heatup and cooldown transients as measured on the pipe exterior at various locations along the pipe wall for test 2. The SRV was discharged for approximately seconds during this test. Note that the pipe temperature had reached a steady state temperature within approximately following valve closure.

8.6 SRV DISCHARGE AIR BUBBLE CHARACTERISTICS

8.6.1 Description of the Phenomena

As the initial air/steam mixture in the SRV discharge line is expelled through the holes in the T-Quencher device, several bubbles* form in the

*Due to the geometry of the T-Quencher (see Figure 1-1) several bubbles are formed initially. These bubbles may coalesce into one or two larger bubbles as they rise to the pool surface.

pool and oscillate as they rise to the pool surface. As initial conditions vary, these bubble oscillations result in pressure loading on the torus shell of varying magnitude, frequency, and duration. In addition, these bubble oscillations create velocity and acceleration fields in the pool, which result in drag loads on submerged structures.

The maximum pressures attained within the air/steam bubbles resulting from SRV discharge are directly related to the rate at which the initial air/steam mixture in the SRV discharge line is discharged into the torus pool. Therefore, the T-Quencher was designed to effect a gradual discharge of the air/steam mixture to the pool. This was accomplished by the use of a graduated hole pattern in the T-Quencher arms which increases in density with distance from the ramshead fitting. In addition, the discharge of the mixture through small holes (see Figure 1-2) results in excellent heat transfer to the pool water. Therefore, the majority of the initial steam in the air/steam mixture is condensed before bubble formation.

During the initial SRV discharge, the line is heated to approximately within sec. When the valve closes, steam in the line begins to condense on the interface of water reentering the line, rapidly lowering the pressure in the pipe. Suppression pool water is then drawn up the SRV line and when the SRVDL to drywell ΔP reaches 0.2 psig (VB set point), the SRV line vacuum breaker valve opens, allowing air in the drywell to enter the pipe. If the SRV is reopened shortly after the first actuation, the resulting SRV air bubble pressures are lower than in the cold pipe, first actuation case. This is because the line has a high steam partial pressure and a reduced air mass prior to a consecutive actuation. As this mixture is expelled through the T-Quencher holes, the steam partial pressure is largely removed as the steam condenses before bubble formation. Therefore, since for a given pipe geometry, the bubble pressure is proportional to the air mass, consecutive actuations result in lower peak bubble pressures than do first actuations, even though with the higher pipe temperatures less steam condenses on the walls during the transient.

8.6.2 Instrumentation and Test Data Summary

Four pressure sensors (P8-P11, Figure 4-6) were installed on the T-Quencher mid-arm supports to record SRV air bubble pressures. Data from these sensors were evaluated using a computer program to plot the difference in pressure across the T-Quencher arms as a function of time during the air bubble oscillation transient.

Peak SRV discharge air bubble pressures for various test conditions and means and standard deviations of these data are presented in Table 8-1.

Peak positive and negative air bubble pressures measured, and peak differences across each arm, are presented in Appendix D for all tests.

8.6.3 Results

Figure 8-9 presents representative SRV air bubble pressure traces for test 801. This was a cold pipe, normal water leg test (single valve actuation) and resulted in the highest pressure loading on the torus shell. Note that the peak positive and negative pressures recorded by sensors P9 and P11 (sensors closer to the reactor pressure vessel) were approximately twice as high as those measured on the opposite side of the T-Quencher arms by sensors P8 and P10. This asymmetry was confirmed by the spatial pressure distribution measured on the torus shell and was repeated consistently throughout the test. In addition, sensor P9 generally read somewhat higher than did sensor P11.

Figure 8-10 presents the SRV air bubble pressures as measured by sensor P9 for various test conditions. Note that on hot pipe tests, when there was less air in the line initially, the bubble pressures are less regular in shape and have lower peak magnitudes than do those resulting from cold pipe tests. The high frequency pressure oscillations recorded during the initial portion of the bubble pressure transients for hot pipe tests are attributed to steam condensation from the bubbles, since on these tests the bubbles would be expected to have a much higher steam content than in the cold pipe tests.

The highest measured bubble pressures were and psid. The positive psid pressure was recorded by sensor P9 during Test 2303 (cold pipe, normal water leg, multiple valve actuation). The negative psid pressure resulted from a hot pipe, elevated water leg test (Test 2306), recorded by P8 and P11.

8.6.4 Air Bubble Pressure Differential Across the T-Quencher Arms

Figure 8-11 presents plots of the pressure differentials across each T-Quencher arm (i.e., P11-P10 and P9-P8) for Test 801. Test 801 was a cold pipe, normal water leg test which resulted in the highest pressures recorded on the torus shell. The maximum pressure differentials across a T-Quencher arm were and psid. The positive sign means that the force is directed away from the reactor. These positive and negative peak pressure differentials were recorded during Tests 2303 and 2306, respectively.

SRV Air Bubble Frequency

The general shape of the SRV air bubble pressure transient was followed by the pressure measurements on the torus shell. See subsection 8.7.3 for a discussion of frequency of the torus shell pressures due to SRV air bubble oscillation.

*On two tests (901 and 2306) singular, extremely short duration pressure spikes (less than 3 milliseconds) were recorded. These pressure spikes had magnitudes of 31.6 and 14.0 psid, respectively. Plots presenting these pressure spikes are presented in Appendix E2. In neither of these tests were the effects of these pressure spikes felt by pressure sensors on the torus shell.

8.7 TORUS SHELL PRESSURES RESULTING FROM SRV AIR BUBBLE OSCILLATION

8.7.1 Description of the Phenomena

The air bubble pressure loading phenomenon is described in subsection 8.6.1. The bubble pressures produced by this phenomenon attenuate with distance from the outer radii of each bubble to the submerged portion of the torus shell. At a given point on the torus shell the resulting pressure is a function of the attenuated pressures occurring from each bubble at that instant in time. This functional relationship is determined by the effects of surrounding free surfaces and pool boundaries.

8.7.2 Instrumentation and Test Data Summary

Thirty-four pressure sensors (P12-P46, Figures 4-4 and 4-5) were mounted on the submerged portion of the torus shell. Sensor P44 failed before the beginning of the test program. Evaluation of calibration data indicates that the calibration of sensors P25, P28, and P32 drifted more than 5 percent during the test. Therefore, data for sensors P44, P25, P28, and P32 are not presented. All other shell pressure sensors functioned normally throughout the test. Peak positive and negative pressures measured by these sensors, means, standard deviations, and frequencies of these data for each test condition are presented in Appendix D.

8.7.3 Results

Figures 8-12A and B present torus shell pressure plots for the sensor that recorded the highest shell pressure in the test bay (Bay D) for various test conditions. The highest shell pressures measured were psid. These pressures resulted from a single valve actuation (SVA) under cold pipe (CP), normal water leg (NWL) conditions, (test 801). Torus shell pressures resulting from all hot pipe tests were lower than those resulting from cold pipe, single valve actuations. The hot pipe tests were single valve actuations and were performed with initially depressed, normal, and slightly elevated water legs in the SRV discharge line.

Multiple valve actuations (3 adjacent valves, valves A, E, and G) were performed under cold pipe conditions. These tests resulted in maximum shell pressures no greater than those resulting from single valve actuations under the same conditions. Table 8-1 presents the highest peak positive and peak negative pressures as measured by P12 and P16 for various test conditions. In addition, mean and standard deviations are provided for the different test conditions.

Spatial Pressure Distribution on the Torus Shell

Figure 8-13 presents the measured pressure distribution on the torus shell along the torus longitudinal axis for the single and multiple valve actuations (MVA) which resulted in the highest pressure loadings on the shell, Tests 801 and 2301, respectively. Note that the pressure loading resulting from a single valve actuation attenuated to approximately psid in the region of the adjacent discharge device. Note also that the pressure distribution resulting from the single valve actuation bounded that resulting from the multiple valve actuation everywhere except in the region approximately midway between the T-Quenchers. This is as expected, since the pressure loadings from each device are approximately of equal magnitude in this region.

Figures 8-14 through 8-18 present the pressure distributions for tests 801 and 2301 at the cross-sectional locations shown in Figure 8-13.

8.7.4 Frequencies of Torus Shell Loadings Due to SRV Air Bubble Oscillation

Table 8-3 presents a summary of the frequencies of the pressure loads on the torus shell resulting from SRV air bubble oscillation for various test conditions. The frequencies reported were determined by taking the inverse of the time periods between successive positive pressure peaks. In general, hot pipe tests resulted in somewhat higher frequencies than did cold pipe tests. In addition, the frequency generally increased slightly from the initial cycle to latter cycles.

Shell frequencies ranged from for cold pipe tests, to from for hot pipe tests. Bubble pressure (P9) frequencies and torus pressure (P16) frequencies are tabulated in Appendix D for the first six cycles for all tests.

8.8 TORUS SHELL PRESSURES DUE TO STEAM CONDENSATION

8.8.1 Description of the Phenomena

Following expulsion of the initial air/steam mixture in the SRV discharge line during an SRV discharge, a steady flow of steam (approximately 200 lbm/sec, corresponding to a reactor pressure of 1000 psia) flows through the T-Quencher holes. As this steam is condensed within the pool, high frequency, low magnitude pressure loads on the torus shell result. Appendix J describes the methods used to evaluate the SRV flowrate.

8.8.2 Instrumentation and Test Data Summary

The instrumentation used to record the steam condensation pressures on the torus shell and within the pool during the T-Quencher discharge were the same as previously discussed in subsections 8.6.2 and 8.7.2.

Plots of steam condensation pressures measured by all pool and shell pressure sensors at local pool temperatures of approximately 50 and 115°F are presented in Appendix E3.

8.8.3 Results

An extended SRV discharge through the T-Quencher in Bay D was performed to determine the pool thermal mixing characteristics of a T-Quencher device, (test 24). During this test, which lasted approximately 6.5 minutes, steam condensation pressures were recorded both near the T-Quencher exit and on the torus shell over a local pool temperature range of from 50 to 115°F.

Figure 8-19 presents a plot of peak to peak shell pressures recorded both near the T-Quencher discharge and on the torus shell as a function of pool temperature in the bay of discharge. Note that the peak to peak shell pressure at a temperature of was less than psid. Also presented in Figure 8-19 are sample plots of the steam condensation pressures measured both in the pool near the T-Quencher and on the torus shell at a local pool temperature of 115°F.

The measured frequencies of the pressure oscillations resulting from SRV steam condensation on the torus shell ranged from approximately to Hz. Steam condensation pressure frequencies and magnitudes increased as pool temperature increased from 50°F to 115°F. The highest pressure measured when the pool temperature was was psid peak to peak. The highest pressure measured at pool temperature of was psid, peak to peak.

In addition to the extended discharge described above, a shakedown test was performed before the test program at a reactor pressure of 155 psia. The SRV flow rate during this test was approximately 30 lbm/sec and the pool temperature was approximately 70°F. Figure 8-20 presents the pressure transients recorded near the T-Quencher exit (P9) and on the torus shell (P24 and P30) for this test. Note that no discernible steam condensation pressures were recorded.

8.9 POOL THERMAL MIXING

8.9.1 Description of the Phenomena

During steady flow of an SRV (at full reactor pressure), steam flows at a rate of approximately 200 lbm/sec into the suppression pool. The methods used to evaluate the SRV steam flow rate are presented in Appendix J. As this energy is added to the local area of a T-Quencher device, convective currents and momentum imparted to the pool water from the inflowing steam result in a circulation of pool water into and out of the test bay. This circulation increases in intensity until a steady state difference in the bulk pool and local bay temperatures is established. When this equilibrium condition is reached, the energy input into the test bay through the T-Quencher is equal to the energy flowing out of the bay via pool circulation. At equilibrium, the bulk pool and local bay heatup rates are approximately equal.

8.9.2 Instrumentation and Test Data Summary

Thirty-four temperature sensors (T16-T49, figures 4-19 to 4-26) were installed throughout the torus pool to record the pool heatup transient. In addition, data from two plant temperature sensors (Figures 4-23 and 4-25) were recorded.

Data for sensors T16-T49 were recorded at one- or two-minute intervals by a data acquisition system whose output was in a printed paper tape format.

Data from pool temperature sensors T31, T33, and T29 indicate that these sensors were not functioning properly. Sensor T29 recorded a temperature of 20°F while the remaining sensors indicated the pool temperature was 50°F. Sensors T31 and T33 showed little response during the extended discharges (unlike numerous sensors near by), indicating that they were possibly above the pool surface; therefore, data for these sensors are not reported. Plots of pool temperature versus time for the remaining sensors for both extended SRV discharge tests are provided in Appendix E4.

8.9.3 Results

Two extended SRV discharge tests through a T-Quencher device were performed. The first test (Test 24) was performed without the RHR System in operation. The second test was similar to Test 24 except that one loop of the RHR System was in operation throughout the test. The RHR system was in the recirculation mode (no cooling) for this test to determine the possible effect of pool motion induced by RHR operation on the thermal mixing characteristics of the T-Quencher.

Before each extended SRV blowdown test the pool was cooled using both RHR loops to a uniform temperature of approximately 50°F. The initial conditions for each test were then set; i.e., RHR was turned off for the test without RHR, and one of the RHR loops was switched to the recirculation mode and the other loop turned off for the test with RHR. A waiting period of at least 50 minutes occurred before test initiation to allow any residual pool motion resulting from previous RHR operation to damp out. After the waiting period, the SRV was actuated and allowed to continue discharging until the average test bay temperature exceeded 110°F. For both tests, the calculated bulk pool temperature remained below 80°F.

Figure 8-21 presents the RHR discharge and suction nozzle locations relative to that of the T-Quencher tested. For the test performed with RHR, the loop containing pumps A and C was used. As a result, water was discharged into the pool at 299° azimuth and suction was taken from the pool at the four locations shown in the figure.

Figure 8-22 presents the measured "average test Bay D" to "calculated bulk" pool temperature difference as a function of time for both extended SRV discharge tests (with and without RHR operation).* Note that the maximum bulk to local temperature differences were 38 and 43°F for the tests with and without RHR, respectively. The calculated bulk pool heatup was based on an SRV flow of 200 lbm/sec. The range of SRV flow was estimated to be from 200 to 226 lbm/sec. If 226 lbm/sec were used for the SRV flow rate, the slopes of the calculated bulk temperatures would increase by 13% and smaller (by 3 to 4°F) bulk to local temperature differences would be obtained. A description of how the SRV flow range was calculated from the test data is presented in Appendix J.

During both SRV extended blowdown tests the pool heatup was most evident in the direction of Bay B, relative to the discharge device location (see Figures 8-23 and 8-25). This phenomenon is attributed to residual pool motion resulting from the previous operation of both RHR loops. The 50-min waiting period discussed earlier was not sufficient to allow complete dissipation of all residual pool motion.

*"Average test Bay D temperature" is the average value measured by Sensors T17, T25, and T28 located as shown in Figure 4-20. "Calculated bulk pool temperature" is that calculated given a known energy input and assuming uniform energy dissipation throughout the pool water.

During the SRV discharge, the temperature distribution within the test bay was fairly uniform, with a maximum difference in temperature from sensor to sensor of only 12°F for both tests (with and without RHR).

In the extended discharge test performed without RHR, the hot water throughout the torus pool quickly rose to the surface following SRV closure, resulting in significant vertical thermal stratification (see Figure 8-24). Thirteen minutes after SRV closure the temperature variation from the pool surface to the torus bottom was ~52°F as can be seen by comparing Figures E.4-1 and E.4-4. Figure E.4-1 shows the data from the sensors closest to the pool surface, while Figure E4-4 presents the data from the sensors closest to the pool bottom, for the bay in which the temperature variation occurred.

Following some initial stratification after valve closure, for the test performed with one RHR loop in operation, the pool temperature began to approach a uniform value. Figure 8-26 presents the azimuthal pool temperature distribution 13 min after valve closure for the test with RHR. The mixing process continued and the pool reached a nearly uniform temperature within 30 min after the valve was closed (see Figure 8-27).

Table 8-1

MONTICELLO T-QUENCHER TEST HYDRODYNAMIC DATA SUMMARY

Test Conditions & Tests Involved		SRVDL Pressure (psig)		T-Quencher Pressure (psid)		Shell Pressures (1) (psid)		Bubble Pressures (1) (psid)			
		P1	P2	P6	P7	P12	P16	P8	P9	P10	P11
CP, NWL, SVA Valve A Tests-2.501,801 901,1301,1601,24	Highest Value(s) Meas'd Mean ($\overline{X}$) Stand'd Deviation (σ) Std Dev/Mean ($\sigma/\overline{X}$)										
HP, NWL, SVA Valve A Tests-802,902, 903,904,905	Highest Value(s) Meas'd Mean ($\overline{X}$) Stand'd Deviation (σ) Std. Dev/Mean (σ/X)										
HP, DWL, SVA Valve A Tests 1303,1602, 1603,1604,1605	Highest Value(s) Meas'd Mean ($\overline{X}$) Stand'd Deviation (σ) Std. Dev/Mean ($\sigma/\overline{X}$)										
HP, EWL, SVA Valve A / Tests 2305, 2306	Highest Value(s) Meas'd										
CP, NWL, MVA Valve A (&E&G) Tests 2301,2302, 2303,2304	Highest Value(s) Meas'd										
CP, NWL, SVA Valve E Tests 1101, 14,18,21	Highest Value(s) Meas'd Mean ($\overline{X}$) Stand'd Deviation (σ) Std. Dev/Mean ($\sigma/\overline{X}$)										
HP, NWL, SVA Valve E Tests 1102, 1103,1104,1105	Highest Values Meas'd Mean ($\overline{X}$) Standard Deviation (σ) Std. Dev/Mean ($\sigma/\overline{X}$)										
CP, NWL, SVA Valve G Tests 12, 15 19, 22	Highest Values Meas'd Mean ($\overline{X}$) Std. Dev. (σ) Std. Dev/Mean ($\sigma/\overline{X}$)										

(1) Shell and bubble pressures are given as follows: Maximum Positive/Maximum Negative; these values did not necessarily occur in the same test.

(2) Pressures measured during CP, NWL, MVA tests are included in these values.

(3) NA = non-applicable.

Table 8-2

SUMMARY OF SRV DISCHARGE LINE REFLOOD DATA

Run No.	Test No.	Range of Reflood Height With Reference To NWL (ft) (1)	Estimated Time From Valve Closure to Peak Reflood (sec)
2	2		
3	501		
4	502		
5	801		
6	802		
7	901		
8	902		
9	903		
10	904		
11	905		
12	1101		
13	1102		
14	1103		
15	1104		
16	1105		
17	12		
18	1301		
18	1302		
18	1303		
19	14		
20	15		
21	1601		
21	1602		
21	1603		
21	1604		
21	1605		
22	18		
23	19		
24	21		
25	22		
26	2301		
28	2302		
30	2303		
31	2304		
31	2305		
31	2306		
31	2307		
32	24 Shakedown		

(1) Positive values refer to reflood above the initial water leg (13.3 ft).

(2) Reflood did not go beyond one foot above T-Quencher centerline.

Table 8-3

WALL PRESSURE (P_{16}) FREQUENCIES FOR VARIOUS TEST CONDITIONS

Test No.	Type of Test Case	Frequency of 1st Cycle (f_1)*	Frequencv of 2nd Cycle (f_2)*	Approximate Frequency From 3rd and Subsequent Cycles
801	CP, NWL, SVA Valve A			
904	HP, NWL, CVA Valve A			
2306	HP, EWL, CVA Valve A			
1604	HP, DWL, CVA Valve A			
2301	CP, NWL, MVA Valves A, E, and G			
22	CP, NWL, SVA Valve G (distant bay)			

*Figure 8-12A shows an example of these two cycles, f_1 and f_2.

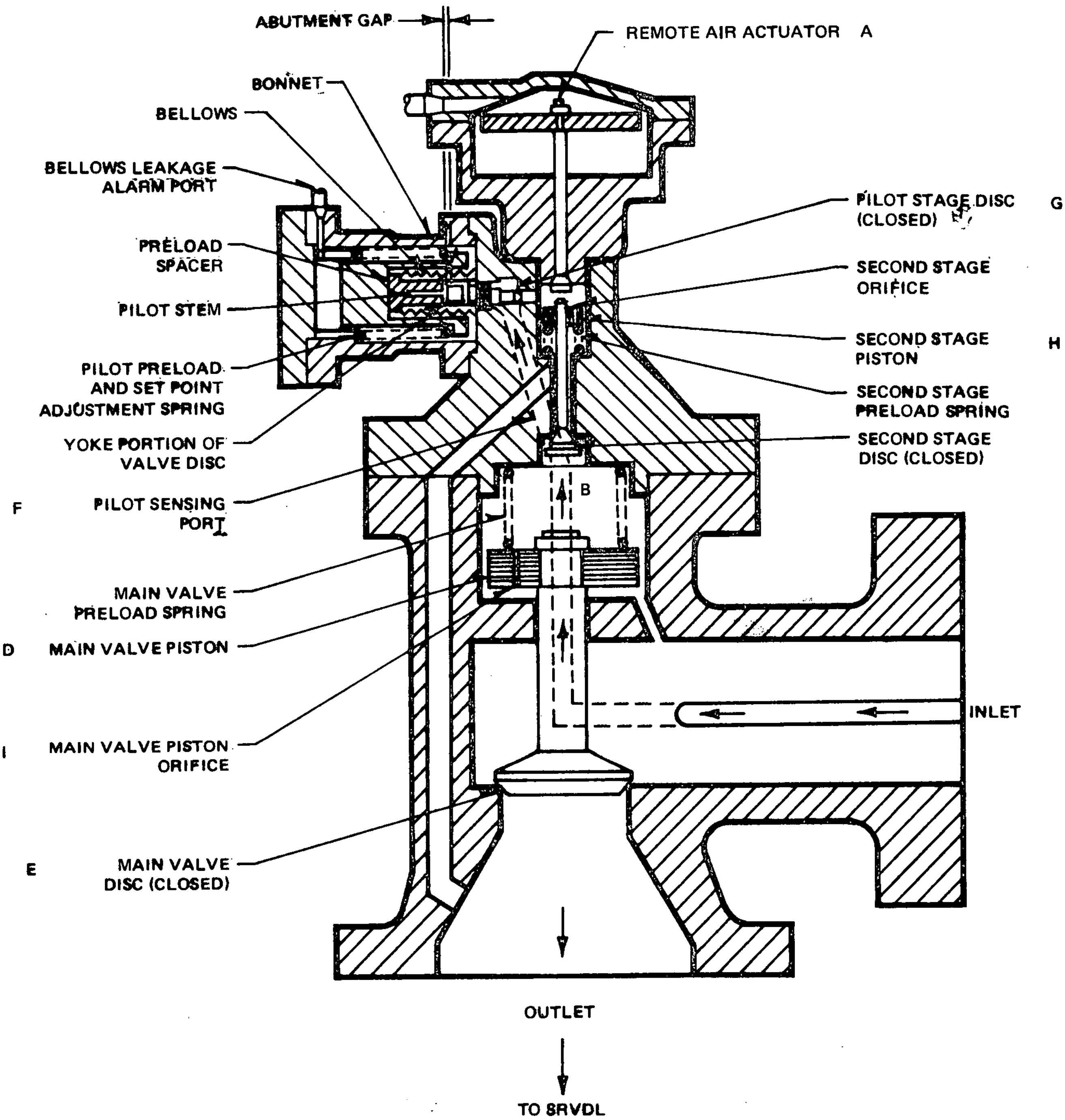

Figure 8-1A. Valve Schematic (Closed)

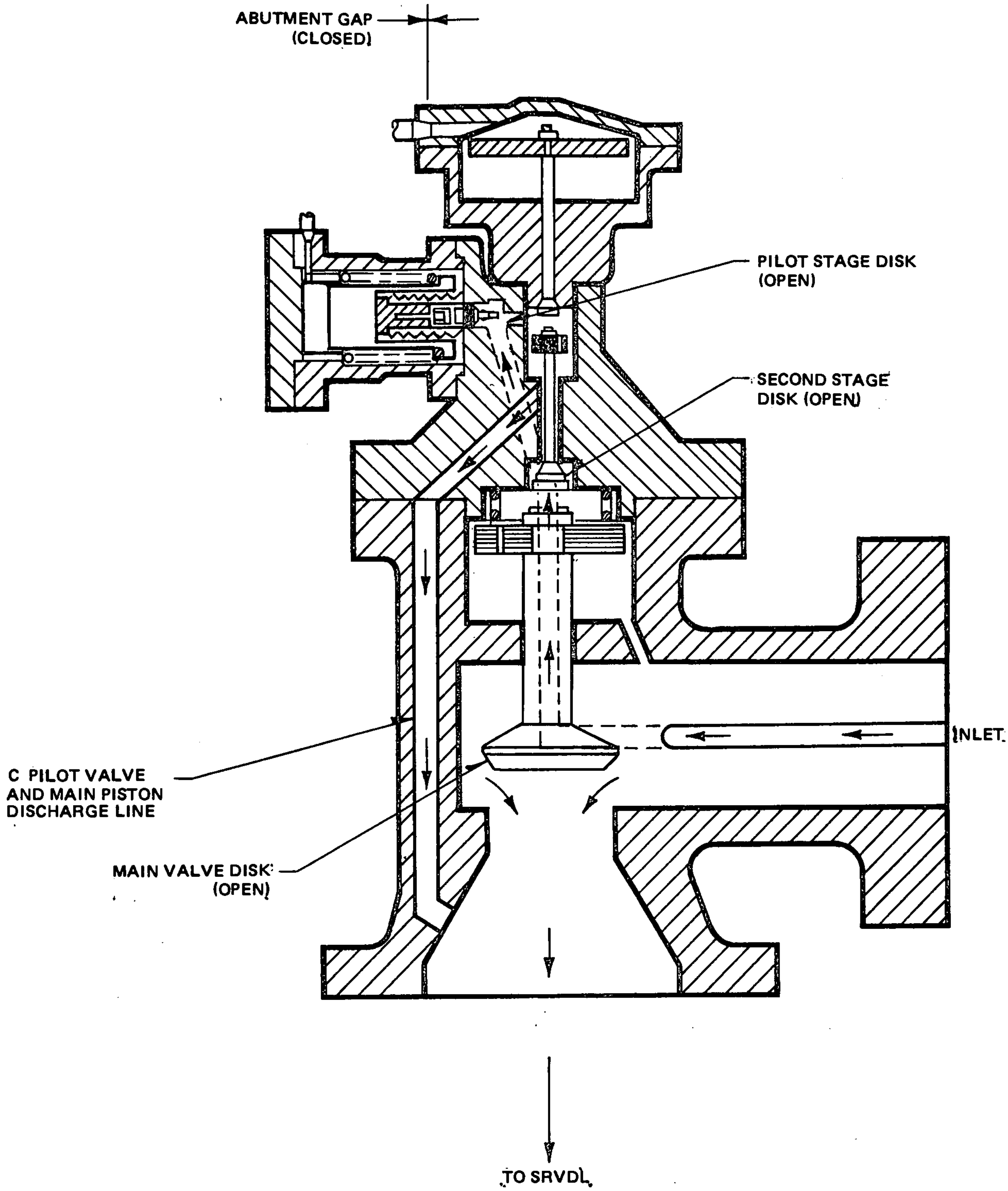

Figure 8-1B. Valve Schematic (Open)

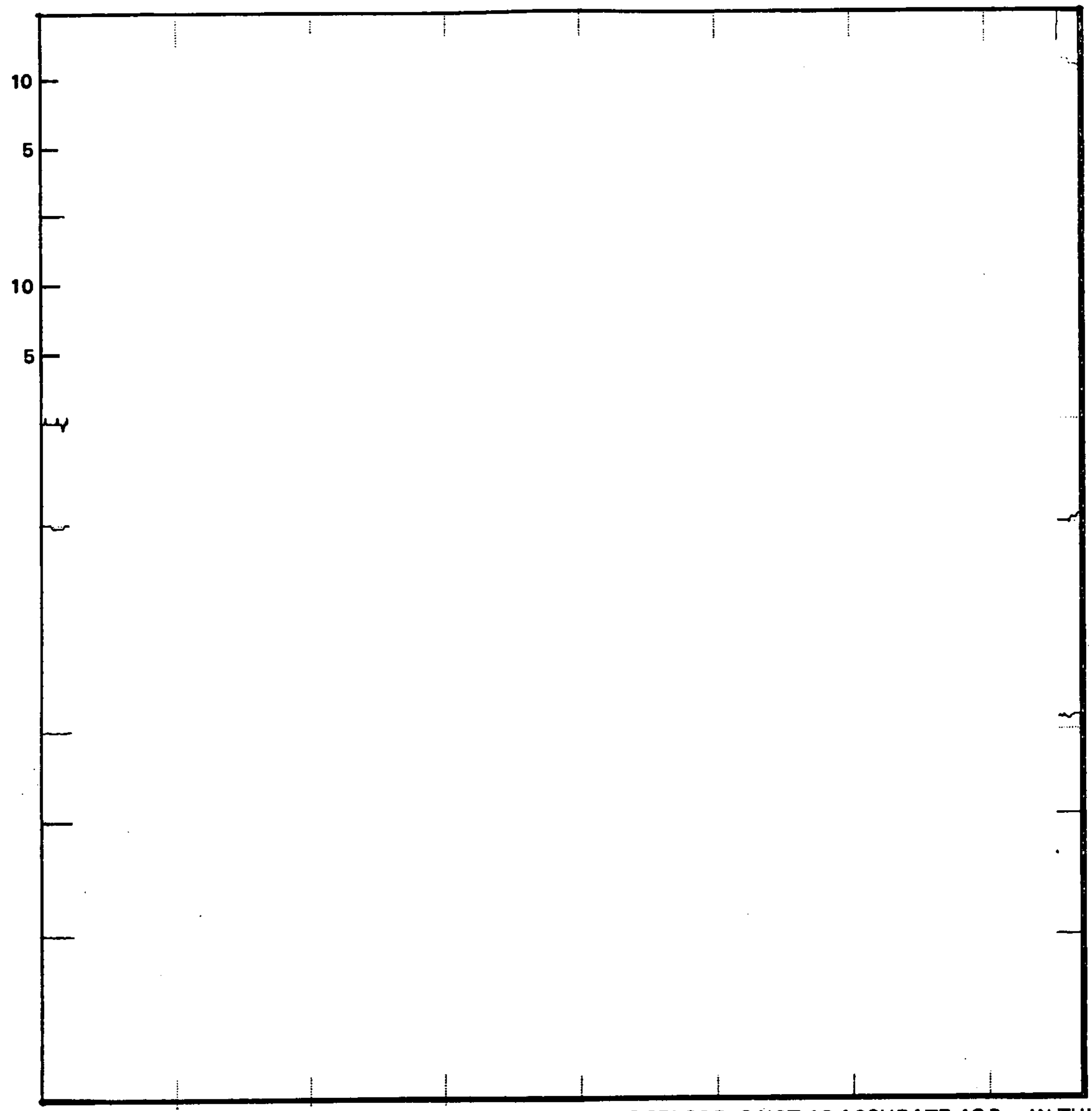

*P_5 IS SHOWN HERE TO DEMONSTRATE TIMING ONLY. THIS SENSOR IS NOT AS ACCURATE AS P_{49} IN THIS LOW PRESSURE RANGE. P_5 FULL RANGE IS 1000 psia WHILE P_{49} HAS A FULL RANGE OF 25 psia

Figure 8-2. Sample Prepressurization Transient Test 2

Figure 8-3. SRVDL and T-Quencher Pressures Measured in Test 2306 (HP, EWL, SVA)

SAMPLE WATER REFLOOD DATA FROM TEST 2

0 1 2 3 4 5 6

TIME FROM SRV CLOSURE (seconds)

Figure 8-4. Sample Reflood Data - Test 2

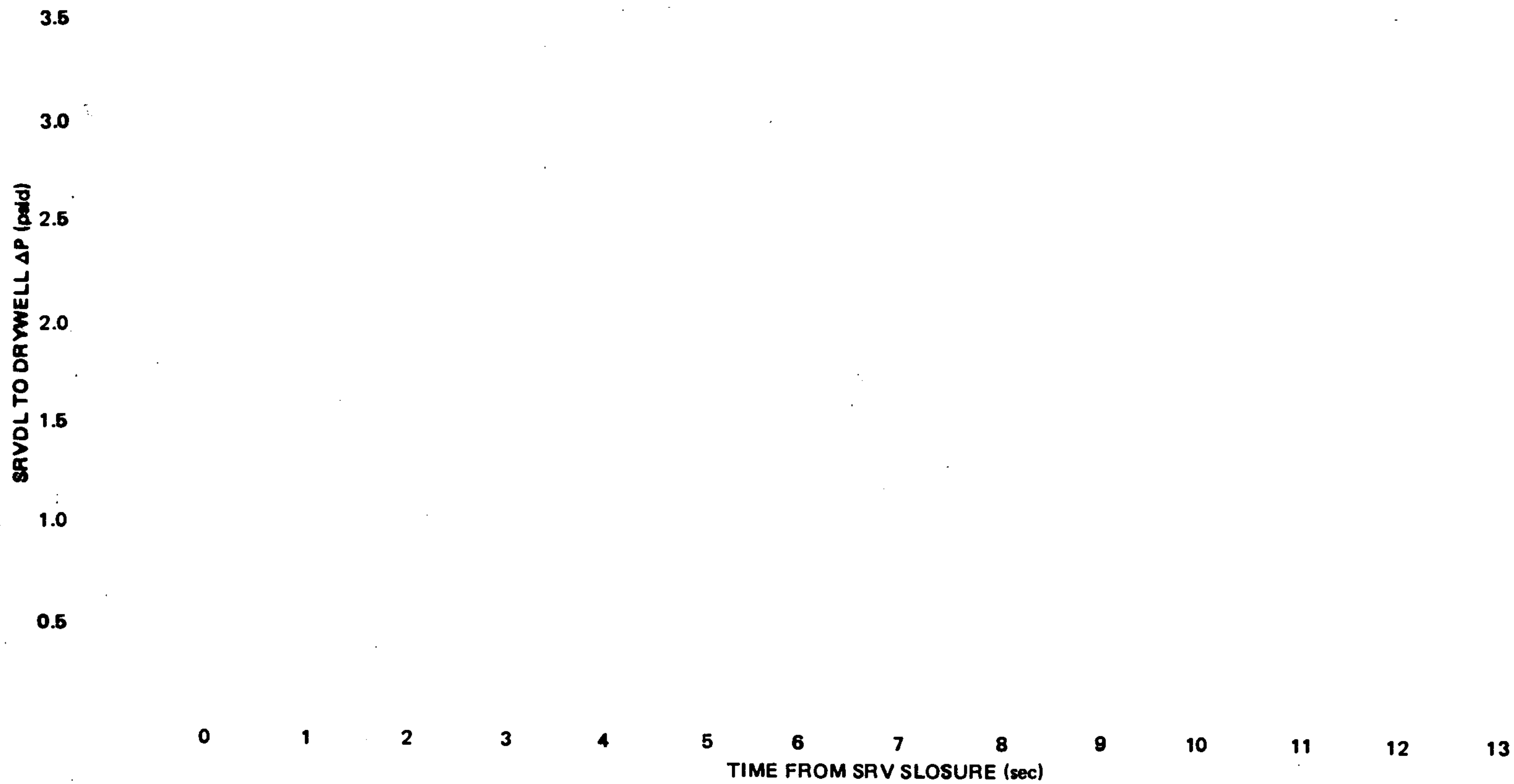

Figure 8-5. SRVDL Pressure Following Initial Reflood Test 2

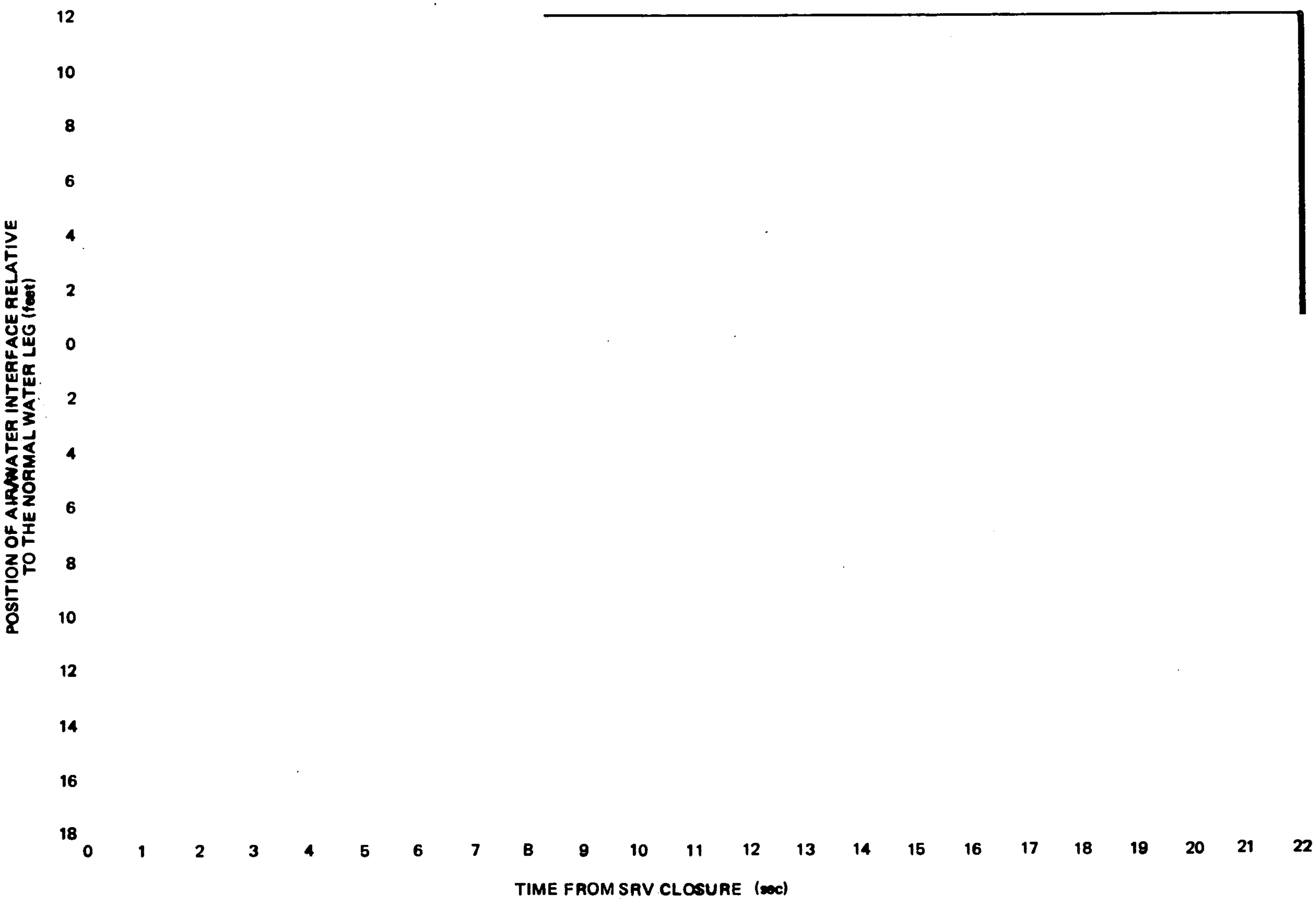

Figure 8-6. SRVDL Water Reflood - 1000 psia Shakedown Test

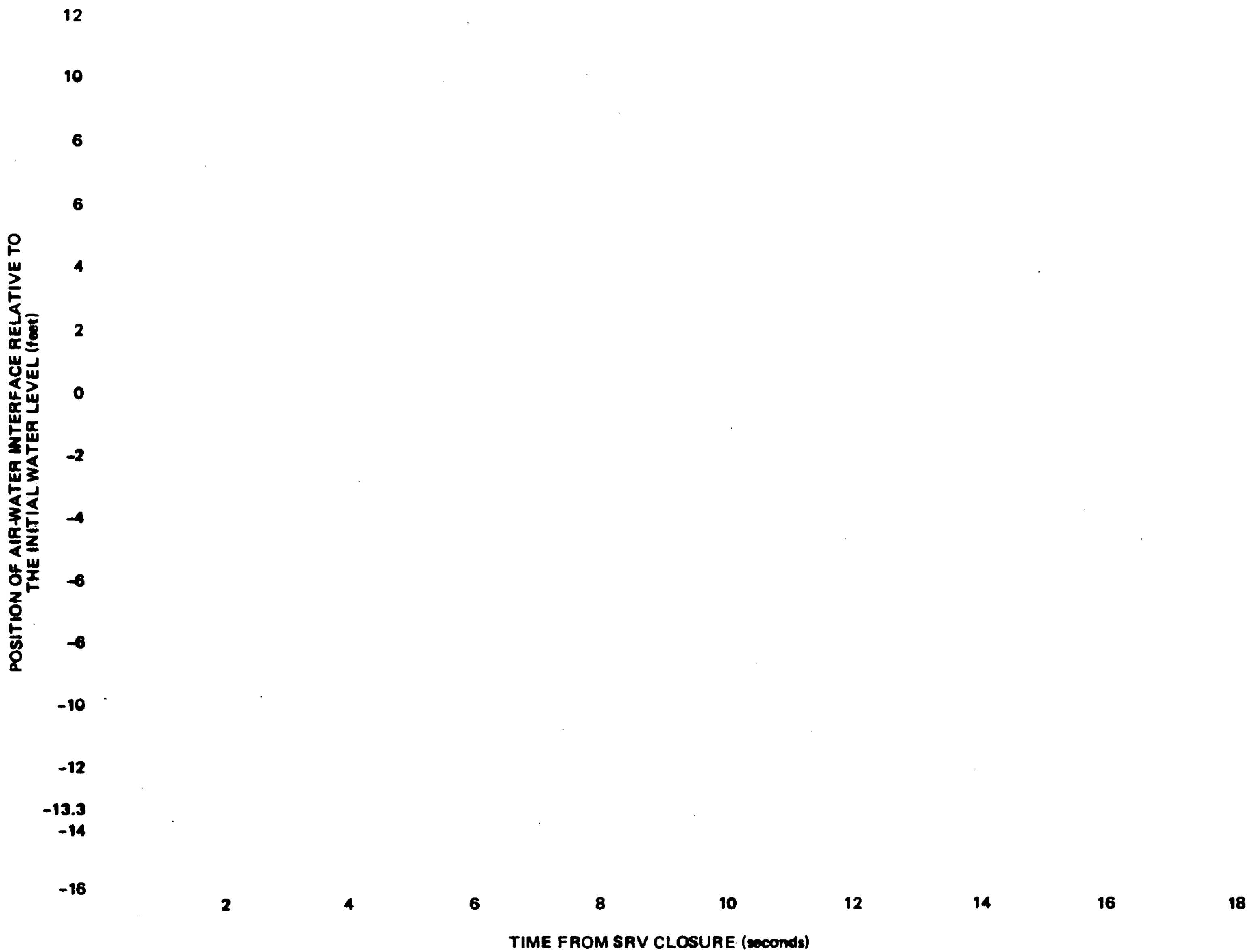

Figure 8-7. SRVDL Water Reflood and Vacuum Breaker Operation - Test 2

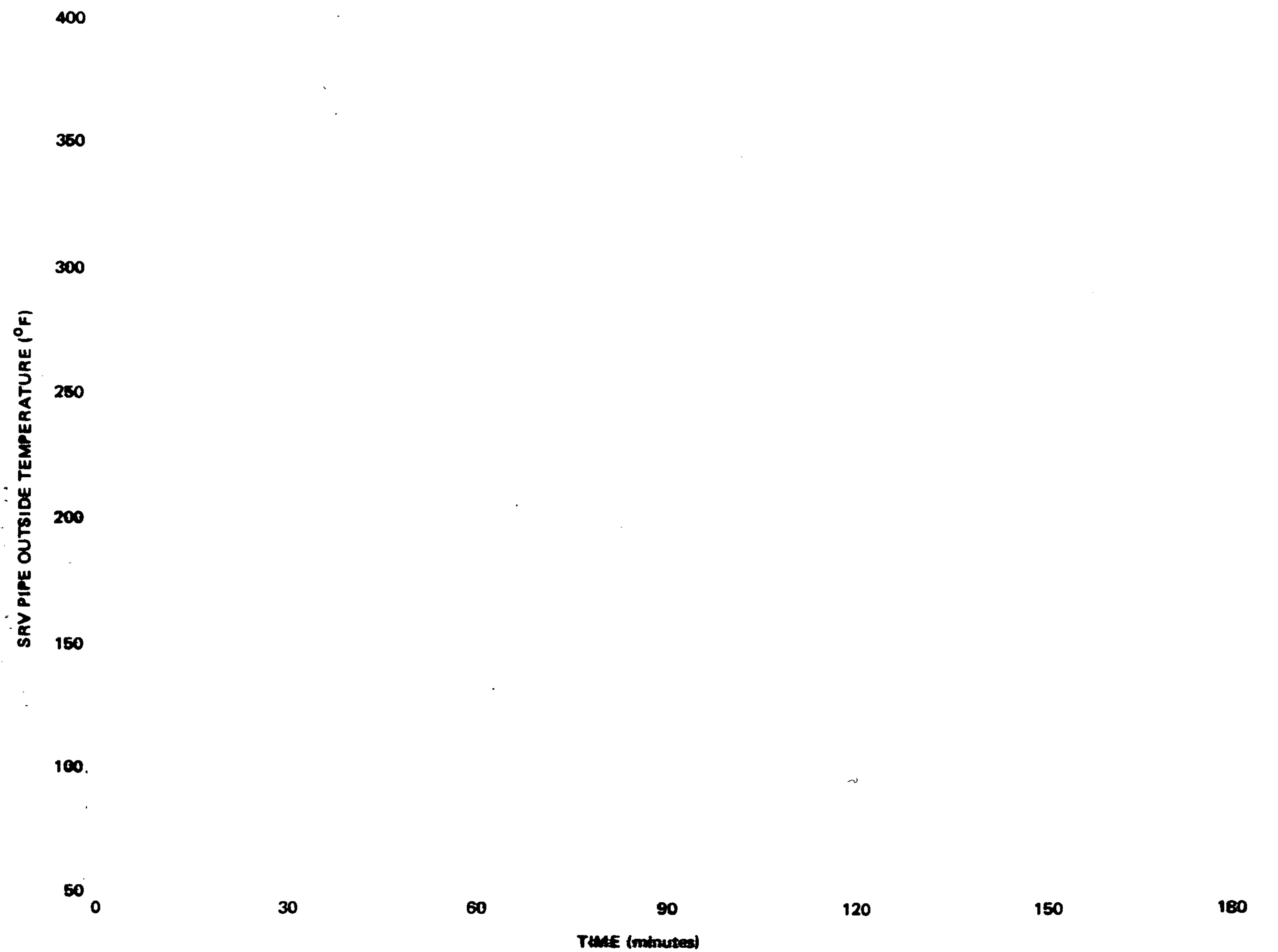

Figure 8-8. SRV Pipe Temperature Transient - Test 2

Figure 8-9. Air Bubble Pressures Test 801 - CP, NWL, SVA

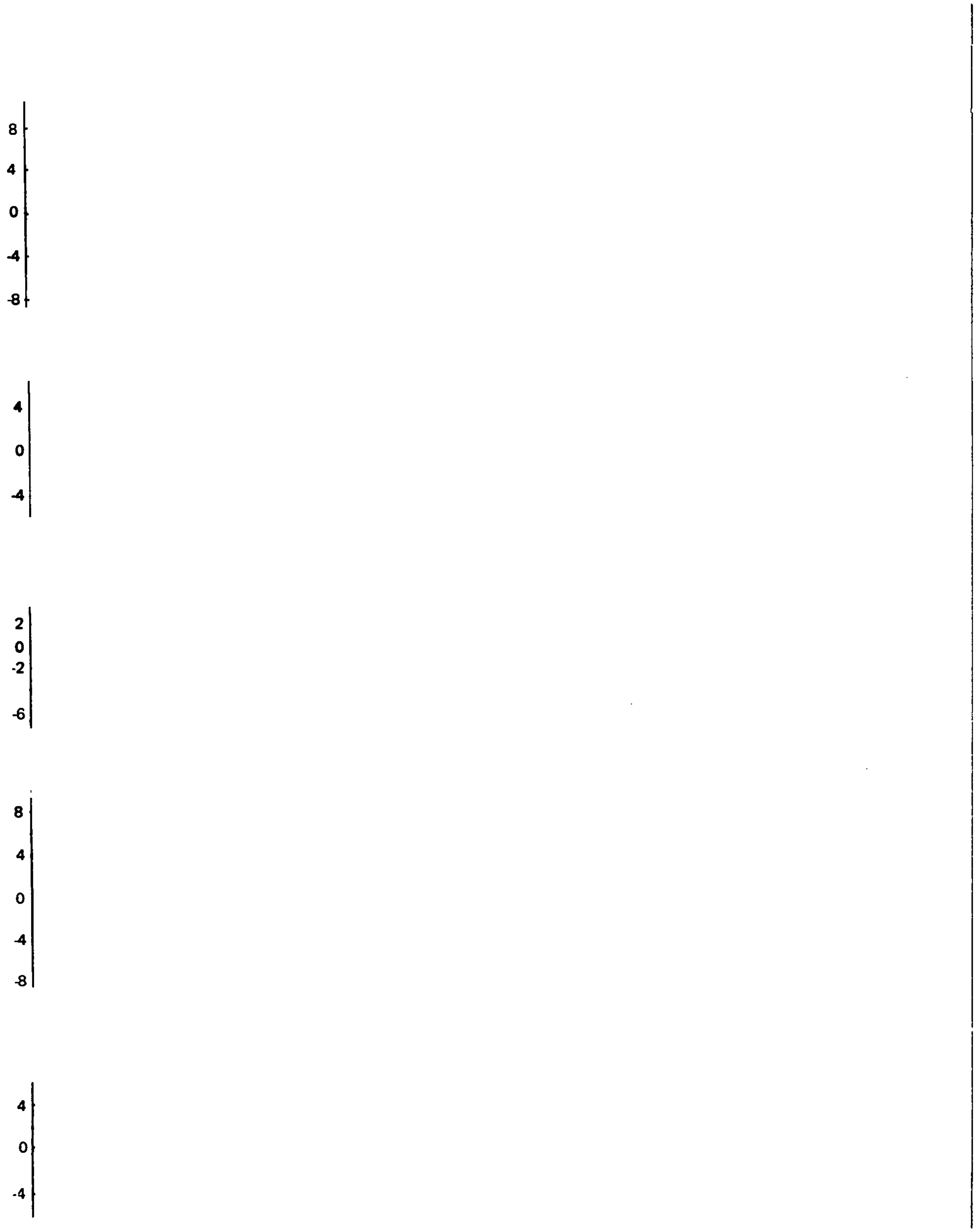

Figure 8-10. Air Bubble Pressures (Recorded by Sensor P9) For Various Test Conditions

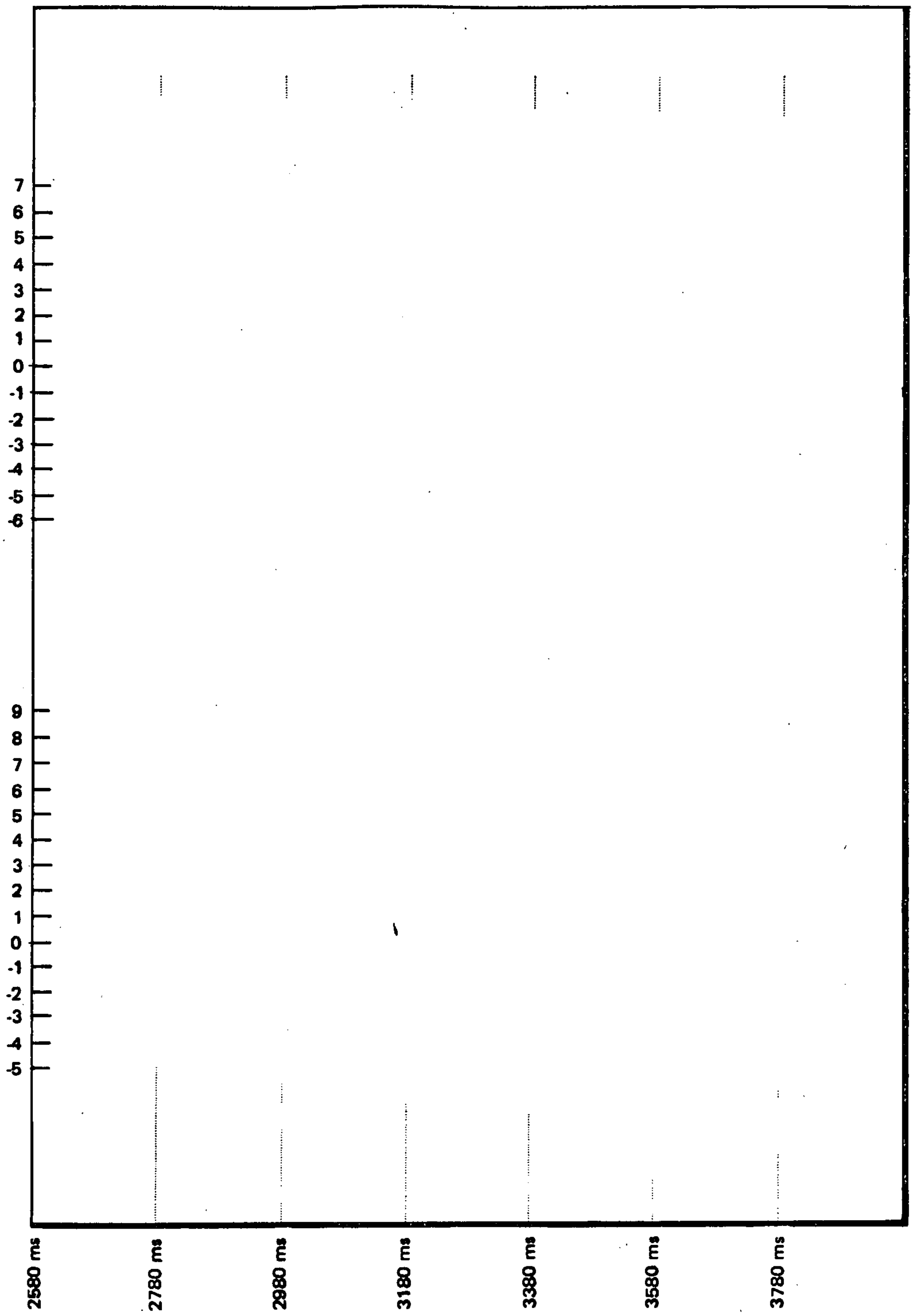

Figure 8-11. Air Bubble Pressure Differential Across the T-Quencher Arms - Test 801

6
4
2
0
-2
-4

6
4
2
0
-2
-4

Figure 8-12A. Highest Measured Shell Pressures (Bay D) for Various Test Conditions

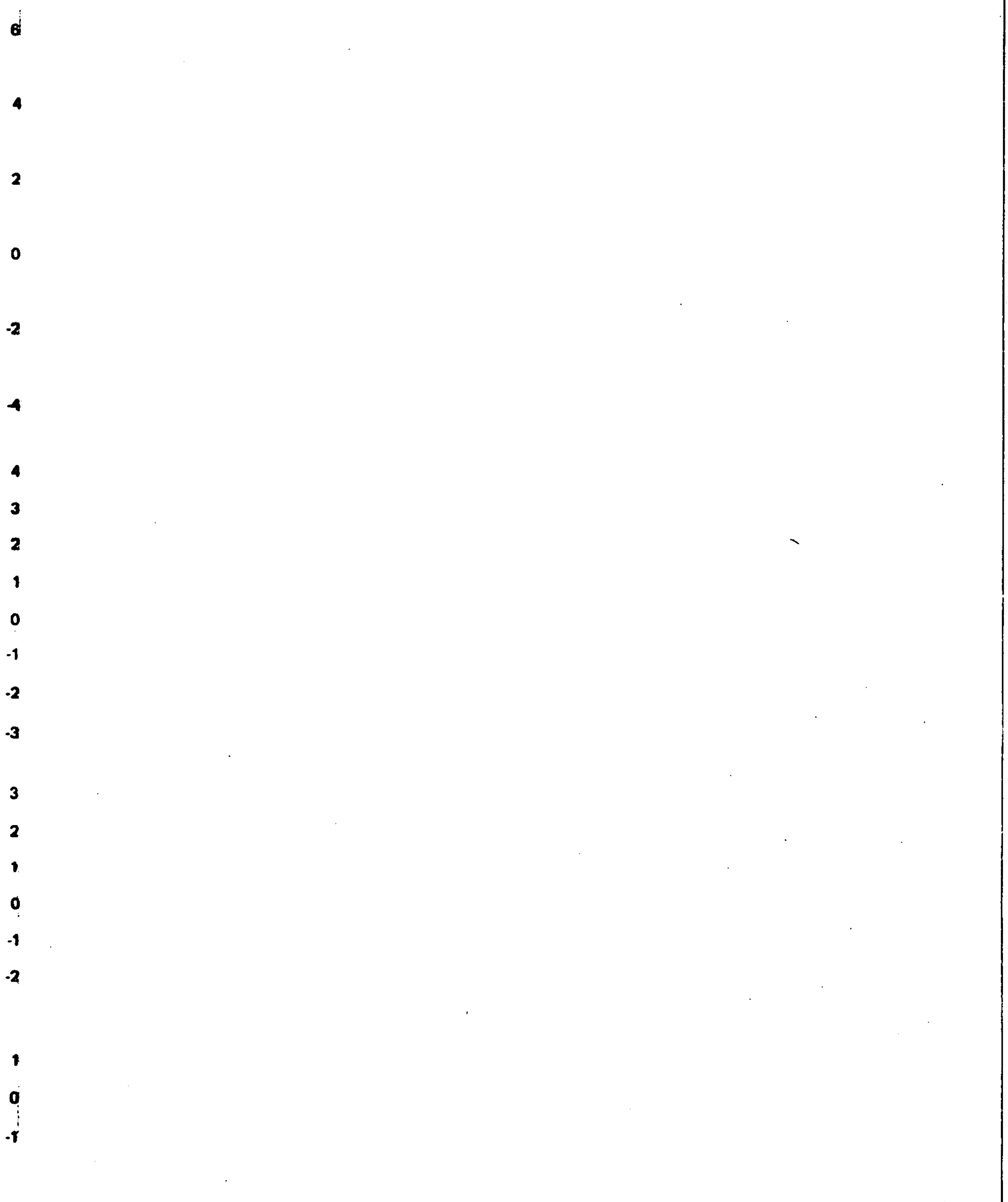

Figure 8-12B. Highest Measured Shell Pressures (Bay D) for Various Test Conditions

Figure 8-13. Pressure Attenuation Along Torus Shell Longitudinal Axis for Test 801 (CP, NWL, SVA) and Test 2301 (CP, NWL, MVA)

Figure 8-14. Spatial Pressure Distribution at Torus Cross-Section A-A, 39 Feet From T-Quencher Center Line as Shown in Figure 9-13.

Figure 8-15. Spatial Pressure Distribution at Torus Cross-Section B-B, 20.4 Feet From T-Quencher Center Line as Shown in Figure 9-13

Figure 8-16. Spatial Pressure Distribution at Torus Cross-Section C-C, 3.75 Feet from T-Quencher Center Line as Shown in Figure 9-13

Figure 8-17. Spatial Pressure Distribution at Torus Cross-Section D-D, at T-Quencher Center Line as Shown in Figure 9-13

Figure 8-18. Spatial Pressure Distribution at Torus Cross-Section E-E, 375 Feet From T-Quencher Center Line as Shown in Figure 9-13

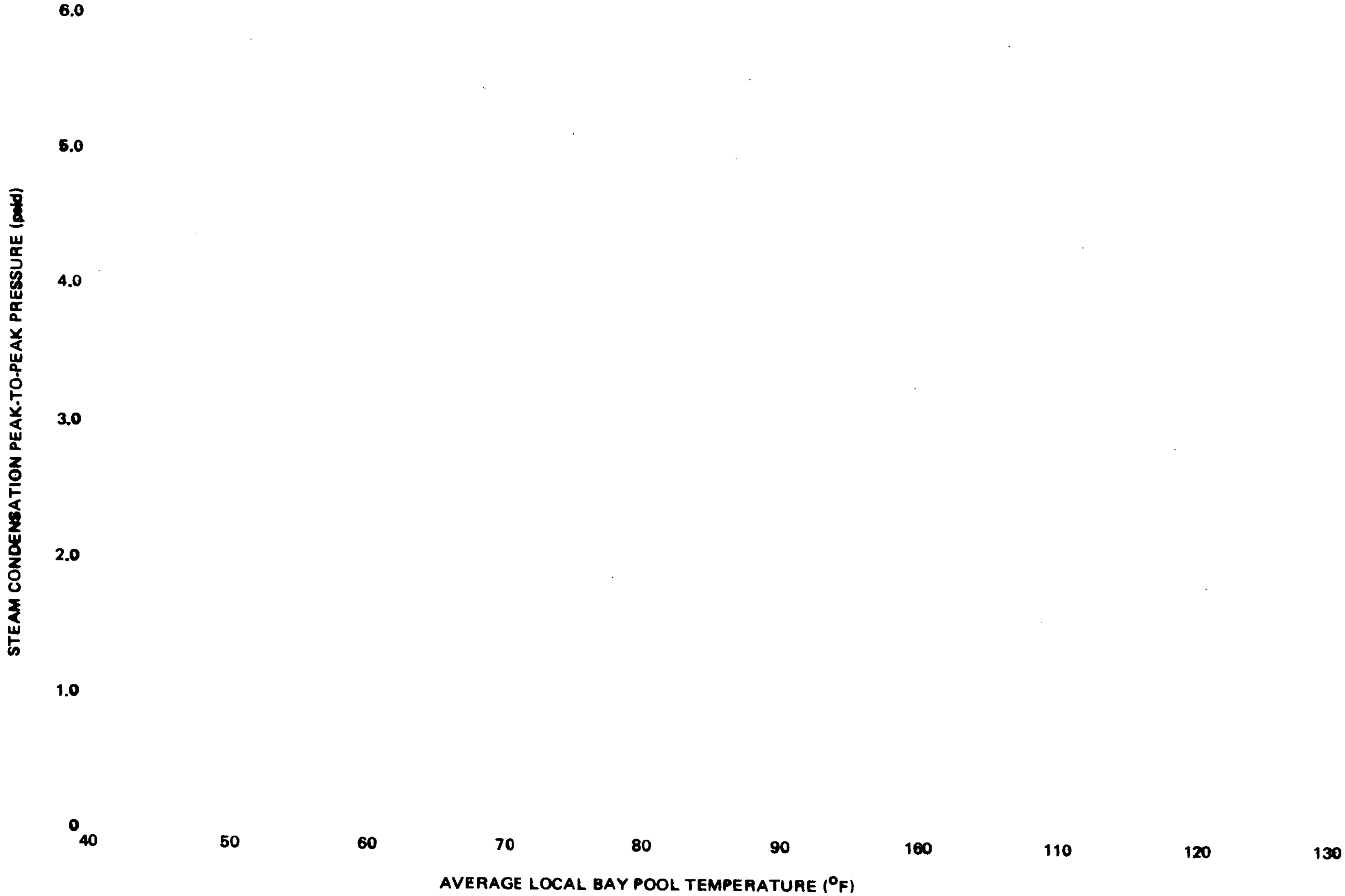

Figure 8-19. Steam Condensation Pressure vs. Pool Temperature

Figure 8-20. Steam Condensation Pressures During the Low (155 psia) Pressure Test

Figure 8-21. Locations of RHR Suction and Discharge Piping in Monticello Torus

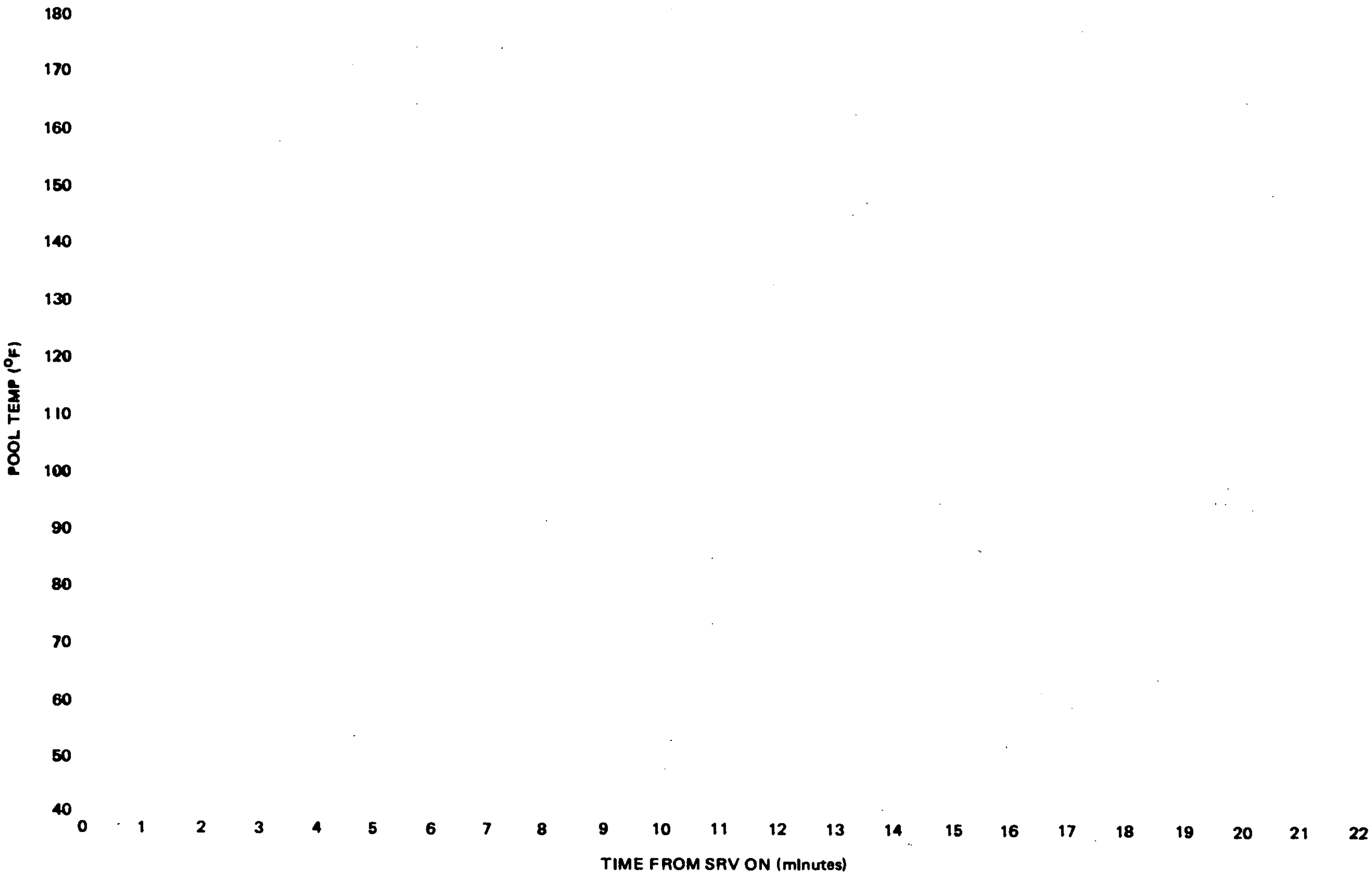

Figure 8-22. Comparisons of Bulk Pool to Local Bay D Temperature for Extended Blowdown Tests (With and Without RHR)

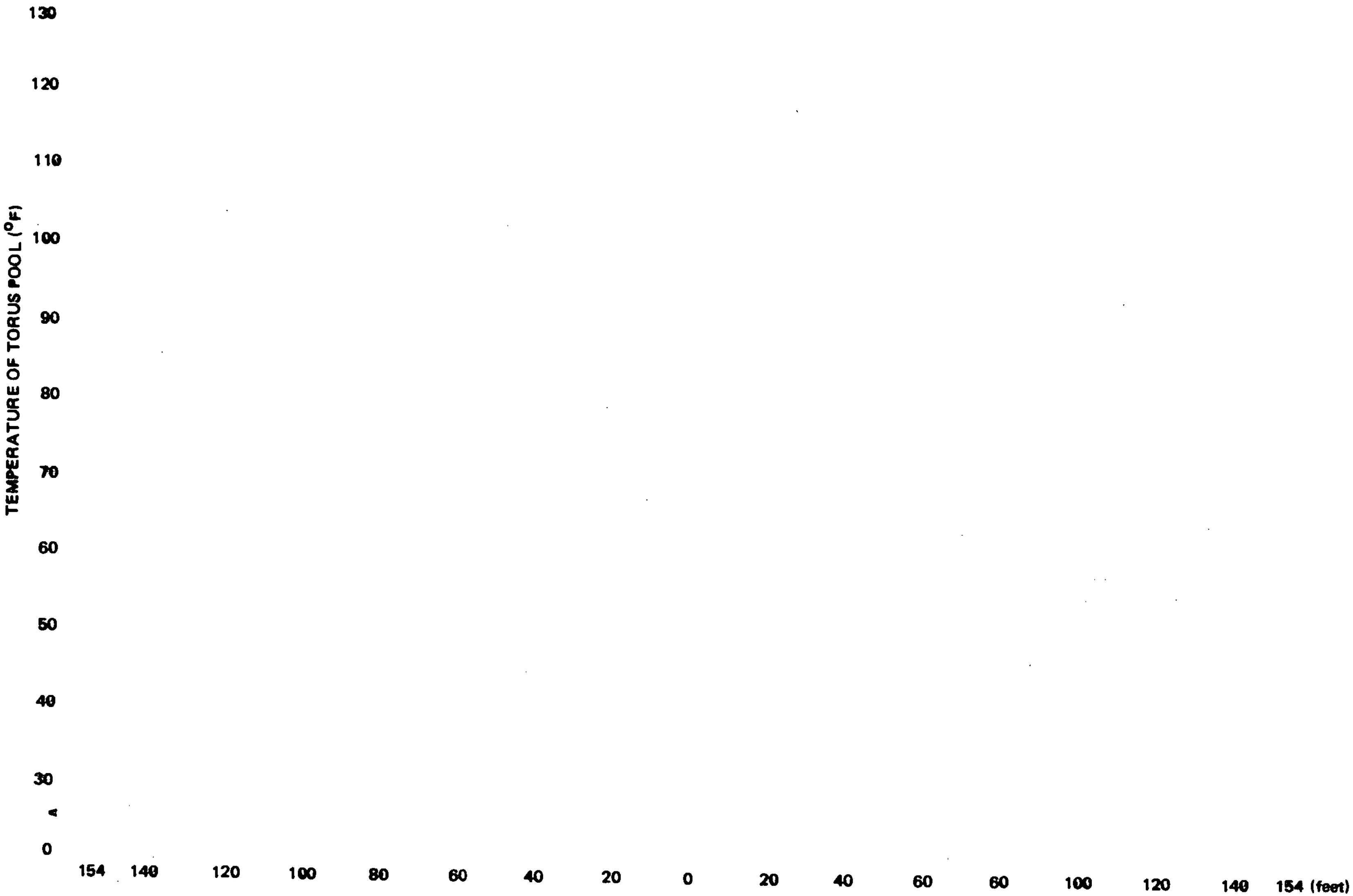

Figure 8-23. Torus Pool Temperature vs. Azimuthal Location Snapshot Just Prior to S/RV Closure Discharge Time: 6 Min. 46 Sec. No RHR

Figure 8-24. Torus Pool Temperature vs. Azimuthal Location Snapshot 13 Minutes After S/RV Closure. Discharge Time: 6 Min. 46 Sec., No RHR

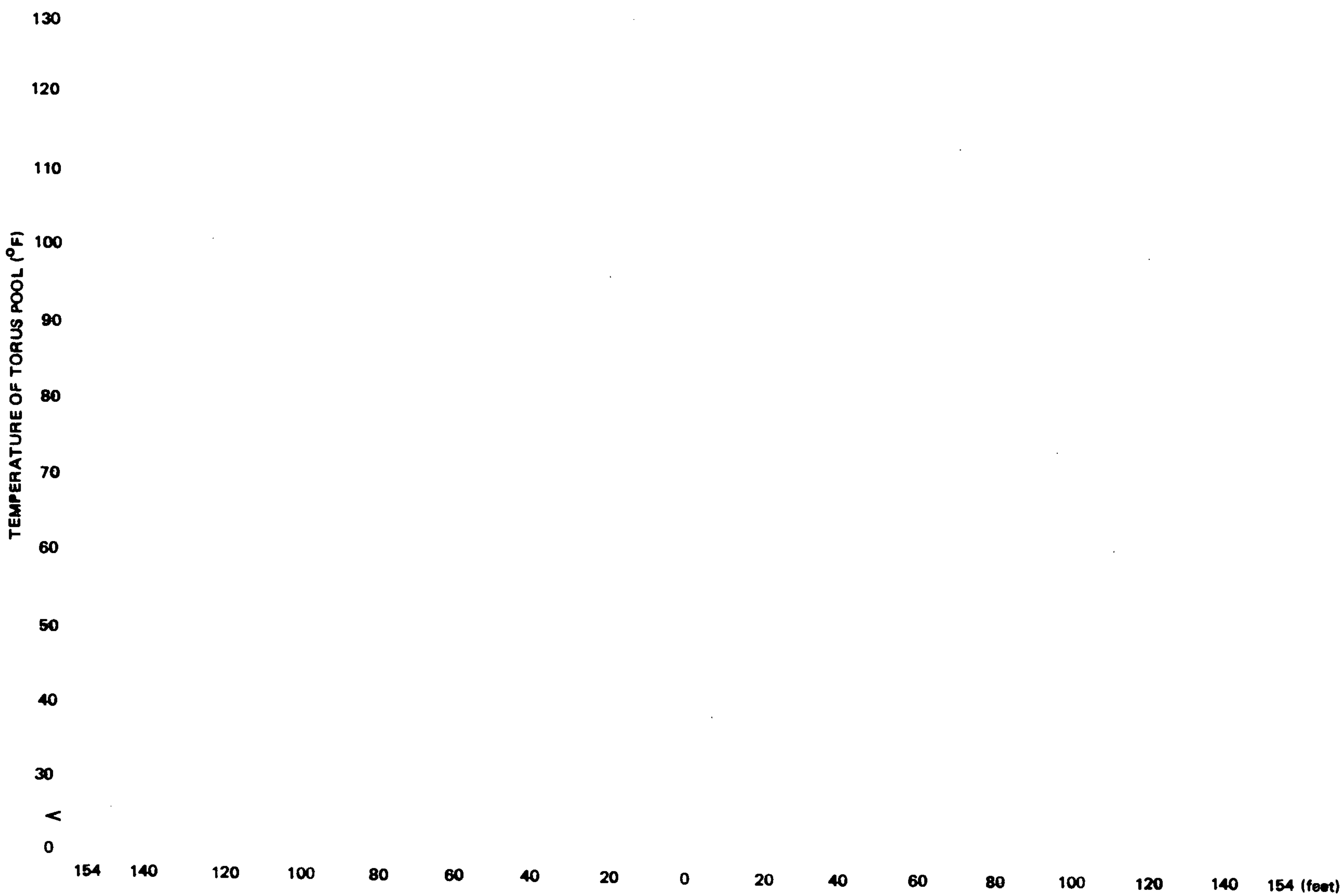

Figure 8-25. Torus Pool Temperature vs. Azimuthal Location Snapshot Just Prior to S/RV Closure. Discharge Time: 7 Min. 55 Sec., With RHR

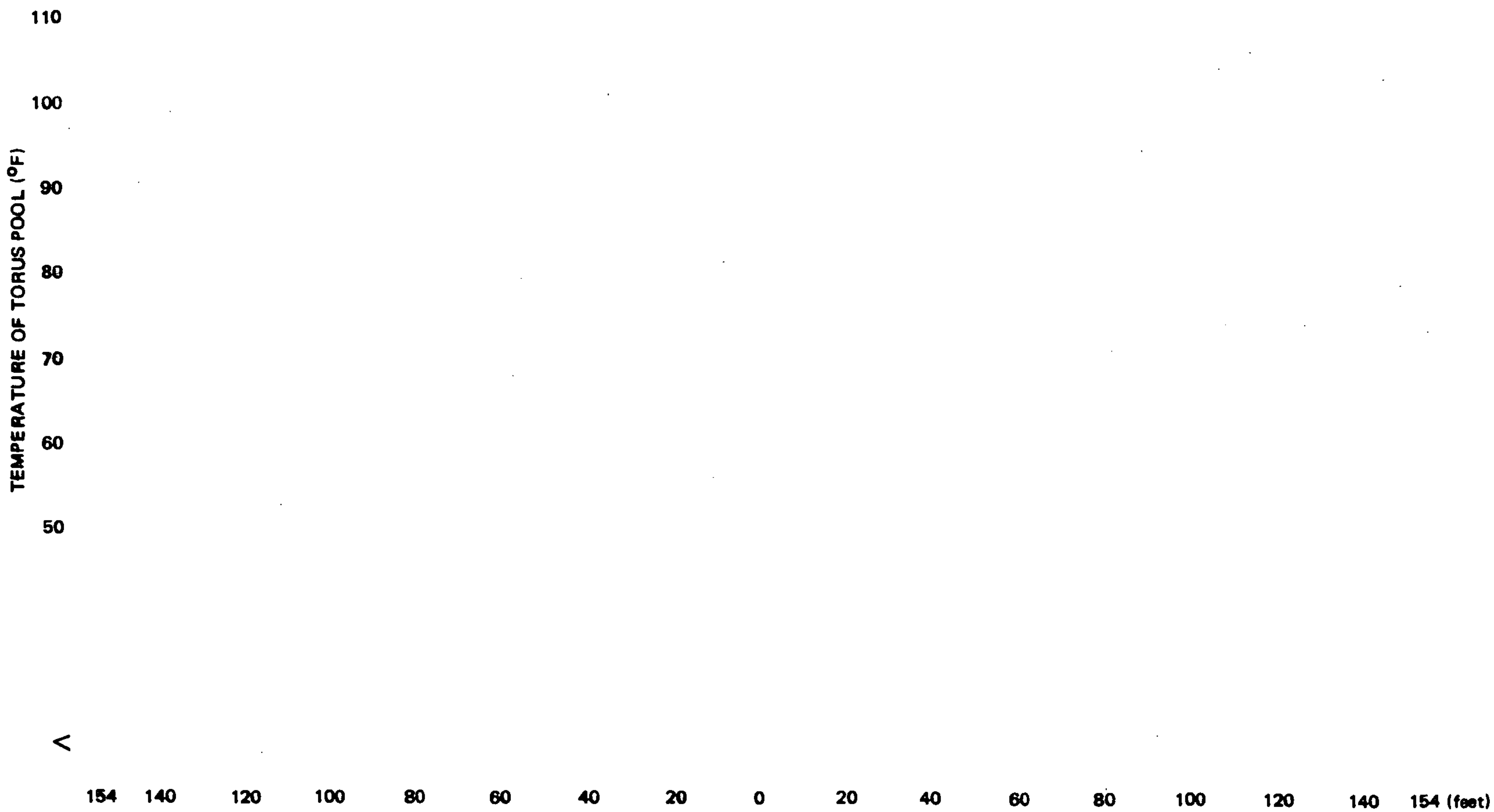

Figure 8-26. Torus Pool Temperature vs. Azimuthal Location Snapshot 13 Minutes After S/RV Closure. Discharge Time: 7 Minutes 55 Sec., With RHR

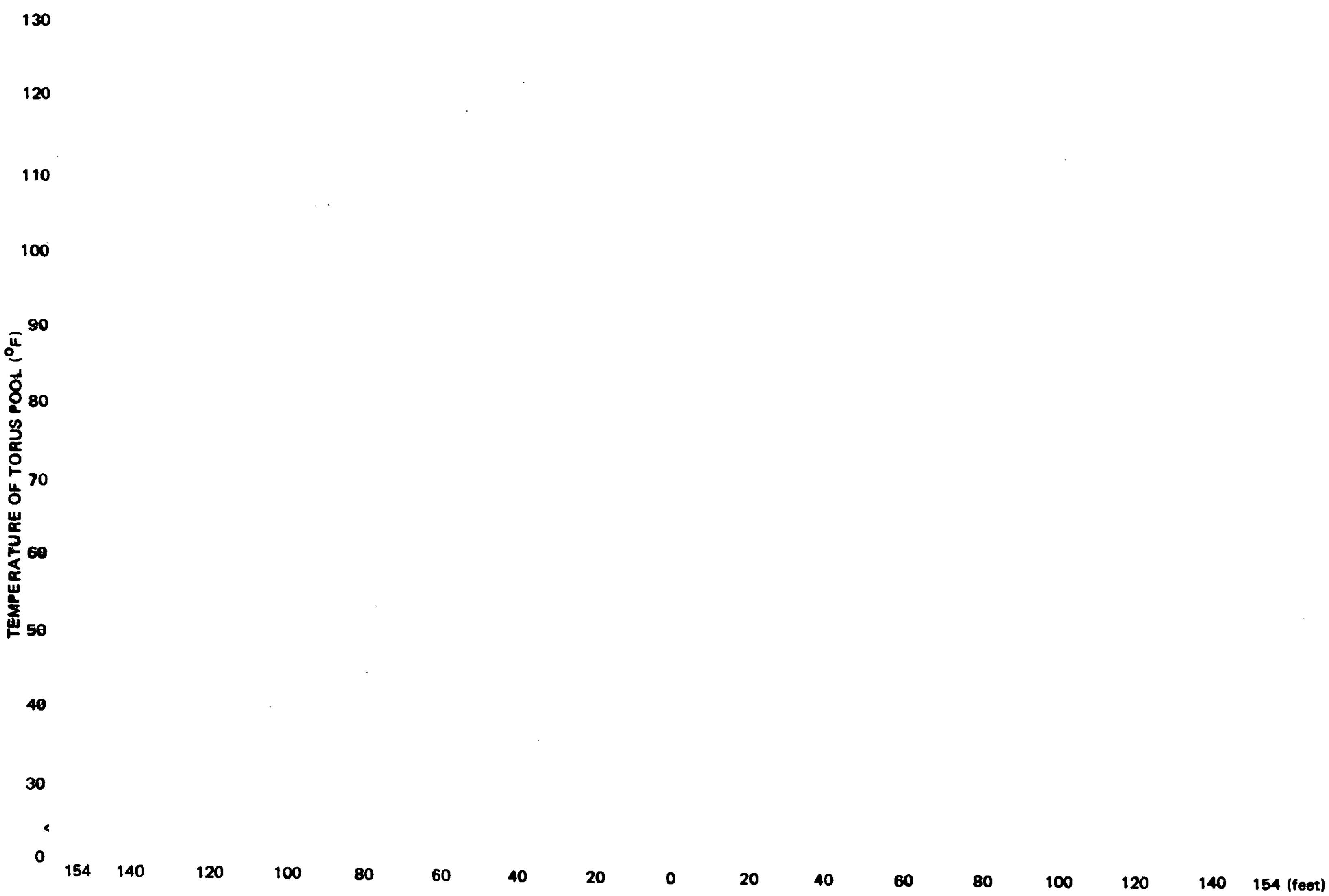

Figure 8-27. Torus Pool Temperature vs. Azimuthal Location Snapshot 30 Minutes After S/RV Closure. Discharge Time: 7 Min. 55 Sec., With RHR

9. DISCUSSION OF STRUCTURAL RESULTS

9.1 INTRODUCTION

The torus shell structure (including suction header nozzle and attachments), torus support column and vent downcomer structural responses are described in this section. Resistance strain gauges were the main instruments used for these components, however, there were also seven uniaxial accelerometers. Bay D was the most heavily instrumented. Strain gauges were also installed on the outside of Bay A, Bay C, and Bay C/D. All four torus support columns of Bay D were instrumented; two columns of Bay A and two of Bay B were also instrumented.

Test data are summarized in this section and tables of the peak stresses for each gauge and test are given in Appendix F. Not all the reduced data are included in this report but a sample of plots from Test 2 is given in Appendix G.

9.2 DATA REDUCTION AND EVALUATION METHODS

Data for most of the gauges were reduced from the pulse code modulator (PCM) recordings. Data from gauges on the remote bays were reduced by an FM analog system. The two systems yield basically the same information although there are differences in the data format.

The strain gauge rosettes were oriented as shown in the following sketch so results would be uniform throughout the tests. In the cases of paired rosettes, the individual gauge elements were named clockwise on the outside surface and counterclockwise on the inside surface so that the corresponding outside and inside elements were parallel to each other. The maximum principal stress angle was measured from the "A" orientation and was defined as positive in the A-to-C direction. Thus, stresses having the same nominal orientation with respect to the gauges have the same orientation in the material.

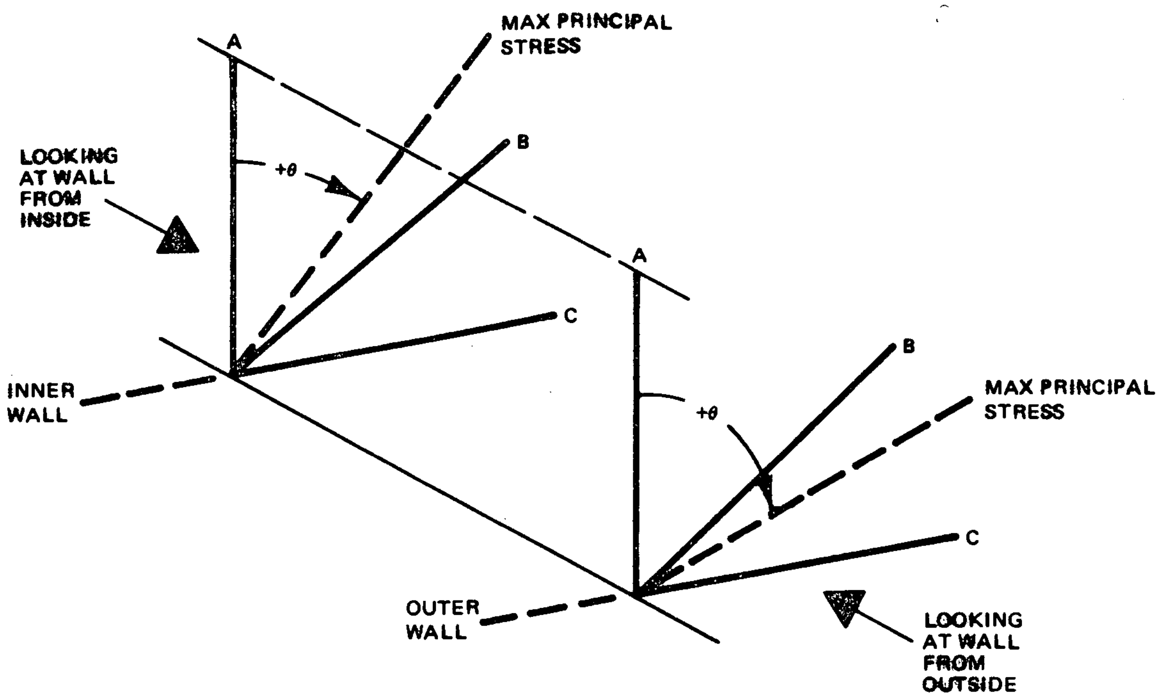

STRAIN GAUGE ROSETTE NOTATION

Membrane stresses were calculated by averaging the inside and outside strains in each pair of corresponding directions and calculating the stresses from these averages.

In cases where rosette gauges were applied only to the outside surface, the gauge arrangement is the same as for the outside gauges shown in the strain gauge location sketch.

Strain data were reduced to yield the following results:

σ_A, σ_C, τ_{AC}:	stresses relative to the A and C directions
σ_1, σ_2, Angle:	maximum and minimum principal stresses and angle of maximum principal stress
SI:	stress intensity.

For single element gauges, the strains were converted to approximate stresses by multiplying by Young's modulus (27.9×10^6 psi). The inside, outside or membrane cases were calculated for the different types of strain gauge installation.

Calculations were presented in plots and as tables. Plots were made of the raw strain data and of the resulting computed stress components: σ_A, σ_C, and τ_{AC}. Tables are presented for the raw strain data, the component stresses, the principal stresses, the stress intensity and the angle of maximum principal stress. In the cases of single element (uniaxial) gauges, only the strain and the calculated stress were calculated.

In the cases of paired inside/outside rosettes, each surface rosette measures the stress condition at that surface. The membrane stress represents the midplane stress condition, assuming a linear distribution of strain through the thickness.

The FM analog plots differ only in the stress and time scales. The tables include the same data as the above tables except for strain data and stress intensity. The two sets of data do not have a common time base.

All data were reduced at 10-millisecond intervals of real time of the tests. Previous tests* had demonstrated that no significant high frequency components were deleted by this procedure. No filtering of PCM data beyond that inherent in the signal conditioning and processing equipment was performed. The FM analog system incorporated a 50-Hz, low-pass filter.

The data reduction program included a peak determination routine that selected and ordered the five highest positive (tensile) and negative (compressive) stresses of each test for each gauge. The largest stress of each of these groups of five is used in the evaluation in this report.

The peak values are tabulated in Appendix G. Where appropriate, stress intensities are tabulated. In cases where stress intensities were not calculated, the stress components are listed.

---

*NEDC-21581-P Final Report: In-Plant Safety/Relief Valve Discharge Load Test - Monticello Plant

Table 9-1 summarizes the results of each test condition. The maximum value observed in all tests of that condition, the mean value, the standard deviation, and the ratio of standard deviation to mean are given for each gauge.

9.3 TORUS SHELL STRESSES

9.3.1 Instrumentation and Test Data Summary

The torus shell strain gauges in Bay D consisted of: a) a row of nine locations (mostly rosettes) along the bottom half at mid-span; b) lesser rows at the quarter-span regions; c) three locations along the ring girder on the Bay C side; and d) four locations near one outer support column (D4). There were also two gauge locations each at the bottom of Bay A, Bay C, and Bay C/D, plus one location 45^{o} from the bottom in Bay C (see Figure 4-9). The maximum values of stress intensity for each group of tests are given in Table 9-4.

9.3.2 Results

The distribution of stress intensity around the periphery of Bay D is shown in Figure 9-1 for the reference case (i.e., cold pipe, normal waterlevel, Bay D discharge). Maximum values for the seven tests of this condition are averaged for each applicable outside surface strain gage in developing this Figure. Stress values tend to be lowest near the water line. They are higher at the bottom, although the discontinuity of the earthquake tie might be expected to influence these values. The highest peak is at the upper hanger pad where load from the ECCS header is supported.

The clear shell region membrane stress intensity (during cold pipe tests) peaked at values ranging between 0.6 ksi and 1.6 ksi, the lower values occurring near the waterline.

The maximum outside stress intensities near the ring girder (cold pipe tests) were between ksi, which is approximately the same as in the vicinity of the earthquake tie. Stresses at the support column attachment were ksi in the column stub plate immediately above the column (Gauge 24), decreasing to ksi in the shell above the column stub plate (Gauge 25). Stresses near the gusset plates were about ksi (Gauges 26 and 31).

9.4 TORUS SUPPORT COLUMN LOADS

9.4.1 Instrumentation and Test Data Summary

The support columns at Bay D were instrumented to give axial load and bending load about two orthogonal planes six inches from the top. The data reduction routine resolved these bending moments into a resultant moment and the angle relative to a radially-outward line (measured positive counterclockwise as viewed from above). Data presentation consisted of plots of the axial load and the radial and circumferential bending moment. The support columns at Bays A and B were instrumented for axial load only. Because of the very small strains, digitizing of the column load data resulted in irregular output in some cases. The data are valid, however, except for a limited resolution of about 7 kips.

9.4.2 Results

Table 9-1 includes the maximum values, standard deviations, etc., for the individual columns. Since the peaks do not necessarily occur at the same time for all columns of a given bay, the sum of these cannot be taken as the total column force. Table 9-2 gives the maximum measured sum of column loads for the four columns of Bay D at any instant of time for the peak column load tests of each condition. It also gives the maximum instantaneous sum of the loads of the two instrumented columns of Bay A and the two of Bay B. Both upward and downward maximum values are given.

The maximum dynamic column load which was observed during the test occurred on outside column D1 during the multiple valve actuation test condition. The compressive load was 101 kips. The dynamic bending moment at that same time was 59 inch-kips. The maximum dynamic bending moment observed during the tests was on Column D3 during an MVA test, having a value of 182 inch-kips.

9.5 ECCS SUCTION NOZZLE STRESSES

9.5.1 Instrumentation and Test Data Summary

Gauges 32 and 33 measure the stresses in the region of the suction nozzle.

9.5.2 Results

Table 9-1 includes the nozzle region stresses under the various test conditions. The maximum measured stress in the nozzle region was encountered under MVA conditions, where a maximum stress intensity of   ksi was encountered on the inside surface. The maximum membrane stress intensity occurred during a depressed water level test, having a value of   ksi.

The stresses in the nozzle region (SG32 and SG33 above and below the nozzle) were predominantly radial with respect to the nozzle. This stress field would indicate that the forces on the nozzle were predominantly vertical loads or punch loads.

9.6 VENTHEADER/DOWNCOMER STRESSES

9.6.1 Instrumentation and Test Data Summary

Single element gauges 131, 132, and 133 were placed near the joints between ventheader and downcomer. Gauges 134 and 135 were placed, one each, on the straps between downcomers. Stresses from these gauges are given in Table 9-1.

9.6.2 Results

Tie strap stresses represented the maximum value for any locations in the torus structure, with SG 135 reaching a value of compression during the MVA. The data plot shows that this gauge undergoes a cyclic stress at about (during MVA) between the maximum first cycle value in compression (peaking at and a lesser value in tension (peaking). Since there was no gauge on the opposite side of the strap, the total behavior cannot be described. The mating tie strap showed about half the stress during this same event even though it was attached between the same two downcomers. The two straps showed stresses approximately equal to each other during the other tests. It should be noted that the tiebar configuration can support only a small static load in compression. Thus, the value observed in the one instrumented surface of each tiebar must represent a predominance of bending stress. Such a stress could arise from the hydrodynamic pressure of the nearby discharge (directly below the tiebars) or from elastic buckling associated with downcomer motion. The ventheader stresses reached a maximum of at gauge 131 during the MVA.

9.7 TORUS COLUMN LOAD/SHELL STRESS ATTENUATION

9.7.1 Column Loads

The attenuation of column load with distance from the discharge is shown in Figure 9-2. This plot uses the mean values of column load for each cold pipe discharge bay. The bay distance axis is divided into half bays, taking each pair of inside/outside columns as being one half bay from a discharge in its bay, etc. (A full bay is considered as one-half the distance between Bay A and Bay B, etc.) On the average, the column loads are reduced by about one half for each two bays distant from the source of the SRV discharge.

9.7.2 Shell Stresses

A measure of the attenuation of shell stress with distance from the discharge is indicated in Figure 9-3. The mean stress intensity at outside gauges on the bottom of Bays A, C, and C/D (gauges W6, W3, W1) and near the bottom of Bay D (gauge 4) are plotted for discharges in Bays C, D, and E. Although there is some data scatter, the curves show that the shell stresses attenuate to about one-third of the maximum value over a distance of two bays and remain at a nearly constant value for more distant bays.

9.8 GENERAL OBSERVATIONS

9.8.1 Structural Response Levels

The relative degrees of structural response to the different test conditions can be observed by examining the values for the various strain gages in Table 9-1. It can be seen that, although general trends are indicated, the detailed response relationships vary from location to location, reflecting the unique excitation resultant and characteristic response of the torus structure.

The general trends mentioned in the preceding paragraph are reasonably consistent if a limited region of the structure is considered. For example, limiting to the immediate vicinity of Bay D (OSG 1 through OSG 23), the effects of pipe temperature and water level can be evaluated. These effects assume then the following values.

HP, NWL, SVA:	17 percent reduction in stress	relative to CP, NWL, SVA
HP, DWL, SVA:	27 percent reduction in stress	
HP, EWL, SVA:	23 percent increase in stress	
MVA (three adjacent bays):	20 percent increase in stress	

9.8.2 Response Frequencies

Predominant frequency responses were observed on many of the strain gauge outputs. Study of the plots revealed the following:

a. The free shell, in the vicinity of gauges 2 and 4, commonly exhibited a 16-Hz component.

b. The torus shell structure in the vicinity of the ECCS header exhibited Hz with some higher frequency components in the early stages of SRV action.

c. Gauge 18 near the ring girder indicates Hz, with a beat frequency of approximately Hz.

d. The columns exhibited a predominant frequency of Hz although the first two or three cycles occurred at about , probably coinciding with bubble frequency.

The Hz initial frequency was also observed in other locations for the first two or three cycles, being particularly apparent on the ventheader/downcomer tie bars. These tie bars, especially for MVA, show a strong Hz signal initially, although Hz is the later predominant frequency in the presence of lesser amplitude at about Hz.

9.8.3 Accelerometer Measurements

Typical accelerometer plots are shown in Appendix G. The plots show a rather random acceleration with a predominance of high-frequency content (30 Hz or greater). Some evidence of the SRV bubble action can be detected at lower frequencies; for example, accelerometer A3 exhibits three negative peaks having spacing of about 150 ms. This spacing corresponds to strain gauge signals on several parts of the structure in the vicinity of the discharge. Other than this observation, the accelerometers on the torus shell reveal no distinctive data. The maximum value of acceleration observed during the tests was . on accelerometer No. 3 during Test 1302. Estimating the dominant frequency content of the wave at this point to be Hz, a shell amplitude of 0.018 in. can be calculated, representing a rough estimate of the degree of motion entailed by that point on the torus shell during the discharge. The next highest acceleration was g on accelerometer No. 3 during Test 2306, corresponding to a shell displacement amplitude of 0.013 in., estimating the dominant frequency component as Hz.

Table 9-1

SUMMARY OF STRAIN GAUGE DATA (1 of 3)
(peak principle stresses--ksi)

		(1)				(2)				(3)				(4)	(5)	(6)				(7)				(8)			
Test Condition		CP, NWL				HP, NWL				HP, DWL				HP EWL	MVA	CP, BAY C				HP, BAY C				CP, BAY E			
Test Numbers		2, 501, 801, 901 1301, 1601, 24				802, 902, 903, 904, 905				1303, 1602, 1603 1604, 1605				2305 2306	2301 2302 2303 2304	1101, 14 18, 21				1102, 1103 1104, 1105				12, 15 19, 22			
Gage		Max.	$\overline{X}$	σ	$\sigma/\overline{X}$	Max	$\overline{X}$	σ	$\sigma/\overline{X}$	Max	$\overline{X}$	σ	$\sigma/\overline{X}$	Max	Max	Max	$\overline{X}$	σ	$\sigma/\overline{X}$	Max	$\overline{X}$	σ	$\sigma/\overline{X}$	Max	$\overline{X}$	σ	$\sigma/\overline{X}$
1	O	.6	.5	.1	.17	.8	.6	.1	.18	.5	.4	.1	.12	.5	.9	.6	.5	.1	.16	.4	.4	0	0	.5	.5	0	0
	I	.8	.6	.1	.12	.8	.7	.1	.12	.7	.6	.1	.20	.6	.9	.7	.7	.1	.09	.7	.6	.1	.08	.8	.7	.1	.20
	M	.6	.5	.1	.16	.6	.5	.1	.16	.6	.4	.1	.34	.5	.7	.6	.5	.1	.16	.4	.4	.1	.13	.6	.5	.1	.20
2	O	1.2	1.0	.1	.09	1.4	1.1	.3	.24	1.1	1.0	.2	.18	.9	2.2	1.7	1.2	.4	.30	.9	.8	.2	.23	1.1	1.0	.1	.08
	I	3.2	2.5	.4	.17	3.0	2.4	.4	.15	1.3	1.9	.3	.17	2.4	4.1	2.0	1.8	.1	.08	1.9	1.4	.5	.34	2.1	1.8	.3	.17
	M	1.1	1.0	.1	.13	.9	.8	.1	.15	.7	.6	.1	.08	.8	1.3	.7	.6	.1	.08	.6	.5	.1	.20	.8	.7	.1	.14
3	O	1.1	.9	.1	.16	1.2	.8	.3	.34	.6	.6	.1	.10	.7	1.2	.8	.6	.2	.30	.5	.5	0	0	.9	.7	.3	.40
4	O	2.2	1.7	.3	.16	1.4	1.2	.2	.13	1.8	1.2	.3	.26	1.6	2.1	.9	.7	.1	.17	.8	.7	.1	.13	.9	.8	.1	.06
	I	2.1	1.6	.6	.37	1.6	1.3	.3	.20	1.1	1.0	.1	.11	1.8	2.8	1.0	.9	.1	.14	1.1	.8	.2	.27	1.4	1.1	.3	.30
	M	1.7	1.4	.3	.22	1.0	.9	.1	.18	1.0	.8	.1	.13	1.6	1.8	.6	.5	.1	.16	.5	.4	.1	.20	.6	.5	.1	.10
6	O	1.7	1.3	.3	.20	1.0	.9	.1	.10	1.2	1.0	.2	.16	.9	1.8	.9	.8	.1	.12	.7	.7	.1	.15	.9	.8	.1	.17
	I	2.0	1.8	.1	.08	1.7	1.4	.2	.17	1.7	1.4	.2	.15	2.2	2.4	.9	.8	.1	.16	.9	.7	.2	.23	.9	.8	.1	.10
	M	1.4	1.1	.2	.17	1.0	.7	.2	.28	.8	.6	.1	.18	1.4	1.2	.5	.5	.1	.13	.5	.4	.1	.12	.5	.5	.1	.11
7	O	2.3	1.7	.4	.25	1.5	1.3	.4	.27	1.0	.8	.2	.23	1.3	3.5	1.3	.9	.3	.28	1.0	.8	.2	.21	2.0	1.4	.4	.32
	I	1.3	1.0	.2	.22	.9	.8	.1	.17	.8	.7	.1	.19	1.2	2.0	1.4	.8	.4	.55	1.1	.7	.3	.41	1.0	..8	.2	.18
	M	1.1	.87	.2	.27	1.0	.5	.3	.5	.5	.3	.1	.34	.7	1.0	.7	.4	.2	.59	.4	.4	.1	.16	.8	.5	.2	.47
8	O	2.3	1.4	.5	.38	2.8	1.9	.6	.29	2.4	1.8	.5	.25	1.8	1.9	1.2	1.1	.2	.18	1.3	.9	.3	.30	1.1	1.0	.1	.11
	I	5.0	3.1	1.2	.39	5.1	3.8	1.0	.27	4.5	3.6	.9	.25	2.8	4.3	2.4	2.2	.3	.14	2.8	1.9	.6	.31	2.3	2.1	.2	.09
	M	1.5	1.0	.3	.26	1.5	1.1	.3	.23	1.4	1.1	.3	.25	.9	1.4	.8	.7	.1	.13	.8	.6	.2	.30	.7	.7	.1	.09
9	O	4.0	3.3	.7	.20	4.1	3.4	.4	.14	4.0	3.2	.7	.22	3.6	4.2	2.0	1.6	.3	.18	2.0	1.5	.3	.22	2.4	2.3	.2	.07
	I	2.2	1.5	.4	.28	2.3	1.8	.4	.20	2.2	1.8	.4	.24	2.3	2.7	.9	.8	.1	.13	1.0	.8	.2	.23	1.2	1.2	.1	.05
	M	1.2	1.2	.2	.16	1.0	.7	.2	.29	.8	.6	.2	.24	1.0	1.2	.5	.5	.1	.11	.5	.4	.1	.20	.5	.5	0	0
10	O	1.6	1.4	.2	.15	.9	.7	.1	.15	.9	.7	.1	.15	1.2	1.7	.9	.7	.2	.22	.8	.6	.1	.20	.7	..7	0	0
	I	1.5	1.1	.2	.20	1.1	.9	.2	.18	1.0	.8	.1	.14	1.4	1.5	1.0	.9	.1	.15	.9	.7	.1	.20	.8	.8	.1	.08
	M	1.5	1.2	.2	.15	.8	.6	.1	.24	.9	.5	.2	.41	.9	1.2	.4	.4	.1	.13	.4	.4	.1	.16	.4	.4	0	0
11	O	.9	.5	.2	.38	.5	.4	.1	.18	.5	.4	.1	.26	.4	.7	.5	.5	.1	.13	.4	.4	0	0	.5	.5	.1	.13
12	O	1.2	1.0	.1	.12	1.0	.9	.1	.10	1.0	.9	.1	.13	1.1	1.7	.8	.7	.1	.07	.7	.6	.1	.18	.8	.8	.1	.06
	I	1.6	1.3	.2	.18	.8	.7	.1	.12	.8	.7	.1	.10	1.1	1.8	.8	.7	.1	.20	.7	.6	.1	.24	.7	.7	0	0
	M	1.3	1.1	.2	.17	.6	.5	.1	.16	.6	.5	.1	.17	1.0	1.6	.6	.5	.1	.18	.6	.5	.1	.16	.7	.6	.1	.17
13	O	1.9	1.6	.3	.16	1.2	1.1	.1	.09	1.2	1.1	.2	.14	1.8	2.4	1.0	.8	.2	.18	.8	.7	.1	.20	1.1	.9	.2	.18
	I	1.9	1.5	.3	.19	1.5	1.0	.3	.27	1.2	.8	.2	.29	1.7	1.6	1.1	.8	.2	.30	1.0	.7	.2	.26	.9	.8	.1	.10
	M	1.6	1.3	.2	.13	1.1	.8	.2	.31	.8	.7	.1	.17	1.5	1.4	.6	.5	.1	.16	.4	.4	.1	.13	.6	.5	.1	.10
14	O	1.9	1.4	.4	.25	1.1	.8	.2	.32	.8	.7	.1	.14	1.1	1.8	.8	.6	.1	.24	.6	.5	.1	.20	.8	.7	.1	.14
	I	1.8	1.6	.2	.10	1.2	1.1	.1	.04	1.5	1.1	.3	.23	1.6	1.9	.8	.6	.2	.24	.8	.6	.1	.20	.9	.7	.2	.21
	M	1.4	1.2	.2	.12	1.0	.7	.2	.25	.8	6	.2	.24	1.2	1.6	.5	.4	.1	.12	.6	.4	.2	.40	.5	.4	.1	.12
15	O	1.3	1.2	.2	.14	1.3	1.1	.2	.18	1.1	1.0	.2	.17	1.3		1.0	.9	.1	.13	1.1	.9	.2	.23	1.1	.9	.2	.22
	I	1.6	1.3	.2	.16	1.1	1.0	.1	.13	1.5	1.0	.3	.33	1.4	1.6	.8	.7	.1	.07	1.0	.7	.2	.29	.7	.7	.1	.09
	M	1.3	1.1	.2	1.5	1.0	.7	.2	.20	1.2	.7	.3	.38	1.3		.7	.5	.1	.24	.6	.5	.1	.20	.6	.5	.1	.11

$\overline{X}$ - Mean
σ - Standard deviation

Gage Units - ksi
Columns - kips and inch-kips

O - Outside torus
I - Inside torus
M - Membrane

CP - Cold pipe
HP - Hot pipe
NWL - Normal water level

DWL - depressed water level
EWL - elevated water level
MVA - multiple valve actuation

Table 9-1

SUMMARY OF STRAIN GAUGE DATA (2 of 3)
(peak principle stresses--ksi)

		(1)				(2)				(3)				(4)	(5)	(6)				(7)				(8)			
Test Condition		CP, NWL				HP, NWL				HP, DWL				HP EWL	MVA	CP, BAY C				HP, BAY C				CP, BAY E			
Test Numbers		2, 501, 801, 901 1301, 1601, 24				802, 902, 903, 904, 905				1303, 1602, 1603 1604, 1605				2305 2306	2301 2302 2303 2304	1101, 14 18, 21				1102, 1103 1104, 1105				12, 15 19, 22			
Gage		Max.	$\overline{X}$	σ	σ/$\overline{X}$	Max	$\overline{X}$	σ	σ/$\overline{X}$	Max	$\overline{X}$	σ	σ/$\overline{X}$	Max	Max	Max	$\overline{X}$	σ	σ/$\overline{X}$	Max	$\overline{X}$	σ	σ/$\overline{X}$	Max	$\overline{X}$	σ	σ/$\overline{X}$
16	O	1.5	1.2	.2	.16	1.1	.8	.2	.25	.9	.8	.1	.12	1.0		.6	.6	.1	.10	.6	.5	.1	.10	.7	.6	.1	.14
17	O	2.5	2.1	.2	.11	2.9	2.3	.5	.22	2.1	1.8	.3	.15		4.3	2.7	2.4	.3	.13	1.6	1.2	.3	.23	2.2	1.9	.2	.11
18	O	1.9	1.7	.2	.11	1.7	1.2	.3	.23	1.5	1.2	.4	.30	1.8	2.6	1.6	1.4	.1	.09	1.4	1.2	.3	.22	1.8	1.7	.1	.08
19	O	2.0	1.5	.3	.16	1.3	1.0	.2	.22	.9	.8	.1	.15	1.6	1.6					1.3	.8	.4	.46	.8	.7	.1	.20
20	O	1.2	1.0	.1	.15	1.2	.8	.3	.32	1.0	.8	.2	.20	.9	1.5	.7	.7	.1	.07	.9	.7	.2	.32	.7	.7	.1	.09
21	O	1.7	1.3	.3	.19	.9	.8	.1	.14	.9	.8	.1	.13	1.0	1.5	.7	.6	.1	.14	.7	.6	.1	.22	.6	.5	.1	.10
22	O	2.7	1.8	.5	.25	1.3	1.1	.2	.16	1.4	1.1	.2	.18	1.5	2.2	.8	.7	.1	.20	1.0	.8	.2	.19	1.0	.8	.1	.18
23	O	1.6	1.4	.3	.2	3.0	1.9	.8	.42	1.8	1.4	.4	.30	1.5	1.7	.8	.7	.1	.14	.9	.8	.1	.17	.9	.8	.1	.12
	I	1.8	1.6	.2	.14	1.3	1.1	.2	.14	1.6	1.1	.3	.30	1.6	1.8	.8	.8	.1	.08	.8	.7	.1	.15	.8	.8	.1	.08
	M	1.6	1.4	.3	.24	1.3	.9	.3	.32	1.1	.8	.2	.27	1.5	1.5	.6	.5	.1	.20	.5	.4	.1	.12	.5	.5	.1	.11
24	O	3.3	2.8	.4	.14	1.3	1.1	.2	.20	1.5	1.2	.3	.22	2.6	4.2	.7	.6	.1	.08	1.1	.7	.3	.36	1.7	1.6	.1	.07
25	O	3.0	2.7	.4	.14	1.8	1.6	.3	.18	2.3	1.7	.4	.25	3.2	3.7	1.0	.8	.2	.18	1.0	.8	.2	.18	1.5	1.4	.2	.11
26	O	1.6	1.4	.2	.16	1.0	.7	.2	.25	.8	.7	.1	.20	1.4	1.9	.5	.5	.1	.11	.5	.4	.1	.12	.9	.8	.1	.10
31	O	1.5	1.2	.2	.16	.8	.7	.1	.12	.8	.6	.3	.50	.9	1.4	.7	.6	.1	.17	.6	.5	.1	.2	.8	.7	.2	.22
32	O	4.4	3.4	.6	.16	3.8	2.7	.7	.25	3.7	2.9	.5	.17	2.7	7.6	5.9	5.2	.6	.11	3.0	2.6	.6	.22	2.7	2.6	.2	.06
	I	5.2	3.9	.8	.19	4.6	3.1	.9	.29	4.2	3.4	.5	.16	3.7	8.8	6.3	5.6	.7	.13	3.5	3.1	.6	.18	2.6	2.4	.2	.09
	M	.8	.6	.1	.21	1.2	.7	.3	.42	.9	.5	.2	.38	.6	1.1	1.6	1.0	.4	.44	.8	.7	.2	.33	.6	.6	.06	.10
33	O	2.5	2.0	.4	.20	1.8	1.7	.1	.06	2.1	1.7	.3	.19	2.2	4.8	4.2	3.1	1.0	.32					2.5	2.3	.3	.11
	I	3.6	2.6	.7	.26	2.7	2.3	.3	.12	4.2	2.8	.8	.30	2.7	5.4	5.7	4.5	1.2	.27					2.8	2.4	.4	.17
	M	.9	.8	.1	.10	.8	.5	.3	.47	1.7	.8	.5	.70	.6	1.1	.9	.8	.1	.13					.9	.7	.2	.21
34	O	1.2	.9	.3	.34	1.2	1.0	.2	.22	1.1	.8	.3	.32	.8	1.6	1.0	.9	.2	.17	.8	.6	.1	.2	1.0	.9	.1	.15
35	O	3.4	1.4	1.4	.99	1.3	.9	.3	.37	1.0	.7	.3	.45	1.0	1.2	.8	.7	.1	.14	.9	.5	.3	.63	1.1	.9	.2	.20
131	I	3.5	2.7	.5	.19	1.7	1.3	.3	.22	1.4	1.0	.3	.28	2.3	4.4	1.2	1.0	.2	.18	.5	.4	.1	.26	1.1	1.0	.1	.10
132	I	1.9	1.6	.2	.14	1.0	.7	.2	.28	.8	.6	.2	.24	1.3	3.2	1.2	1.0	.2	.16	.5	.4	.1	.34	1.2	1.1	.1	.13
133	I	2.1	1.3	.4	.27	1.0	.8	.1	.17	.8	.6	.2	.26	1.1	2.2	.5	.4	1	.26	.4	.3	1	.27	.6	.5	1	.10
134	I	16.0	12.6	2.3	.18	4.9	4.2	.5	.13	5.1	3.9	1.0	.25	6.5	17.0	10.0	9.2	.7	.08	4.5	2.5	1.4	.59	11.4	11.2	1.6	.14
135	I	22.0	11.8	5.4	.46	4.7	3.0	.6	.20	2.4	2.3	.5	.20	3.8	31.0	8.8	.7	1.0	.14	2.0	1.5	.4	.28	9.5	8.2	1.7	.21

Table 9-1

SUMMARY OF STRAIN GAUGE DATA (3 of 3)
(peak principle stresses--ksi)

		(1)				(2)				(3)				(4)
Test Condition		CP, NWL				HP, NWL				HP, DWL				HP EWL
Test Numbers		2, 501, 801, 901 1301, 1601, 24				802, 902, 903, 904, 905				1303, 1602, 1603 1604, 1605				2305 2306
Gage		Max.	$\bar{X}$	σ	$\sigma/\bar{X}$	Max	$\bar{X}$	σ	$\sigma/\bar{X}$	Max	$\bar{X}$	σ	$\sigma/\bar{X}$	Max
W1	0	1.4	1.2	.2	.13	.9	.7	.2	.20	.9	.8	.1	.14	.8
W2	0	.8	.6	.1	.20	.6	.5	.1	.25	.6	.6	0	0	.5
W3	0	.8	.7	.1	.17	.6	.5	.1	.10	.7	.6	.1	.14	.6
W4	0	.6	.5	.1	.20	.5	.4	.1	.25	.4	.4	.1	.2	.4
W5	0	.4	.3	.1	.35	.3	.3	.1	.22	.3	.3	.1	.22	.2
W6	0	.7	.6	.1	.17	.6	.4	.1	.26	.5	.4	.1	.20	.7
W7	0	.6	.5	.1	.20	.5	.4	.1	.32	.4	.3	1	.26	.6
W8	0	.8	.6	.1	.18	.8	.6	.1	.18	.7	.6	.1	.24	.8
COLUMNS														
A1	UP	7	3.3	2.0	.60	3	.8	1.9	2.40	3	.8	1.3	1.63	3
	DN	6	4.2	1.6	.38	5	3.2	1.3	.41	5	2.8	1.8	.64	0
A2	UP	7	5.3	1.1	.21	6	4.2	1.9	.46	6	5.4	.9	.17	0
	DN	7	6.0	1.2	.19	7	4.6	1.5	.33	6	3.2	2.6	.81	6
B1	UP	18	12.7	3.0	.23	11	6.0	2.6	.44	8	7	.7	.10	8
	DN	15	12.1	2.1	.17	9	6.4	1.8	.28	8	6.8	1.6	.24	10
B2	UP	8	5.3	1.7	.32	8	6.0	1.2	.20	6	4.4	1.1	.26	6
	DN	7	5.6	1.6	.29	8	5.6	2.0	.35	6	4.6	1.1	.25	3
D1	UP	56	49.0	6.6	.14	40	28	8.3	.30	30	23.4	5.0	.21	50
	DN	91	66.7	14.9	.22	50	36	11.3	.31	40	29.0	7.2	.25	60
	MOM	125	108.4	17.0	.16	185	142	29.9	.21	171	121.8	32.7	.27	83
D2	UP	47	38.3	4.9	.13	31	23	8.0	.34	28	22.2	3.8	.17	45
	DN	66	55.4	9.7	.17	40	31	5.6	.18	35	28.0	7.3	.26	63
	MOM	98	83.3	12.3	.15	61	46	8.7	.19	42	37.0	4.6	.13	74
D3	UP	51	35.1	8.1	.23	33	24	8.9	.37	29	20.0	7.9	.39	38
	DN	63	50.6	9.2	.18	35	26	6.4	.25	39	30.0	5.9	.20	57
	MOM	105	94.0	8.1	.09	49	44	3.6	.08	47	42.0	6.8	.16	74
D4	UP	49	40.0	6.2	.16	39	25	8.6	.34	31	18.8	8.1	.43	35
	DN	66	49.6	12.8	.26	29	22	3.9	.18	37	24.6	8.3	.34	53
	MOM	88	63.7	12.7	.20	46	40	7.3	.19	43	30.6	7.0	.23	51

		(5)	(6)				(7)				(8)			
Test Condition		MVA	CP, BAY C				HP, BAY C				CP, BAY E			
Test Numbers		2301 2302 2303 2304	1101, 14 18, 21				1102, 1103 1104, 1105				12, 15 19, 22			
Gage		Max	Max	$\bar{X}$	σ	$\sigma/\bar{X}$	Max	$\bar{X}$	σ	$\sigma/\bar{X}$	Max	$\bar{X}$	σ	$\sigma/\bar{X}$
W1	0	2.7	1.5	1.3	.2	.19	1.7	1.0	.5	.5	1.5	1.1	.3	.26
W2	0	1.6	.8	.7	.1	.13	1.5	.8	.5	.55	.8	.7	.1	.13
W3	0	3.4	2.8	2.7	.2	.1	2.9	1.7	.8	.47	1.0	.9	.1	.11
W4	0	3.1	2.4	2.2	.3	.13	2.0	1.4	.4	.33	2.0	1.2	.6	.51
W5	0	2.4	2.2	2.0	.2	.09	1.3	1.0	.3	.26	.7	.5	.1	.28
W6	0	1.2	.7	.7	.1	.15	1.8	.9	.7	.76	1.1	.9	.1	.16
W7	0	.9	.6	.5	.1	.16	.6	.5	.1	.29	1.2	.8	.3	.32
W8	0	.7	.4	.3	.1	.29	.4	.3	.1	.27	.6	.4	.2	.40
COLUMNS														
A1	UP	39	35	31.2	3.3	.11	14	12.3	1.5	.12	3	1.5	1.3	.86
	DN	28	27	24.5	2.9	.12	17	12.8	4.2	.33	2	2	2.2	8.9
A2	UP	6	2	.8	1.5	2.00	1	.3	1.3	5.03	9	9	0	0
	DN	11	7	4.3	2.1	.49	5	2.5	2.7	1.06	13	11.0	1.8	.17
B1	UP	63	50	46	5.4	.12	26	20.0	4.2	.21	15	13.0	1.8	.14
	DN	53	43	39.5	4.0	.10	25	21.8	3.8	.17	18	14.3	3.0	.21
B2	UP	52	43	39.3	3.5	.09	22	19.3	2.5	.13	3	1.5	1.3	.86
	DN	34	34	30.3	3.0	.10	21	19.0	1.4	.07	5	2.0	2.5	1.22
D1	UP	61	20	14.3	6.1	.43	20	14	4.3	.31	39	31.8	4.9	.16
	DN	101	20	13.3	4.6	.35	18	13.5	4.1	.31	50	43.3	4.6	.11
	MOM	159	91	84.8	7.2	.09	92	73.8	16.0	.22	99	85.3	10.4	.12
D2	UP	59	18	4.3	4.5	.32	12	9.0	2.9	.33	27	22.5	3.7	.16
	DN	87	24	19.5	3.0	.15	15	11.3	3.3	.29	40	36.0	3.3	.09
	MOM	159	87	78.3	8.5	.11	50	35.8	11.1	.31	101	80.0	14.7	.18
D3	UP	59	27	26.3	.5	.02	21	13.5	6.6	.49	17	13.0	4.6	.36
	DN	58	50	40.3	7.8	.19	31	25.0	5.8	.23	17	13.0	4.6	.36
	MOM	182	107	100.0	8.3	.08	53	44.3	6.1	.14	74	71.5	2.7	.04
D4	UP	59	39	35.8	4.7	.13	29	20.0	6.5	.32	10	10	0	0
	DN	59	49	37.3	10.0	.27	20	14.5	4.2	.29	10	10	0	0
	MOM	111	67	57.3	8.8	.15	41	31.3	6.5	.21	64	52.0	8.5	.16

UP - Column Upload

DN - Column download

MOM - Column moment

Table 9-2

MAXIMUM INSTANTANEOUS COLUMN LOADS (KIPS)

		Test Numbers						
Column	Time & Direction	904	1301	1605	18	22	2302	2306
	Time[1] (ms)	1740	4720	2030	4340	3770	4520	2170
D1	UP	40	49	30	19	39	59	50
D2	UP	31	36	28	18	27	57	45
D3	UP	33	26	29	26	9	53	38
D4	UP	29	39	31	36	10	49	35
	Sum	133	150	118	99	85	218	168
	Time	1700	4660	1990	4290	3720	4610	2120
D1	DN	50	91	40	11	41	91	60
D2	DN	40	63	35	18	36	87	63
D3	DN	35	51	31	43	9	58	57
D4	DN	29	59	37	42	10	59	53
	Sum	154	264	143	114	96	295	233
	Time[1]	1360	1350	980	950	290	1100	590
A1	UP	4	7	1	32	2	32	3
A2	UP	6	7	6	0	9	3	(1)
	Sum	10	14	7	32	11	35	2
	Time	1540	1300	1340	1000	400	1150	880
A1	DN	4	6	3	27	(3)	26	(2)
A2	DN	7	5	6	4	13	10	6
	Sum	11	11	9	31	10	36	4
	Time	1120	1410	810	940	290	1090	730
B1	UP	11	18	7	48	14	44	8
B2	UP	8	8	6	38	2	41	(2)
	Sum	19	26	13	86	16	85	6
	Time	1160	1610	1020	990	330	1140	68-
B1	DN	9	14	8	42	18	46	10
B2	DN	8	7	5	34	(1)	33	(2)
	Sum	17	21	13	76	17	79	8

[1]For reference only. There is no time correlation between tests or between Columns D and Columns A and B.

[2]Parentheses denote UP load in "DN" group and vice versa.

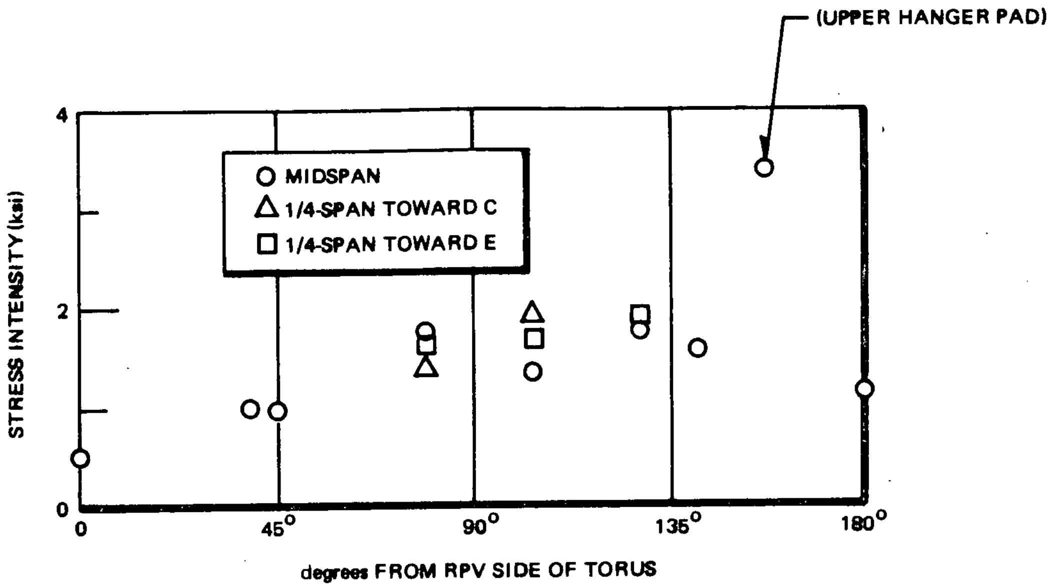

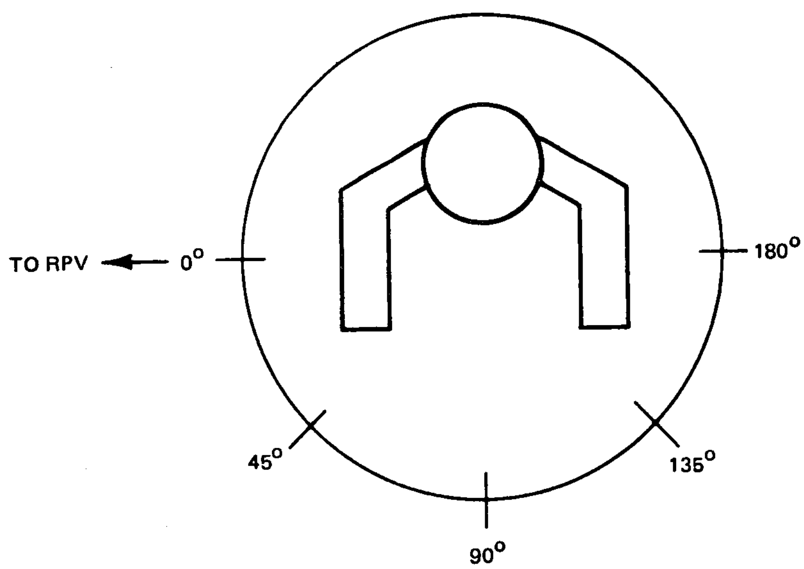

Figure 9-1. Stress Variation Around Bay D (Average of maximum values from cold pipe tests)

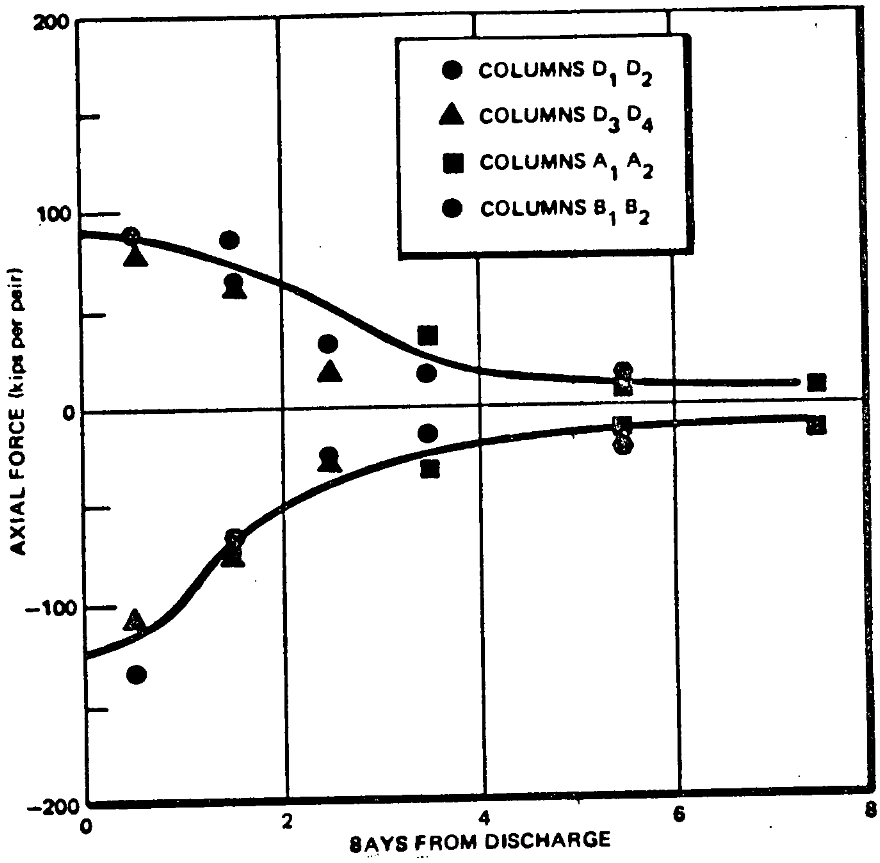

Figure 9-2. Attenuation in Columns (Sum of maximum values of inside and outside column from cold pipe tests)

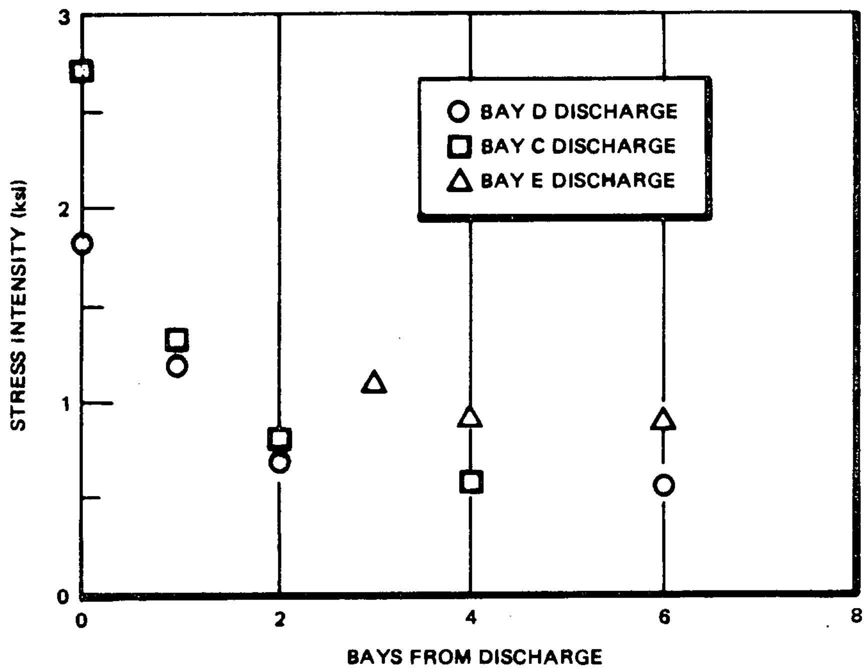

Figure 9-3. Attenuation in Shell (Average of maximum values from cold pipe tests.)

10. DISCUSSION OF T-QUENCHER AND SRV PIPING RESULTS

10.1 INTRODUCTION

The SRV piping is 10-in. schedule 40 in the drywell and schedule 80 in the torus. The material of the pipe is ASTM 106, Grade B, carbon steel; total length is about 103 feet with a normal water leg of 13.50 ft.

10.2 DATA REDUCTION AND EVALUATION METHOD

There were ten uniaxial strain gauges, ten rosettes and two biaxial accelerometers on the SRV piping, SRV supports, quencher and quencher support (see Figures 4-14, 4-15, 4-16, 4-17). Strain gauge locations were selected so that the stress concentration factor would be close to unity. The two rosettes on the ramshead of the T-Quencher SG 55 and SG 56 are an exception. They were placed on the expected maximum stress concentration locations to determine if stresses exceeded safe limits during the test. Strain measurements on the SRV piping and quencher contained thermal stresses caused by the temperature gradient through the pipe wall thickness. The stresses reported are the dynamic oscillations from the mean of the strain measurements.

Appendix H tables H-1 through H-3 show the maximum stresses for each strain gauge measurement. The principal stresses for all the rosettes were also tabulated. Because of possible different thermal stresses in each strain gauge of the rosette, the principal stress calculations may not be accurate.

All the A direction legs of the rosettes and all the uniaxial strain gauges were aligned along the center line of the pipe. The C direction legs of rosettes were in the circumferential direction of the pipe. Since all the dynamic loads caused bending stresses in the longitudinal direction (except for the rosettes on the T-Quencher of the ramshead), the longitudinal stresses will be close to the principal stress direction; therefore, the A direction legs of the rosettes or uniaxial strain gauge measurement were used for all comparisons. SG55 is located on the center of the ramshead of the quencher.

The B direction leg of this rosette measured higher stress than the other two directions; therefore, the B direction leg measurements will be used for comparison.

The transient pressure inside the pipe increases the strains in the circumferential direction. The strain increment due to the pressure in the longitudinal direction is less than one-fourth the increment in the circumferential direction. The strain measured in the longitudinal direction is considered to be caused by dynamic bending loads alone.

10.3 T-QUENCHER STRESSES

10.3.1 Instrumentation and Test Data Summary

There were five rosettes and one uniaxial strain gauge on the T-Quencher, and one biaxial accelerometer on the ramshead of the T-Quencher. The accelerometer on the ramshead of the T-Quencher did not provide reasonable wave forms or magnitude data (see Figure 10-20) and therefore cannot be used in the load assessment.

The maximum stresses due to dynamic loads for the gauges on the T-Quencher were summarized from gauges SG51 through SG56 (see Tables 10-1 to 10-3). The data are grouped according to test conditions.

Typical strain time history plots for SG54 and SG55A for each test condition are shown in Figures 10-2, 10-5, 10-8, 10-11 and 10-14.

10.3.2 Results of T-Quencher Stresses

Strain gauge 55B, located on the center of the ramshead of the T-Quencher, recorded the maximum stresses on the T-Quencher under the water clearing thrust load. The highest stress recorded by this sensor was 4480 psi during a cold pipe, single valve, normal water level test (Test 501). This is about 1/3 to 1/4 of the ASME allowable stress.

For single valve actuation and normal water level condition, cold pipe conditions produced slightly higher stress than did hot pipe conditions (about 10 percent).

There were no significant differences between the stress values for hot pipe normal water level, elevated water level or depressed water level.

10.4 T-QUENCHER SUPPORT STRESSES

10.4.1 Instrumentation and Test Data Summary

There were two rosettes and one uniaxial strain gauge on the T-Quencher support and one biaxial accelerometer on the center of the support. The accelerometer in the vertical direction did not provide consistent data, but good data was obtained in the horizontal direction perpendicular to the quencher.

The maximum stresses due to dynamic loads for the gauges on the T-Quencher support were summarized from gauge SG50 through A9H on the Tables 10-1 through 10-3. The data are grouped according to test conditions.

Typical strain time history plots for SG60 and A9H for each test condition are shown in Figures 10-3, 10-6, 10-9, 10-12 and 10-15.

10.4.2 Results

Strain gauge 60 was located on the middle span of the T-Quencher support pipe and recorded the maximum stresses on the support under water clearing thrust load.

The highest stress measured for the quencher support was   psi from single valve, normal water level, both cold pipe and hot pipe conditions (SG60, Tests 801 and 903). This about 1/3 to 1/4 of the ASME allowable stress.

SG61A also recorded a high stress   psi during Test 2306, elevated water level.

The maximum horizontal acceleration recorded from A9H was   from Test 2306, elevated water level. The acceleration from Test 2305 is   In most of the tests the accelerations are about   Further discussions of the measured values are presented in paragraph 10.6 (g), (h), (c).

10.5 SRV DISCHARGE PIPE/PIPE SUPPORT STRESSES

10.5.1 Instrumentation and Test Data Summary

The strain gauge type and locations for SRV discharge pipe/pipe support are tabulated below.

SG39	Uniaxial	On main steam branch pipe
SG40	Uniaxial	On vent pipe at the SRV pipe penetration
SG 41, 42, 45, 46	Uniaxial	On SRV pipe in the torus
SG43	Uniaxial	On beam A for SRV pipe support
SG44	Uniaxial	On beam B for SRV pipe support
SG 47, 48, 49	Rosette	On SRV pipe near T-Quencher

The maximum stresses due to dynamic loads recorded by these gauges are summarized from SG39 through SG49 of Tables 10-1 through 10-3.

Typical strain time history plots for SG41 and SG39 for each test condition are shown in Figures 10-1, 10-4, 10-7, 10-10 and 10-13.

10.5.2 Results

Strain gauge 39, located on the branch pipe between the main steam pipe and the SRV in the direction of bending due to SRV blowdown transient wave load, recorded highest stress,   psi, during test 901, cold pipe condition. Water level should not affect the measurement in this area if the pipe is properly supported. Multiple valve actuation did not create higher stresses than single valve actuation in either hot pipe or cold pipe condition. The highest stress recorded from SG40 was psi.

The maximum stresses measured for the SRV pipe in the torus was psi during cold pipe, normal water level test. This is about 1/3 to 1/4 of ASME allowable stress. There is no significant difference of stress reading for each test condition. An approximate order of magnitude comparison is: cold pipe > elevated water level > hot pipe > multiple valve cold pipe > depressed water level.

The maximum stress measured for the SRV pipe support in the torus was psi during elevated water level test.

10.6 GENERAL OBSERVATIONS

a. Approximation of time relationship of the SRV blowdown events were as follows (data obtained from Test 501, cold pipe, normal water level, single valve actuation, see Figures 10-16 and 10-17):

		Time (sec)
(1)	SRV opened	
(2)	Stress at branch pipe started	
	Significant stress at branch pipe ended (25% peak value)	
	All stress at branch pipe ended (10% peak value) peak stress occurred	
(3)	Quencher stress started (SG55B)	
	Peak stress occurred at (55B due to peak pressure, See Figure 10-16)	
	Significant stress in quencher arm	
	Peak bending stresses in the quencher arm	
(4)	Pressure in pool due to air clearing started	
	Significant different pressure on both side of quencher	
	Peak pressure in pool occurred at	

	Time (sec)
(5) Pressure rise in the ramshead of the T-Quencher started	
Peak pressure occurred at	
Pressure rise in the ramshead of the T-Quencher ended	

b. Peak bubble pressure existed after the significant stress in the SRV branch pipe disappeared, indicating that the stresses in the drywell piping were not affected by the air clearing phenomenon.

c. Peak stress in the SRV piping, T-Quencher and quencher support appeared before peak air bubble pressure occurred. Therefore, water clearing thrust load is considered the most important load for the design of the wetwell SRV pipe, T-Quencher and its support structure.

d. The approximate magnitude of the stresses in the quencher resulting from various dynamic loads associated with SRV actuation are tabulated below:

	Stress	Location	Test No.	Time (sec)
Water clearing	5000	55B	501	
Air clearing	2100	55B	501	
Drag due to adjacent valve blowdown	500	55B	1104	

e. The measured stresses in the T-Quencher ramshead were only slightly higher than those near the support points, indicating that the support points of the quencher were not only well chosen resulting in a uniform stress distribution, but also that the ramshead was well reinforced.

f. SRV piping in the torus vibrated at a frequency of approximately Hz. The quencher support vibrated at approximately Hz.

g. The accelerometer A9H measured the acceleration of the quencher support. During the blowdown in the adjacent bay, a low frequency vibration at about Hz, was measured. The maximum accelerations of the low frequency vibrations are tabulated below:

Test No.	Bay	Acceleration (g)
14	F	
18	F	
21	F	
1101	C	
1102	C	
1103	C	
1104	C	
1105	C	
15	E	
19	E	
22	E	

Double integration of the accelerations at the low frequency vibration resulted in large displacements in the order of 50 inches.

The low frequency vibrations had only half-cycle duration and always along the same direction. After the half-cycle of the low frequency vibration, the vibration decayed rapidly to zero.

The low frequency vibration indicates that the magnitude of the measurement of the accelerometer A9H is not consistent with the fact that the quencher displacements are small.

The accelerations of the torus support column were compared and no low frequency vibrations were found, indicating that the measurements from A9H contain zero shift and the magnitude of the measurement may not be proportional for the whole range.

h. The acceleration of the quencher support from Test 2306 was 99g at a frequency of 10 Hz. The displacement calculated from the acceleration is excessive, but the strain measurement did not show the same result; this leads to the same conclusion - that the magnitude of the measurement of A9H may not be accurate.

i. Although the magnitude of the measurement of A9H may not be accurate, there is an indication that the peak accelerations not only function with the peak pressure from P7, but also function with the duration of the pressure transient. Therefore, the measurements of A9H are also an indication of water clearing thrust loads. Strain measurements indicated the total effect of water clearing loads; A9H measurements indicated instantaneous effect (peak load may be only in the order of one thousandth of a second) (see Figure 10-19). The following table shows the peak pressures from P7 and the maximum g loads from A9H (see Figure 10-19).

Test No.	2	501	801	901	1301	1601	24	802	902	903	904
P7	180	278	234	180	182	161	155	142	140	149	189
A9H	10.8	26.6	14.2	10.1	19.0	12	8.2	11.2	11.5	23.7	13.0

Test No.	905	2305	2306	1303	1602	1603	1604	1605
P7	169	198	418	200	122	176	207	141
A9H	11.6	39.2	99	14.5	10.4	38.8	17.7	10.6

j. Test 2306, elevated water level test, the peak water clearing load is much higher than other tests. The duration of the peak thrust load must be short (in the order of one thousand of a second) because the peak thrust is still unable to stress the pipe to a level higher than other test conditions (see appendix tables H1 and H2) (i.e., the load may be high but for a short duration; therefore, the energy content is insufficient to put large stresses in the system).

k. The difference of pressure difference from P8, P9, P10 and P11 for Test 2 is shown in Figure 10-18. The strain measurement from 47A, which indicates the effect due to the difference of pressure difference, is also shown in Figure 10-18. By comparing the figure, the first peak which occurred at time 4922 MS did not create significant stresses because of its short duration. The subsequent peak at time 5020 MS and 5100 MS created significant stresses because of its longer duration.

l. SG51A, SG52A, SG53A were the strain gauges in the longitudinal direction of the T-quencher; they are at the same location but 90° apart in circumferential direction. There were no high stresses recorded at the same time, and same direction for those three gauges, indicating that the stresses caused by internal pressure or axial forces are not significant for the quencher arm.

m. SG55B and SG56A at the ramshead of the T-quencher measured high stress. The direction and timing are the same as the peak pressure in the ramshead of the quencher (See Figures 10-16 and 10-17). This indicated that water clearing thrust load plus peak pressure created peak stresses.

n. Thermal stresses, primarily due to temperature gradient effects, have been found in the strain gauges on the SRV pipe and T-quencher. Only minor portions of the thermal stresses are caused by bending loads on the pipe due to thermal expansion. This conclusion is based on the fact that thermal stresses on both sides of the pipe have about the same magnitude and direction, which would not occur if loads were due to bending. The magnitude of the thermal stresses have been found to be less than 25000 psi.

The temperature gradient stresses measured by SG41 and SG42 during hot pipe tests are smaller than cold pipe tests because the initial temperature differences between steam and pipe are smaller for hot pipe tests than for cold pipe tests. For all gauges under the water there are no big differences of temperature gradient between cold pipe tests and hot pipe tests because of the cooling effect of the water.

Table 10-1

SUMMARY OF SRV STRESS DATA*

TEST COND	Sensors 39	40	41	42	43	44	45	46	47A	47B	47C	48A	48B	48C	49A	49B	49C	51A	51B	51C
SVA,CP,NWL																				
MAX. VAL	5600	1960	5600	4760	4200	3920	3640	3920	3360	1400	1680	3080	1680	1120	4200	2240	700	3360	1960	1680
MEAN VAL	4660	1820	4360	4100	3080	2580	2360	2700	2660	1000	980	2380	1220	900	3120	1760	580	2480	1580	980
STND DEV	0.10	0.11	0.24	0.15	0.20	0.37	0.27	0.28	0.26	0.33	0.39	0.24	0.20	0.28	0.17	0.15	0.17	0.22	0.20	0.60
CVA,HP,NWL																				
MAX. VAL	4760	1960	5320	4760	4480	3500	3640	3080	2240	980	840	2520	1400	1120	3080	1400	840	2800	1680	1120
MEAN VAL	4396	1624	4760	3976	3696	2212	2884	2800	1904	812	700	2324	1036	756	2688	1344	672	2576	1344	1008
STND DEV	0.05	0.14	0.12	0.17	0.15	0.34	0.26	0.07	0.12	0.19	0.20	0.08	0.26	0.31	0.12	0.09	0.27	0.09	0.17	0.18
CVA,HP,EWL																				
MAX. VAL	5040	1960	5320	4480	6160	3360	2800	3500	2240	1120	1120	1680	1680	1960	2800	1680	1120	2240	1120	840
CVA,HP,DWL																				
MAX. VAL	4480	1680	4760	3920	4200	1820	0	3080	2520	1820	1120	2800	1400	840	3920	1960	1120	3640	2240	1680
MEAN VAL	4396	1512	4368	3584	3780	1736	0	2688	1960	1232	840	2156	1120	784	3192	1512	784	2744	1680	1120
STND DEV	0.03	0.08	0.08	0.10	0.12	0.04		0.16	0.20	0.42	0.20	0.20	0.18	0.10	0.21	0.21	0.30	0.20	0.31	0.40
MVA,CP,NWL																				
MAX. VAL	5180	1960	4760	4480	3220	2520	2520	2800	3360	1400	1120	2800	1120	840	3080	2240	560	2380	1260	1120
MEAN VAL	4445	1750	3955	3640	2625	1890	1890	2170	2590	945	945	2625	910	770	2660	1715	560	1995	1050	280
STND DEV	0.12	0.08	0.14	0.17	0.16	0.25	0.31	0.19	0.24	0.33	0.22	0.08	0.15	0.18	0.20	0.21	0.	0.14	0.17	2.00
BAY C CP																				
MAX. VAL	1400	420	840	840	1120	700	840	560	1120	560	280	1120	560	280	560	560	280	840	420	420
MEAN VAL	1260	280	735	665	945	490	420	525	875	350	210	805	420	210	420	350	140	560	210	175
STND DEV	0.13	0.41	0.29	0.20	0.14	0.37	0.86	0.13	0.27	0.40	0.38	0.36	0.27	0.38	0.27	0.40	0.82	0.41	0.86	1.01
BAY C HP																				
MAX. VAL	1820	140	560	560	840	700	420	560	700	280	280	840	280	280	420	140	140	560	140	280
MEAN VAL	1505	140	385	455	770	595	315	385	490	175	210	455	245	175	315	140	140	420	140	175
STND DEV	0.24	0.	0.35	0.29	0.10	0.23	0.22	0.35	0.37	0.40	0.38	0.68	0.29	0.40	0.22	0.	0.	0.38	0.	0.40
BAY E CP																				
MAX. VAL	560	280	700	560	1120	560	560	700	1120	560	560	1120	560	560	560	560	140	560	280	140
MEAN VAL	315	245	560	525	875	455	455	630	875	490	385	875	420	315	315	280	140	525	245	70
STND DEV	0.56	0.29	0.35	0.13	0.20	0.29	0.15	0.13	0.20	0.29	0.35	0.20	0.27	0.56	0.67	0.71	0.	0.13	0.29	1.15

*For notes see Table 10-3

Table 10-2

SUMMARY OF SRV STRESS DATA

TEST COND	52A	52B	52C	53A	53B	53C	54	55A	55B	55C	56A	56B	56C	60	61A	61B	61C	62A	62B	62C	A9H
SVA,CP,NWL																					
MAX. VAL	2800	2240	1680	2520	1400	1960	3920	3920	4480	4200	3360	3080	2800	5600	3360	1960	840	3360	1680	1120	
MEAN VAL	2420	1720	1160	1620	1100	1320	3380	2220	3480	2960	2720	2180	2200	4800	2420	1440	640	2600	1240	860	
STND DEV	0.10	0.22	0.32	0.31	0.24	0.24	0.14	0.38	0.19	0.24	0.19	0.25	0.15	0.11	0.24	0.31	0.17	0.23	0.29	0.24	
CVA,HP,NWL																					
MAX. VAL	3080	1680	1960	2240	1400	1680	3360	1960	3920	3360	2800	1960	3080	5600	2660	1400	700	2240	1120	1120	
MEAN VAL	2296	1428	1764	1596	1176	1092	2996	1624	3304	2968	2408	1624	2408	5208	2016	1008	504	1876	868	784	
STND DEV	0.20	0.15	0.11	0.26	0.11	0.32	0.13	0.19	0.13	0.11	0.10	0.14	0.19	0.06	0.21	0.25	0.25	0.12	0.18	0.27	
CVA,HP,EWL																					
MAX. VAL	2520	1680	1960	2240	1120	1120	3220	1960	3080	2800	2240	1960	1960	4760	5600	1960	1400	4200	1680	1260	
CVA,HP,DWL																					
MAX. VAL	3080	1680	2240	2520	1540	1120	3360	1960	4200	3640	2800	1960	3640	5320	2240	1120	700	2240	840	840	
MEAN VAL	2352	1456	1848	1792	1232	924	2604	1680	3332	2856	2268	1736	2632	4788	1736	924	560	1708	728	756	
STND DEV	0.23	0.25	0.17	0.34	0.22	0.14	0.23	0.12	0.18	0.19	0.27	0.21	0.27	0.08	0.22	0.20	0.18	0.23	0.21	0.17	
MVA,CP,NWL																					
MAX. VAL	3360	1820	1960	1960	1400	1260	3360	2520	3080	2800	3080	2800	2940	5460	3220	1820	700	3080	1400	1400	
MEAN VAL	2660	1330	1470	1680	1050	1050	3080	1960	2940	2590	2590	2205	2345	4655	2765	1470	560	2625	1260	1120	
STND DEV	0.22	0.28	0.24	0.19	0.26	0.17	0.10	0.23	0.05	0.05	0.14	0.30	0.20	0.13	0.20	0.20	0.20	0.19	0.16	0.23	
BAY C CP																					
MAX. VAL	280	140	140	560	280	280	420	560	840	840	420	560	420	700	840	420	140	700	280	280	
MEAN VAL	210	105	105	455	210	175	315	385	630	560	315	490	280	595	665	385	140	560	245	245	
STND DEV	0.38	0.67	0.67	0.29	0.38	0.77	0.22	0.55	0.43	0.41	0.22	0.29	0.41	0.12	0.20	0.18	0.	0.20	0.29	0.29	
BAY C HP																					
MAX. VAL	280	140	140	420	140	140	560	560	700	700	280	560	280	700	840	560	140	560	280	140	
MEAN VAL	210	140	70	315	140	105	350	385	420	350	280	280	175	630	630	280	105	525	210	105	
STND DEV	0.38	0.	1.15	0.22	0.	0.67	0.40	0.35	0.61	0.77	0.	0.71	0.40	0.13	0.22	0.71	0.67	0.13	0.38	0.67	
BAY E CP																					
MAX. VAL	280	420	280	560	420	280	840	840	840	560	280	420	560	560	1400	420	420	980	420	420	
MEAN VAL	245	280	175	385	245	210	700	595	735	385	245	315	420	420	1050	350	280	840	280	315	
STND DEV	0.29	0.41	0.40	0.35	0.55	0.38	0.23	0.30	0.18	0.69	0.29	0.22	0.38	0.27	0.26	0.23	0.41	0.14	0.41	0.43	

Table 10-3

SUMMARY OF SRV STRESS DATA*

*Max. Val = Maximum Stress Value (psi)

Mean Val = Mean stress value (psi)

STND Dev = Standard Deviation divided by mean value.

Test condition terminology such as SVA, CP, NWL, see Table 3-1.

TEST COND	47	48	49	51	52	53	55	56	61	62
SVA, CP, NWL										
MAX. VAL	3300	2850	3000	3000	3000	2400	4800	3000	3600	3300
MEAN VAL	2250	2343	2587	2456	2625	1950	3225	2175	2812	2587
STND DEV	0.30	0.13	0.09	0.21	0.16	0.12	0.25	0.22	0.21	0.21
CVA, HP, NWL										
MAX. VAL	2100	2850	2400	3000	2700	2700	3600	2700	2850	2550
MEAN VAL	1680	2250	2220	2370	2340	1980	3360	2250	2340	2190
STND DEV	0.20	0.26	0.07	0.16	0.11	0.30	0.04	0.15	0.13	0.13
CVA, HP, EWL										
MAX. VAL	2400	1200	2100	2100	2700	2400	2400	2400	4800	4200
CVA, HP, DWL										
MAX. VAL	1800	2550	3900	3000	2700	3000	3900	2400	2400	2400
MEAN VAL	1410	1950	2670	2340	2130	1950	2880	1980	2040	1770
STND DEV	0.18	0.20	0.26	0.18	0.20	0.31	0.22	0.17	0.19	0.24
MVA, CP, NWL										
MAX. VAL	2700	2700	4500	2700	2400	1800	3900	3000	3600	3000
MEAN VAL	2475	2400	3150	2362	2400	1650	3000	2175	3075	2700
STND DEV	0.12	0.10	0.30	0.11	0.	0.18	0.22	0.28	0.17	0.16
BAY C CP										
MAX. VAL	1500	1350	900	900	600	900	1050	900	3600	900
MEAN VAL	1087	1050	637	750	412	750	900	675	1650	787
STND DEV	0.34	0.31	0.30	0.28	0.35	0.23	0.24	0.29	0.80	0.18
BAY C HP										
MAX. VAL	900	900	600	750	600	750	900	750	900	750
MEAN VAL	675	750	487	675	450	562	712	487	562	487
STND DEV	0.22	0.16	0.15	0.13	0.27	0.26	0.32	0.68	0.70	0.68
BAY E CP										
MAX. VAL	1200	1350	600	1200	900	900	1200	750	1650	1350
MEAN VAL	975	1087	562	900	637	675	1012	637	1462	1087
STND DEV	0.29	0.21	0.13	0.24	0.40	0.22	0.14	0.23	0.13	0.21

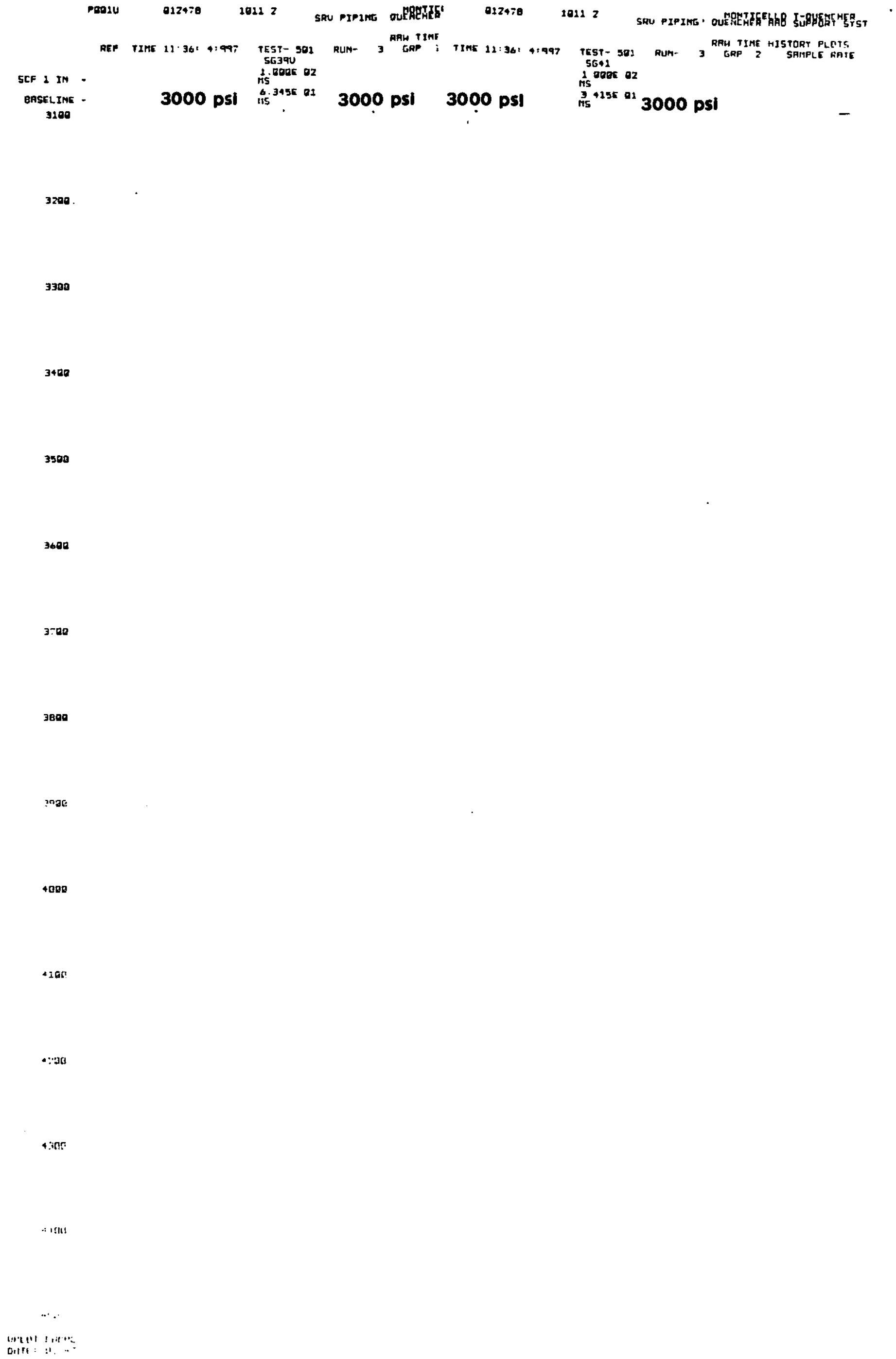

Figure 10-1. Typical Plot for SRV Pipe and Support for SVA, NWL, CP, Valve A Bay D Test, From Test 501, SG39 and SG 49

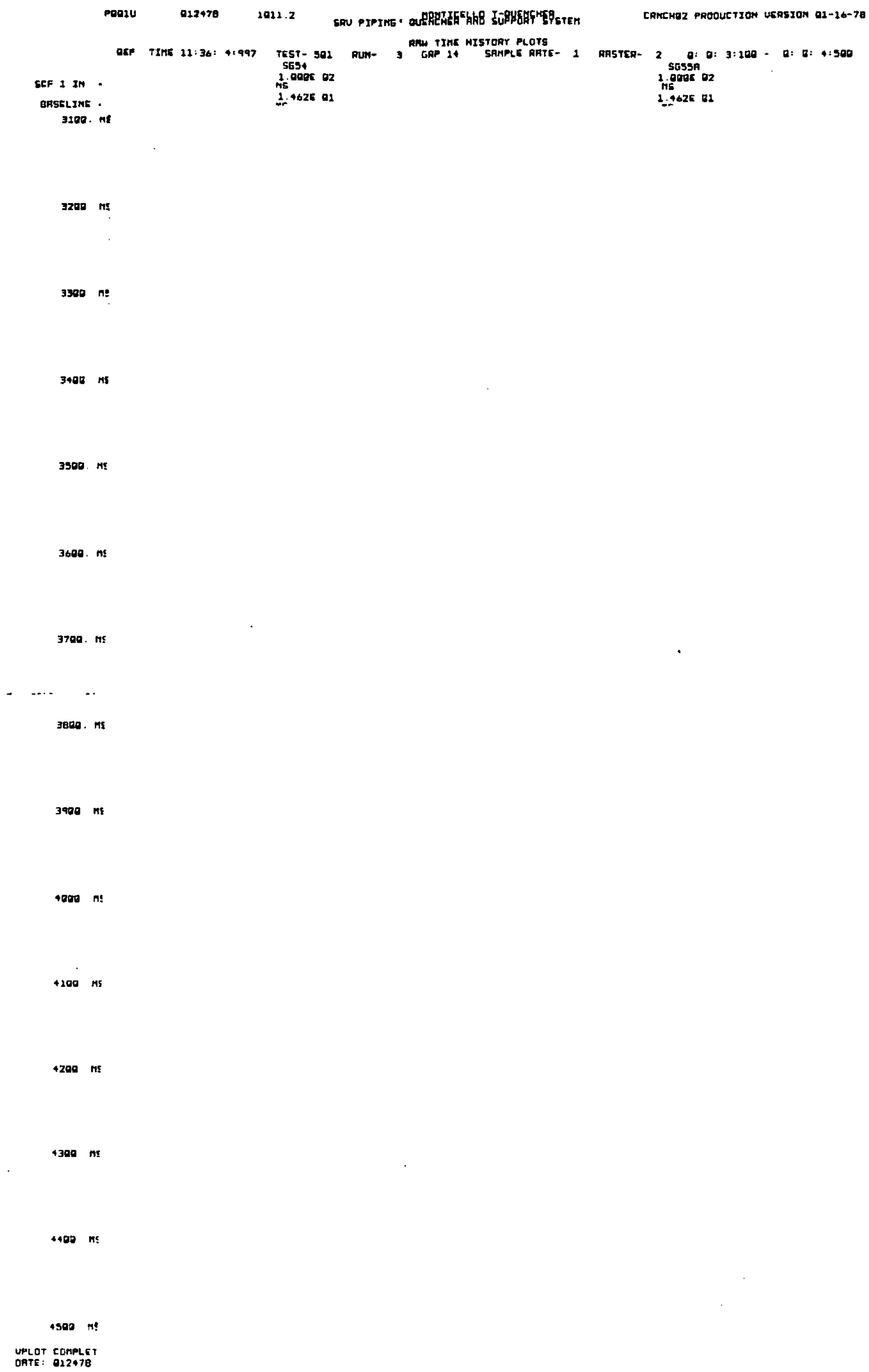

Figure 10-2. Typical Plot for Quencher for SVA, CP, NWL From Test 501, SG54 and SG55A

Figure 10-3. Typical Plot for Quencher Support for SVA, CP, NWL From Test 501, SG60 and A9H

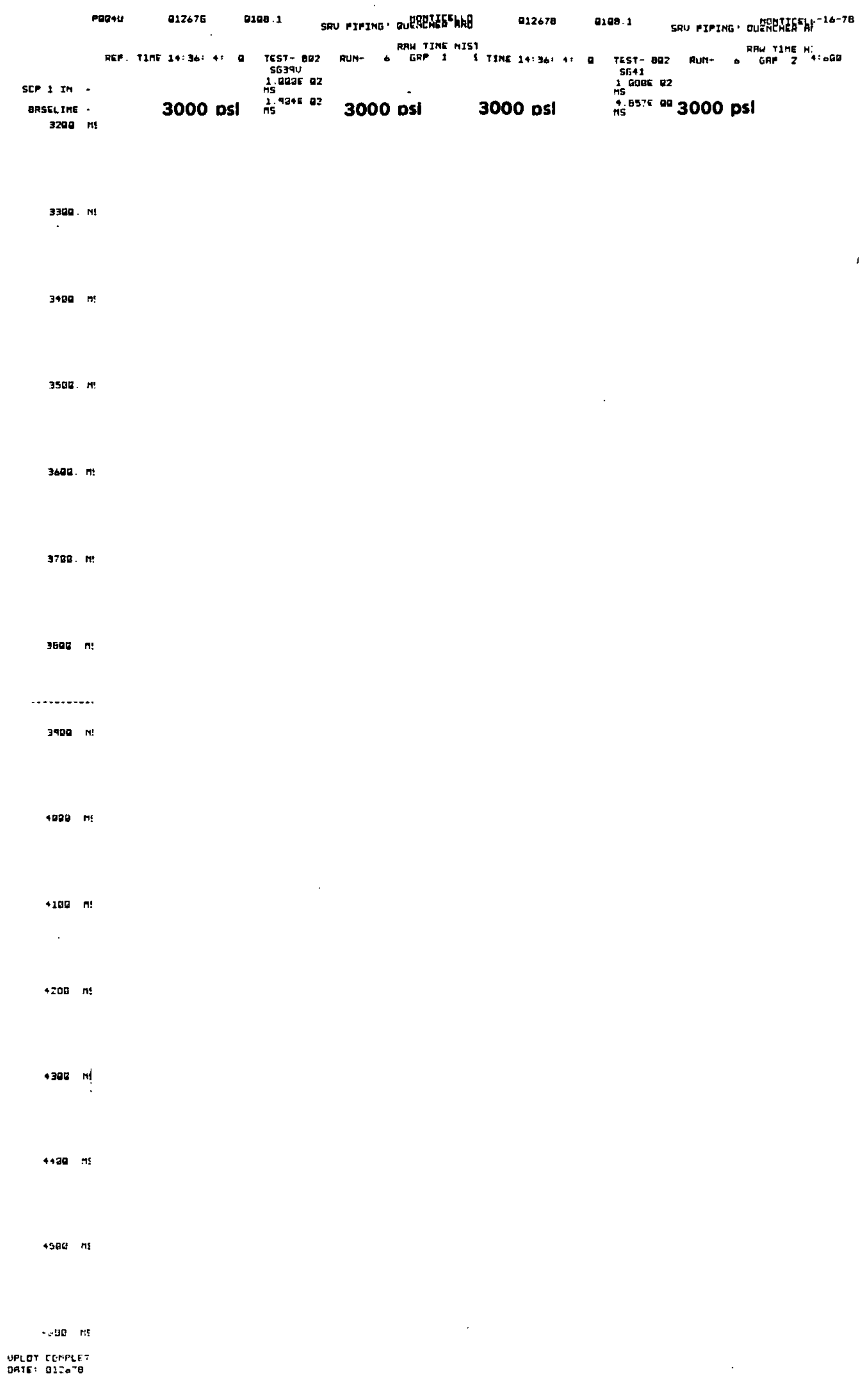

Figure 10-4. Typical Plot for SRV Pipe for SVA, NWL, HP From Test 802, SG39 and SG41

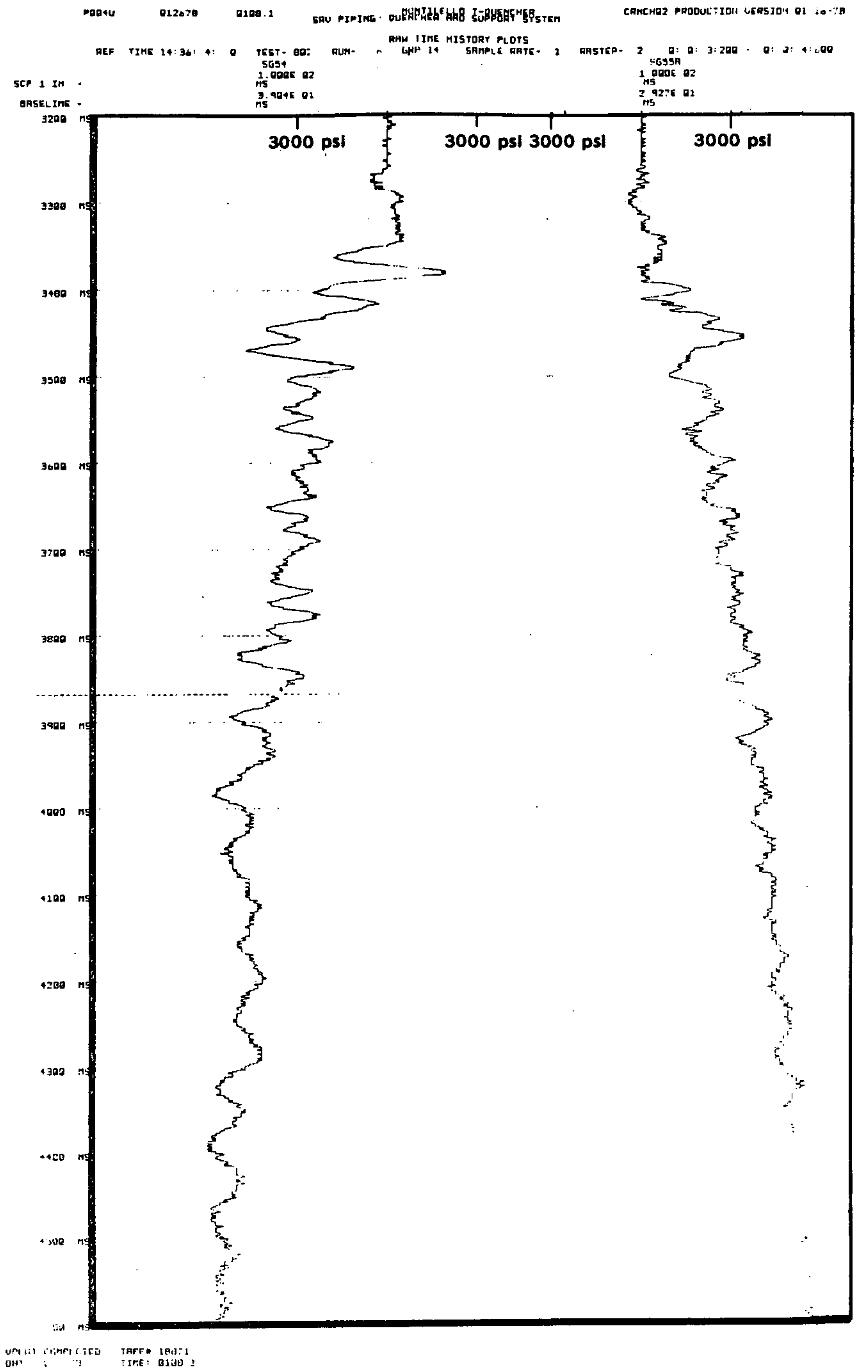

Figure 10-5. Typical Plot for Quencher for SVA, NWL, HP From Test 802, SG54 and 55A

Figure 10-6. Typical Plot for Quencher Support for SVA, NWL, HP From Test 802, SG60 and A9H

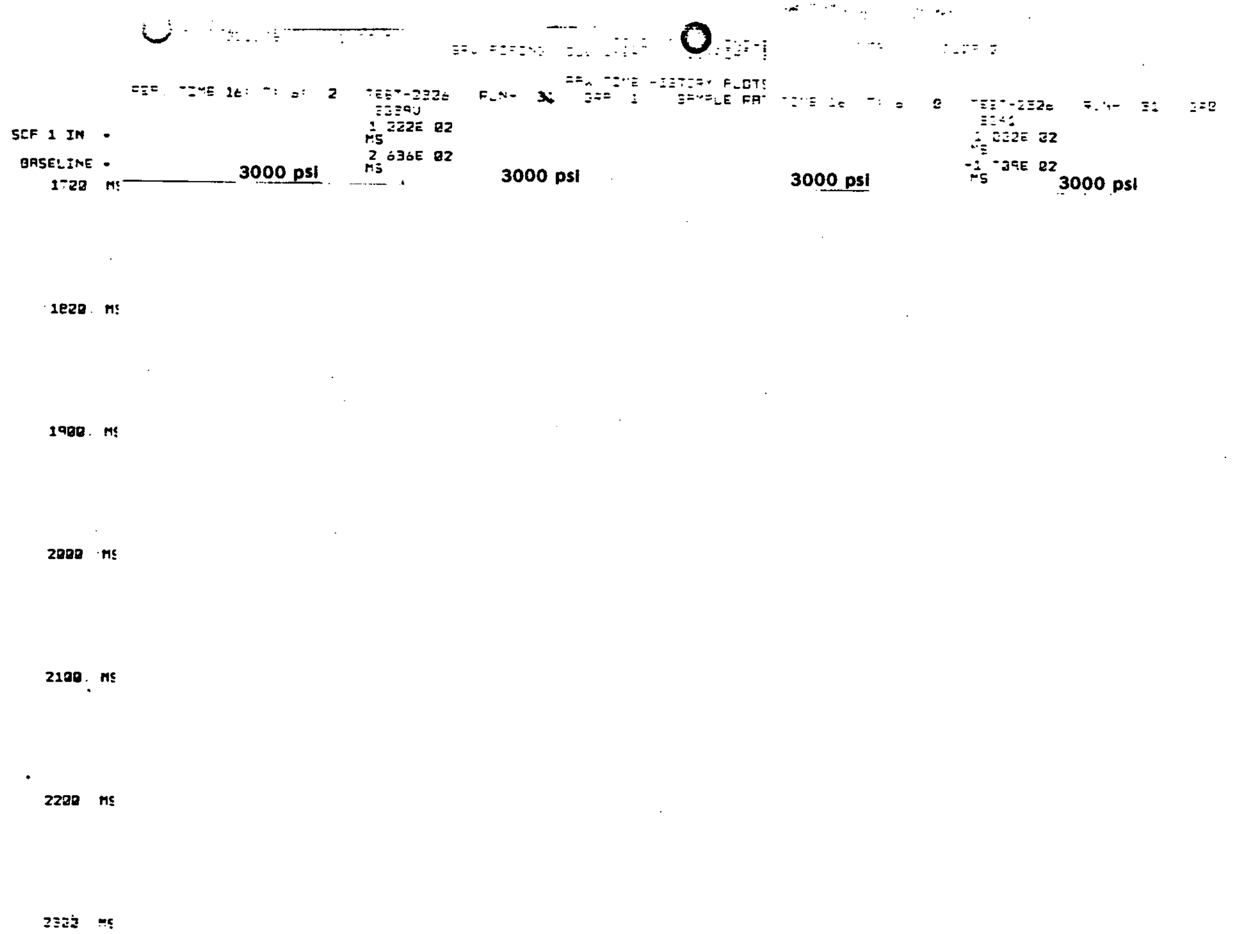

Figure 10-7. Typical Plot for SRV for SVA, CP, EWL From Test 2306, SG39 and SG41

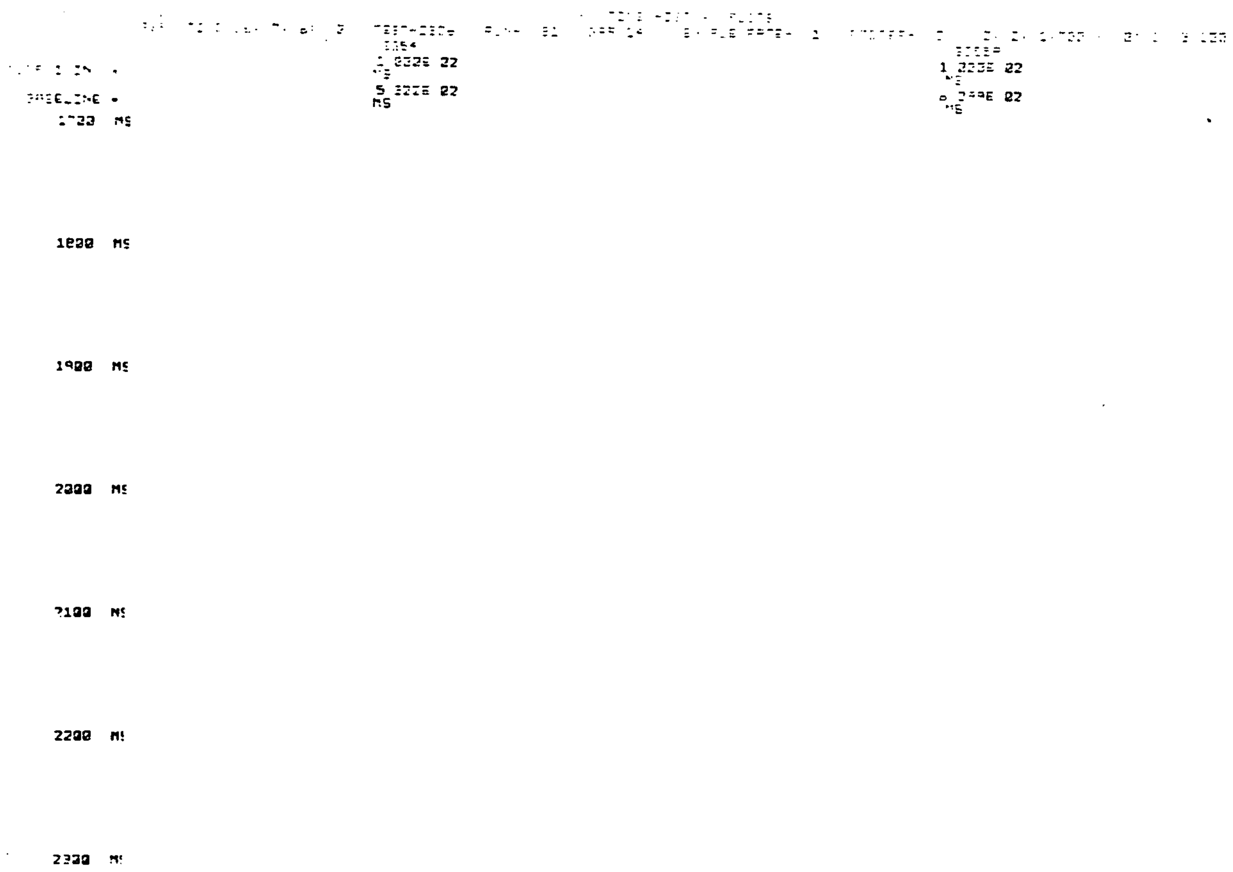

Figure 10-8. Typical Plot for Quencher for CP, SVA, EWL
From Test 2306, SG54 and SG55A

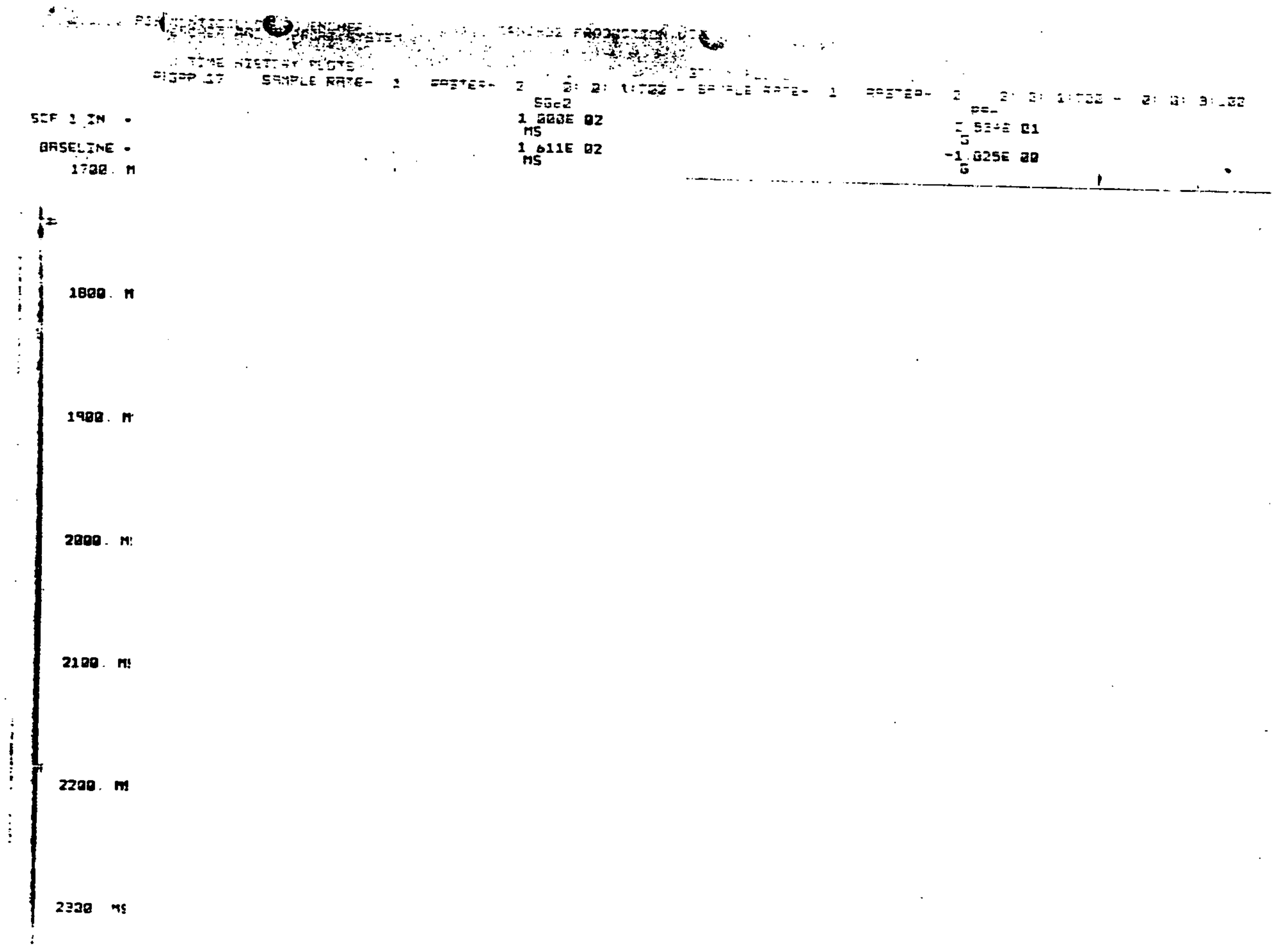

Figure 10-9. Typical Plot for Quencher Support for SVA, CP, EWL
From Test 2306, SG60 and A9H

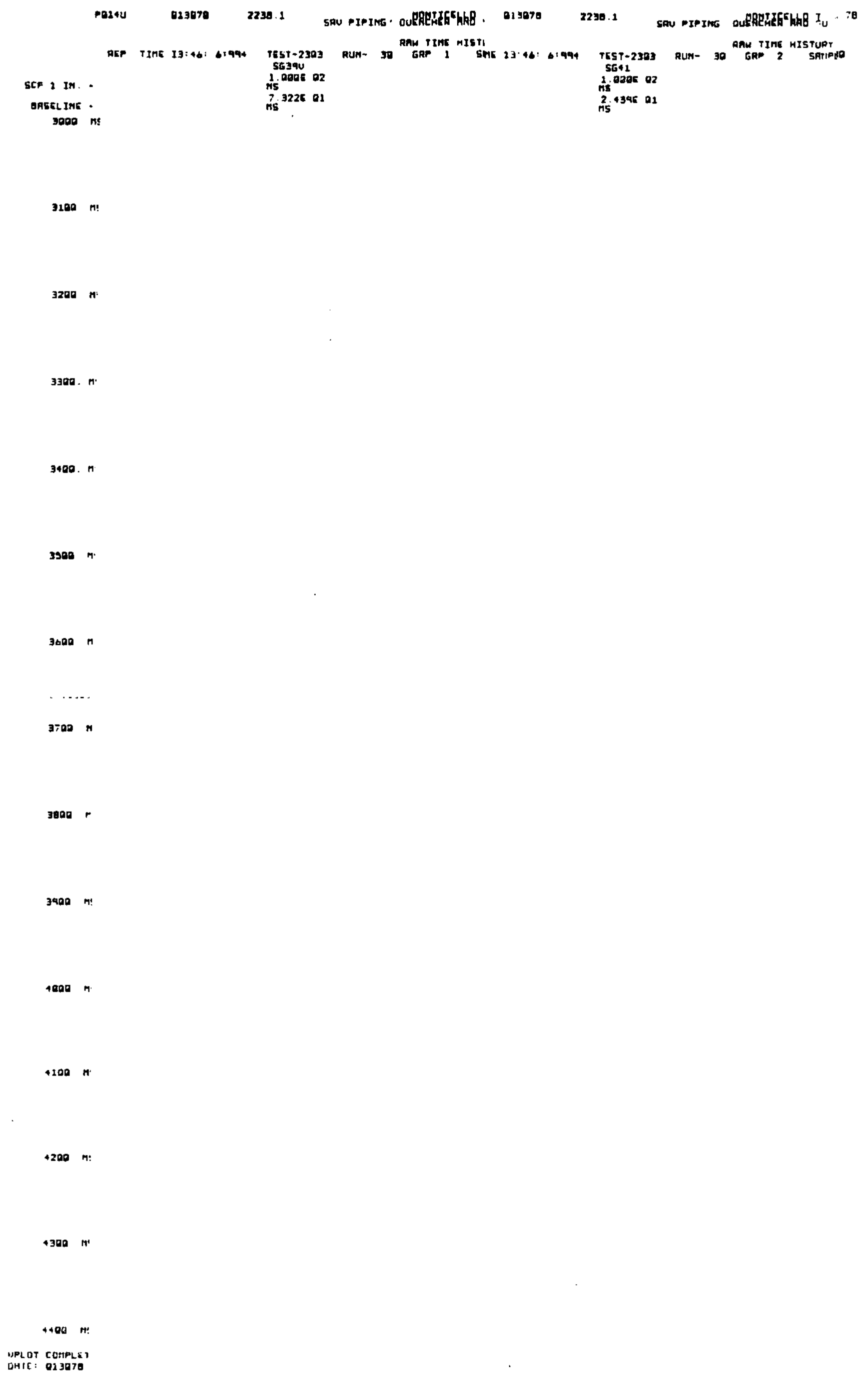

Figure 10-10. Typical Plot for SRV Pipe for CP, MVA, NWL From Test 2303, SG39 and SG41

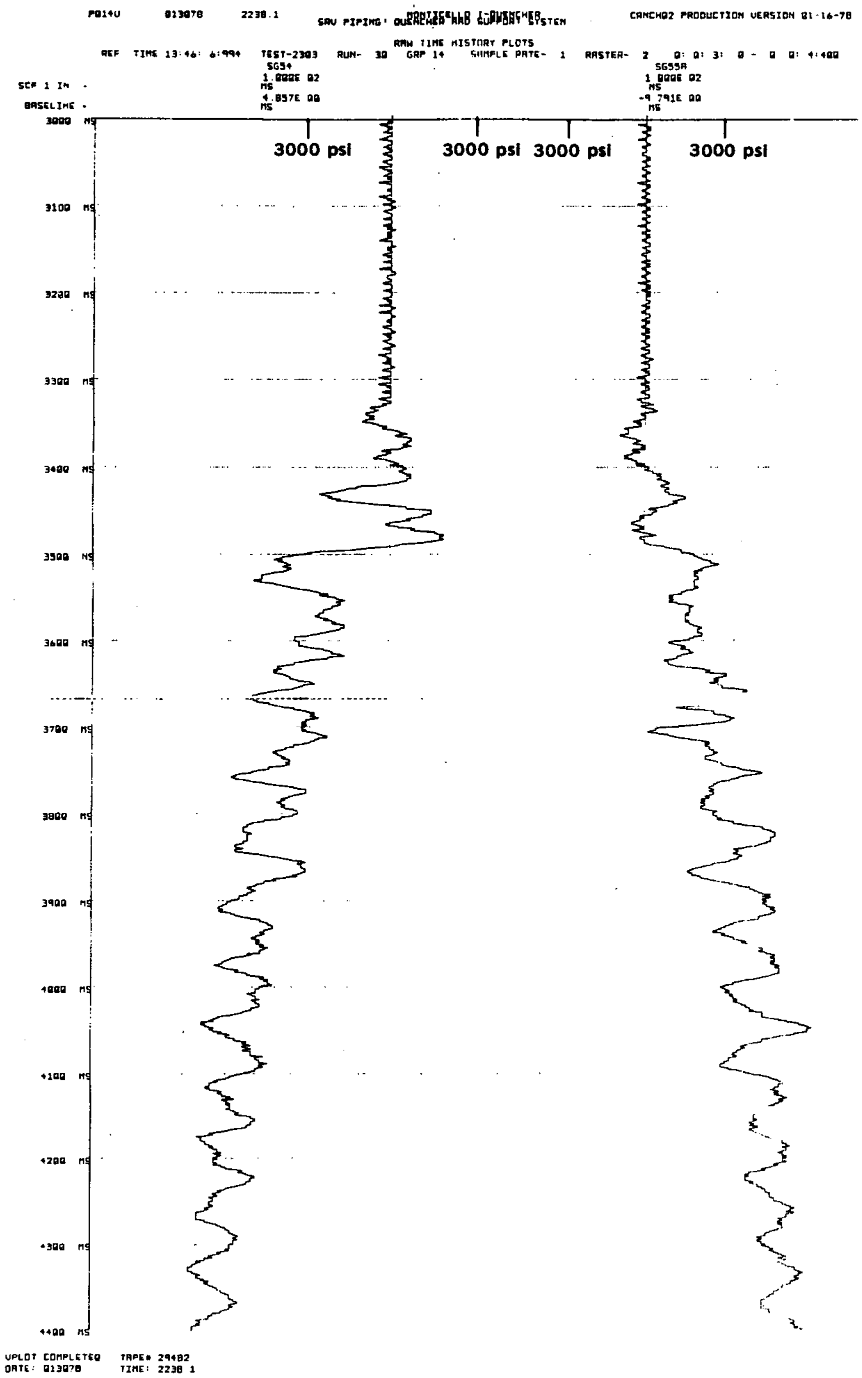

Figure 10-11. Typical Plot for Quencher for MVA, CP, NWL From Test 2303, SG54 and SG55A

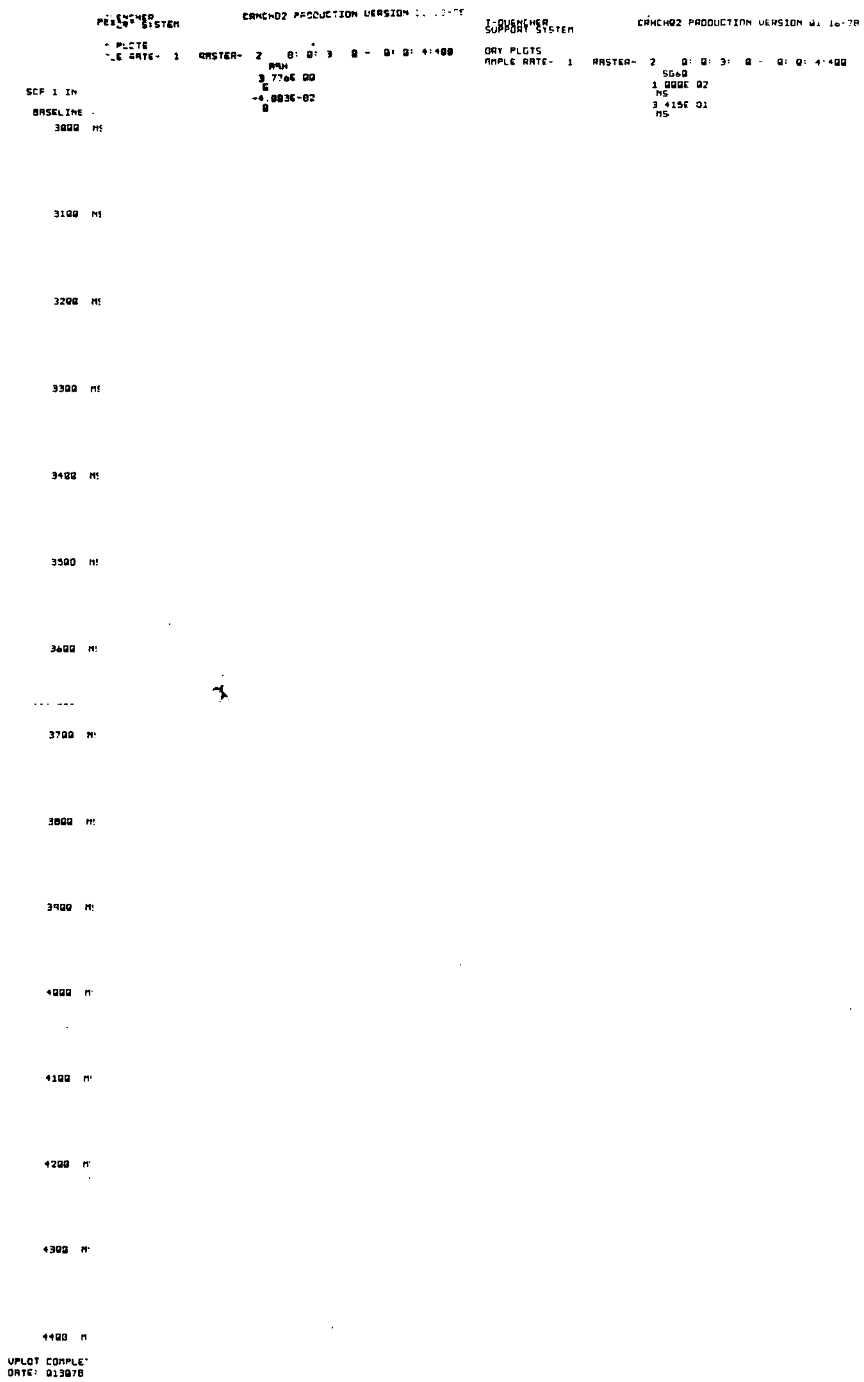

Figure 10-12. Typical Plot for Quencher Support for MVA, CP, NWL From Test 2303, SG60 and A9H

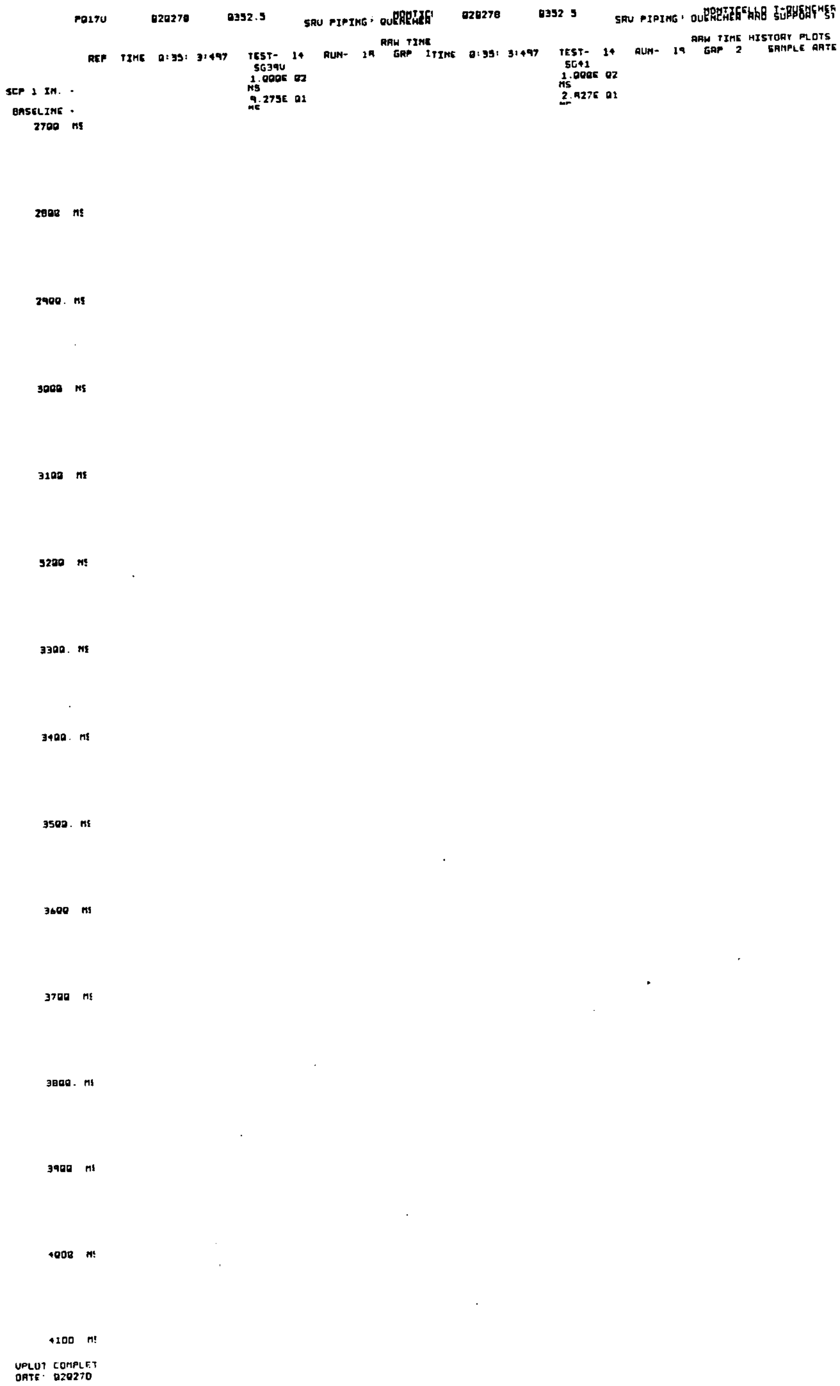

Figure 10-13. Typical Plot for SRV Piping for SVA (Bay C) From Test 14, SG39 and SG41

Figure 10-14. Typical Plot for Quencher for SVA at Bay C From Test 14, SG54 and SG55A

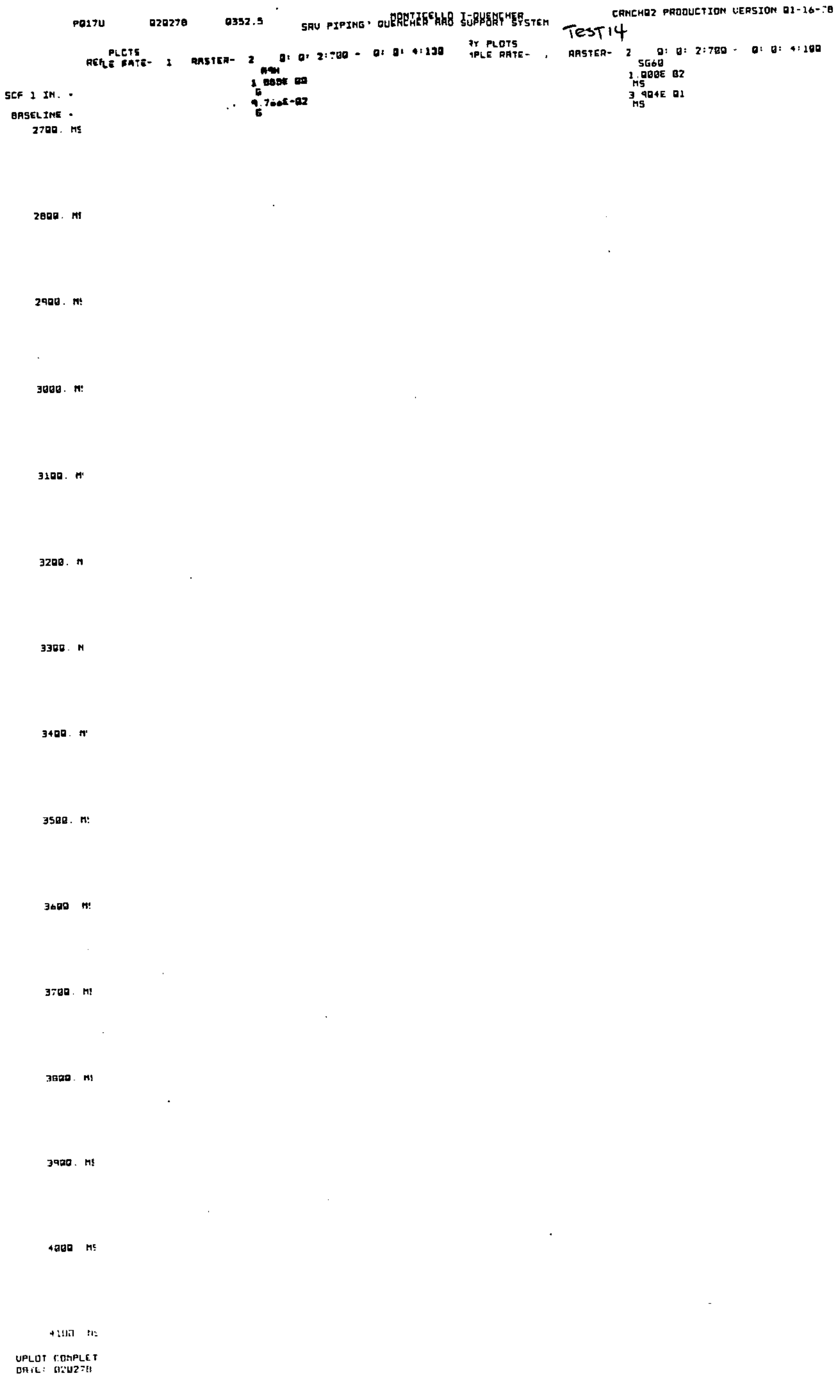

Figure 10-15. Typical Plot for SVA, CP at Bay C From Test 14, SG60 and A9H

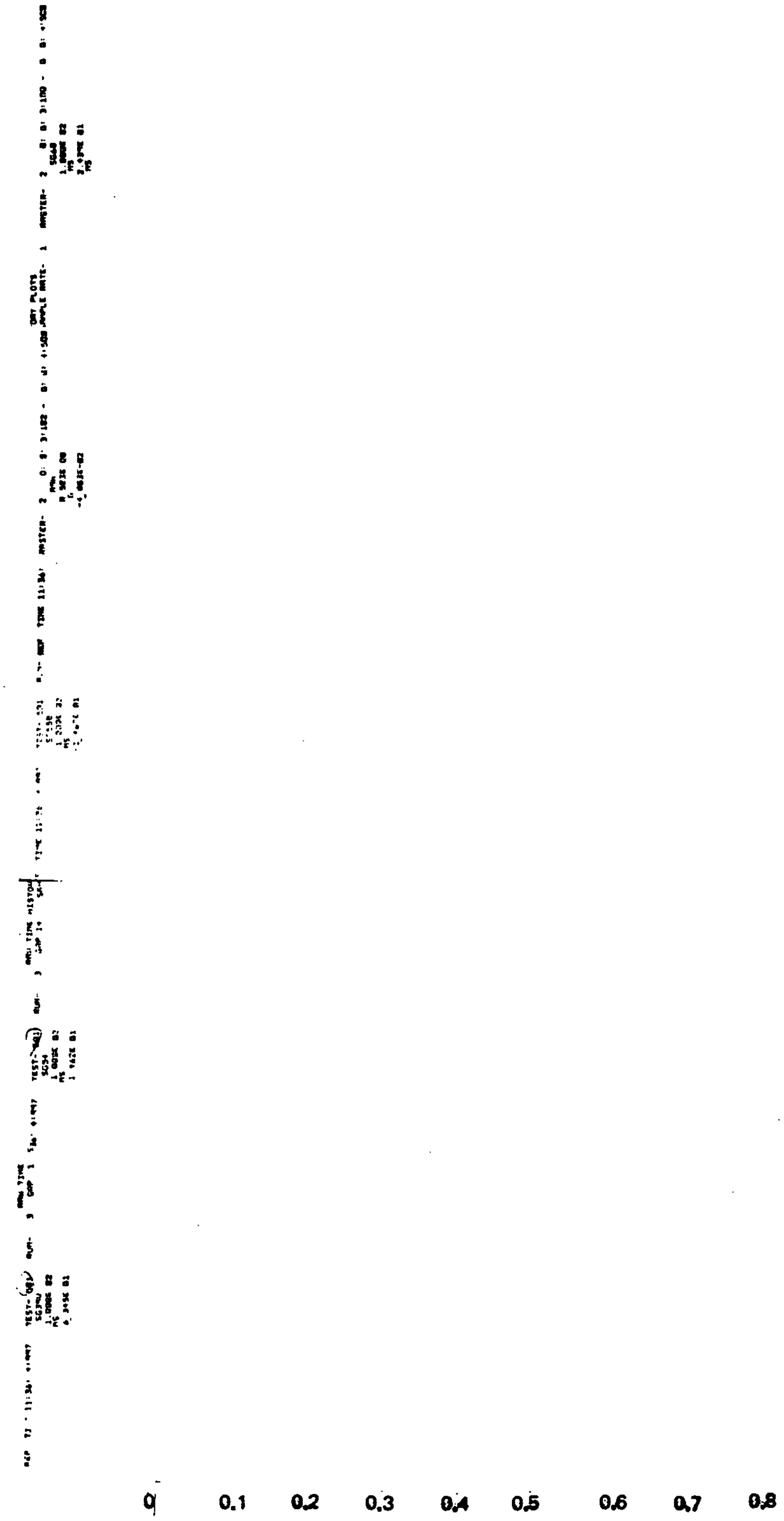

Figure 10-16. Time Sequence for SRV, SRV Pipe, Quencher and Quencher Support From Test 501

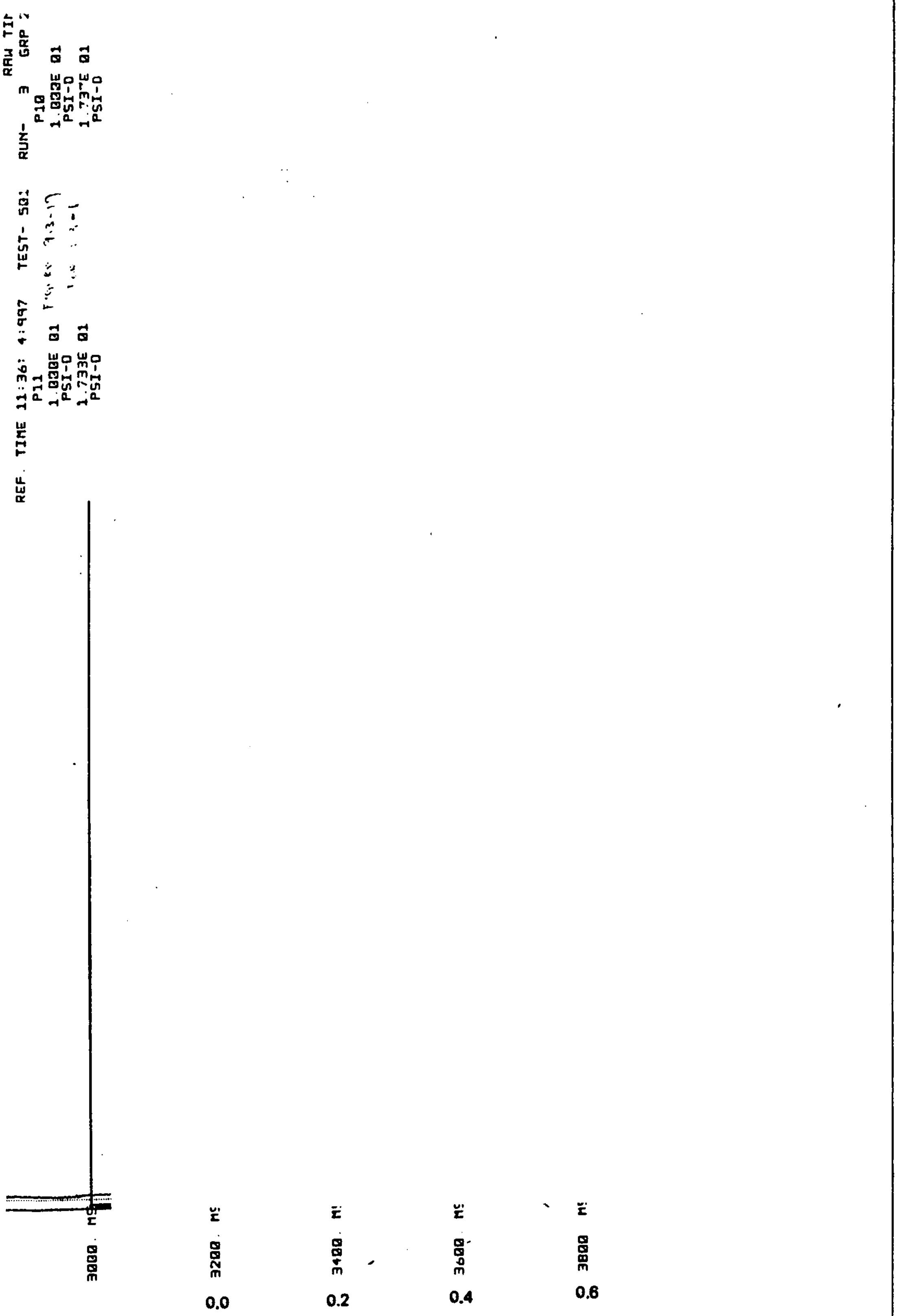

Figure 10-17. Time Sequence for Pressure in SRV, Pipe, Ramshead, and Pool To be Compared With 10-16 From Test 501

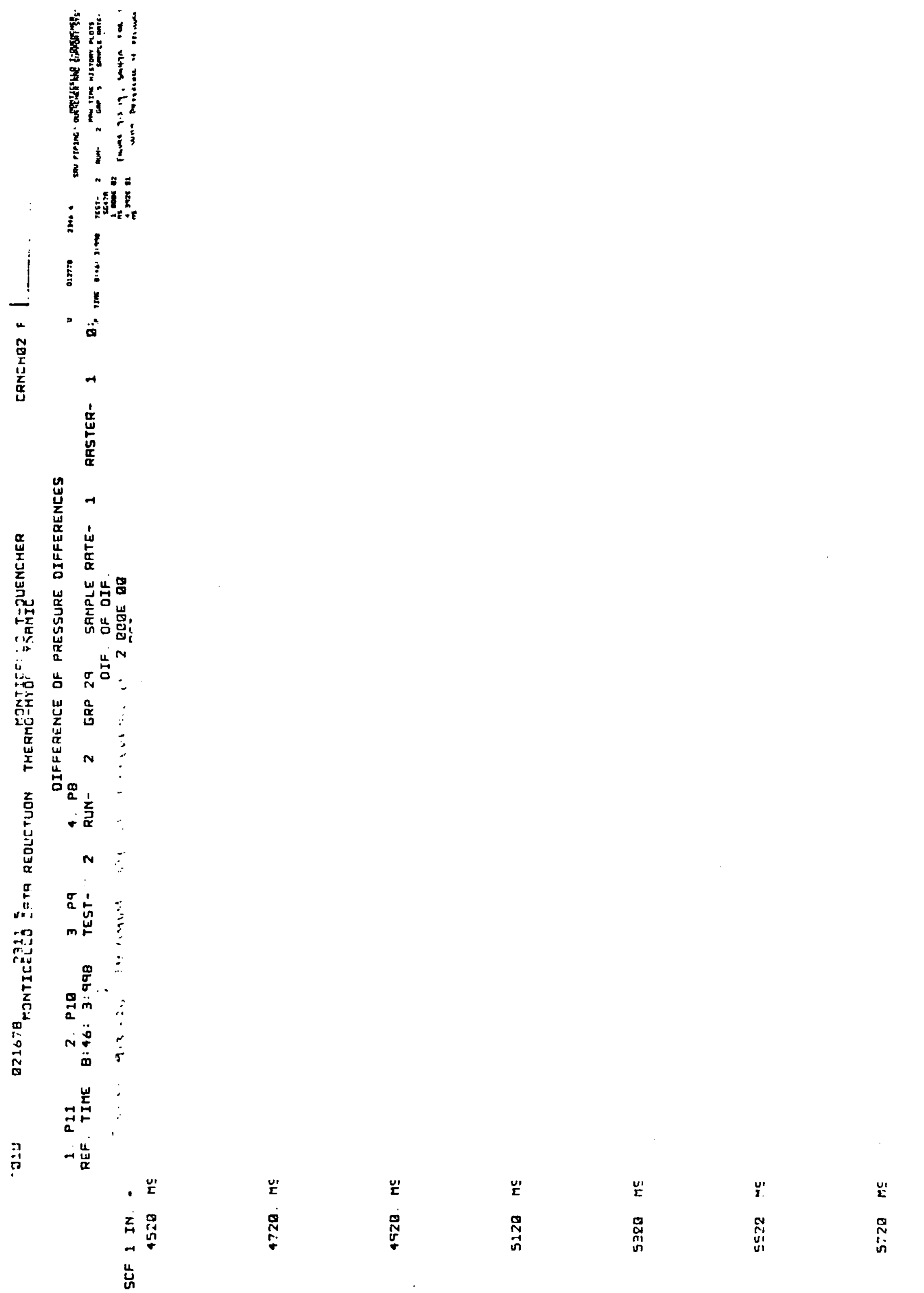

Figure 10-18. Time Relation Between Difference of Difference of Pressure and SG-47

Figure 10-19. P7, Pressure in Ramshead of Quencher Near Support

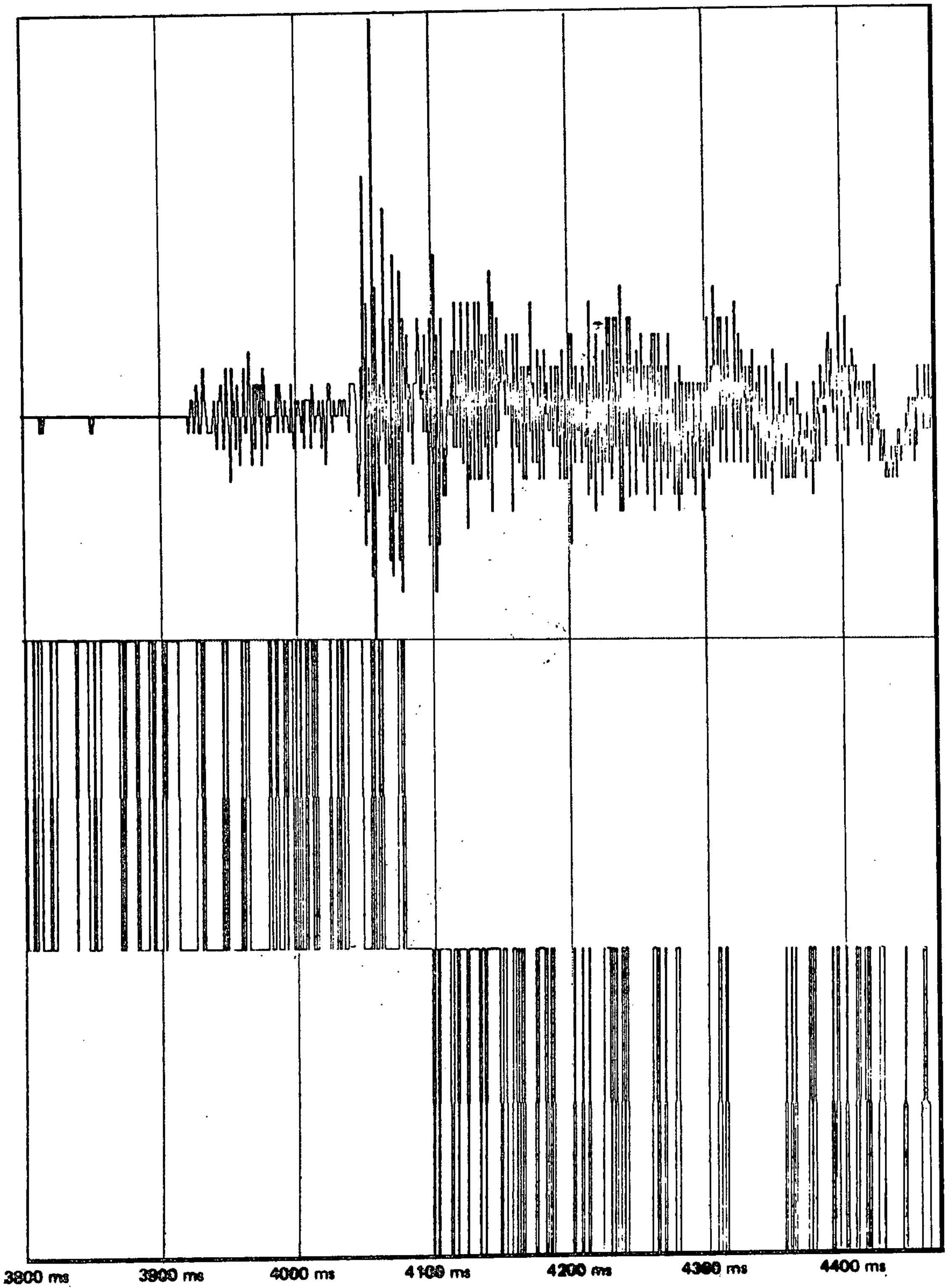

*THE PRODUCTION VERSIONS HAVE FILTERED GAGES A8V, A8H AND A9V WITH SINE BUTTERWORTH LOW-PASS FILTER WITH CUTOFF FREQUENCY OF 100 Hz

Figure 10-20. Sample of Unfiltered Gages A8V, A8H and A9V

APPENDIX A

SENSOR LISTING AND SPECIFICATIONS

Table A-1

PCM RECORDING SYSTEM INSTRUMENTATION SUMMARY

(Sheet 1 of 13)

Sensor ID		Type	Sensor Category	Location	PCM Channel No.
ISG1	A	Rosette	Structural	Bay D. Torus shell, inside. See Figure 4-9	1-1
	B				1-2
	C				1-3
ISG2	A	Rosette	Structural	↓	1-4
	B				1-5
	C				1-6
ISG4	A	Rosette	Structural		1-7
	B				1-8
	C				1-9
ISG6	A	Rosette	Structural		1-10
	B				1-11
	C				1-12
ISG8	A	Rosette	Structural		1-13
	B				1-14
	C				1-15
ISG10	A	Rosette	Structural		1-16
	B				1-17
	C				1-18
ISG12	A	Rosette	Structural		1-19
	B				1-20
	C				1-21
ISG13	A	Rosette	Structural		1-22
	B				1-23
	C				1-24
ISG14	A	Rosette	Structural		1-25
	B				1-26
	C				1-27

Table A-1

PCM RECORDING SYSTEM INSTRUMENTATION SUMMARY

(Sheet 2 of 13)

Sensor ID		Type	Sensor Category	Location	PCM Channel No.
ISG15	A B C	Rosette	Structural	Bay D. Torus shell, inside. See Figure 4-9.	1-28 1-29 1-30
ISG23	A B C	Rosette	Structural	↓	1-31 1-32 1-33
ISG32	A B C	Rosette	Structural	Bay D. Torus shell, inside. See Figure 4-11.	1-34 1-35 1-36
ISG33	A B C	Rosette	Structural	↓	1-37 1-38 1-39
ISG7		Uniaxial	Structural	Bay D. Torus shell, inside. See Figure 4-11.	1-40
IGS9		Uniaxial	Structural	Bay D. Torus shell, inside. See Figure 4-11.	1-41
OSG1	A B C	Rosette	Structural	Bay D. Torus shell, outside. See Figure 4-9.	1-42 1-43 1-44
OSG2	A B C	Rosette	Structural	↓	1-45 1-46 1-47
OSG3	A B C	Rosette	Structural	↓	1-48 1-49 1-50
OSG4	A B C	Rosette	Structural	↓	1-51 1-52 1-53

Table A-1
PCM RECORDING SYSTEM INSTRUMENTATION SUMMARY
(Sheet 3 of 13)

Sensor ID		Type	Sensor Category	Location	PCM Channel No.
OSG6	A	Rosette	Structural	Bay D. Torus shell, outside. See Figure 4-9.	1-54
	B				1-55
	C				1-56
OSG7		Uniaxial	Structural	↓	1-57
OSG8	A	Rosette	Structural		1-58
	B				1-59
	C				1-60
OSG9A		One leg of Rosette	Structural		1-61
OSG10	A	Rosette	Structural		1-62
	B				1-63
	C				1-64
OSG11	A	Rosette	Structural		1-65
	B				1-66
	C				1-67
OSG12	A	Rosette	Structural		1-68
	B				1-69
	C				1-70
OSG13	A	Rosette	Structural		1-71
	B				1-72
	C				1-73
OSG14	A	Rosette	Structural		1-74
	B				1-75
	C				1-76
OSG15	A	Rosette	Structural		1-77
	B				1-78
	C				1-79
OSG16	A	Rosette	Structural	↓	1-80
	B				1-81
	C				1-82

Table A-1

PCM RECORDING SYSTEM INSTRUMENTATION SUMMARY

(Sheet 4 of 13)

Sensor ID		Type	Sensor Category	Location	PCM Channel No.
OSG17	A B C	Rosette	Structural	Bay D. Torus shell, outside. See Figure 4-9.	1-83 1-84 1-85
OSG18	A B C	Rosette	Structural	↓	1-86 1-87 1-88
OSG19	A B C	Rosette	Structural	↓	1-89 1-90 1-91
OSG20	A B C	Rosette	Structural	↓	1-92 1-93 1-94
OSG21	A B C	Rosette	Structural	↓	1-95 1-96 1-97
OSG22	A B C	Rosette	Structural	↓	1-98 1-99 1-100
OSG23	A B C	Rosette	Structural	↓	1-101 1-102 1-103
FSG24	A B C	Rosette	Structural	Bay D. Torus support column. See Figure 4-9.	1-104 1-105 1-106
FSG25	A B C	Rosette	Structural	Bay D. Torus shell, outside. See Figure 4-9.	1-107 1-108 1-109
FSG26	A B C	Rosette	Structural	↓	1-110 1-111 1-112

Table A-1

PCM RECORDING SYSTEM INSTRUMENTATION SUMMARY

(Sheet 5 of 13)

Sensor ID	Type	Sensor Category	Location	PCM Channel No.
FSG31 A FSG31 B FSG31 C	Rosette	Structural	Bay D. Torus shell, outside. See Figure 4-9.	1-113 1-114 1-115
OSG32 A OSG32 B OSG32 C	Rosette	Structural	Bay D. Torus shell, outside. See Figure 4-11.	1-116 1-117 1-118
OSG33 A OSG33 B OSG33 C	Rosette	Structural	↓	1-119 1-120 1-121
SG34	Uniaxial	Structural	Bay D. Hanger strap. See Figure 4-11.	1-122
SG35	Uniaxial	Structural	Bay D. Hanger strap. See Figure 4-11.	1-123
BB1-D4	Column Bending Bridge	Structural	Bay D. Torus support column. See Figure 4-9.	1-124
AB-D4	Column Axial Bridge	Structural	Bay D. Torus support column. See Figure 4-9.	1-125
Hand Switch	-	-	Connected to safety/relief valve hand switch.	1-126
SG39	Uniaxial	T-Quencher & Piping	SRV inlet pipe branch. See Figure 4-18.	2-1
SG40	Uniaxial	T-Quencher & Piping	Vent header pipe. See Figure 4-14.	2-2
SG41	Uniaxial	T-Quencher & Piping	SRV pipe. See Figure 4-14.	2-3
SG42	Uniaxial	T-Quencher & Piping	SRV pipe. See Figure 4-14.	2-4
SG43	Uniaxial	T-Quencher & Piping	SRV pipe support beam. See Figure 4-14.	2-5

Table A-1

PCM RECORDING SYSTEM INSTRUMENTATION SUMMARY

(Sheet 6 of 13)

Sensor ID		Type	Sensor Category	Location	PCM Channel No.
SG44		Uniaxial	T-Quencher & Piping	SRV pipe support beam. See Figure 4-14.	2-6
SG45		Uniaxial	T-Quencher & Piping	SRV pipe. See Figure 4-14.	2-7
SG46		Uniaxial	T-Quencher & Piping	SRV pipe. See Figure 4-14.	2-8
SG47	A B C	Rosette	T-Quencher & Piping	SRV pipe. See Figure 4-15.	2-9 2-10 2-11
SG48	A B C	Rosette	T-Quencher & Piping	↓	2-12 2-13 2-14
SG49	A B C	Rosette	T-Quencher & Piping	↓	2-15 2-16 2-17
SG51	A B C	Rosette	T-Quencher & Piping	T-Quencher. See Figure 4-16.	2-18 2-19 2-20
SG52	A B C	Rosette	T-Quencher & Piping	↓	2-21 2-22 2-23
SG53	A B C	Rosette	T-Quencher & Piping	↓	2-24 2-25 2-26
SG54		Uniaxial	T-Quencher & Piping	↓	2-27
SG55	A B C	Rosette	T-Quencher & Piping	↓	2-28 2-29 2-30

Table A-1

PCM RECORDING SYSTEM INSTRUMENTATION SUMMARY

(Sheet 7 of 13)

Sensor ID	Type	Sensor Category	Location	PCM Channel No.
SG56 { A B C	Rosette	T-Quencher & Piping	T-Quencher. See Figure 4-16.	2-31 2-32 2-33
SG60	Uniaxial	T-Quencher & Piping	T-Quencher pipe support. See Figure 4-16.	2-34
SG61 { A B C	Rosette	T-Quencher & Piping	↓	2-35 2-36 2-37
SG62 { A B C	Rosette	T-Quencher & Piping	↓	2-38 2-39 2-40
SG131	Uniaxial	Structural	Vent header. See Figure 4-12.	2-41
SG132	Uniaxial	Structural	↓	2-42
SG133	Uniaxial	Structural	↓	2-43
SG134	Uniaxial	Structural	Downcomer brace. See Figure 4-12.	2-44
SG135	Uniaxial	Structural	Downcomer brace. See Figure 4-12.	2-45
P1	Pressure Trans-ducer	Hydro-dynamic	Inside SRV pipe. See Figure 4-6.	2-46
P2	Pressure Trans-ducer	Hydro-dynamic	↓	2-47
P3	Pressure Trans-ducer	Hydro-dynamic	↓	2-48
P4	Pressure Trans-ducer	Hydro-dynamic	↓	2-49
P5	Pressure Trans-ducer	Hydro-dynamic	↓	2-50

Table A-1

PCM RECORDING SYSTEM INSTRUMENTATION SUMMARY

(Sheet 8 of 13)

Sensor ID	Type	Sensor Category	Location	PCM Channel No.
P6	Pressure Transducer	Hydro-dynamic	Inside T-Quencher. See Figure 4-6.	2-51
P7	Pressure Transducer	Hydro-	Inside T-Quencher. See Figure 4-6.	2-52
P8	Pressure Transducer	Hydro-dynamic	Pool, near T-Quencher. See Figure 4-6.	2-53
P9	Pressure Transducer	Hydro-dynamic	↓	2-54
P10	Pressure Transducer	Hydro-dynamic	↓	2-55
P11	Pressure Transducer	Hydro-dynamic	↓	2-56
P12	Pressure Transducer	Hydro-dynamic	Bay D. Torus shell. See Figure 4-4.	2-57
P13	Pressure Transducer	Hydro-dynamic	↓	2-58
P14	Pressure Transducer	Hydro-dynamic	↓	2-59
P15	Pressure Transducer	Hydro-dynamic	↓	2-60
P16	Pressure Transducer	Hydro-dynamic	↓	2-61
P17	Pressure Transducer	Hydro-dynamic	↓	2-62
P18	Pressure Transducer	Hydro-dynamic	↓	2-63
P19	Pressure Transducer	Hydro-dynamic	↓	2-64
P20	Pressure Transducer	Hydro-dynamic	↓	2-65

Table A-1

PCM RECORDING SYSTEM INSTRUMENTATION SUMMARY

(Sheet 9 of 13)

Sensor ID	Type	Sensor Category	Location	PCM Channel No.
P21	Pressure Transducer	Hydro-dynamic	Bay D. Torus shell. See Figure 4-4.	2-66
P22	Pressure Transducer	Hydro-dynamic	↓	2-67
P23	Pressure Transducer	Hydro-dynamic	↓	2-68
P24	Pressure Transducer	Hydro-dynamic	↓	2-69
P25	Pressure Transducer	Hydro-dynamic	↓	2-70
P26	Pressure Transducer	Hydro-dynamic	↓	2-71
P27	Pressure Transducer	Hydro-dynamic	↓	2-72
P28	Pressure Transducer	Hydro-dynamic	↓	2-73
P29	Pressure Transducer	Hydro-dynamic	↓	2-74
P30	Pressure Transducer	Hydro-dynamic	↓	2-75
P31	Pressure Transducer	Hydro-dynamic	↓	2-76
P32	Pressure Transducer	Hydro-dynamic	↓	2-77
P33	Pressure Transducer	Hydro-dynamic	↓	2-78
P34	Pressure Transducer	Hydro-dynamic	↓	2-79

Table A-1

PCM RECORDING SYSTEM INSTRUMENTATION SUMMARY

(Sheet 10 of 13)

Sensor ID	Type	Sensor Category	Location	PCM Channel No.
P35	Pressure Transducer	Hydro-dynamic	Bay D. Torus shell. See Figure 4-4.	2-80
P36	Pressure Transducer	Hydro-dynamic	↓	2-81
P37	Pressure Transducer	Hydro-dynamic	↓	2-82
P38	Pressure Transducer	Hydro-dynamic	↓	2-83
P39	Pressure Transducer	Hydro-dynamic	↓	2-84
P40	Pressure Transducer	Hydro-dynamic	Bay C/D. Torus shell. See Figure 4-5.	2-85
P41	Pressure Transducer	Hydro-dynamic	↓	2-86
P42	Pressure Transducer	Hydro-dynamic	↓	2-87
P43	Pressure Transducer	Hydro-dynamic	↓	2-88
P44	Pressure Transducer	Hydro-dynamic	↓	2-89
P46	Pressure Transducer	Hydro-dynamic	↓	2-90
P48	Differ-ential Pressure Transducer	Hydro-dynamic	Vacuum breaker flow.	2-91
A8V	Acceler-ometer	T-Quencher & Piping	T-Quencher. See Figure 4-16	2-92

Table A-1

PCM RECORDING SYSTEM INSTRUMENTATION SUMMARY

(Sheet 11 of 13)

Sensor ID	Type	Sensor Category	Location	PCM Channel No.
A8H	Accelerometer	T-Quencher & Piping	T-Quencher. See Figure 4-16.	2-93
A9V	Accelerometer	T-Quencher & Piping	T-Quencher pipe support. See Figure 4-16.	2-94
A9H	Accelerometer	T-Quencher & Piping	T-Quencher pipe support. See Figure 4-16.	2-95
T1	Temperature Sensor	Hydrodynamic	SRV pipe, inside. See Figure 4-6.	2-96
OT1	Temperature Sensor	Hydrodynamic		2-97
T3	Temperature Sensor	Hydrodynamic		2-98
W4	Water Level Sensor	Hydrodynamic		2-99
W3	Water Level Sensor	Hydrodynamic		2-100
T6	Temperature Sensor	Hydrodynamic		2-101
T7	Temperature Sensor	Hydrodynamic		2-102
T8	Temperature Sensor	Hydrodynamic		2-103
OT11	Temperature Sensor	Hydrodynamic		2-104
P49	Pressure Transducer	Hydrodynamic		2-105

Table A-1

PCM RECORDING SYSTEM INSTRUMENTATION SUMMARY

(Sheet 12 of 13)

Sensor ID	Type	Sensor Category	Location	PCM Channel No.
W1	Water Level Sensor	Hydro-dynamic	SRV pipe, inside. See Figure 4-6.	2-106
W5	Water Level Sensor	Hydro-dynamic	SRV pipe, inside. See Figure 4-6.	2-107
A1	Acceler-ometer	Structural	Bay D. Torus shell, outside. See Figure 4-13.	2-108
A2	Acceler-ometer	Structural	↓	2-109
A3	Acceler-ometer	Structural	↓	2-110
A4	Acceler-ometer	Structural	↓	2-111
A5	Acceler-ometer	Structural	↓	2-112
A6	Acceler-ometer	Structural	↓	2-113
A7	Acceler-ometer	Structural	↓	2-114
BB2-D1	Column Bending Bridge	Structural	Bay D. Torus support column. See Figures 4-10, 4-19.	2-115
BB1-D2	Column Bending Bridge	Structural	↓	2-116
AB-D1	Column Axial Bridge	Structural	↓	2-117
BB1-D2	Column Bending Bridge	Structural	↓	2-118

Table A-1

PCM RECORDING SYSTEM INSTRUMENTATION SUMMARY

(Sheet 13 of 13)

Sensor ID	Type	Sensor Category	Location	PCM Channel No.
BB2-D2	Column Bending Bridge	Structural	Bay D. Torus support column. See Figures 4-10, 4-25.	2-119
AB-D2	Column Axial Bridge	Structural	↓	2-120
BB1-D3	Column Bending Bridge	Structural	↓	2-121
BB2-D3	Column Bending Bridge	Structural	↓	2-122
AB-D3	Column Axial Bridge	Structural	↓	2-123
OSG9B	One Leg of Rosette	Structural	Bay D. Torus shell, outside. See Figure 4-9.	2-124
BB2-D4	Column Bending Bridge	Structural	Bay D. Torus support column. See Figures 4-10, 4-25.	2-125
OSG9C	One Leg of Rosette	Structural	Bay D. Torus shell, outside. See Figure 4-10.	2-126

Table A-2

DS-83 RECORDING SYSTEM INSTRUMENTATION SUMMARY

Sensor ID	Type	Location	See Figure	DS-83 Channel No.
T11	Hy-Cal RTD	SRV Pipe Strap-on. 24.6' along pipe above quencher		1
T12	Hy-Cal RTD	SRV Pipe Strap-on. 18.25' along pipe below T13.		2
T13	Hy-Cal RTD	SRV Pipe Strap-on. 9.75' along pipe below T14.		3
T14	Hy-Cal RTD	SRV Pipe Strap-on. 5.25' along pipe below T15.		4
T15	Hy-Cal RTD	SRV Pipe Strap-on. 1.08' along pipe below SRV flange.		5
T16	Rosemount RTD	Bay D. Off of pool wall.	4-19	6
T17	Rosemount RTD	Bay D. Off of downcomer	↓	7
T18	↓	Bay D. See 17		8
T19		Bay D. See 16		9
T20		Bay D. See 16		10
T21		Bay D. See 17		11
T22		Bay D. Off of quencher support pipe.		12
T23		Bay D. See 16		13
T24		Bay D. See 17		14
T25		Bay D. Off of downcomer brace		15
T26		Bay D. See 25		16
T27		Bay D. See 17		17
T28		Bay D. See 25		18
T29		Bay D. See 25		19
T30		Bay D. See 16	4-19	20
T31		Bay D/E. Off of ring girder	4-21	21
T32		Bay D/E. Off of vent header support.	↓	22
T33		Bay D/E. See 31		23
T34	Rosemount RTD	Bay D/E. See 31	4-21	24

Table A-2 (Continued)

DS-83 RECORDING SYSTEM INSTRUMENTATION SUMMARY

Sensor ID	Type	Location	See Figure	DS-83 Channel No.
T35	Rosemount RTD	Bay D/E. See 32	4-21	25
T36		Bay D/E. See 32		26
T37		Bay D/E. See 32	4-21	27
T38		Bay E. See 32	4-22	28
T39		Bay E. See 32	4-22	29
T40		Bay E. See 32	4-22	30
T41		Bay E/F. See 32	4-23	31
T42		Bay E/F. See 32	4-23	32
T43		Bay E/F. See 32	4-23	33
T44		Bay H. See 32	4-24	34
T45		Bay H. See 32	4-24	35
T46		Bay H. See 32	4-24	36
T47		Bay B. See 32	4-26	37
T48		Bay B. See 32	4-26	38
T49	Rosemount RTD	Bay B. See 32	4-26	39

Table A-3

FM RECORDING SYSTEM INSTRUMENTATION SUMMARY

Strain Gage No.		Type	Location	Channel No.
	A			1
WSG1	B	Rosette	Bay C/D - Bottom Centerline	2
	C			3
	A			4
WSG2	B	Rosette	Bay C/D - 1/4 Point, Bottom	5
				6
	A			7
WSG3	B	Rosette	Bay C - Bottom Centerline	8
				9
	A			10
WSG4	B	Rosette	Bay C - 1/4 Point, Bottom	11
	C			12
	A			13
WSG5	B	Rosette	Bay C - 45° from Bottom Centerline	14
	C			15
	A			16
WSG6	B	Rosette	Bay A - Bottom Centerline	17
	C			18
	A			19
WSG7	B	Rosette	Bay A - 1/4 Point, Bottom	20
	C			21
WSG8		Uniaxial	Bay D - Adjacent SG15C	22
WSG9 Through 16 (WAB-B1)		Column Axial Bridge	Column B1. See Figure 4-19	23
WSG17 Through 24 (WAB-B2)		Column Axial Bridge	Column B2. See Figure 4-19	24
WSG25 Through 32 (WAB-A1)		Column Axial Bridge	Column A1. See Figure 4-19	25
WSG33 Through 40 (WAB-A2)		Column Axial Bridge	Column A2. See Figure 4-19	26

Table A-4

PCM SENSOR

Type	Locations	Specifications	
Weldable Strain Gages Ailtech SG-125-09	SG1-23, 32-35 39-49, 51-56 60-62, 131-135	Resistance:	120 ±1 ohm
		Gage Factor:	1.94 ±3%
		Active Gage Length:	3/4 inch
		Dynamic Range:	±20,000 microstrain
		Temperature Compensation:	75 to 560F
Foil Strain Gages Micromeasurements Type CEA-06-250 UR-120	FSG 24, 25, 26, 31	Resistance:	120 ohms ±0.4%
		Gage Factor:	2.05 ±0.5%
		Active Gage Length:	1/4 inch
		Dynamic Range:	±50,000 microstrain
Micromeasurements Type CEA-06-250 UW-120	SG67-130 (Columns)	Resistance:	120 ohms ±0.3%
		Gage Factor:	2.065 ±0.5%
		Active Gage Length:	1/4 inch
Accelerometers Entran EGAL-125-10 (Uniaxial)	A1-A7 Outside torus wall	Range:	±10g
		Nominal Sensitivity:	12 mv/g
		Nonlinearity:	±1% of reading
		Transverse Sensitivity:	3% max.
Endevco 7717-50 (biaxial)	A8H, V; A9H, V Quencher and quencher support	Range:	±100g

Table A-4

PCM SENSOR (Continued)

Type	Locations	Specifications	
Pressure, Absolute			
Validyne AP-10 with isolator	P1, 2, 4, 5, 6, 7 Inside relief valve discharge piping or quencher	Range: Linearity:	0 - 1000 psia ±1/2% f.s. best straight line
Validyne AP-10 with isolator	P8-13, 15, 16, 18, 19, 22, 23, 24, 26, 27, 31-34, 36, 38-44, 46 In suppression pool	Range: Linearity:	0 - 100 psia ±1/2% f.s. best straight line
Validyne AP-10, preconditioned for 800 psia with isolator	P3, P49 On SRV piping	Range: Linearity:	0 - 25 psia ±1/2% f.s. best straight line
Sensometric, flush mount	P14, 17, 20, 21, 25, 28, 29, 30, 35, 37 In suppression pool	Range:	0 - 100 psia
Pressure, Differential Validyne DP-103	P48 (vacuum breaker air flow)	Range:	±2.0 psid
Resistance Temperature Detector			
Micromeasurements STG-50A (JPW-assembled)	T1, 3, 6, 7, 8 Relief valve piping, in wall near inner surface	Range:	0°F to + 500°F
Micromeasurements ETG-50C (GE-assembled)	OT2, OT11 Relief valve piping, temperature of contained fluid	Range:	0°F to + 500°F
Water Leg Detector custom built by GE	W1, W3, W4, W5	ON/OFF	

Table A-5

DS-83 SENSOR

Type	Locations	Specifications
Resistance Temperature Detector		
Hy-Cal Nickel RTD	T11-15 Outside wall, relief valve piping	0°F to + 500°F/±3°F Steady state
Rosemount Series 78 Platinum RTD	T16-49 Wetwell-pool	0°F to + 500°F/±3°F

Table A-6

FM SYSTEM SENSOR

Type	Locations	Specifications	
Foil Strain Gages			
Micromeasurements CEA-06-250UR-350	WSG1-7 torus shell	Resistance: Gage Factor: Active Gage Length: Dynamic Range	305 ohms ±0.4% 2.05 ±0.5% 1/4 inch ±50,000 microstrain
Micromeasurements CEA-06-250UW-350	WSG8 (torus) WSG9-40 (columns)	Resistance: Gage Factor: Active Gage Length: Dynamic Range:	350 ohms ±0.3% 2.085 ±0.5% 1/4 inch ±50,000 microstrain

APPENDIX B

DATA ACQUISITION AND REDUCTION SYSTEM ACCURACY EVALUATION

APPENDIX B. DATA ACQUISITION AND REDUCTION SYSTEM ACCURACY EVALUATION

I. INTRODUCTION AND SUMMARY

This accuracy evaluation considers the various physical elements of the system and makes an estimate of the accuracy with which the final data represent the physical phenomena being measured. The evaluation is confined to the predictable tolerances based on known uncertainties. It cannot assure that every data point is within these tolerances, however. True confidence in the accuracy of the data must result from a combination of this analysis with a detailed examination of the data in context. This is especially true because of the appearance of some spurious ("wild") data points in the raw plots and edits. Both computer and manual techniques have been used to eliminate these points in the structural data, because it was desired to use the computer to list maximum values. Hydrodynamic data, however, which have been scaled manually from plots, and wild points, when they occur, have been ignored through the engineering judgment of the data analyst. Examination of the data in context is necessary also to reveal unpredictable zero shifts which may affect the apparent absolute data amplitudes.

This system accuracy evaluation considers first the characteristics of the various transucers, and then proceeds through the signal conditioning, digitizing, recording, and reduction systems to arrive at the overall estimates.

II. TRANSDUCERS

A. Strain Gages

1. Weldable gages

Most of the strain gages used were Ailtech weldable gages, temperature-compensated for use over the range 75° to 560°F on steel with a temperature coefficient of 6 ppm. A special lot (#206-L) was purchased for use in Type-316 stainless steel (9 ppm). The gage factor stated by the manufacturer is 1.94 ±3% (1.93 for the 9 ppm gages). The resistance of the gage is given as 120 ±1 ohm.

The effect of tolerances in these parameters can be examined by investigating the circuit used and the way the strain gages were calibrated. Figure B-1 shows the strain gage wiring to the Validyne CD173-1207 input terminals, and the schematic circuit. The circuit used (all rosette elements and single gages) is the conventional "three-wire" quarter-bridge circuit, which provides important advantages. As shown in the schematic, the corner of the bridge from which the positive signal is taken is located such that wire resistance is placed in two adjacent arms. Thus, changes in wire resistance due to temperature will be the same in both arms and the effects of such changes will not appear in the output signal. A second and very important advantage is that shunt calibration across the adjacent arm completion resistor, R1, will generate exactly the same signal as will either real stress or shunt calibration at the active gage. The wire resistance is not included in the shunt calibration equation, and wire resistance may be ignored as long as it is known to be the same in both adjacent arms.

The strain simulated by shunt calibration across R1 is given by

$$\text{Microstrain} = \frac{R_g \times 10^6}{K(R_g + R_c)}$$

where

$R_g = 120 \pm 1$ ohm

$R_c = 59{,}900$ ohms

$K = 1.94 \pm 3\%$ (weldable gages)

The nominal strain signal simulated for weldable gages is 1030 microstrain.

If gage factor, gage resistance, and calibration resistance are at their extreme, worst-case values (assuming 0.1% calibration resistor):

$$\text{Microstrain} = \frac{(120 - 1) \times 10^6}{1.94 \times 1.03 \times (59{,}900 \times 1.001 + 120 - 1)}$$

$$= \frac{119 \times 10^6}{1.998 \times 60{,}078} = 991$$

$$\text{Max \% error} = \frac{1030 - 991}{1030} = 3.8\%$$

It is probable, of course, that the error is within the root-sum-square of the three accuracy tolerances, or 3.1%. Therefore, the accuracy of the single weldable strain gage signal, based on scaling against the calibration signal, is ±3.1% of true strain at the input terminals to the signal conditioning.

2. Rosette and single foil gages

Four rosettes on Bay D (FSG-24, 25, 26, and 31) the single gage WSG-8 on Bay D, and the seven rosettes on Bays A, C, and C/D were foil gages with different properties and tolerances. The rosettes on Bay D were Micromeasurements Type CEA-06-250UR-120 having individual elements with nominal gage factors of 2.05 ± 0.5%. The resistance of each element is given as 120 ± 0.4%.

The rosettes on Bays A, C, and C/D (recorded on the analog system) were CFA-06-250UR-350, with similar properties except for resistance. The single gage WSG-8 was Type CEA-06-250-UW-350, having a gage factor of 2.085 ± 0.5%, and a resistance of 350Ω ± 0.3%. Using the same basic calibration equation for FSG-24, 25, 26, and 31:

$$\text{Microstrain} = \frac{120 \times 10^6}{2.05(59{,}900 + 120)} = 975$$

Applying the worst-case tolerances:

$$\text{Microstrain} = \frac{120(0.996) \times 10^6}{2.05(1.005)(59{,}900 \times 1.001 + 119.5)}$$

$$= \frac{119.52}{2.06 \times 60{,}079} = 966$$

$$\text{Max \% error} = \frac{975-966}{975} = 0.9\%$$

The value of the calibration resistor in both cases has been taken from a Validyne drawing. The FSG gages were part of the PCM system, and were shunt-calibrated in the same manner as described above.

The 350-ohm foil gages used in the analog system (WSG-1 through -7 rosettes, WSG-8 single gage) were calibrated using a somewhat different technique. Rather than using the same calibration resistor value for each circuit, the value was changed to compensate for slight variations in gage factor so that a specific microstrain (500) signal was simulated. The oscillographs were then adjusted to give a 2-inch span for this signal, and the signal to the tape recorder was measured in order to establish the scale factor for digitizing. Even though the three-wire circuit was used, shunt calibration was performed manually at the active gage, and thereafter all scaling was done on a voltage basis. The calibration signal itself was not used directly in the data reduction process.

The calibration values and tolerances are different, and yield a different probable error, as shown in the following calculation.

An R_c value of 341,948 ohms was set in a decade resistance box to simulate 500 microstrain for a 350-ohm gage element with a gage factor of 2.045:

$$500 = \frac{350 \times 10^6}{2.045(341{,}948 + 350)}$$

Given the tolerances stated above, the worst-case error is

$$\varepsilon_c = \frac{350(0.997) \times 10^6}{2.045 \times 1.005(341,948 \times 1.001 + 350(0.997)}$$

$$\varepsilon_c = \frac{348.95}{2.055(342,639)}$$

$$\varepsilon_c = 495.6 \text{ microstrain}$$

$$\text{Max \% error} = \frac{500 - 495.6}{500} = 0.88\%$$

3. Single foil gages in four-arm bridges

In order to measure the bending moment and axial load at the tops of selected columns, single gages were installed and connected together to form complete bridges. The PCM systems included an axial bridge and two orthogonal bending bridges on each of 4 columns surrounding Bay D, labeled D_1 - D_4. Two columns at Bay A and two columns at Bay B had axial bridges only, labeled A1, A2, B1 and B2, respectively. These latter signals were recorded on the analog system.

For D_1 - D_4, sixteen 120-ohm foil gages were installed and interconnected on each column to form the two bending and one axial bridge. The physical arrangement and circuits are shown in Figure 4-10. The calibration was accomplished as before by shunting one arm of the bridge with the standard 59,900-ohm resistor. Since the wire resistance must now be considered, the calibration equation* becomes

$$\varepsilon_c = \frac{1}{nK} \quad \frac{(R_g + 2R_L)^2}{R_g R_c}$$

*See Statham Instrument Notes No. 36, Nov. 1959 "The Effect of Transmission Line Resistance in the Shunt Calibration of Bridge Transducer" by Peter R. Perino.

For the bending bridges, assuming R_L = 14 ohms, and n = 4 arms:

$$\varepsilon_c = \frac{1}{4 \times 2.085} \; \frac{(120 + 28)^2}{120 \times 59{,}900} = 365 \text{ microstrain}$$

For the axial bridges, assuming R_L = 14 ohms, and n = 2.6 arms (Poisson gages):

$$\varepsilon_c = \frac{1}{2.6 \times 2.085} \; \frac{(240 + 28)^2}{240 \times 59{,}900} = 921.6$$

Assuming the worst-case tolerance on these values:

$$\varepsilon_c = \frac{1}{2.6 \times 2.085 \times 1.005} \; \frac{((240 \times 0.996) + 28)^2}{(240 \times 0.996)(59{,}900 \times 1.001)} = 913.2$$

$$\text{Max \% error} = \frac{921.6 - 913.2}{921.6} = 0.91\%$$

The actual average values of R_L were determined from a table of measurements made by G.E. Using these actual values, the calibration values were determined to be:

Bridge	R_L Average (Ω)	Calibration Microstrain
BB1-D1	13.8	364
BB2-D1	13.8	364
AB-D1	15.2	939
BB1-D2	15.9	385
BB2-D2	14.3	368
AB-D2	17.0	964
BB1-D3	17.0	396
BB2-D3	14.0	366
AB-D3	13.8	919
BB1-D4	13.1	357
BB2-D4	13.4	360
AB-D4	13.7	918

The test data were recorded using 242 and 747 microstrain, respectively, to establish the scale factor for the bending and axial bridges. A correction was made during the data reduction process, discussed below.

4. Additional Factors

Additional factors potentially affecting the accuracy of the strain gage data were also investigated:

a. Type/Size. The weldable strain gages were selected because they could be installed more quickly, and did not require extensive waterproofing treatment. Their only disadvantage from the standpoint of data accuracy was their relatively long gage length, 3/4 inch, and the 3 percent tolerance on gage factor.

b. Transverse Sensitivity. The manufacturer's data sheet indicates that the transverse sensitivity is negligibly small.

c. Temperature sensitivity. The weldable gages are self-temperature compensated for the range from 75 to 560°F. Because only dynamic data is of interest, and the data reduction process forces the initial level to zero, slow temperature variations will not affect the accuracy of the strain data.

d. Sensitivity to Curvature. Information from Ailtech indicated that the weldable gages could be applied to curved surfaces with radii as small as 1.5 inches by using the conventional welding techniques. Examination of the installation drawings and photographs did not reveal any situations where gages were applied to highly-curved surfaces.

e. Environmental Protection. The weldable gages were contained in a stainless steel tube which was hermetically sealed to the cable.

f. Miscellaneous Gage Considerations. The gages were rated for a strain range of ±20,000 microstrain, much higher than the strains actually experienced. There is no hysteresis within this range, and neither frequency response nor acceleration sensitivity are considerations in the accuracy evaluation. From a polarity standpoint, it is a characteristic of the material used to increase its resistance with increasing strain.

B. Pressure Transducers

1. Validyne AP-10

Validyne AP-10 absolute pressure transducers were used in two ranges, 0-1000 psia and 0-100 psia, as indicated in Table A-4. Those mounted on the torus shell in Bays D and C/D were modified to include a special sealed cavity with an external flush diaphragm. This modification was developed and tested to eliminate amplitude distortion and ringing for pressure transients.

These transducers operate on the variable reluctance principle, and are compatible with the Validyne carrier signal-conditioning system. The specification value for linearity is ±1/2 percent full scale of the best straight line.

2. Sensometric

Sensometric transducers were also installed in Bay D as a way of verifying the performance of the Validyne units. These are flush-mounted, strain-gage pressure transducers not susceptible to potential frequency response problems with cavities, and were used as a standard of comparison during the qualification tests of the modified AP-10s.

C. Accelerometers

The Entran Model EGAL-125-10 accelerometers are piezo-resistive devices using semiconductor strain gages. Therefore, they are capable of responding to static accelerations with a frequency response of at least 0-100 Hz. The non-linearity is quoted as ±1% of reading. Although they are somewhat temperature-sensitive, the torus environment is quite stable thermally, and any long-term drift would be removed during data reduction.

The Endevco units are connected to charge amplifiers having a 2-Hz low-frequency cutoff. Any data at this frequency or lower should be examined carefully, and compared with nearby strain information.

D. Temperature Detectors

The Micro-Measurements ETG-50A resistance temperature detectors were used in a four-wire system, with the output signal in millivolts as a function of temperature (10 mv per °F). The limitation on overall accuracy appears to be the uncertainty in the original resistance versus temperature table supplied by the manufacturer plus any signal conditioning calibration uncertainty.

III. SIGNAL CONDITIONING

A. PCM System

The signal-conditioning system converted the low-level transducer signals to the 10-volt full-scale level required by the analog-to-digital converter. The equipment used was a Validyne MC170 carrier system having various types of modules for the different transducers.

The most common module used was the CD173, designed to condition strain gage bridge circuits. It was used for strain gages, accelerometers, and pressure transducers. With an arbitrary scale factor of 1.0 volt output for 1,000 microstrain input, the CD173 was operating at a very reduced level for most of the strain signals recorded. For example, reviewing the raw strain data, it appears that the maximum recorded signal was 230 microstrain (except for the downcomer tie-bar, at over 600 microstrain). The CD173 output from this signal, therefore, was only 230 millivolts, or only 2.3% of full-scale output. At this level the basic electronic noise present becomes significant. The vast majority of data, of course, was much lower.

For the pressure data, better use was made of the available dynamic range. SRVDL pipe pressure maxima were on the order of 27% of full scale, and the shell and air bubble pressures were about 5 to 10% of full scale. These latter values are still relatively low, however.

The Validyne PT-174 module was used for the temperature detectors, and provides separate supply and sense leads. It amplifies and filters the output to indicate probe temperature with a scale factor of +1.0 volt output for a ΔT of +100°F over a range of -300°F to +1,000°F.

A common element in the Validyne MC170 system is the PS 176 Modular Oscillator Power Supply. This module provides the 5-volt, 3 kHz carrier excitation to all of the transducers in the PCM system, as well as ±15V DC power for the electronics.

B. FM Analog System

The analog system consisted of 26 channels of strain gage data conditioned by a Vishay 2100 System. Accuracy quoted for this system is ±2%. Amplifier bandwidth is flat within 5% of 5 kHz.

IV. DIGITIZING EQUIPMENT

The signals from the Validyne signal-conditioning system were presented as inputs to the two Preston Scientific GM Series PCM multiplexers. These devices scan all the input signals once each millisecond and generate a 12-bit word which represents the data amplitude on a scale of 0 to 4095 counts with 0 counts representing negative full-scale, and 4095 representing positive full scale. For example, with full-scale pressure of 100 psi producing an output of 10 volts, and zero pressure producing zero volts (2048 counts), 20 psi at the transducer generates an output of 2458 counts. The overall accuracy of the multiplexer, sample-and-hold circuit, and analog-to-digital converter is 0.06 percent of full scale, plus or minus half the least significant bit. The accuracy translates to a tolerance of ±12 millivolts.

Although the accuracy of the digitizer in converting analog signals to digital words is excellent at full scale, for very low-level signals the 5-millivolt resolution becomes significant. The strain gage data suffers in particular in this respect, because of the arbitrary establishment of a 1.0 volt/ 1,000 microstrain scale factor. The actual slope in microstrain per digitizing count is given by the "Engineering Unit Channel Description." For single strain gages the slope is 5 microstrain per count. A signal of 30 millivolts from a CD173, representing 30 microstrain, would generate only 6 counts (out of a full scale of 2,048).

This lack of resolution is compounded in the conversion to axial force for the column gages. With each microstrain representing more than one KIP, and about 5 microstrain per count, the least step in KIPS becomes about 9 KIPS. Since the maximum axial load reported is 101 KIPS, this is significant.

V. RECORDING EQUIPMENT

A. PCM System

The digitized data were applied serially to two tracks of a Sangamo Sabre III Model 3600, high-speed, direct-mode tape recorder. The probability of error in the digital format is much lower than that of other uncertainties discussed above.

B. Analog System

Analog data were recorded on two Honeywell 5600E FM tape recorders operating at 7-1/2 inches per second, giving a bandwidth of 0–2500 Hz. The accuracy of this equipment is quoted as ±2% in the Instrumentation Equipment Sheet. At the beginning of each tape a 1.0 volt peak, 100 Hz calibration signal was recorded.

C. Oscillographs

Real-time data going to the PCM system were recorded on eight 6-channel Brush oscillographs. Full scale in one direction covers 25 chart divisions, at 1 mm each. Since it is difficult to read these charts to any better than one-half division, the accuracy of data recorded on the oscillographs is no better than 2 percent. Three Honeywell 1508 oscillographs were used in association with the analog system, but were not used to present any final data.

VI. COMPUTER SYSTEMS

A. On-Site Equipment

A Hewlett-Packard HP2100 minicomputer, a Versatec plotter, and a printer (see system block diagram) were used at Monticello to monitor the results of the shakedown tests. This equipment was useful in improving system accuracy by locating sources of questionable data.

B. Computer System at San Jose

Conversion of the PCM data serially recorded on two tracks of the Sabre III tape to nine-track digital tape format is accomplished at the site by a Hewlett-Packard 2100 minicomputer. At San Jose, the bulk of the data reduction is performed by a Honeywell 6000 computer system. In this process, an Engineering Unit tape is generated which can then provide either tabular ("edits") or plotted output. The accuracy of the hardware part of this system is virtually perfect. The source of potential error, therefore, is in the software. By a number of comparisons, however, of computer output with known data input, there appears to be no inaccuracies that can be attributed to computer software. The occurrence of spurious data points is suspected to arise from the reproduction of the PCM tape at a very reduced speed.

The analog strain gage data were also converted to digital data in a system based on a XDS Sigma 5 computer. Again, the accuracy of the digital processing is much better than that of other elements in the total system.

VII. CALIBRATION METHODS

A. PCM System

1. Strain gages

All strain gages connected to the PCM system were shunt-calibrated using a 59,900 ohm resistor. The microstrain simulated by this calibration was calculated (as demonstrated above) and amplifier gains set so that the

1.0 volt per 1,000 microstrain transfer function was achieved. All strain gages were calibrated simultaneously before and after each test, and the calibration signals were recorded on the PCM tape. The accuracy of this calibration depends upon the accuracy of the strain gage and calibration resistances, and the tolerance on the gage factor. For the weldable strain gages this tolerance, ±3 percent, is the principal uncertainty.

2. Pressure Transducers

Calibration of the Validyne pressure transducer output was established primarily by the manufacturer using a ratio transformer. Each transducer was pressurized individually, and the entire torus was also pressurized as a calibration check. System calibrations were accomplished by using a ratio transformer to simulate the transducer output for zero and full-scale pressure.

Sensometric pressure transducer calibration was based upon manufacturer's data.

3. Accelerometers

Accelerometer data depended upon application of the manufacturer's given sensitivity in setting the signal-conditioning amplifier gains.

4. Temperature Detectors

The RTDs were calibrated by substituting resistances calculated to simulate the output for the desired full-scale temperature range.

B. FM Analog System

The strain gages on the FM analog system were shunt calibrated manually at each gage location, and amplifier gains adjusted to produce the desired output. No shunt calibration signals were recorded during the tests. Scaling was accomplished by comparing recorded signal levels with a standard 1.0 volt signal recorded for that purpose.

VIII. CUMULATIVE SYSTEM ACCURACY

Over and above the detailed examination of the specification accuracy of individual system components, there are other investigations which must be conducted in order to arrive at a rational value for system accuracy. One of these is the question of proper installation of the transducers and wiring. These installations were done by qualified, experienced personnel, and were inspected in accordance with established procedures. Further inspection by those involved in test planning and data interpretation served to heighten confidence in the installations. Confidence in the transducers themselves is gained from the fact that only one out of more than 200 individual strain gages is known to have failed during the test.

Another very important area for consideration is the final conversion of raw strain data to maximum and minimum principal stresses, uniaxial stresses, and column axial and bending loads. These conversions are accomplished by the equations in the software for producing the Engineering Units tape. These equations incorporate properties of the material and, for the columns, dimensions of the structure.

Two properties of the steel are used in the equations: Young's Modulus (E), given as 27.9×10^6 PSI, and Poisson's Ratio (μ), given as 0.300 for the computations. All stress values are directly proportional to E, but μ enters the equations in a variety of ways. Because it appears in the denominator of the component stress equations as $1 - \mu^2$, a small variation in μ can have a significant effect. Since there is no practical way to determine μ for the structure tested, an error value cannot be assigned. It is important to recognize this source of uncertainty in the final results, however, to avoid the unnecessary pursuit of very high accuracy in the other parts of the entire data path.

For the significant structural data, then, derived from weldable strain gages, the principal sources of uncertainty appear to be the following:

gage factor:	3%
gage resistance:	1%

signal conditioning (low levels):	1%
Poisson's Ratio:	2%
digitizing:	±140 PSI (least count)

Disregarding the uncertainty in Poisson's Ratio, and accepting $E = 27.9 \times 10^6$ psi with no assigned tolerance, the root-sum-square of the remaining percentage tolerances is about ±3.3 percent. For the lower values of strain data, where the 5 microstrain per count (about 140 psi) digitizing resolution becomes important, the uncertainty in the results can be much higher. Quantitatively, stress values reported as 2.8 ksi would have an additional 5 percent uncertainty from the digitizing, for a total root-sum-square accuracy of

$$RSS = \sqrt{3^2 + 1^2 + 1^2 + 5^2} = \pm 6 \text{ percent}$$

Regarding the column axial and bending data, the conversion factors from strain to axial load and bending moment are based on calculations using the nominal dimensions of the columns. Manufacturing tolerances for pipe allow a 12 percent variation of wall thickness less than the nominal value. Nevertheless, in considering the real meaning of the column data, the actual loads on the columns may be somewhat higher than those reported if the pipe wall thickness is less than nominal.

In summary, for each type of measurement there is a unique set of circumstances to consider in evaluating the accuracy of the results. Stress values below 2.8 ksi have an accuracy of no better than 6 percent, and this accuracy degrades as the value decreases. Column axial loads are limited to about 10 percent accuracy by the digitizing resolution alone, ignoring the other uncertainties discussed above. Temperature data has a basic tolerance of 2°F based on the resistance/temperature characteristic. Accelerations and pressures have no known sources of error other than the given transducer accuracies and calibration accuracies, and the resulting data may be considered accurate to about 1 percent. Strain data from the FM analog system are limited to ±2 percent by the tolerance on signal conditioning equipment.

IX. ERROR CORRECTION PROCEDURES

Because of the analysis of the column strain gage circuits was continuing until just before the tests began, scale factors based on earlier calculations had already been used to set up the voltages on the strain gage circuits. To avoid an unnecessary disruption of the other work involved at that time, it was decided to leave the voltages as set, and to make the necessary corrections in the data reduction process.

The data were corrected during the data reduction process by changing the slope and intercept of the transfer function relating PCM counts to microstrain. For example, the Axial Bridge on Column D1 (AB-D1, Engineering Unit Channel 243) was recorded with the calibration signal assumed to represent 747 microstrain. Since the final calculation resulted in a value of 939 microstrain, all data should be raised proportionately. This was accomplished by changing the slope value by the ratio 939/747, and calculating the new intercept.

The new slopes and intercepts were calculated at the time of the test, and now appear in the Engineering Unit Channel Description (Production Version, January 6, 1978).

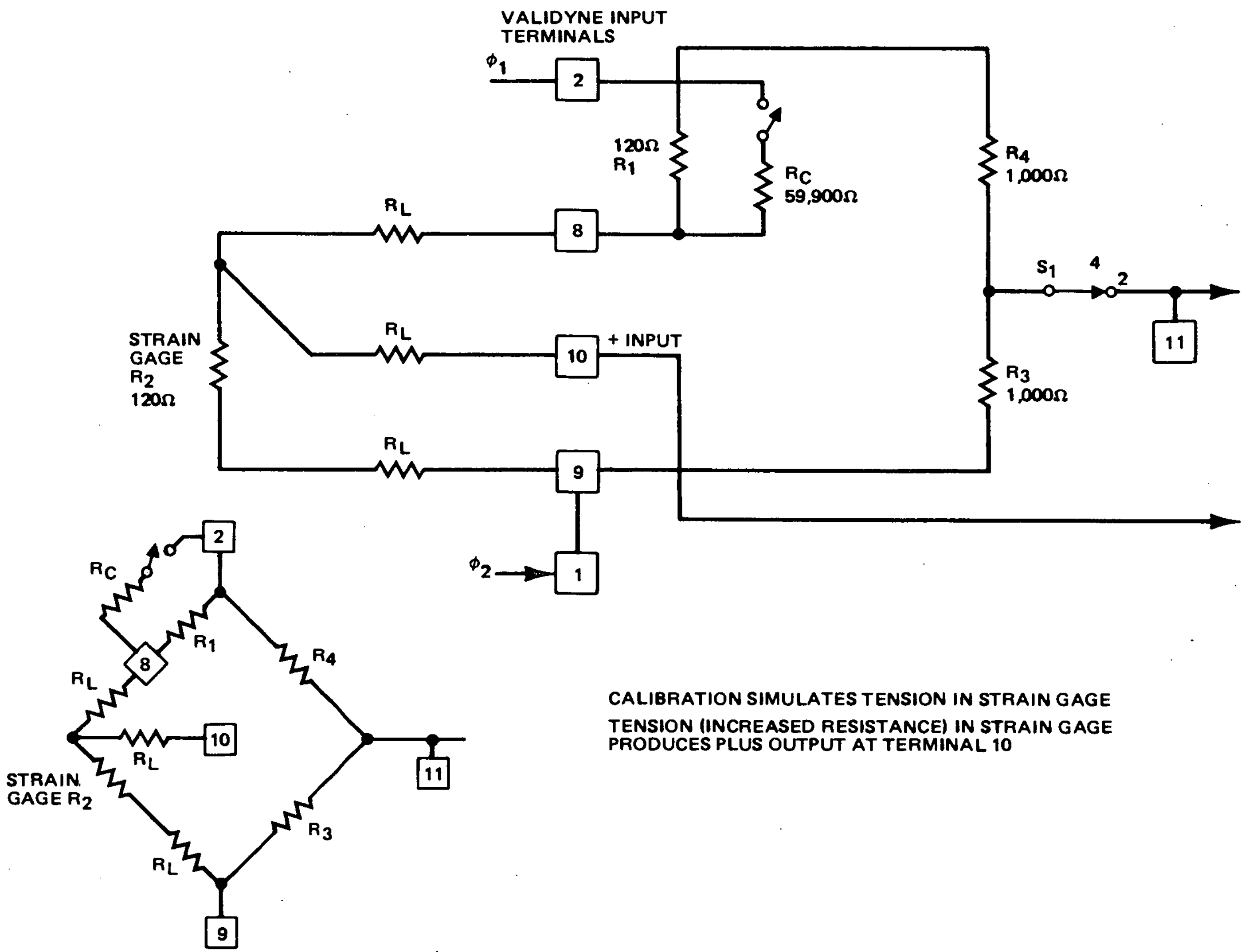

Figure B-1. Quarter Bridge Input Circuit (Modified Validyne CD173-1207)

APPENDIX C
MAXIMUM MEASURED PRESSURES - SRV PIPING AND T-QUENCHER

This appendix presents a tabulation of maximum pressures in the SRVDL and in the T-Quencher as measured by P1, P2, P4 and P5 for the SRV line and by P6 and P7 for the T-Quencher, for all valve A tests. In addition, statistical evaluations for these sensors are tabulated for different test conditions.

Table C-1

S/RV PIPE AND T-QUENCHER PRESSURES
Peak/Steady State

Run No.	Test No.	S/RV Pipe Pressures (psig) P1	P2	P4	P5	T-Quencher Pressures (psid) P6	P7
2	2						
3	501						
4	502						
5	801						
6	802						
7	901						
8	902						
9	903						
10	904						
11	905						
12	1101						
13	1102						
14	1103						
15	1104						
16	1105						
17	12						
18	1301						
18	1302						
18	1303						
19	14						
20	15						
21	1601						
21	1602						
21	1603						
21	1604						
21	1605						
22	18						
23	19						
24	21						
25	22						

Table C-1 (Continued)

Run No.	Test No.	S/RV Pipe Pressures (psig) P1	P2	P4	P5	T-Quencher Pressures (psid) P6	P7
26	2301						
28	2302						
30	2303						
31	2304						
31	2305						
31	2306						
31	2307						
32	24						

Table C-2

STATISTICAL EVALUATIONS FOR SRV PIPE AND T-QUENCHER PRESSURES

Test Conditions and Tests Involved		SRVDL Pressures (psig)				T-Quencher Pressures (psid)	
		P_1	P_2	P_4	P_5	P_6	P_7
CP, NWL, SVA Valve A Tests: 2,501, 806, 901, 1301, 1601, 24	Highest Value(s) Meas'd						
	Mean $(\bar{x})$						
	Standard Deviation (σ)						
	Std Dev./Mean $(\sigma/\bar{x})$						
HP, NWL, SVA Valve A Tests: 802, 902, 903 904, 905	Highest Value(s) Meas'd						
	Mean $(\bar{x})$						
	Standard Deviation (σ)						
	Std. Dev./Mean $(\sigma/\bar{x})$						
HP, DWL, SVA Valve A Tests: 3103, 1602, 1603, 1604, 1605	Highest Value(s) Meas'd						
	Mean $(\bar{x})$						
	Standard Deviation (σ)						
	Std. Dev./Mean $(\sigma/\bar{x})$						
HP, EWL, SVA Valve A Tests 2305, 2306	Highest Value(s) Meas'd						

*Pressures measured during CP, NWL, MVA tests are included in these values.

Table C-2 (Continued)

Test Conditions and Tests Involved		SRVDL Pressures (psig) P_1	P_2	P_4	P_5	T-Quencher Pressures (psid) P_6	P_7
CP, NWL, MVA Valve A (and E and G) Tests: 2301, 2302, 2303, 2304	Highest Value(s) Meas'd						
CP, NWL, SVA Valve E Tests 1101, 14, 18, 21	Highest Value(s) Meas'd Mean $(\bar{x})$ Standard Deviation (σ) Std. Dev./Mean $(\sigma/\bar{x})$				NA		
HP, NWL, SVA Valve E Tests: 1102, 1103, 1104, 1105	Highest Values Meas'd Mean $(\bar{x})$ Standard Deviation (σ) Std. Dev./Mean $(\sigma/\bar{x})$				NA		
CP, NWL, SVA Valve G Tests: 12, 15, 19, 22	Highest Values Meas'd Mean $(\bar{x})$ Std. Dev. (σ) Standard Deviation (σ)				NA		

APPENDIX D

MAXIMUM MEASURED PRESSURES - AIR BUBBLE AND TORUS SHELL

This appendix contains the following tables:

Table	Description
D-1	Maximum positive and maximum negative bubble and pool pressures measured by P8, P9, P10, P11 for all tests.
D-2	Statistical evaluations for the sensors in Table D-1.
D-3	Maximum positive and maximum negative torus shell pressures (all sensors) for all tests.
D-4	Statistical evaluations for all Torus shell pressure sensors reported in Table D-3.
D-5	Maximum positive and maximum negative T-Quencher bubble pressure differential for all tests.
D-6	Torus shell (P16) and bubble pressure (P9) frequencies for all valve A tests.

Table D-1

DATA FOR BUBBLE PRESSURES*
Peak Positive/Peak Negative (psid)

Run No.	Test No.	P8	P9	P10	P11
2	2				
3	501				
4	502				
5	801				
6	802				
7	901				
8	902				
9	903				
10	904				
11	905				
12	1101				
13	1102				
14	1103				
15	1104				
16	1105				
17	12				
18	1301				
18	1302				
18	1303				
19	14				
20	15				
21	1601				
21	1602				
21	1603				
21	1604				

*Pressures are given as follows: Maximum positive/maximum negative. These sensors (P8, P9, P10, P11) measure bubble pressures for Valve A tests and pool water pressures, otherwise.

**This bubble pressure was above psid for less than milliseconds and therefore, psid was taken as the maximum positive pressure.

Table D-1 (Continued)

DATA FOR BUBBLE PRESSURES*
Peak Positive/Peak Negative (psid)

Run No.	Test No.	P8	P9	P10	P11
21	1605				
22	18				
23	19				
24	21				
25	22				
26	2301				
28	2302				
30	2303				
31	2304				
31	2305				
31	2306				
31	2307				
32	24				

*Pressures are given as follows: Maximum positive/maximum negative. These sensors (P8, P9, P10, P11) measure bubble pressures for Valve A tests and pool water pressures, otherwise.

**This Bubble Pressure was above psid for less than milliseconds and thus, psid was taken as the maximum positive pressure.

Table D-2

STATISTICAL EVALUATIONS FOR BUBBLE PRESSURES*

Test Conditions and Tests Involved		Bubble Pressures* (psid) or Pool Water Pressures (psid)			
		P_8	P_9	P_{10}	P_{11}
CP, NWL, SVA Valve A Tests: 2, 501, 801, 901, 1301, 1601, 24	Highest Value(s) Measured				
	Mean ($\bar{x}$)				
	Standard Deviation (σ)				
	Std Dev./ Mean ($\sigma/\bar{x}$)				
HP, NWL, SVA Valve A Tests: 802, 902, 903, 904, 905	Highest Value(s) Measured				
	Mean ($\bar{x}$)				
	Standard Deviation (σ)				
	Std. Dev./Mean ($\sigma/\bar{x}$)				
HP, DWL, SVA Valve A Tests: 1303, 1602, 1603, 1604, 1605	Highest Value(s) Measured				
	Mean ($\bar{x}$)				
	Standard Deviation (σ)				
	Std. Dev./Mean ($\sigma/\bar{x}$)				
HP, EWL, SVA Valve A Tests 2305, 2306	Highest Value(s) Measured				

*Pressures are given as follows: Maximum positive/maximum negative and did not necessarily occur in the same test. These sensors (P8, P9, P10, P11) measured bubble pressures for valve A tests and pool water pressures, otherwise.

Table D-2 (Continued)

STATISTICAL EVALUATIONS FOR BUBBLE PRESSURES*

Test Conditions and Tests Involved		Bubble Pressures* (psid) or Pool Water Pressures (psid)			
		P_8	P_9	P_{10}	P_{11}
CP, NWL, MVA Valve A (and E and G) Tests: 2301, 2302, 2303, 2304	Highest Value(s) Measured				
CP, NWL, SVA Valve E Tests 1101, 14, 18, 21	Highest Value(s) Measured				
	Mean ($\overline{x}$)				
	Standard Deviation (σ)				
	Std. Dev./Mean ($\sigma/\overline{x}$)				
HP, NWL, SVA Valve E Tests: 1102, 1103, 1104, 1105	Highest Values Measured				
	Mean ($\overline{x}$)				
	Standard Deviation (σ)				
	Std. Dev./Mean ($\sigma/\overline{x}$)				
CP, NWL, SVA Valve G Tests: 12, 15, 19, 22	Highest Values Measured				
	Mean ($\overline{x}$)				
	Standard Deviation (σ)				
	Std. Dev./Mean ($\sigma/\overline{x}$)				

*Pressures are given as follows: Maximum positive/maximum negative and did not necessarily occur in the same test. These sensors (P8, P9, P10, P11) measured bubble pressures for valve A tests and pool water pressures, otherwise.

Table D-3

TORUS SHELL PRESSURES

Peak Positive/Peak Negative (psid)
(Sheet 1 of 8)

Run No.	Test No.	P12	P13	P14	P15
2	2				
3	501				
4	502				
5	801				
6	802				
7	901				
8	902				
9	903				
10	904				
11	905				
12	1101				
13	1102				
14	1103				
15	1104				
16	1105				
17	12				
18	1301				
18	1302				
18	1303				
19	14				
20	15				
21	1601				
21	1602				
21	1603				
21	1604				
21	1605				
22	18				
23	19				
24	21				
25	22				
26	2301				
28	2302				
30	2303				
31	2304				
31	2305				
31	2306				
31	2307				
32	24				

Table D-3

TORUS SHELL PRESSURES
Peak Positive/Peak Negative (psid)
(Sheet 2 of 8)

Run No.	Test No.	P16	P17	P18	P19
2	2				
3	501				
4	502				
5	801				
6	802				
7	901				
8	902				
9	903				
10	904				
11	905				
12	1101				
13	1102				
14	1103				
15	1104				
16	1105				
17	12				
18	1301				
18	1302				
18	1303				
19	14				
20	15				
21	1601				
21	1602				
21	1603				
21	1604				
21	1605				
22	18				
23	19				
24	21				
25	22				
26	2301				
28	2302				
30	2303				
31	2304				
31	2305				
31	2306				
31	2307				
32	24				

Table D-3

TORUS SHELL PRESSURES
Peak Positive/Peak Negative (psid)
(Sheet 3 of 8)

Run No.	Test No.	P20	P21	P22	P23
2	2				
3	501				
4	502				
5	801				
6	802				
7	901				
8	902				
9	903				
10	904				
11	905				
12	1101				
13	1102				
14	1103				
15	1104				
16	1105				
17	12				
18	1301				
18	1302				
18	1303				
19	14				
20	15				
21	1601				
21	1602				
21	1603				
21	1604				
21	1605				
22	18				
23	19				
24	21				
25	22				
26	2301				
28	2302				
30	2303				
31	2304				
31	2305				
31	2306				
31	2307				
32	24				

Table D-3

TORUS SHELL PRESSURES
Peak Positive/Peak Negative (psid)
(Sheet 4 of 8)

Run No.	Test No.	P24	P26	P27	P29
2	2				
3	501				
4	502				
5	801				
6	802				
7	901				
8	902				
9	903				
10	904				
11	905				
12	1101				
13	1102				
14	1103				
15	1104				
16	1105				
17	12				
18	1301				
18	1302				
18	1303				
19	14				
20	15				
21	1601				
21	1602				
21	1603				
21	1604				
21	1605				
22	18				
23	19				
24	21				
25	22				
26	2301				
28	2302				
30	2303				
31	2304				
31	2305				
31	2306				
31	2307				
32	24				

Table D-3

TORUS SHELL PRESSURES
Peak Positive/Peak Negative (psid)
(Sheet 5 of 8)

Run No.	Test No.	P30	P31	P33	P34
2	2				
3	501				
4	502				
5	801				
6	802				
7	901				
8	902				
9	903				
10	904				
11	905				
12	1101				
13	1102				
14	1103				
15	1104				
16	1105				
17	12				
18	1301				
18	1302				
18	1303				
19	14				
20	15				
21	1601				
21	1602				
21	1603				
21	1604				
21	1605				
22	18				
23	19				
24	21				
25	22				
26	2301				
28	2302				
30	2303				
31	2304				
31	2305				
31	2306				
31	2307				
32	24				

Table D-3

TORUS SHELL PRESSURES
Peak Positive/Peak Negative (psid)
(Sheet 6 of 8)

Run No.	Test No.	P35	P36	P37	P38
2	2				
3	501				
4	502				
5	801				
6	802				
7	901				
8	902				
9	903				
10	904				
11	905				
12	1101				
13	1102				
14	1103				
15	1104				
16	1105				
17	12				
18	1301				
18	1302				
18	1303				
19	14				
20	15				
21	1601				
21	1602				
21	1603				
21	1604				
21	1605				
22	18				
23	19				
24	21				
25	22				
26	2301				
28	2302				
30	2303				
31	2304				
31	2305				
31	2306				
31	2307				
32	24				

*P35 shifted at beginning of reading by +1.1 psid.

Table D-3

TORUS SHELL PRESSURES
Peak Positive/Peak Negative (psid)
(Sheet 7 of 8)

Run No.	Test No.	P39	P40	P41	P42
2	2				
3	501				
4	502				
5	801				
6	802				
7	901				
8	902				
9	903				
10	904				
11	905				
12	1101				
13	1102				
14	1103				
15	1104				
16	1105				
17	12				
18	1301				
18	1302				
18	1303				
19	14				
20	15				
21	1601				
21	1602				
21	1603				
21	1604				
21	1605				
22	18				
23	19				
24	21				
25	22				
26	2301				
28	2302				
30	2303				
31	2304				
31	2305				
31	2306				
31	2307				
32	24				

Table D-3

TORUS SHELL PRESSURES
Peak Positive/Peak Negative (psid)
(Sheet 8 of 8)

Run No.	Test No.	P43	P46
2	2		
3	501		
4	502		
5	801		
6	802		
7	901		
8	902		
9	903		
10	904		
11	905		
12	1101		
13	1102		
14	1103		
15	1104		
16	1105		
17	12		
18	1301		
18	1302		
18	1303		
19	14		
20	15		
21	1601		
21	1602		
21	1603		
21	1604		
21	1605		
22	18		
23	19		
24	21		
25	22		
26	2301		
28	2302		
30	2303		
31	2304		
31	2305		
31	2306		
31	2307		
32	24		

Table D-4

STATISTICAL EVALUATIONS FOR SHELL PRESSURES
(Sheet 1 of 5)

Test Conditions and Tests Involved		Shell Pressures* (psid) P_{12}	P_{13}	P_{14}	P_{15}	P_{16}	P_{17}
CP, NWL, SVA Valve A Tests: 2,501, 801, 901, 1301, 1601, 24	Highest Value(s) Measured Mean ($\overline{x}$) Standard Deviation (σ) Std. Dev./Mean ($\sigma/\overline{x}$)						
HP, NWL, SVA Valve A Tests: 802, 902, 903, 904, 905	Highest Value(s) Measured Mean ($\overline{x}$) Standard Deviation (σ) Std. Dev./Mean ($\sigma/\overline{x}$)						
HP, DWL, SVA Valve A Tests: 1303, 1602, 1603, 1604, 1605	Highest Value(s) Measured Mean ($\overline{x}$) Standard Deviation (σ) Std. Dev./Mean ($\sigma/\overline{x}$)						
HP, EWL, SVA Valve A Tests 2305, 2306	Highest Value(s) Measured						
CP, NWL, MVA Valve A (and E and G) Tests: 2301, 2302, 2303, 2304	Highest Value(s) Measured						
CP, NWL, SVA Valve E Tests 1101, 14, 18, 21	Highest Value(s) Measured Mean ($\overline{x}$) Standard Deviation (σ) Std. Dev./Mean ($\sigma/\overline{x}$)						
HP, NWL, SVA Valve E Tests: 1102, 1103, 1104, 1105	Highest Values Measured Mean ($\overline{x}$) Standard Deviation (σ) Std. Dev./Mean ($\sigma/\overline{x}$)						
CP, NWL, SVA Valve G Tests: 12, 15, 19, 22	Highest Values Measured Mean ($\overline{x}$) Std. Dev. (σ) Std. Dev./Mean ($\sigma/\overline{x}$)						

*Shell Pressures are given as follows: Maximum Positive/Maximum Negative and did not necessarily occur in the same test.

Table D-4

STATISTICAL EVALUATIONS FOR SHELL PRESSURES
(Sheet 2 of 5)

Test Conditions and Tests Involved		Shell Pressures* (psid) P_{18}	P_{19}	P_{20}	P_{21}	P_{22}	P_{23}
CP, NWL, SVA Valve A Tests: 2,501, 801, 901, 1301, 1601, 24	Highest Value(s) Measured						
	Mean ($\bar{x}$)						
	Standard Deviation (σ)						
	Std. Dev./Mean ($\sigma/\bar{x}$)						
HP, NWL, SVA Valve A Tests: 802, 902, 903, 904, 905	Highest Value(s) Measured						
	Mean ($\bar{x}$)						
	Standard Deviation (σ)						
	Std. Dev./Mean ($\sigma/\bar{x}$)						
HP, DWL, SVA Valve A Tests: 1303, 1602, 1603, 1604, 1605	Highest Value(s) Measured						
	Mean ($\bar{x}$)						
	Standard Deviation (σ)						
	Std. Dev./Mean ($\sigma/\bar{x}$)						
HP, EWL, SVA Valve A Tests 2305, 2306	Highest Value(s) Measured						
CP, NWL, MVA Valve A (and E and G) Tests: 2301, 2302, 2303, 2304	Highest Value(s) Measured						
CP, NWL, SVA Valve E Tests 1101, 14, 18, 21	Highest Value(s) Measured						
	Mean ($\bar{x}$)						
	Standard Deviation (σ)						
	Std. Dev./Mean ($\sigma/\bar{x}$)						
HP, NWL, SVA Valve E Tests: 1102, 1103, 1104, 1105	Highest Values Measured						
	Mean ($\bar{x}$)						
	Standard Deviation (σ)						
	Std. Dev./Mean ($\sigma/\bar{x}$)						
CP, NWL, SVA Valve G Tests: 12, 15, 19, 22	Highest Values Measured						
	Mean ($\bar{x}$)						
	Std. Dev. (σ)						
	Std. Dev./Mean ($\sigma/\bar{x}$)						

*Shell Pressures are given as follows: Maximum Positive/Maximum Negative and did not necessarily occur in the same test.

Table D-4

STATISTICAL EVALUATIONS FOR SHELL PRESSURES
(Sheet 3 of 5)

Test Conditions and Tests Involved		Shell Pressures* (psid) P_{24}	P_{26}	P_{27}	P_{29}	P_{30}	P_{31}
CP, NWL, SVA Valve A Tests: 2,501, 801, 901, 1301, 1601, 24	Highest Value(s) Measured Mean ($\bar{x}$) Standard Deviation (σ) Std. Dev./Mean ($\sigma/\bar{x}$)						
HP, NWL, SVA Valve A Tests: 802, 902, 903, 904, 905	Highest Value(s) Measured Mean ($\bar{x}$) Standard Deviation (σ) Std. Dev./Mean ($\sigma/\bar{x}$)						
HP, DWL, SVA Valve A Tests: 1303, 1602, 1603, 1604, 1605	Highest Value(s) Measured Mean ($\bar{x}$) Standard Deviation (σ) Std. Dev./Mean ($\sigma/\bar{x}$)						
HP, EWL, SVA Valve A Tests 2305, 2306	Highest Value(s) Measured						
CP, NWL, MVA Valve A (and E and G) Tests: 2301, 2302, 2303, 2304	Highest Value(s) Measured						
CP, NWL, SVA Valve E Tests 1101, 14, 18, 21	Highest Value(s) Measured Mean ($\bar{x}$) Standard Deviation (σ) Std. Dev./Mean ($\sigma/\bar{x}$)						
HP, NWL, SVA Valve E Tests: 1102, 1103, 1104, 1105	Highest Values Measured Mean ($\bar{x}$) Standard Deviation (σ) Std. Dev./Mean ($\sigma/\bar{x}$)						
CP, NWL, SVA Valve G Tests: 12, 15, 19, 22	Highest Values Measured Mean ($\bar{x}$) Std. Dev. (σ) Std. Dev./Mean ($\sigma/\bar{x}$)						

*Shell Pressures are given as follows: Maximum Positive/Maximum Negative and did not necessarily occur in the same test.

Table D-4

STATISTICAL EVALUATIONS FOR SHELL PRESSURES
(Sheet 4 of 5)

Test Conditions and Tests Involved		Shell Pressures* (psid) P_{33}	P_{34}	P_{35}	P_{36}	P_{37}	P_{38}
CP, NWL, SVA Valve A Tests: 2,501, 801, 901, 1301, 1601, 24	Highest Value(s) Measured Mean ($\overline{x}$) Standard Deviation (σ) Std. Dev./Mean ($\sigma/\overline{x}$)						
HP, NWL, SVA Valve A Tests: 802, 902, 903, 904, 905	Highest Value(s) Measured Mean ($\overline{x}$) Standard Deviation (σ) Std. Dev./Mean ($\sigma/\overline{x}$)						
HP, DWL, SVA Valve A Tests: 1303, 1602, 1603, 1604, 1605	Highest Value(s) Measured Mean ($\overline{x}$) Standard Deviation (σ) Std. Dev./Mean ($\sigma/\overline{x}$)						
HP, EWL, SVA Valve A Tests 2305, 2306	Highest Value(s) Measured						
CP, NWL, MVA Valve A (and E and G) Tests: 2301, 2302, 2303, 2304	Highest Value(s) Measured						
CP, NWL, SVA Valve E Tests 1101, 14, 18, 21	Highest Value(s) Measured Mean ($\overline{x}$) Standard Deviation (σ) Std. Dev./Mean ($\sigma/\overline{x}$)						
HP, NWL, SVA Valve E Tests: 1102, 1103, 1104, 1105	Highest Values Measured Mean ($\overline{x}$) Standard Deviation (σ) Std. Dev./Mean ($\sigma/\overline{x}$)						
CP, NWL, SVA Valve G Tests: 12, 15, 19, 22	Highest Values Measured Mean ($\overline{x}$) Std. Dev. (σ) Std. Dev./Mean ($\sigma/\overline{x}$)						

*Shell Pressures are given as follows: Maximum Positive/Maximum Negative and did not necessarily occur in the same test.

Table D-4

STATISTICAL EVALUATIONS FOR SHELL PRESSURES
(Sheet 5 of 5)

Test Conditions and Tests Involved		Shell Pressures* (psid) P_{39}	P_{40}	P_{41}	P_{42}	P_{43}	P_{46}
CP, NWL, SVA Valve A Tests: 2,501, 801, 901, 1301, 1601, 24	Highest Value(s) Measured Mean ($\bar{x}$) Standard Deviation (σ) Std. Dev./Mean ($\sigma/\bar{x}$)						
HP, NWL, SVA Valve A Tests: 802, 902, 903, 904, 905	Highest Value(s) Measured Mean ($\bar{x}$) Standard Deviation (σ) Std. Dev./Mean ($\sigma/\bar{x}$)						
HP, DWL, SVA Valve A Tests: 1303, 1602, 1603, 1604, 1605	Highest Value(s) Measured Mean ($\bar{x}$) Standard Deviation (σ) Std. Dev./Mean ($\sigma/\bar{x}$)						
HP, EWL, SVA Valve A Tests 2305, 2306	Highest Value(s) Measured						
CP, NWL, MVA Valve A (and E and G) Tests: 2301, 2302, 2303, 2304	Highest Value(s) Measured						
CP, NWL, SVA Valve E Tests 1101, 14, 18, 21	Highest Value(s) Measured Mean ($\bar{x}$) Standard Deviation (σ) Std. Dev./Mean ($\sigma/\bar{x}$)						
HP, NWL, SVA Valve E Tests: 1102, 1103, 1104, 1105	Highest Values Measured Mean ($\bar{x}$) Standard Deviation (σ) Std. Dev./Mean ($\sigma/\bar{x}$)						
CP, NWL, SVA Valve G Tests: 12, 15, 19, 22	Highest Values Measured Mean ($\bar{x}$) Std. Dev. (σ) Std. Dev./Mean ($\sigma/\bar{x}$)						

*Shell Pressures are given as follows: Maximum Positive/Maximum Negative and did not necessarily occur in the same test.

Table D-5

BUBBLE PRESSURE* DIFFERENTIAL
Peak Positive/Peak Negative

Run No.	Test No.	P9-P8	P11-P10
2	2		
3	501		
4	502		
5	801		
6	802		
7	901		
8	902		
9	903		
10	904		
11	905		
12	1101		
13	1102		
14	1103		
15	1104		
16	1105		
17	12		
18	1301		
18	1302		
18	1303		
19	14		
20	15		
21	1601		
21	1602		
21	1603		
21	1604		
21	1605		
22	18		
23	19		
24	21		
25	22		
26	2301		
28	2302		
30	2303		
31	2304		
31	2305		
31	2306		
31	2307		
32	24		

*Pressures are given as follows: Maximum Positive/Maximum Negative. These sensors (P8, P9, P10, P11) measure bubble pressures for valve A tests and pool water pressures, otherwise.

**See note on P11, test 901 of Table D-1.

***See note on P11, test 2306 of Table D-1.

Table D-6

TORUS SHELL AND BUBBLE PRESSURE FREQUENCIES
DUE TO SRV AIR BUBBLE OSCILLATION (Hz)

Run No.	Cycle Test No.	1st P9[1]	1st P16[2]	2nd P9	2nd P16	3rd P9	3rd P16	4th P9	4th P16	5th P9	5th P16	6th P9	6th P16
2	2												
3	501												
4	502												
5	801												
6	802												
7	901												
8	902												
9	903												
10	904												
11	905												
12	1101												
13	1102												
14	1103												
15	1104												
16	1105												
17	12												
18	1301												
18	1302												
18	1303												
19	14												
20	15												
21	1601												
21	1602												
21	1603												
21	1604												
21	1605												

1. P9 is a sensor measuring bubble pressures.

2. P16 is a sensor measuring shell pressures.

*Pressure cycles due to air bubble oscillation could not be separated from the high frequency steam condensation pressures.

Table D-6 (Continued)

TORUS SHELL AND BUBBLE PRESSURE FREQUENCIES
DUE TO SRV AIR BUBBLE OSCILLATION (Hz)

Run No.	Cycle Test No.	1st P9[1]	1st P16[2]	2nd P9	2nd P16	3rd P9	3rd P16	4th P9	4th P16	5th P9	5th P16	6th P9	6th P16
22	18												
23	19						NA						
24	21												
25	22												
26	2301												
28	2302												
30	2303												
31	2304												
31	2305												
31	2306												
31	2307												
32	24												

1. P9 is a sensor measuring bubble pressures.
2. P16 is a sensor measuring shell pressures.

*Pressure cycles due to air bubble oscillation could not be separated from the high frequency steam condensation pressures.

APPENDIX E

SAMPLES OF HYDRODYNAMIC DATA PLOTS

Appendix E presents the following Hydrodynamic Data Plots:

E-1 Sample data plots for test 801 (CP,NWL,SVA).

E-2 Bubble pressures for tests 901 (CP,NWL,SVA) and 2306 (HP,EWL,SVA).

E-3 Pool pressures and torus shell pressures for test 24 (CP,NWL,SVA) during steam condensation phase.

E-4 Pool temperature transient plots for the long discharge tests, with RHR and without RHR.

E-1

Sample data plots for test 801, for pipe pressure sensors, T-Quencher pressure sensors, torus shell pressure sensors, bubble pressure sensors, pressure differential on T-quencher arms, air flow through vacuum breaker, SRVDL prepressurization, and pipe pressure transient during water reflood.

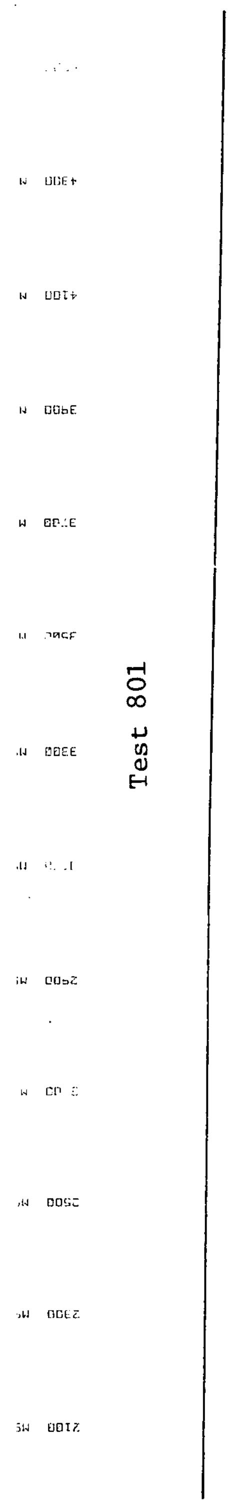

Test 801

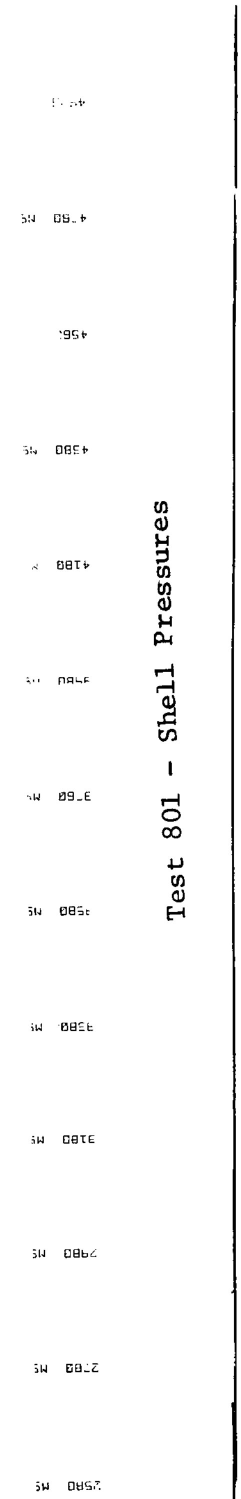

Test 801 - Shell Pressures

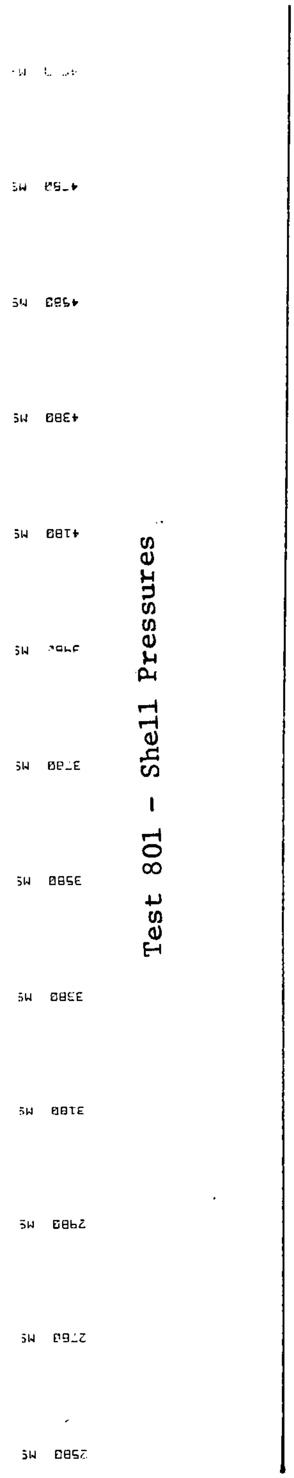

Test 801 - Shell Pressures

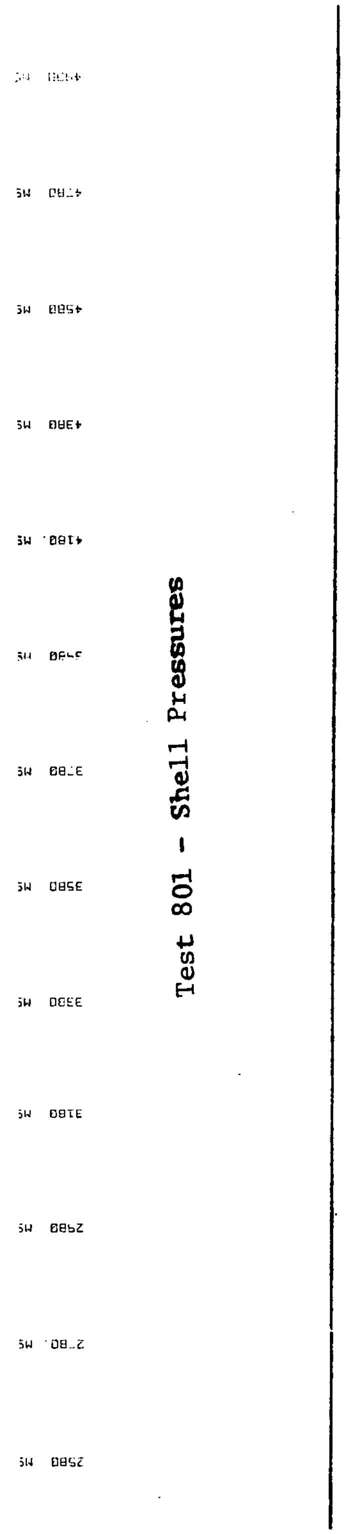

Test 801 - Shell Pressures

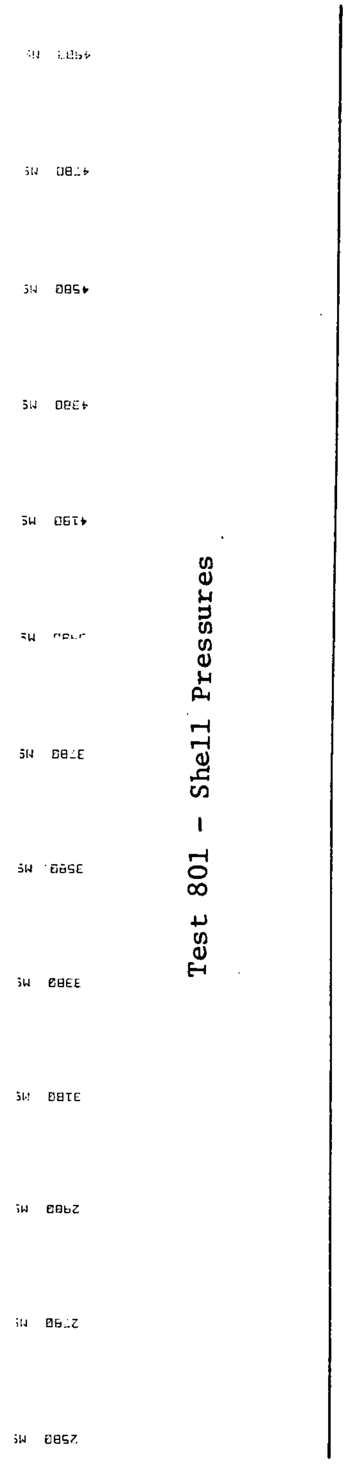

Test 801 - Shell Pressures

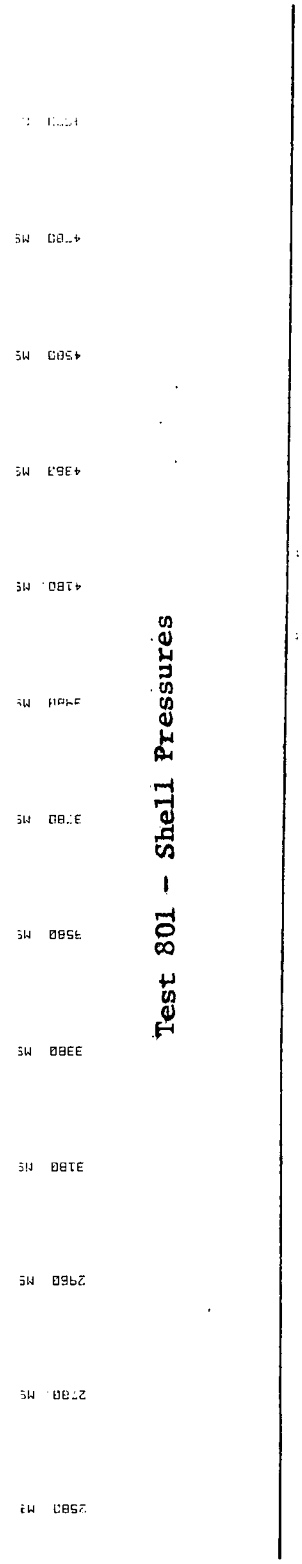

Test 801 - Shell Pressures

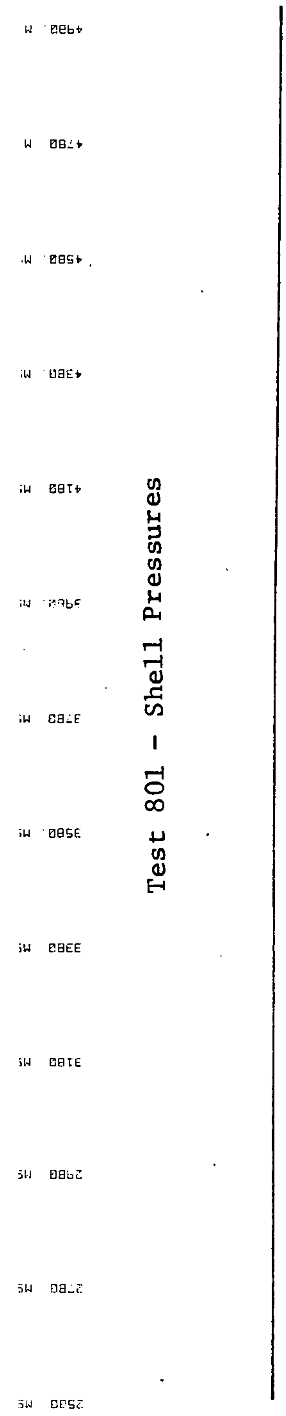

Test 801 - Shell Pressures

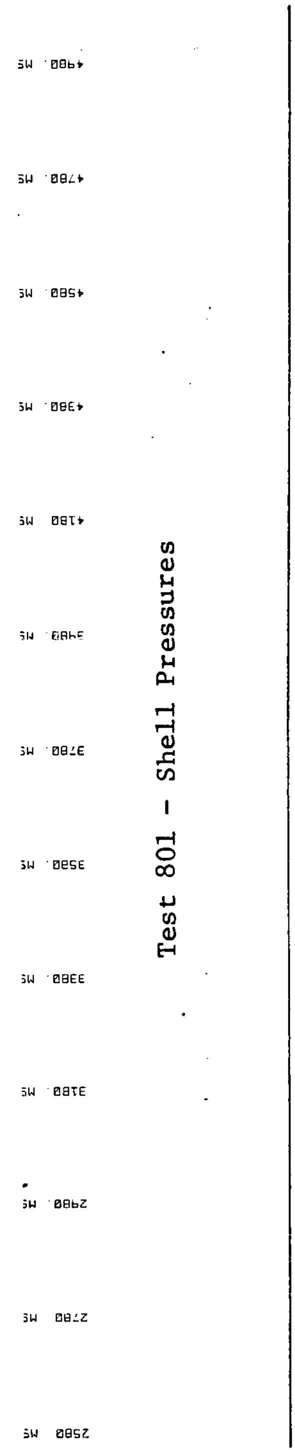

Test 801 - Shell Pressures

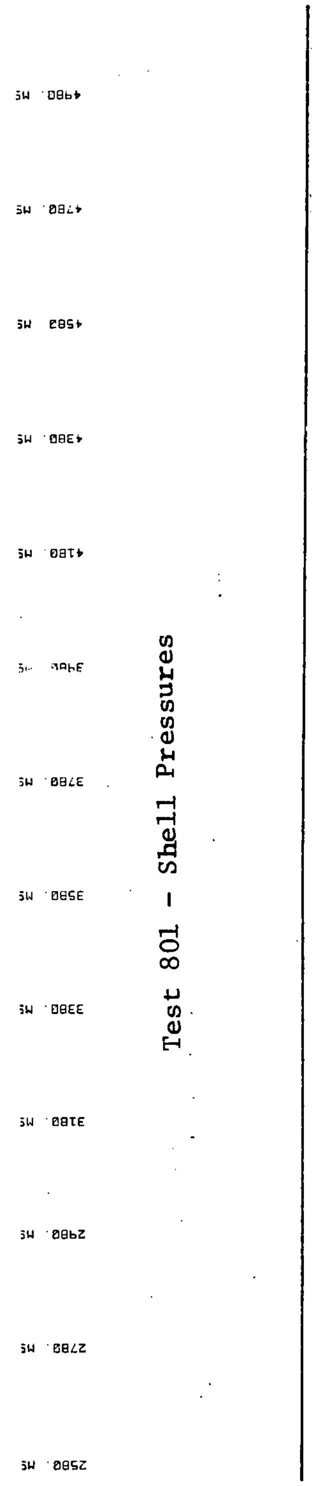

Test 801 - Shell Pressures

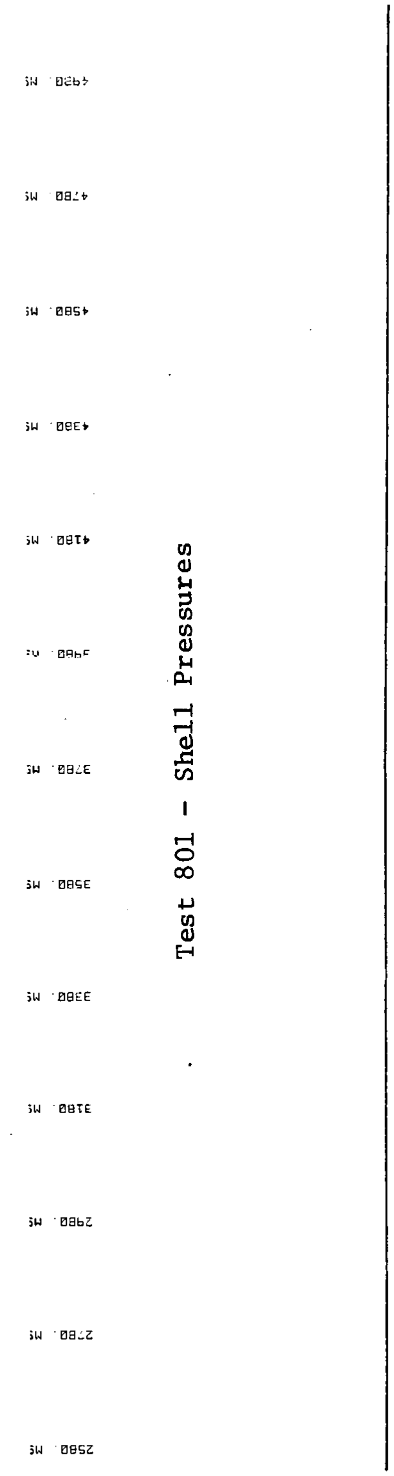

Test 801 - Shell Pressures

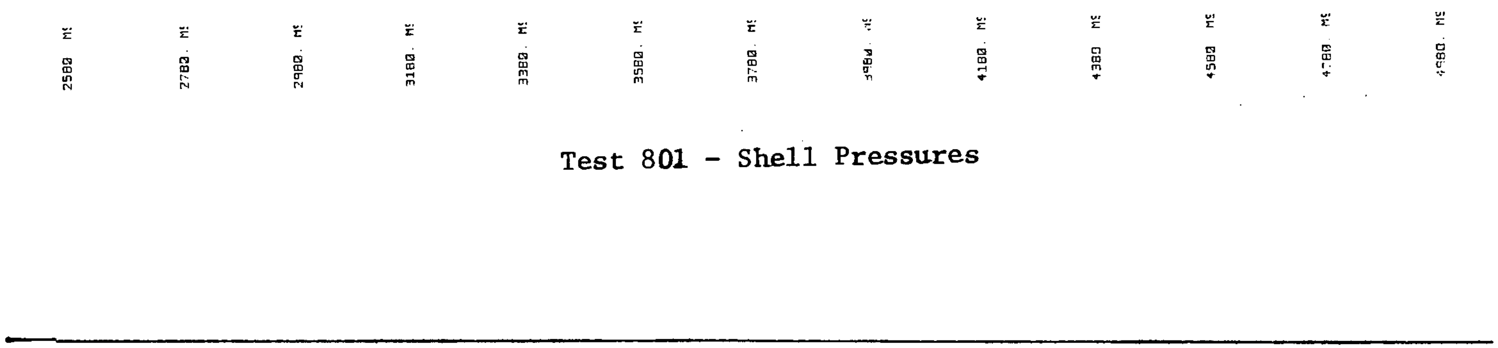

Test 801 - Shell Pressures

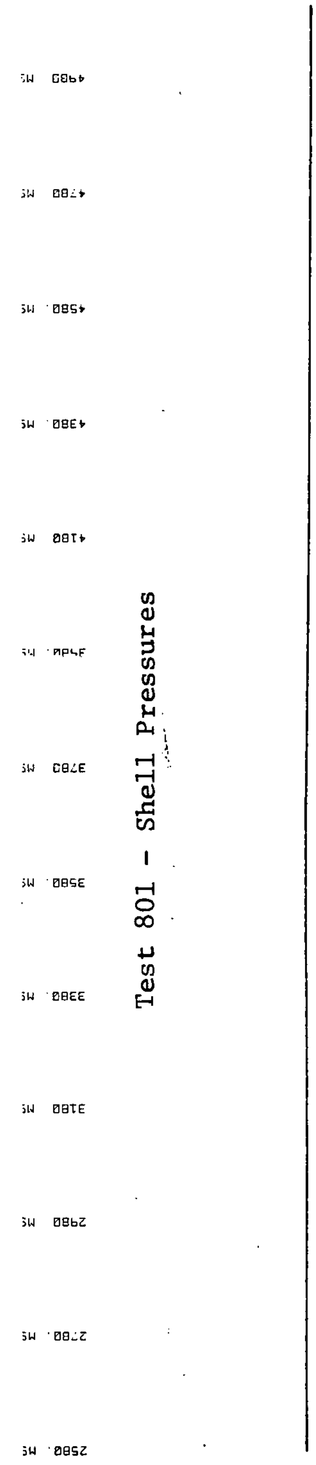

Test 801 - Shell Pressures

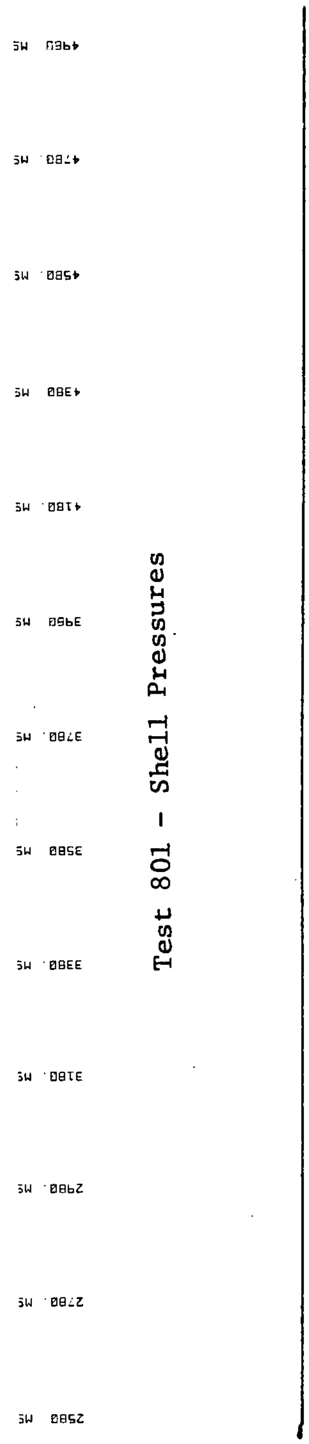

Test 801 - Shell Pressures

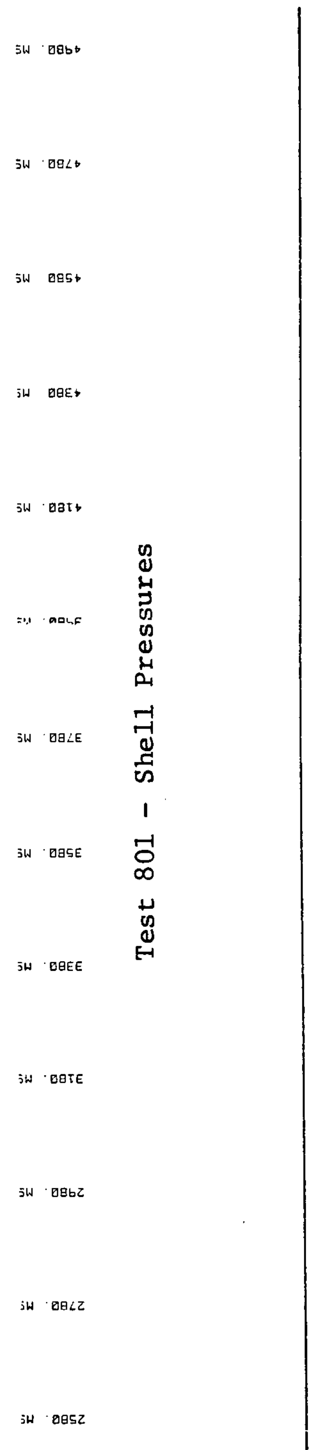

Test 801 - Shell Pressures

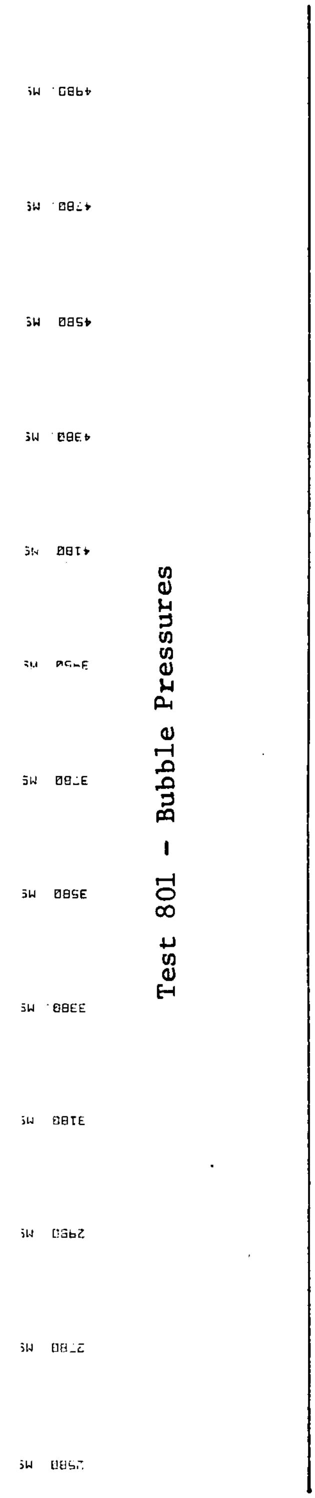

Test 801 - Bubble Pressures

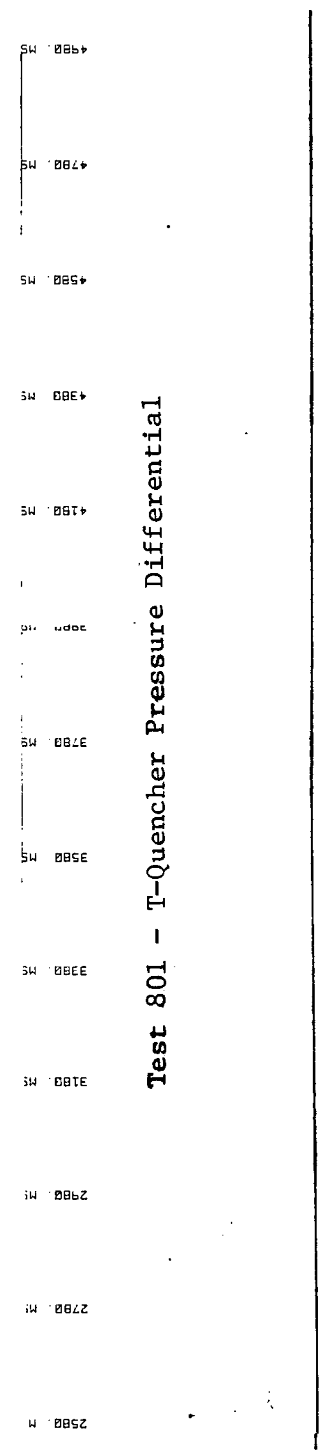

Test 801 - T-Quencher Pressure Differential

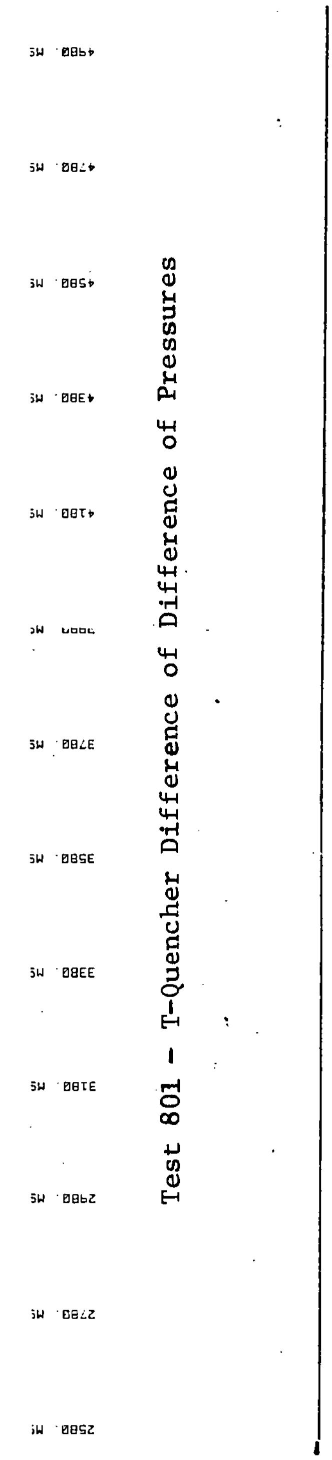

Test 801 - T-Quencher Difference of Pressures

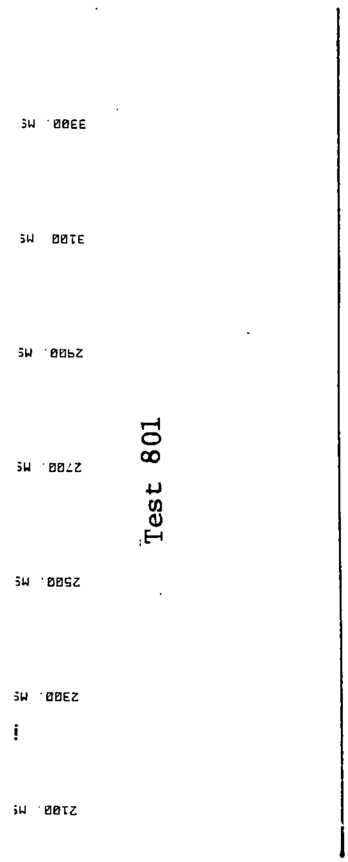
3300. MS
3100. MS
2900. MS
2700. MS
2500. MS
2300. MS
2100. MS
Test 801

Test 801 - SRVDL Pressure Transient During Water Reflood

Test 801 - SRVDL Pressure Transient During Water Reflood

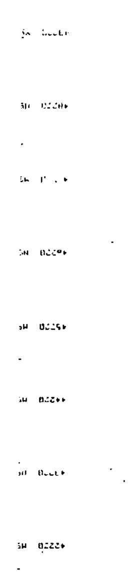

Test 801 - SRVDL Pressure Transient During Water Reflood
(Continuation of Previous Figure)

Test 801 - Air Flow Through SRVDL Vacuum Breaker

20420 ms
20520 ms
20620 ms
20720 ms
20820 ms
20920 ms
21020 ms
21120 ms
21220 ms
21320 ms
21420 ms
21520 ms
21620 ms
21720 ms

2739. MS
2939. MS
3139. MS
3339. MS
3539. MS
3739. MS
3939. MS

Test 901 - Bubble Pressures

E-3

Pool pressures and torus shell pressures for test 24 during the steam condensation phase. Plots are shown for two different local pool temperatures in bay of discharge, and , which correspond to the beginning and the end of the test, respectively.

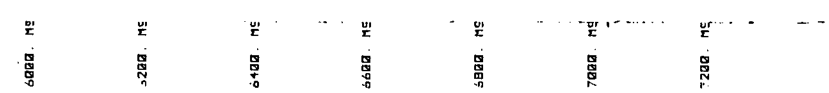

Test 24 - Shell Pressures

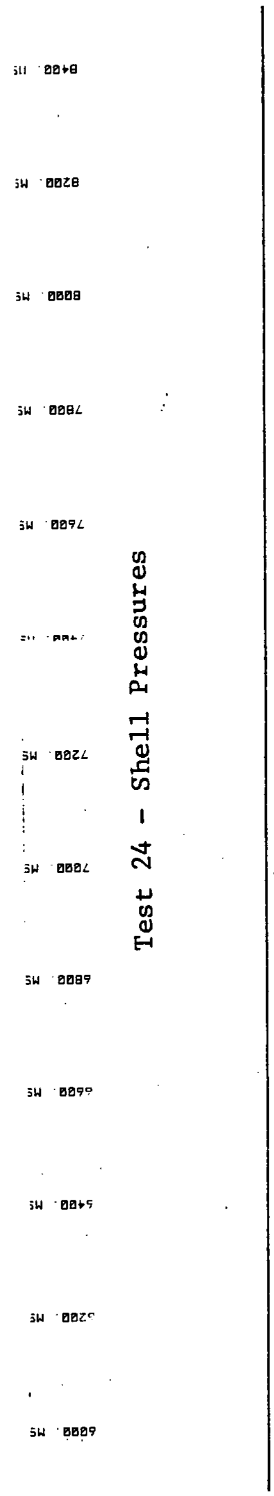

Test 24 - Shell Pressures

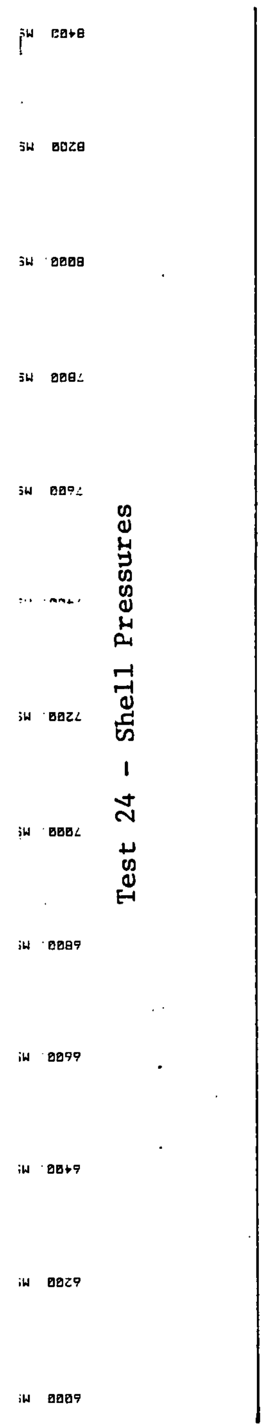

Test 24 - Shell Pressures

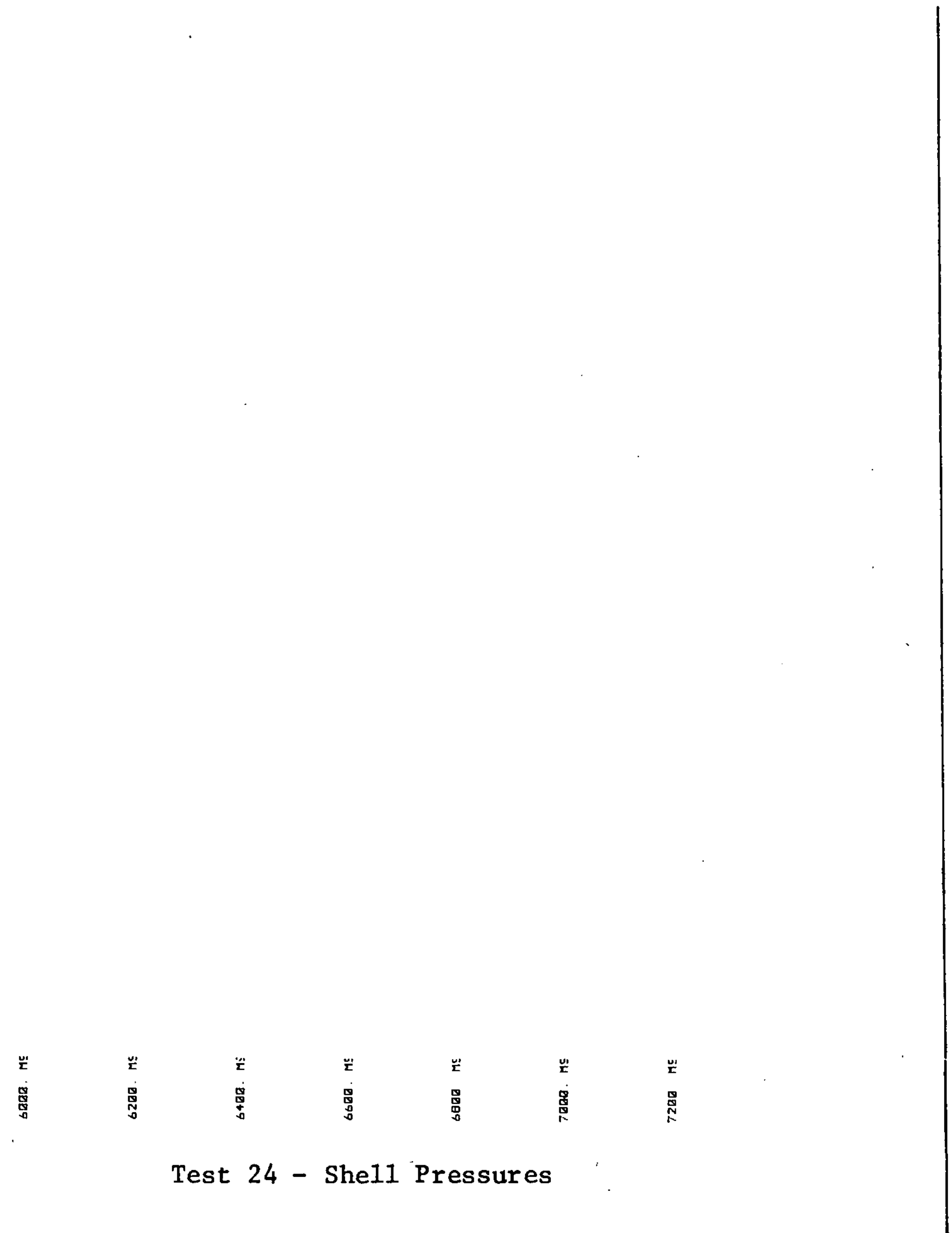

Test 24 - Shell Pressures

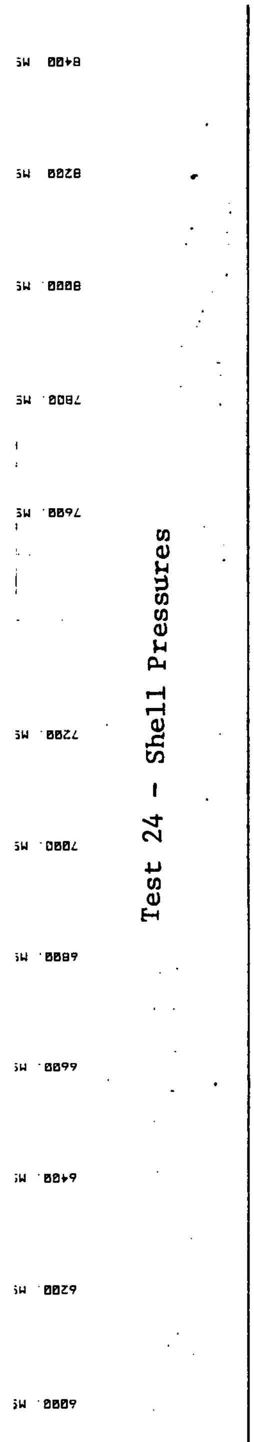

Test 24 - Shell Pressures

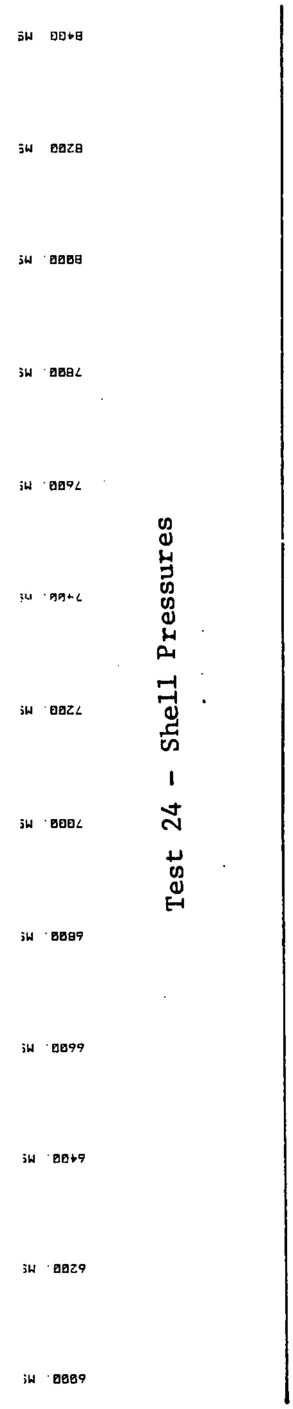

Test 24 - Shell Pressures

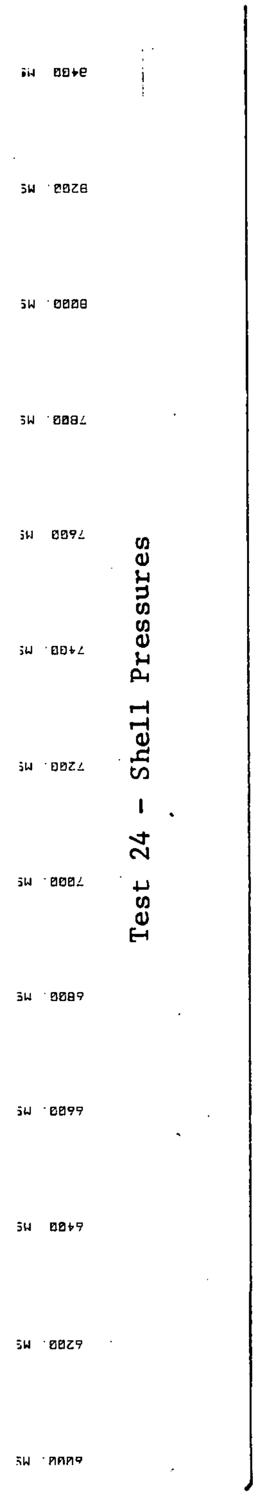

Test 24 - Shell Pressures

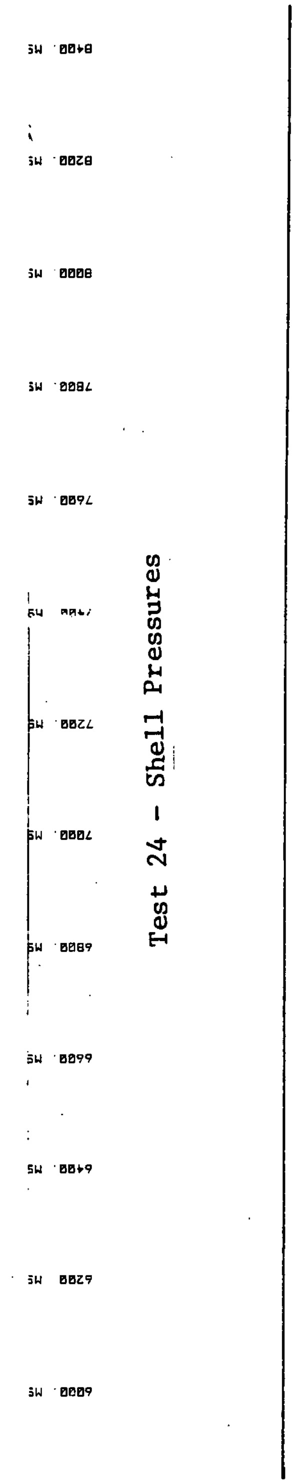

Test 24 - Shell Pressures

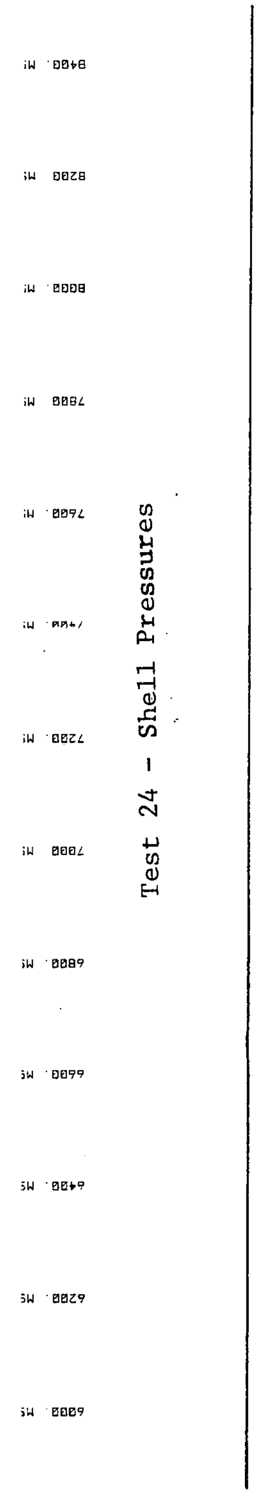

Test 24 - Shell Pressures

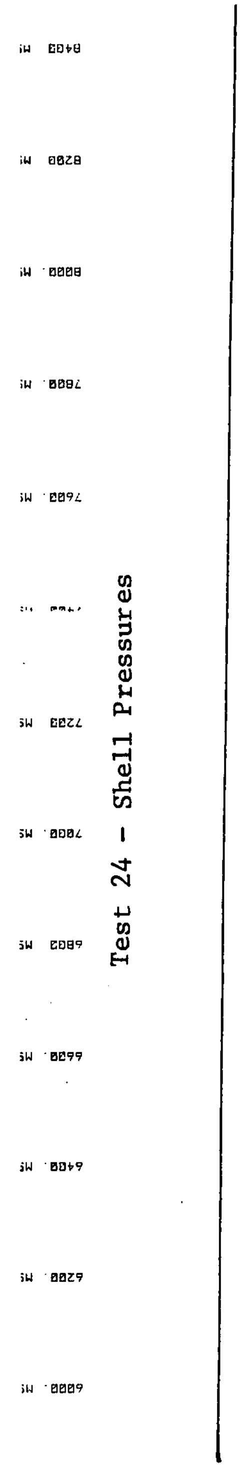
Test 24 - Shell Pressures
8400 MS
8200 MS
8000 MS
7800 MS
7600 MS
7200 MS
7000 MS
6800 MS
6600 MS
6400 MS
6200 MS
6000 MS

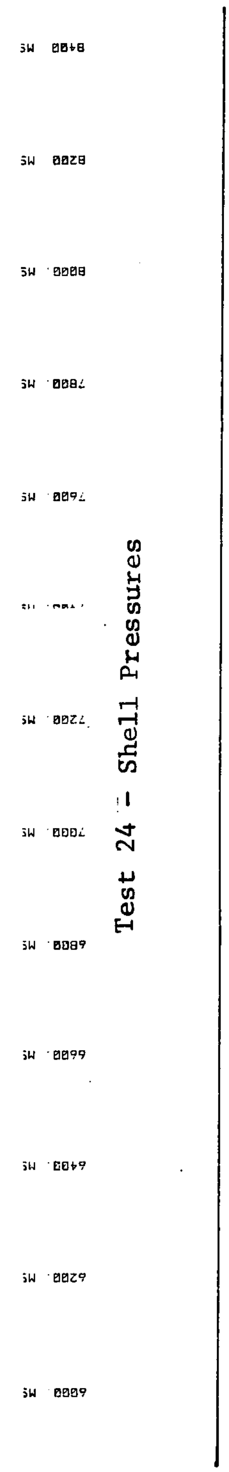

Test 24 - Shell Pressures

Test 24 - Shell Pressures

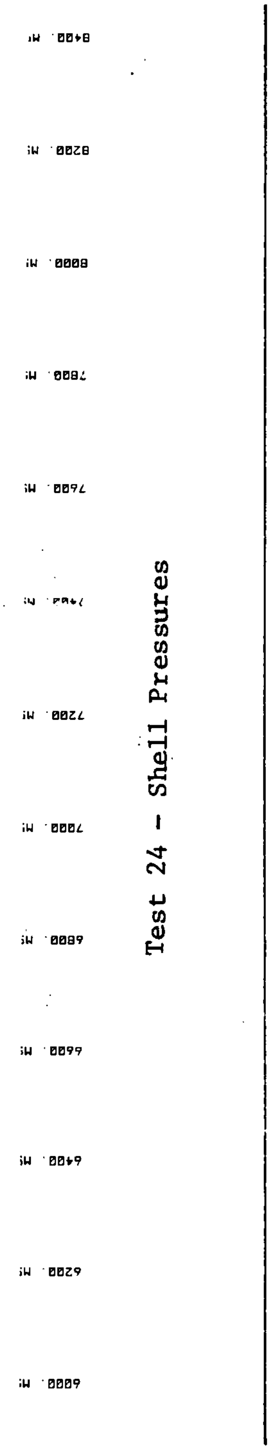

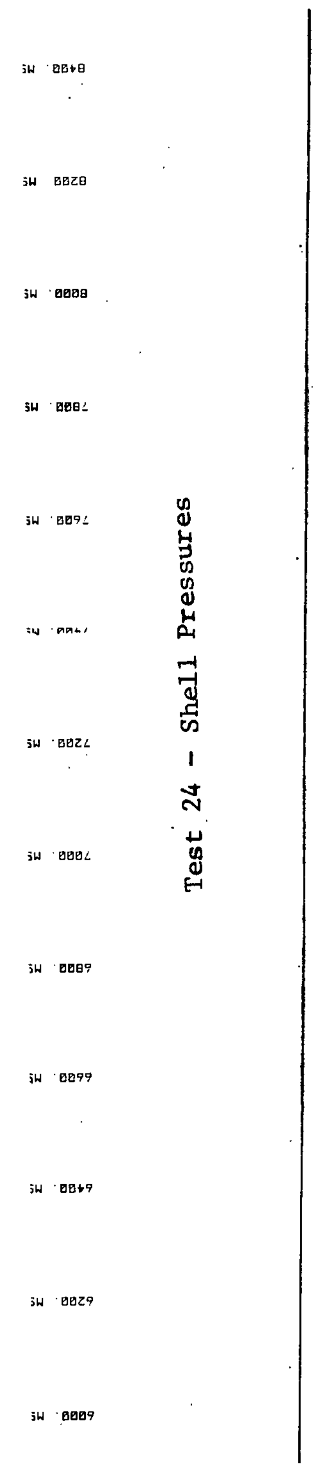

Test 24 - Shell Pressures

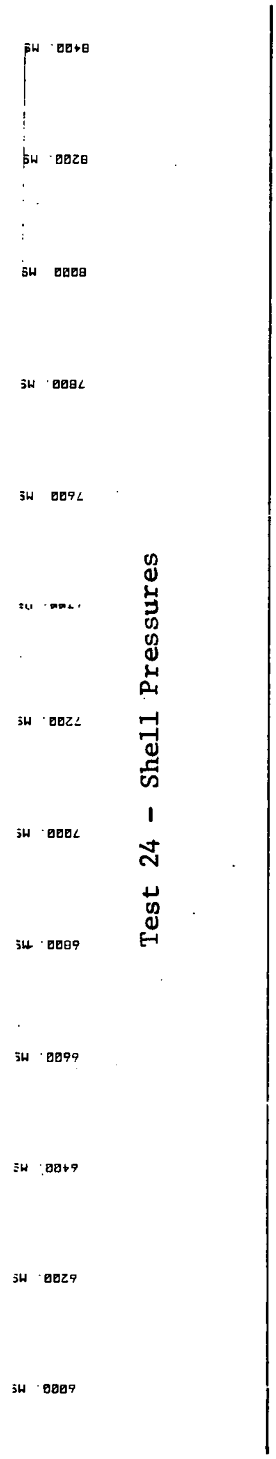

Test 24 - Shell Pressures

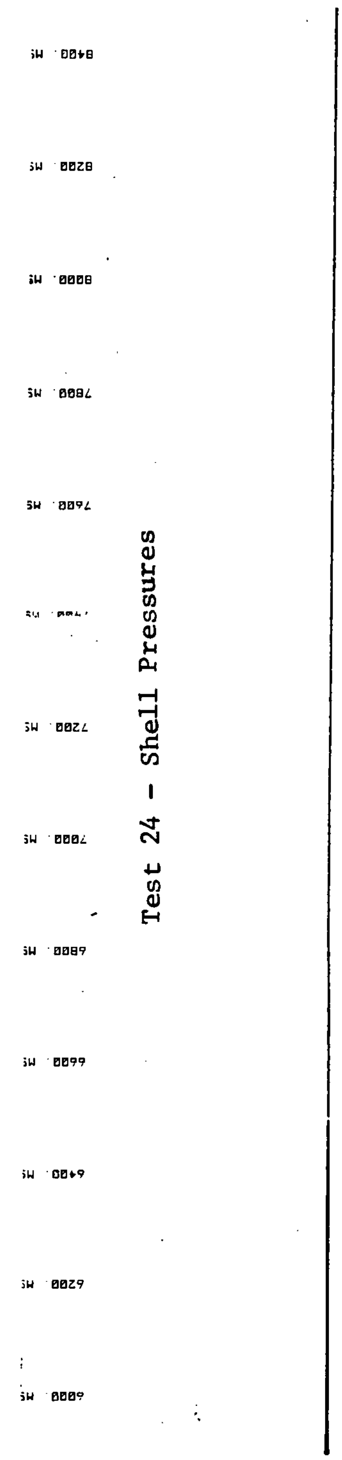

Test 24 - Shell Pressures

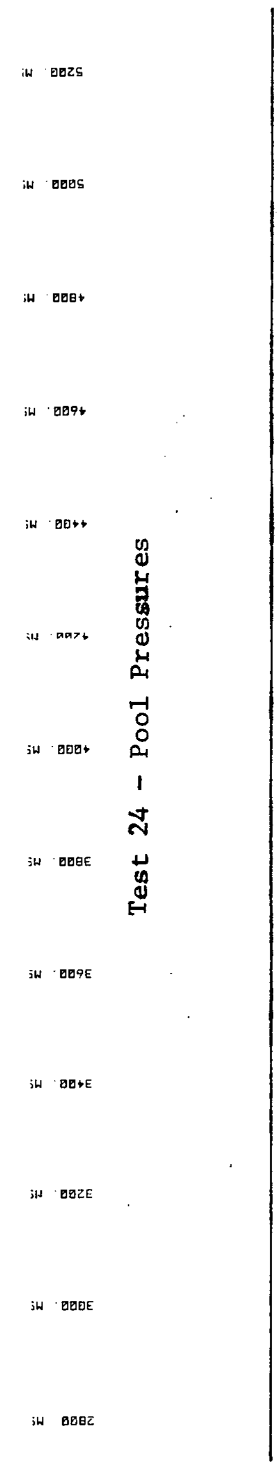

Test 24 - Pool Pressures

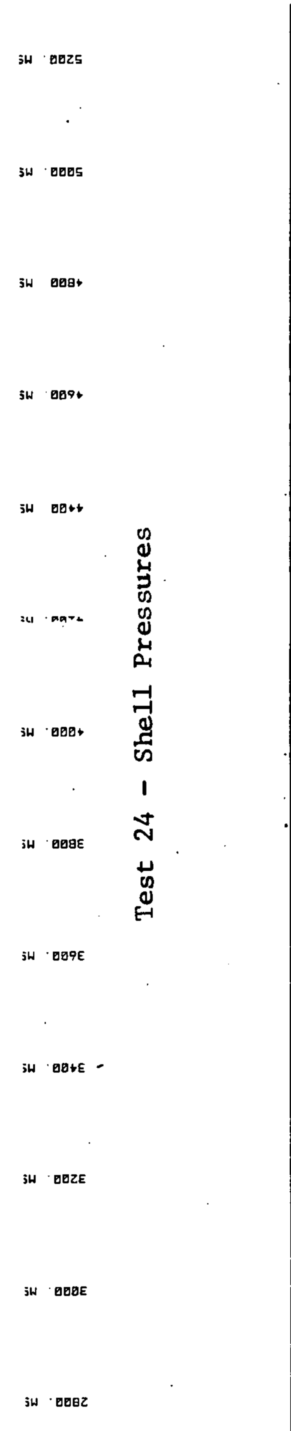

Test 24 - Shell Pressures

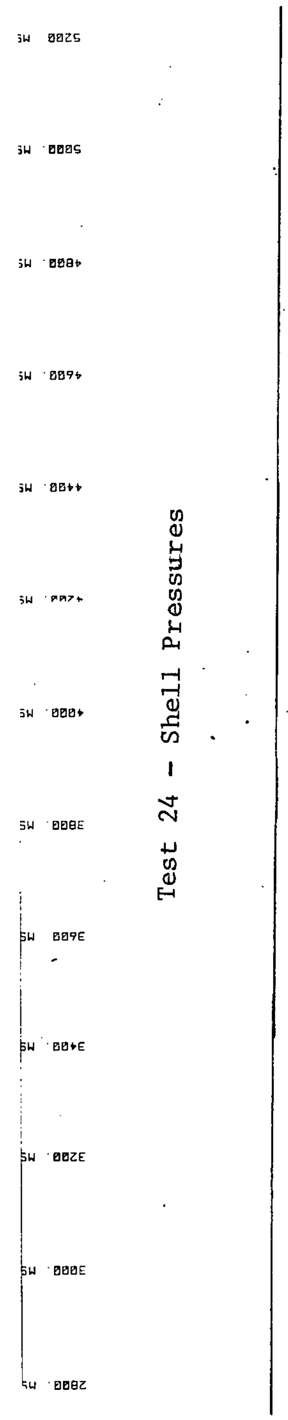

Test 24 - Shell Pressures

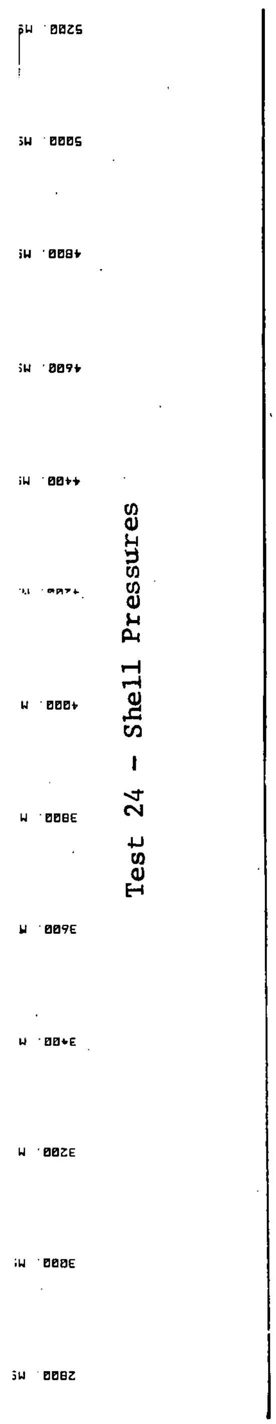

Test 24 - Shell Pressures

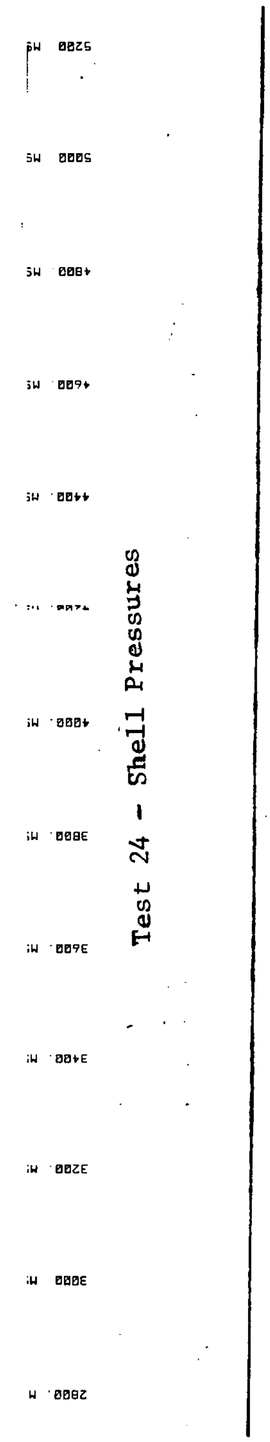

Test 24 - Shell Pressures

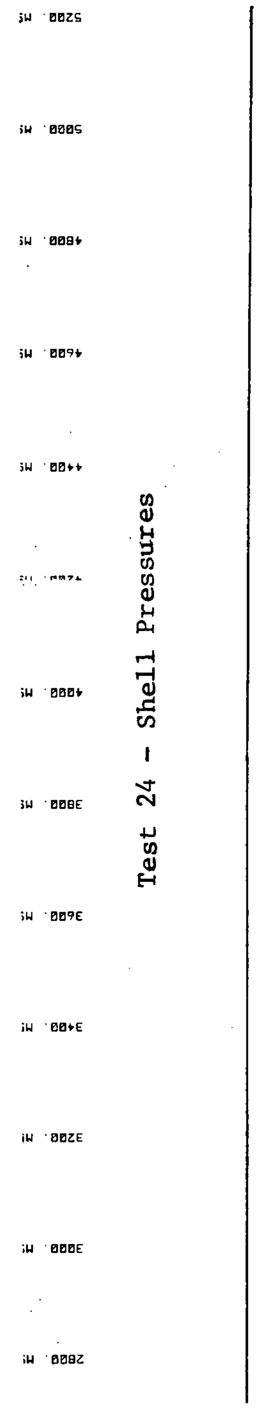

Test 24 - Shell Pressures

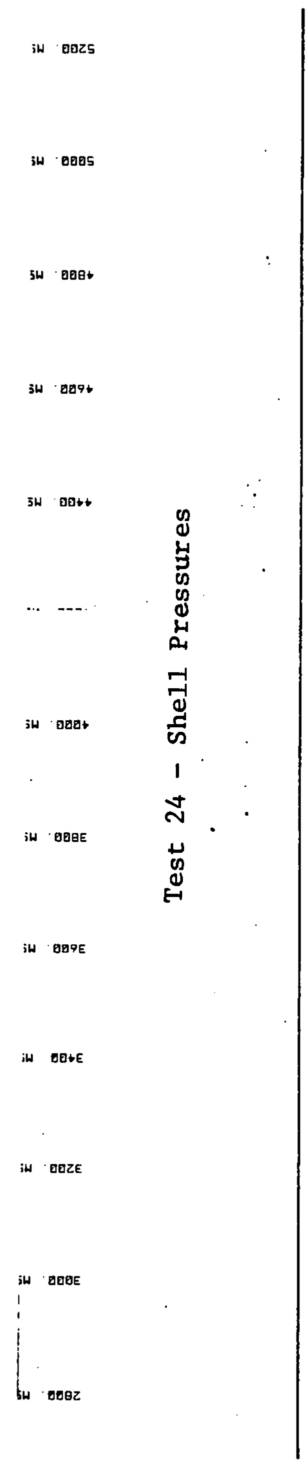

Test 24 - Shell Pressures

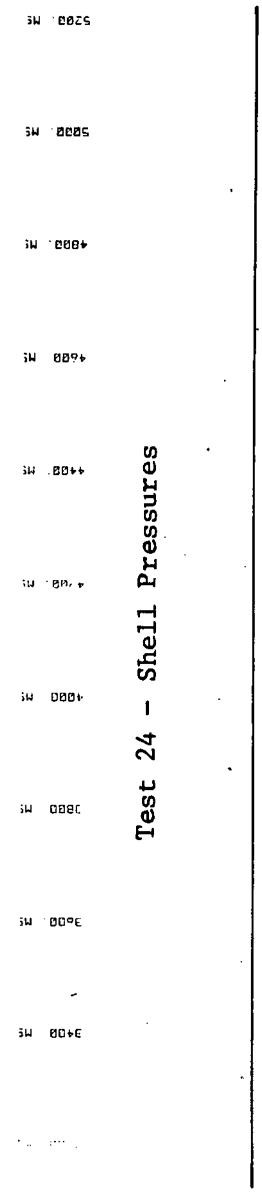

Test 24 - Shell Pressures

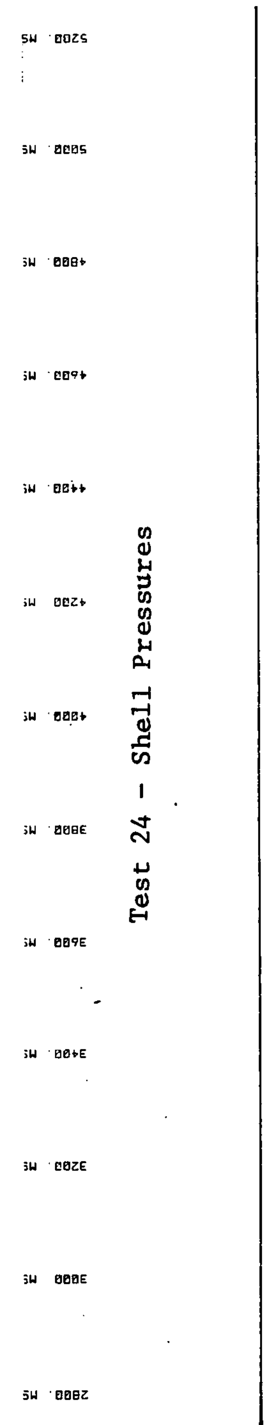

Test 24 - Shell Pressures

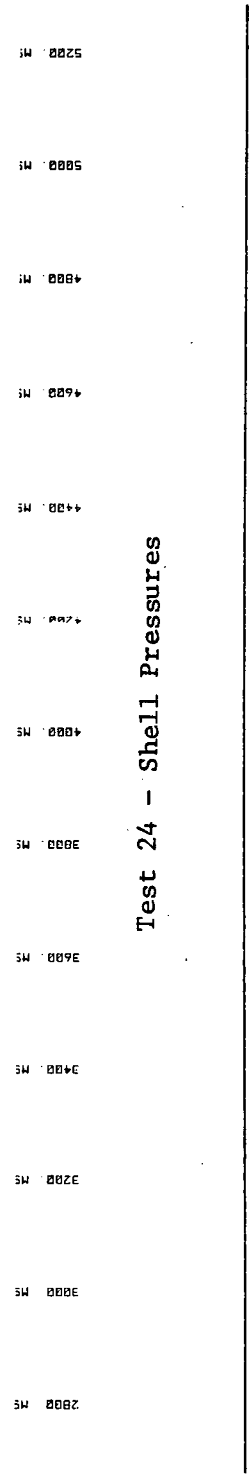

Test 24 - Shell Pressures

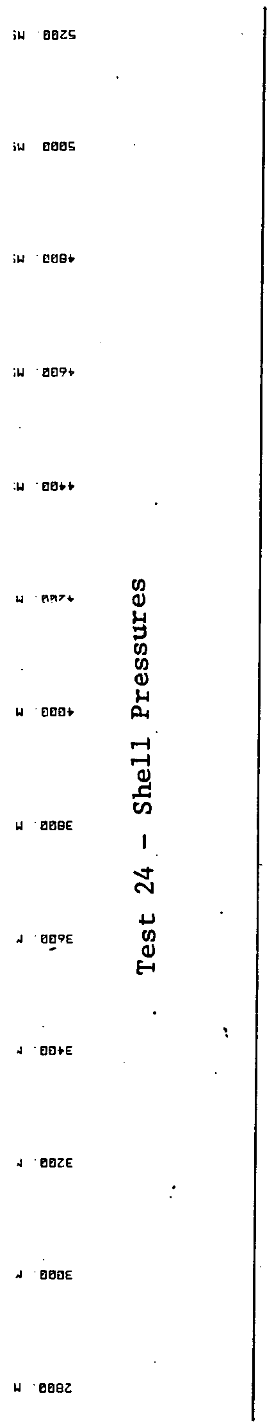

Test 24 - Shell Pressures

Test 24 - Shell Pressures

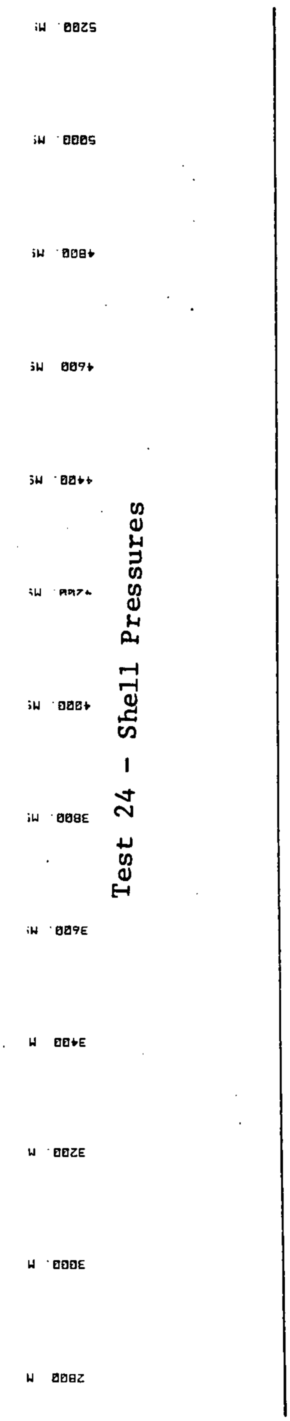

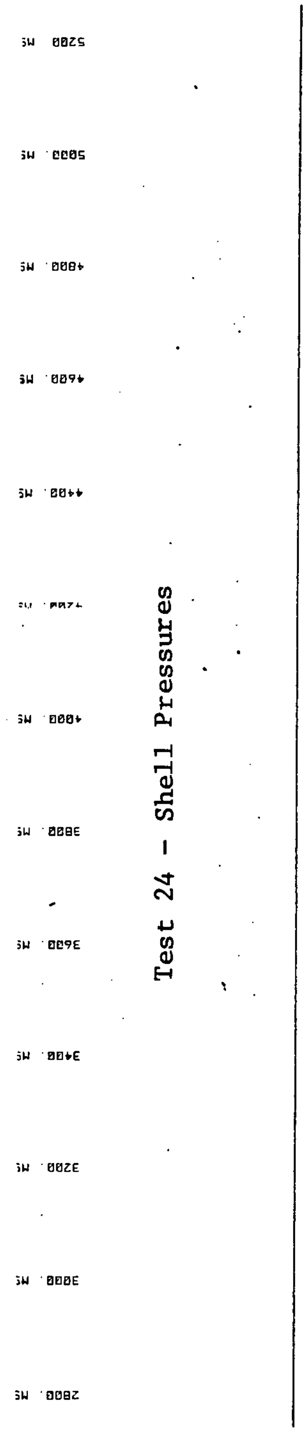

Test 24 - Shell Pressures

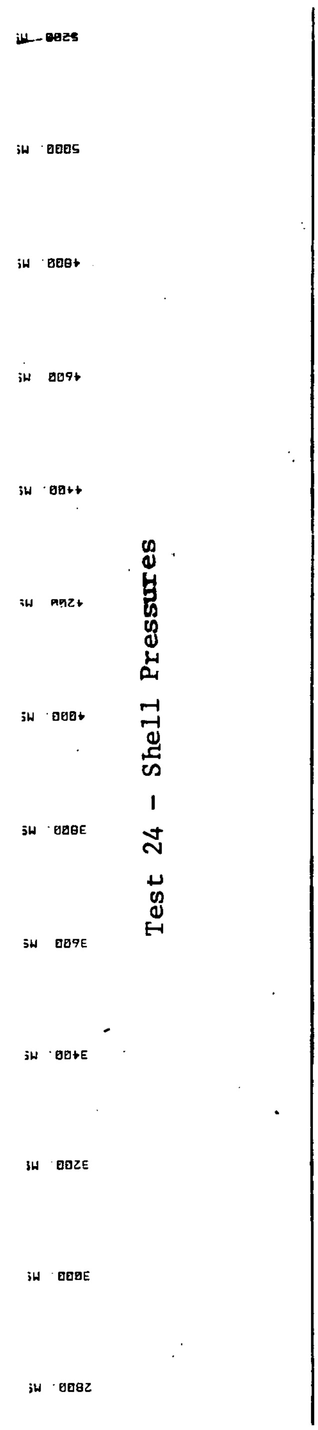

Test 24 - Shell Pressures

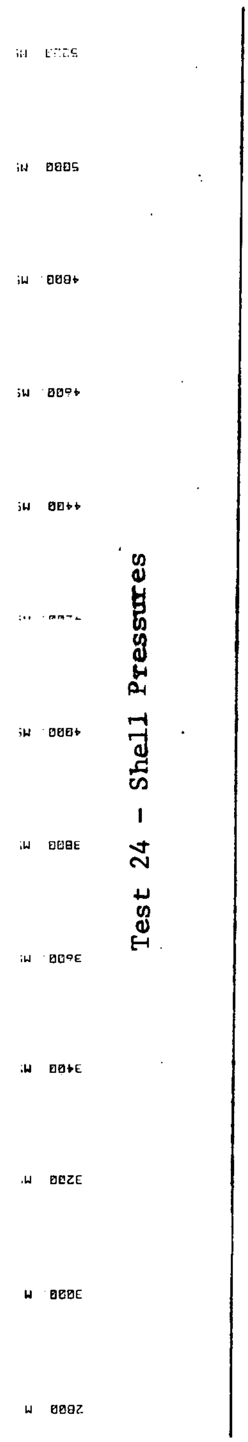

Test 24 - Shell Pressures

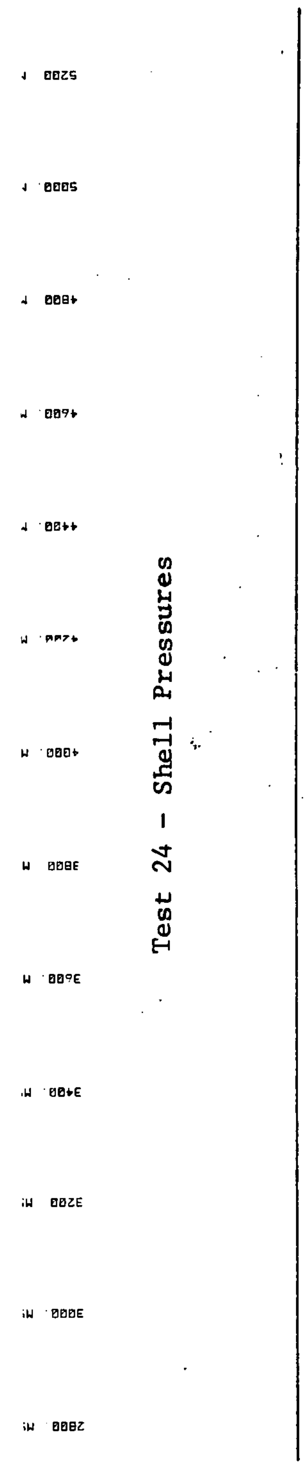

Test 24 - Shell Pressures

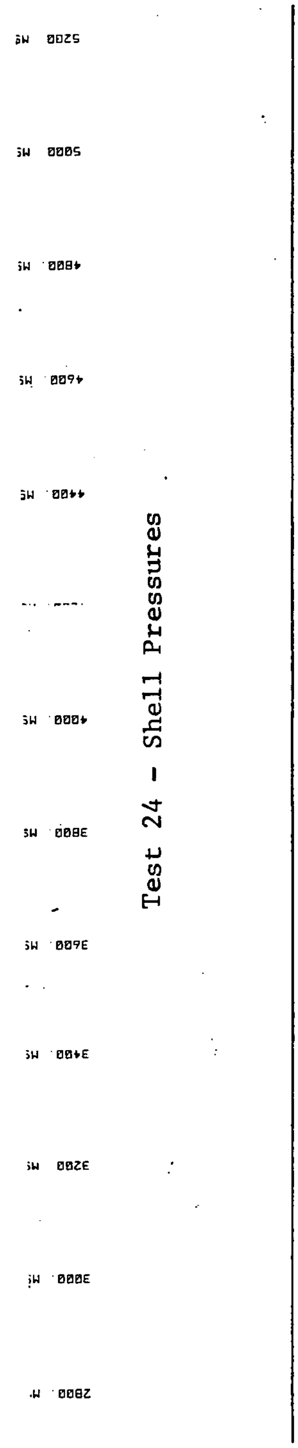

Test 24 - Shell Pressures

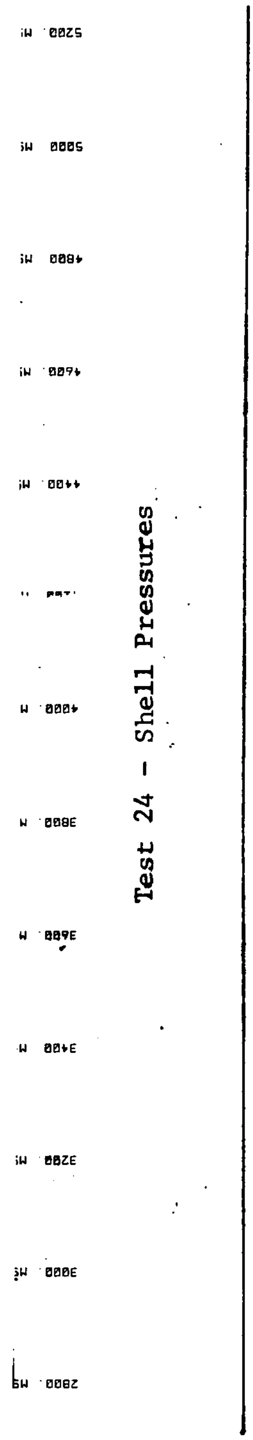

Test 24 - Shell Pressures

E-4

Pool temperature transient plots as recorded by pool temperature sensors and plant sensors during the two extended discharge tests, with and without RHR.

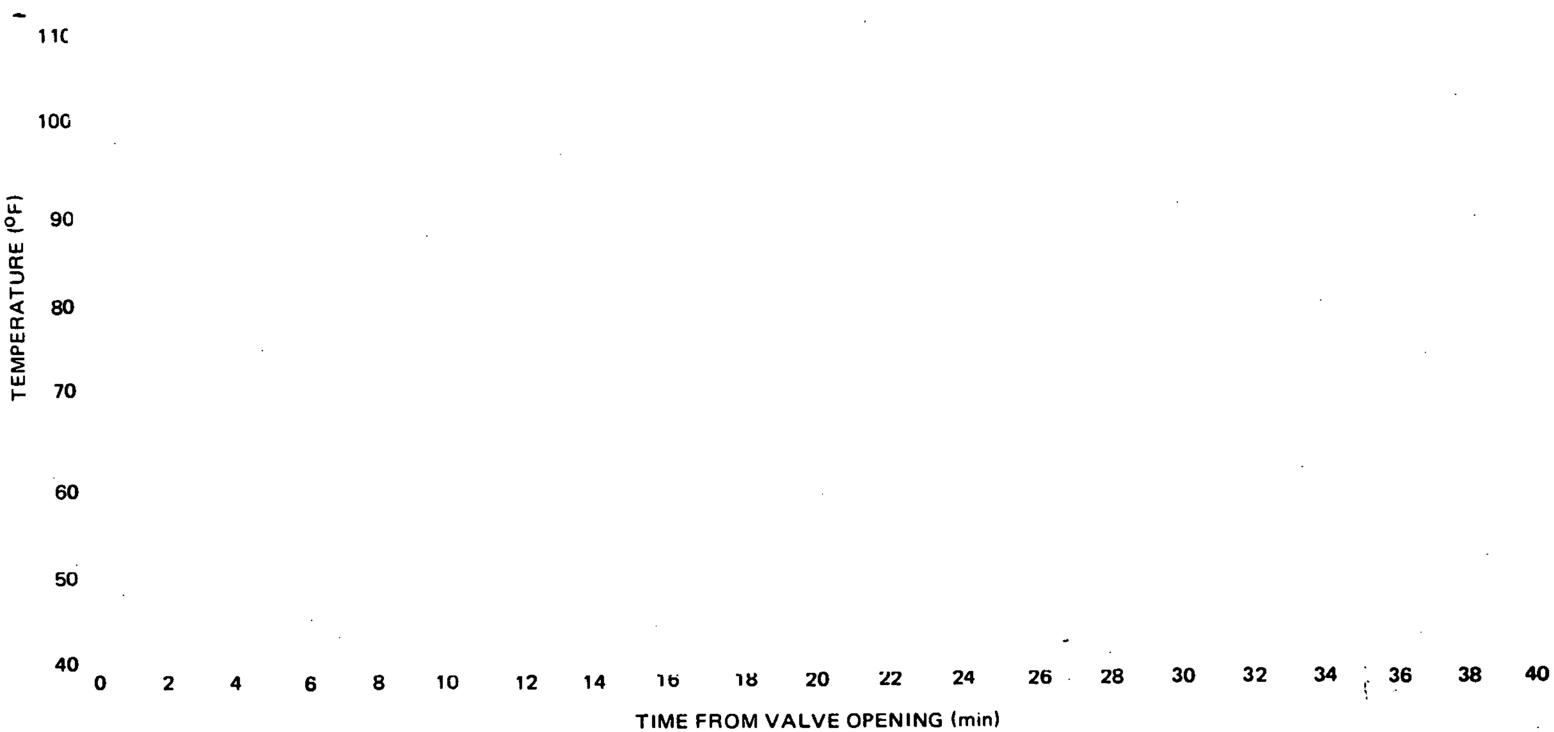

Figure E.4-1. Temperature Histories of the Sensors 7" Below the Pool Surface of Azimuth 74° for Test #24 (No RHR)

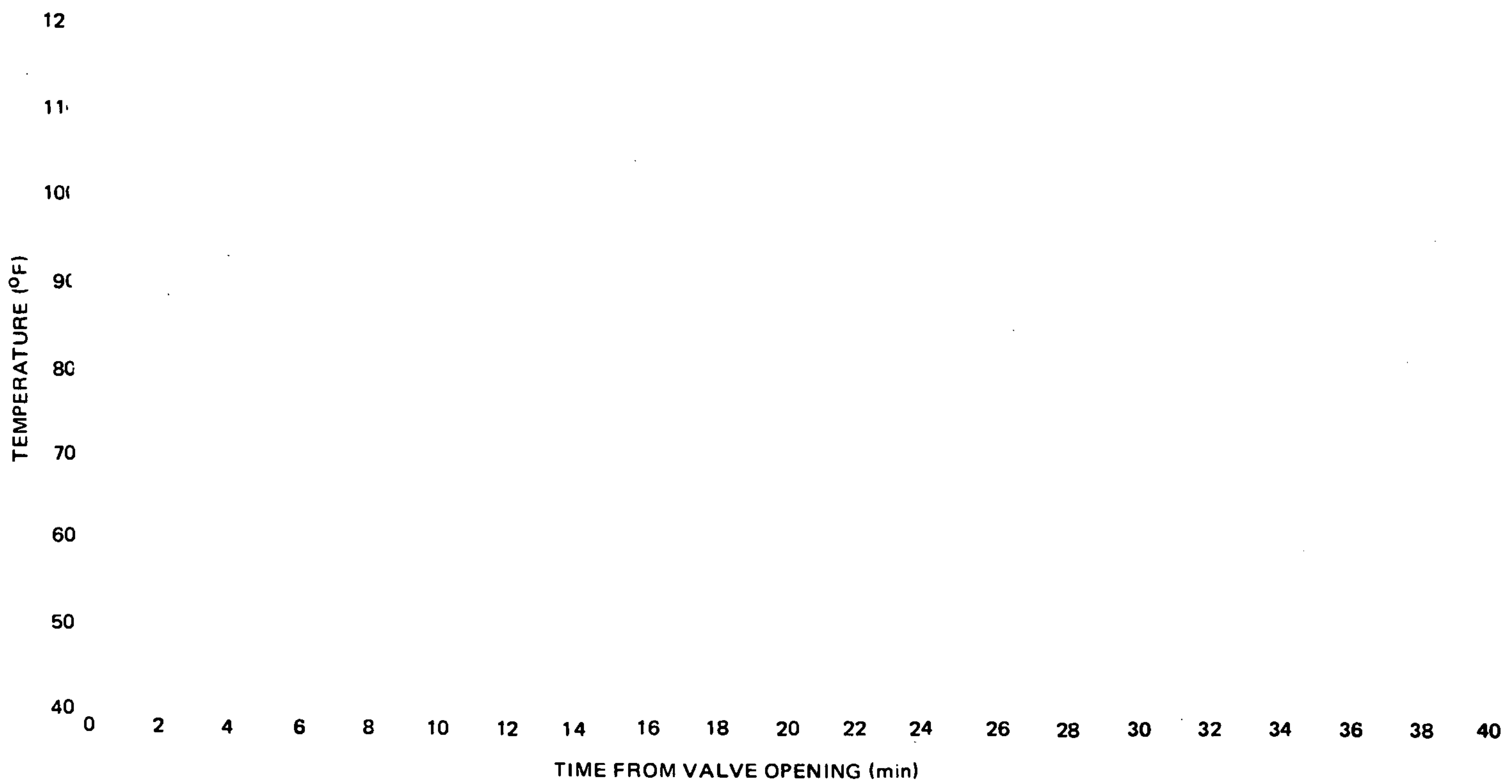

Figure E.4-2. Temperature Histories of the Sensors Below the Pool Surface at Azimuth 74° for Test #24 (No RHR)

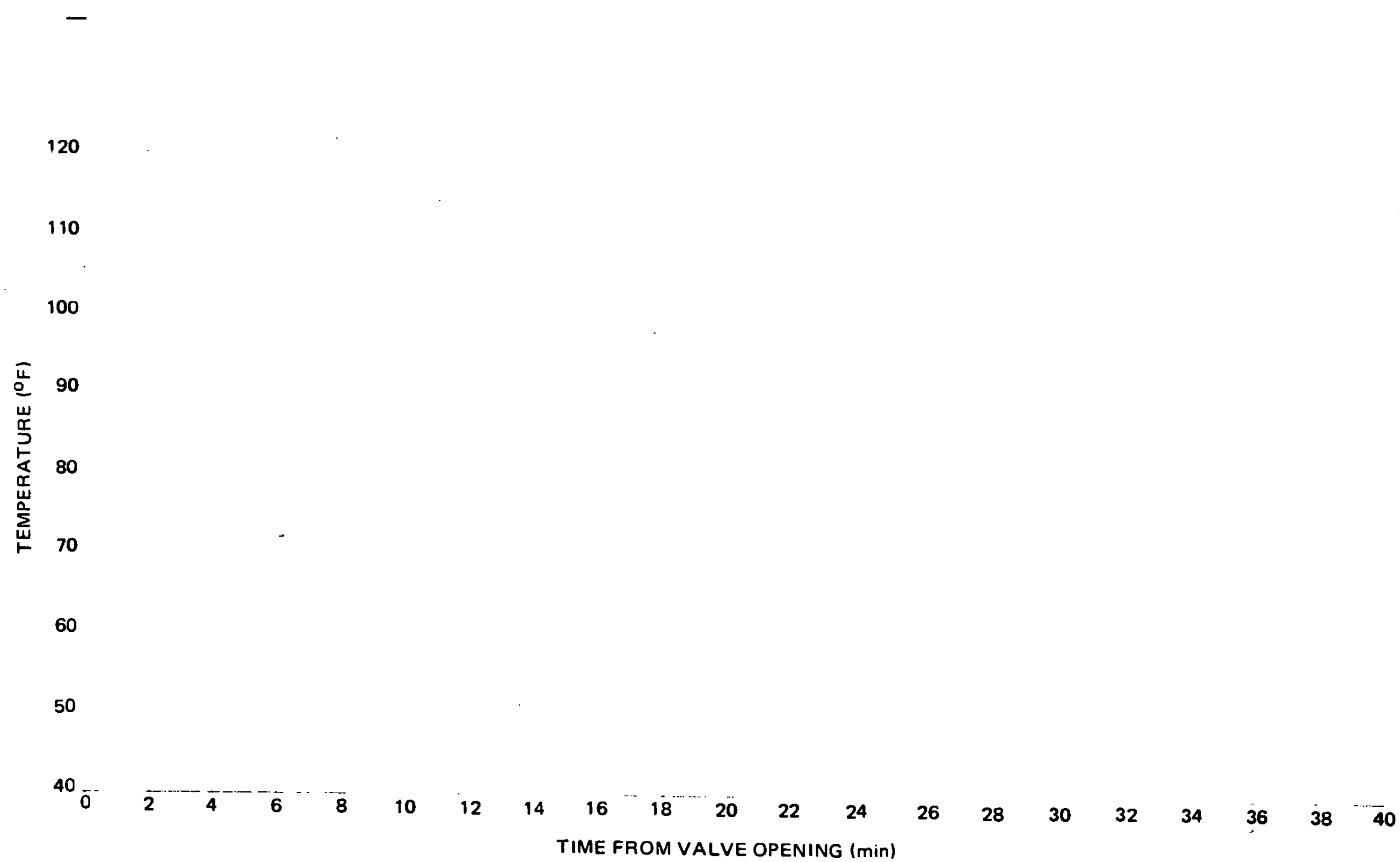

Figure E.4-3. Temperature Histories of the Sensors 51" Below the Pool Surface at Azimuth 74° for Test #24 (No RHR)

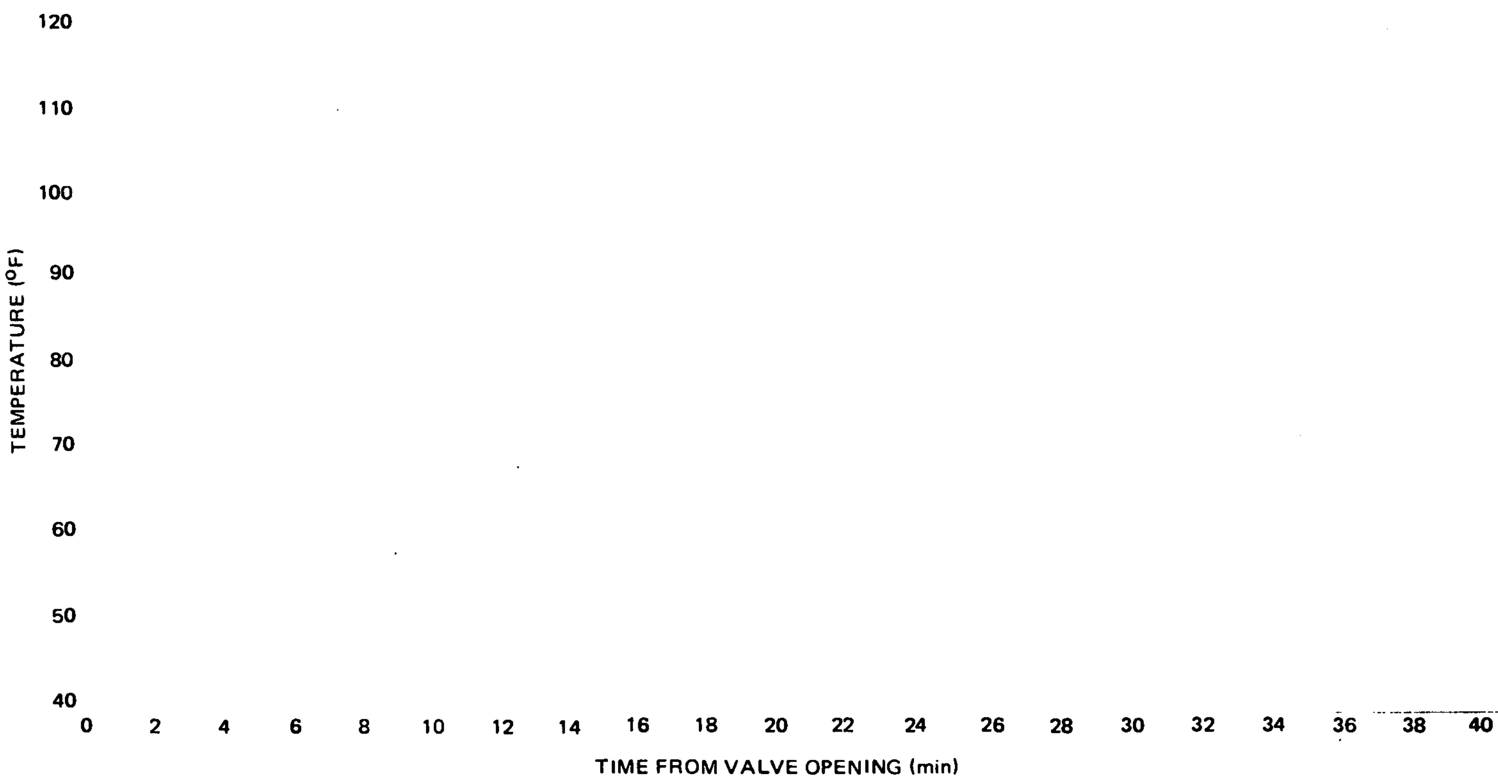

Figure E.4-4. Temperature Histories of the Bottom 4 Sensors at Azimuth 74° for Test #24 (No RHR)

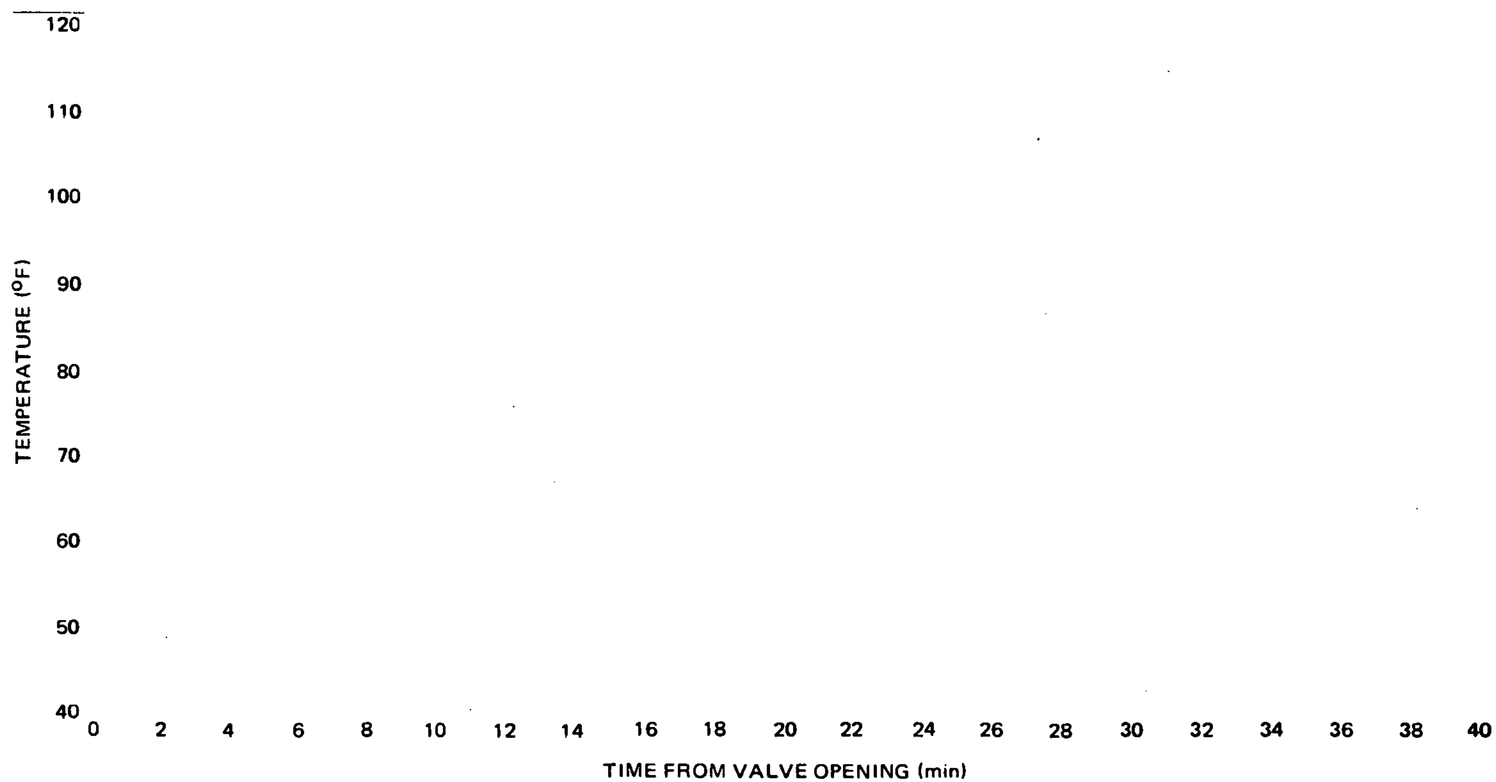

Figure E.4-5. Temperature Histories of RTD Sensors at Azimuth 101° For Test #24 (No RHR)

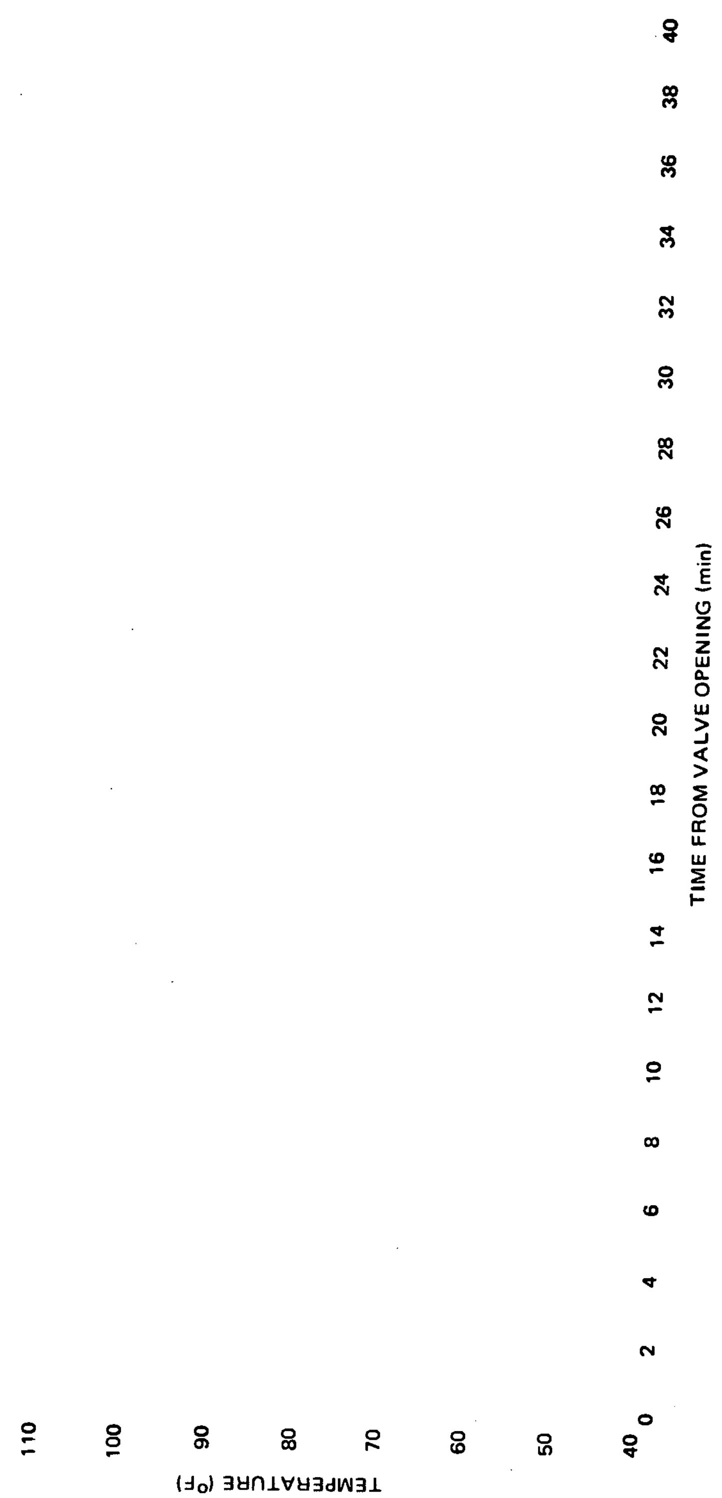

Figure E.4-6. Temperature Histories of RTD Sensors at Azimuth 124° for Test #24 (No RHR)

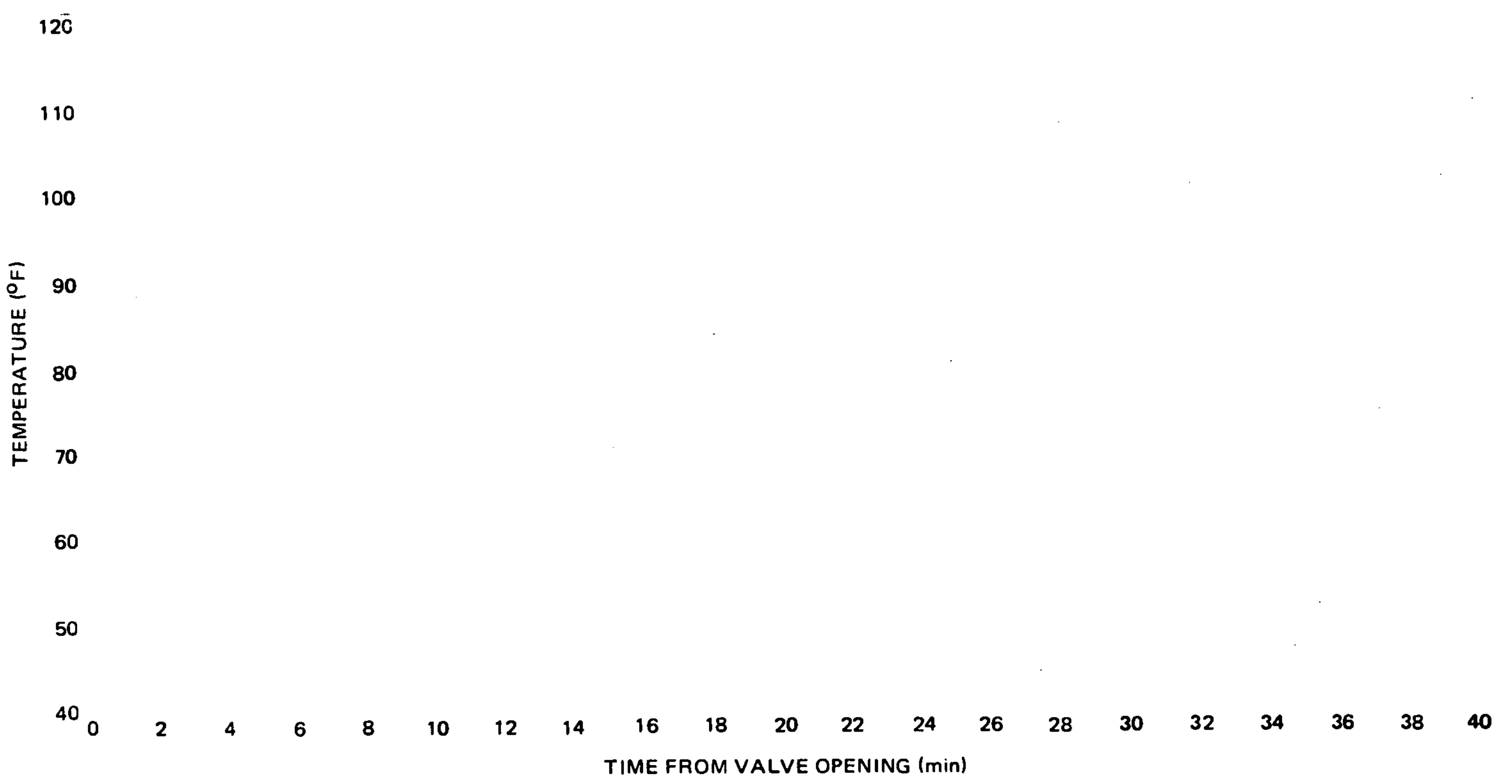

Figure E.4-7. Temperature Histories of RTD Sensors at Azimuth 146° for Test #24 (No RHR)

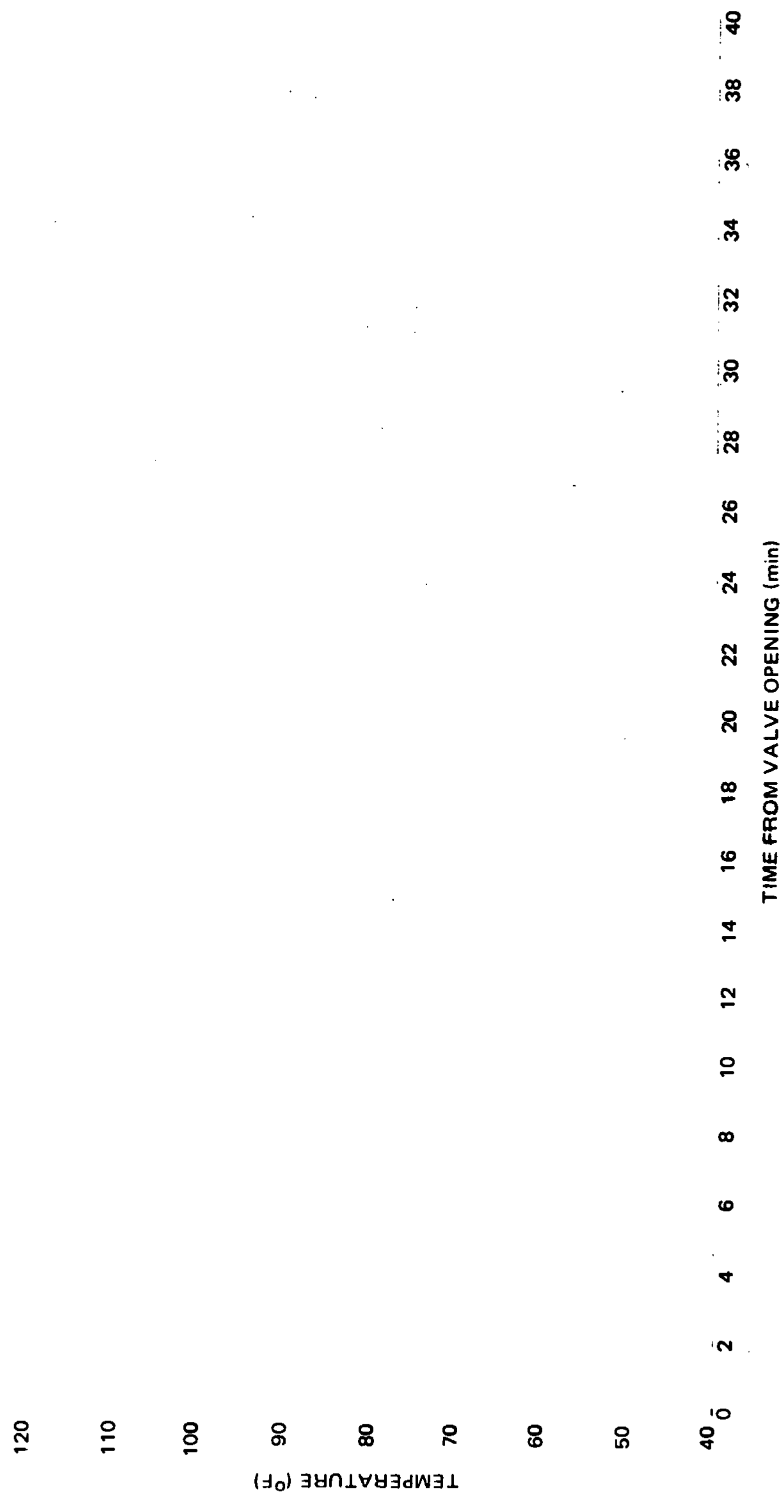

Figure E.4-8. Temperature Histories of RTD Sensors at Azimuth 259° for Test No. 24 (No RHR)

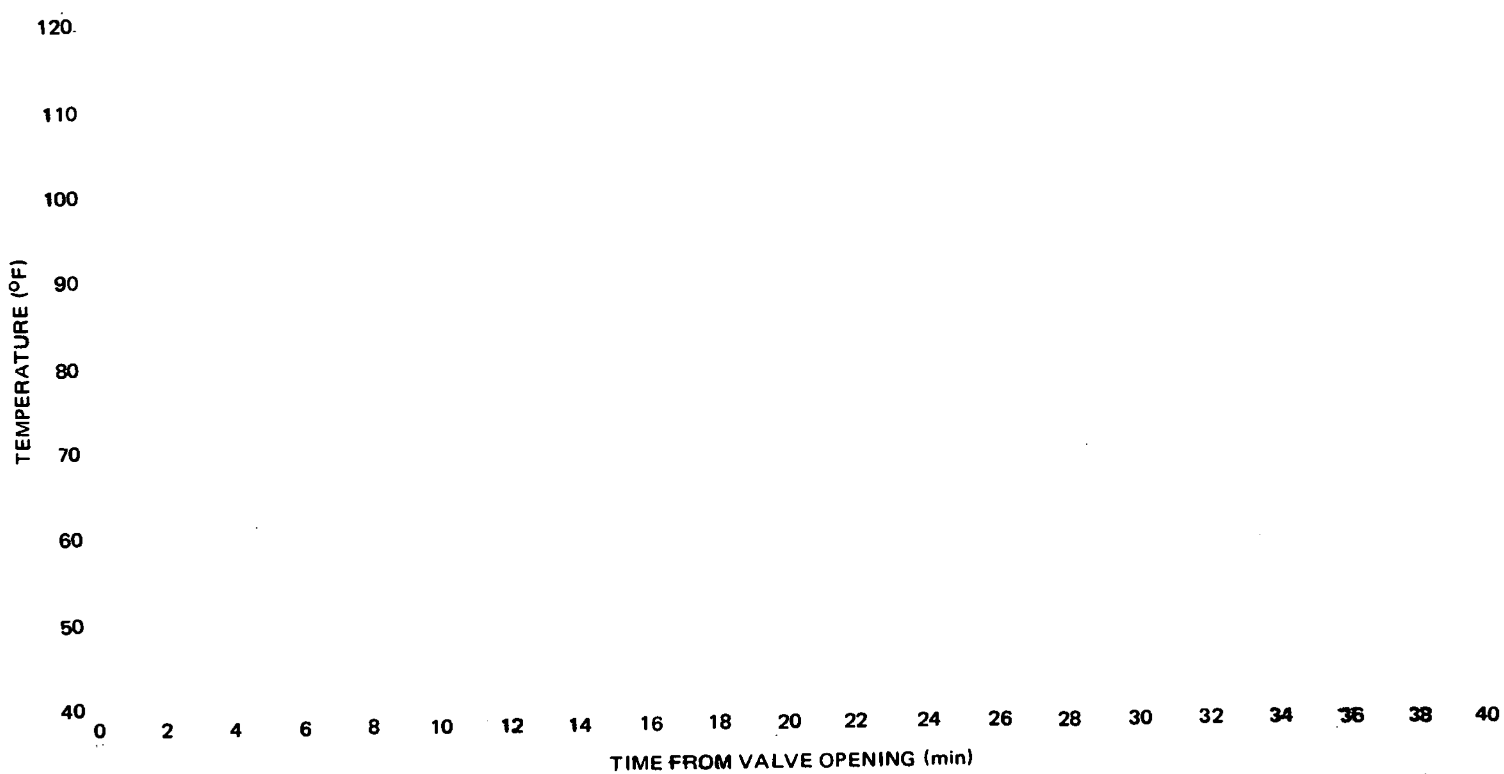

Figure E.4-9. Temperature Histories of RTD Sensors at Azimuth 349° for Test No. 24 (No RHR)

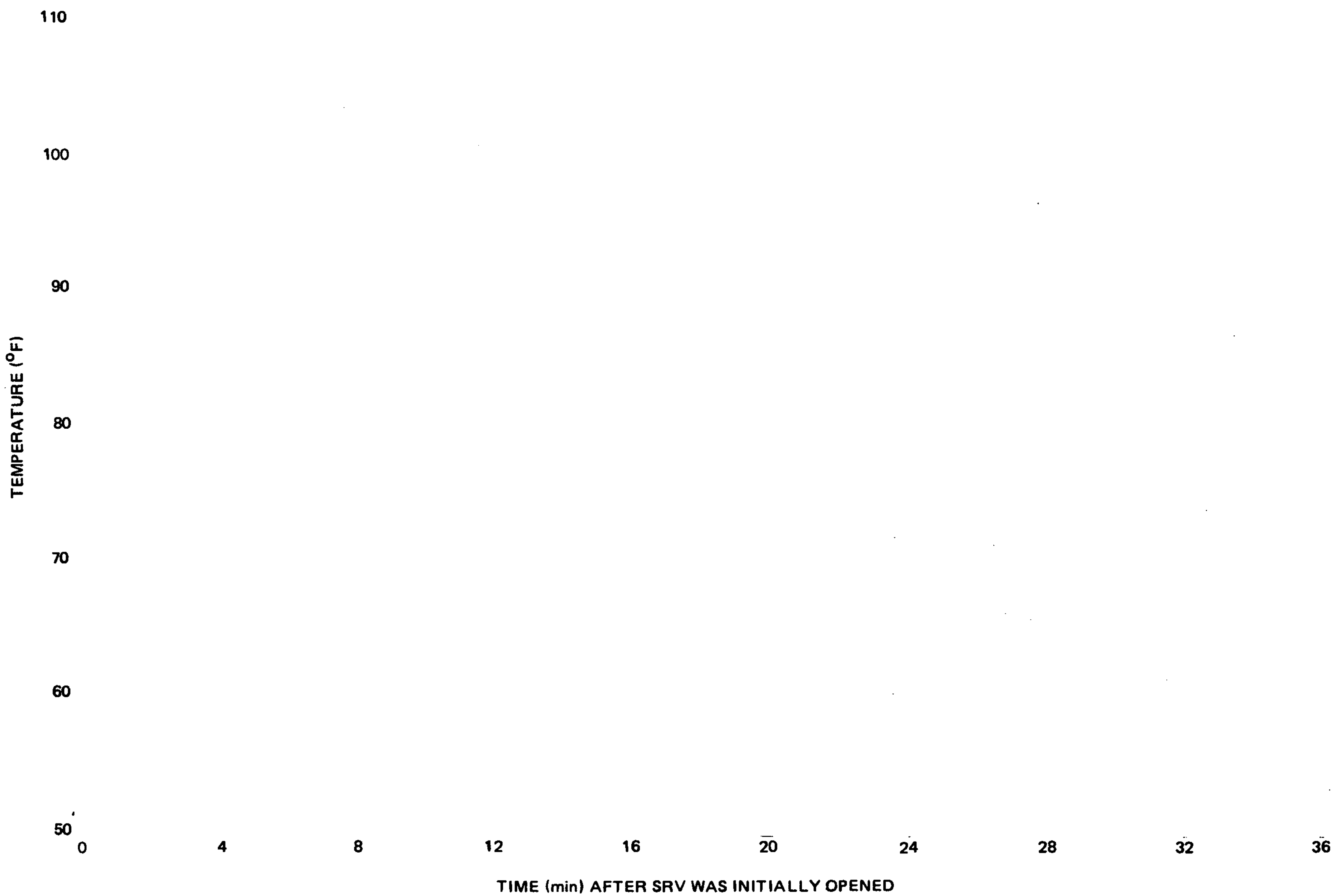

Figure E.4-10. Temperature Histories of Plant Temperature Sensors in Bays E/F and G/H for Test #24 (12/20/77) - No RHR

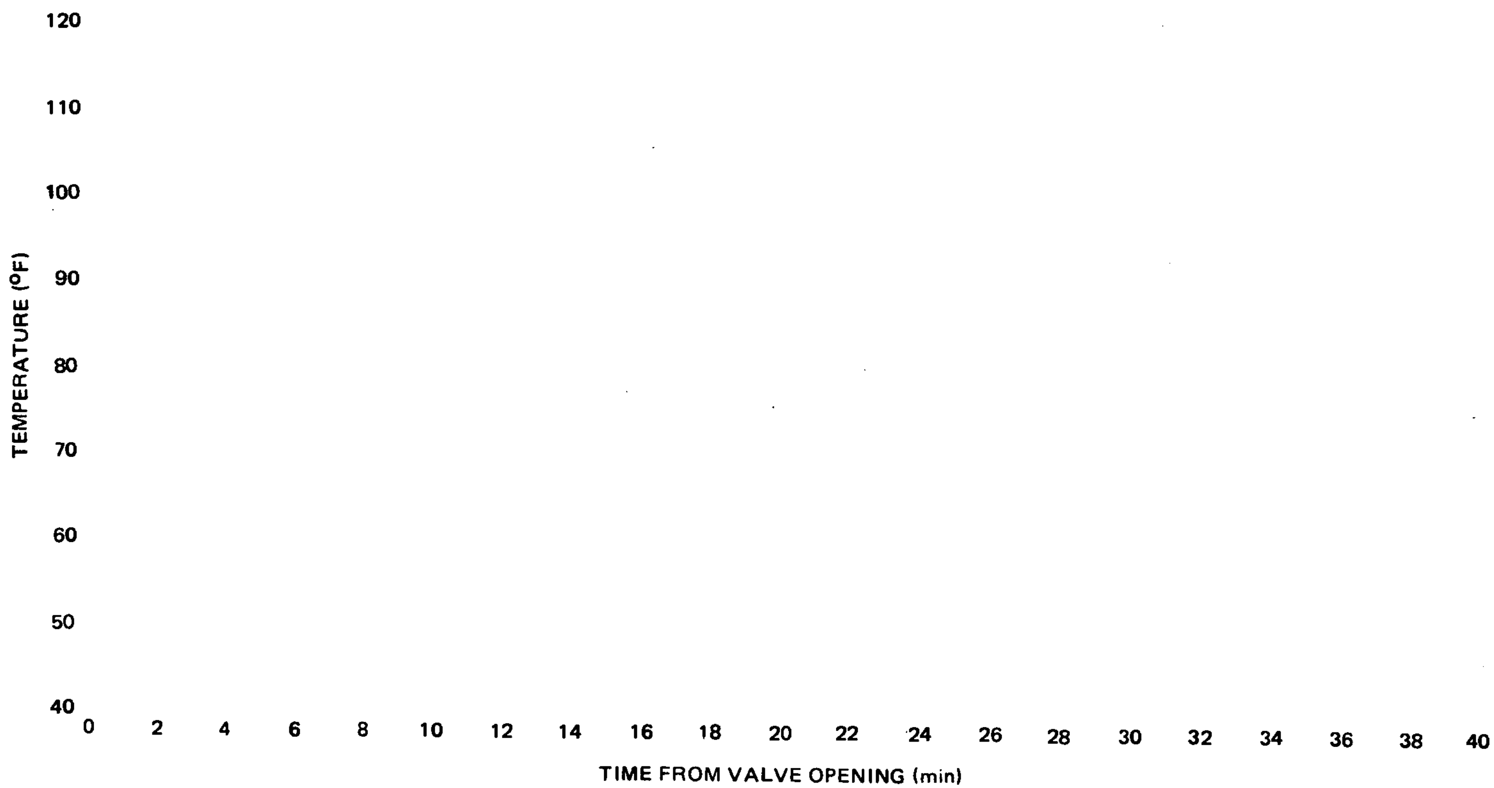

Figure E.4-11. Temperature Histories of the Sensors 7" Below the Surface at Azimuth 74° for Test with RHR (2/24/78)

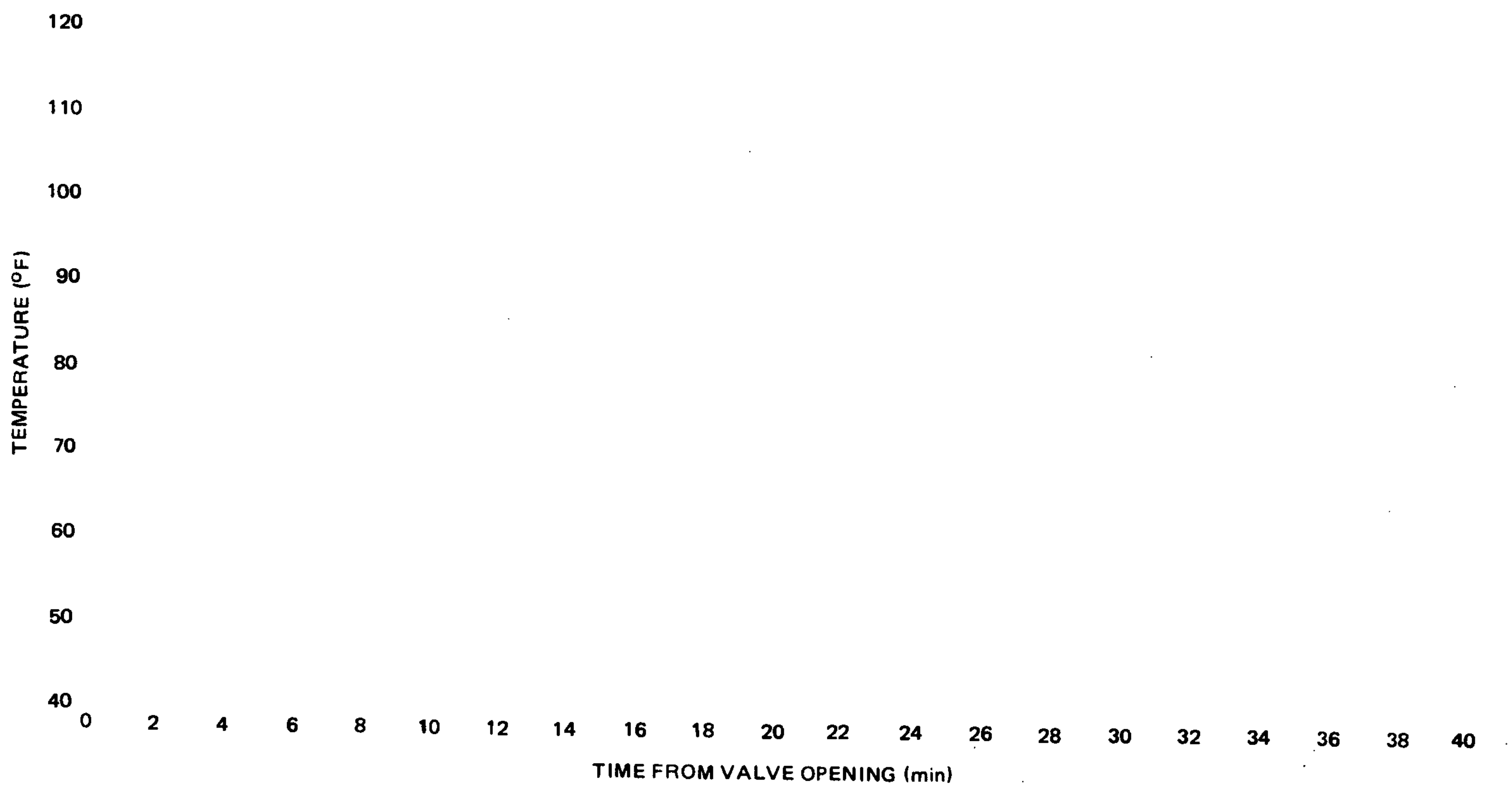

Figure E.4-12. Temperature Histories of the Sensors 12" Below the Pool Surface at Azimuth 74° for Test with RHR (2/24/78)

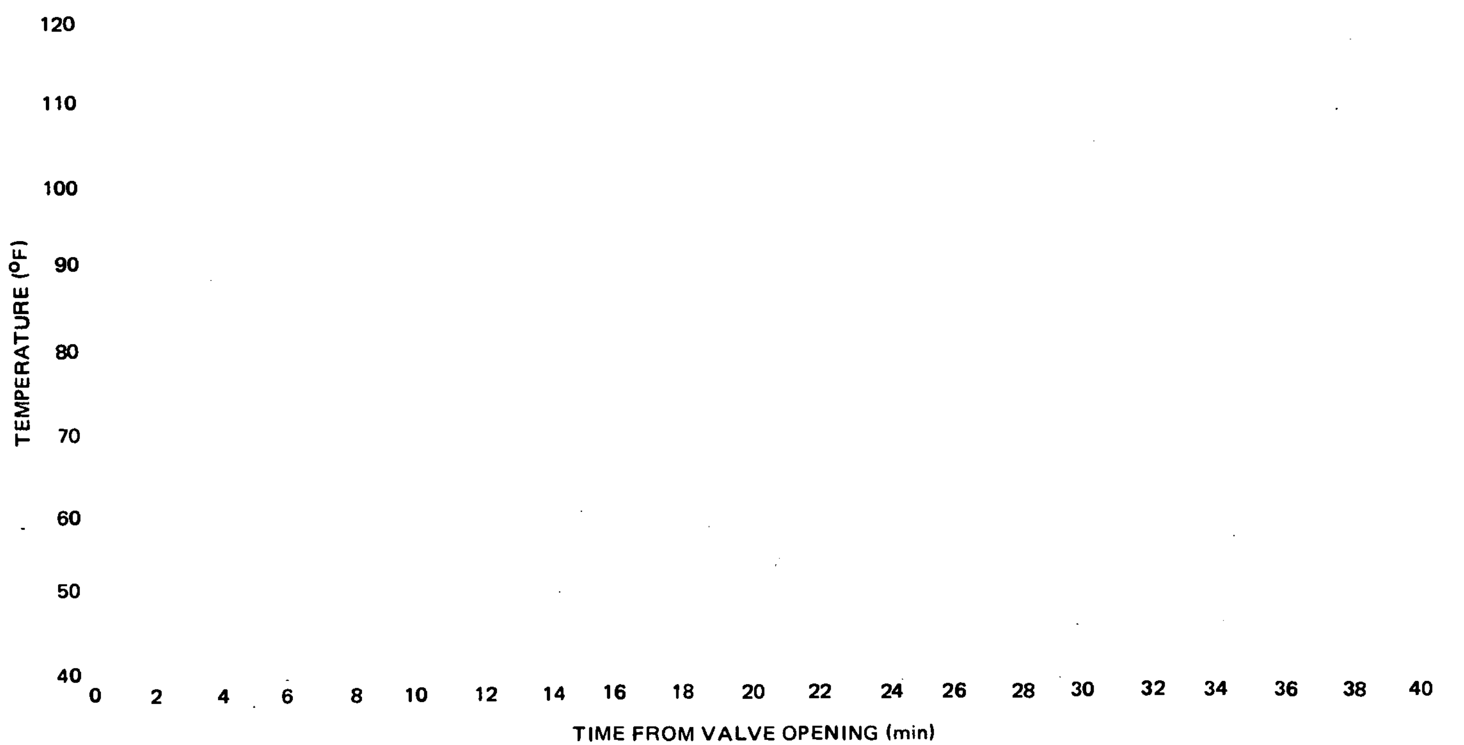

Figure E.4-13. Temperature Histories of the Sensors 51" Below the Pool Surface at Azimuth 74° For Test with RHR (2/24/78)

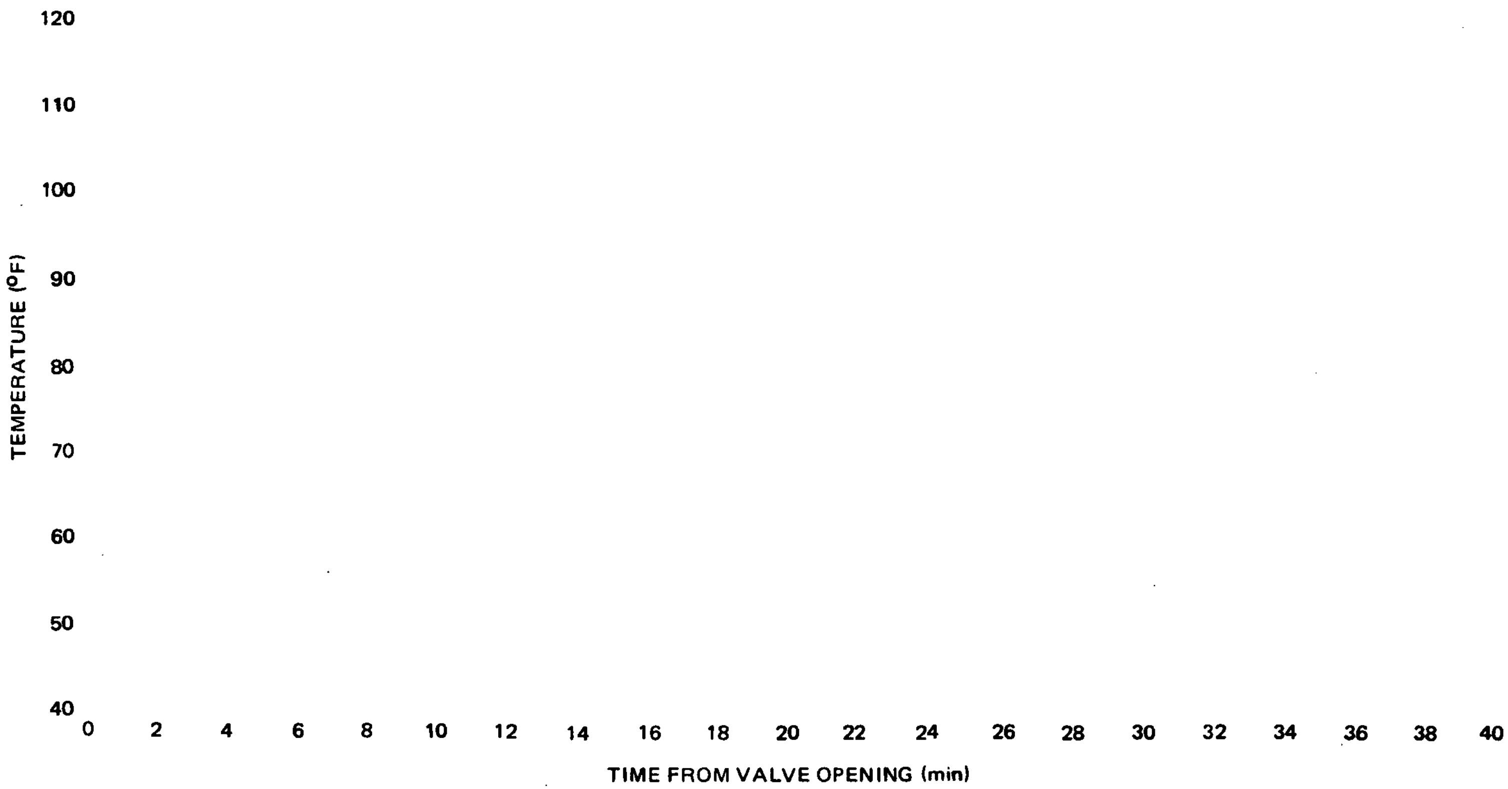

Figure E.4-14. Temperature Histories of the Bottom 4 Sensors at Azimuth 74° for Test with RHR (2/24/78)

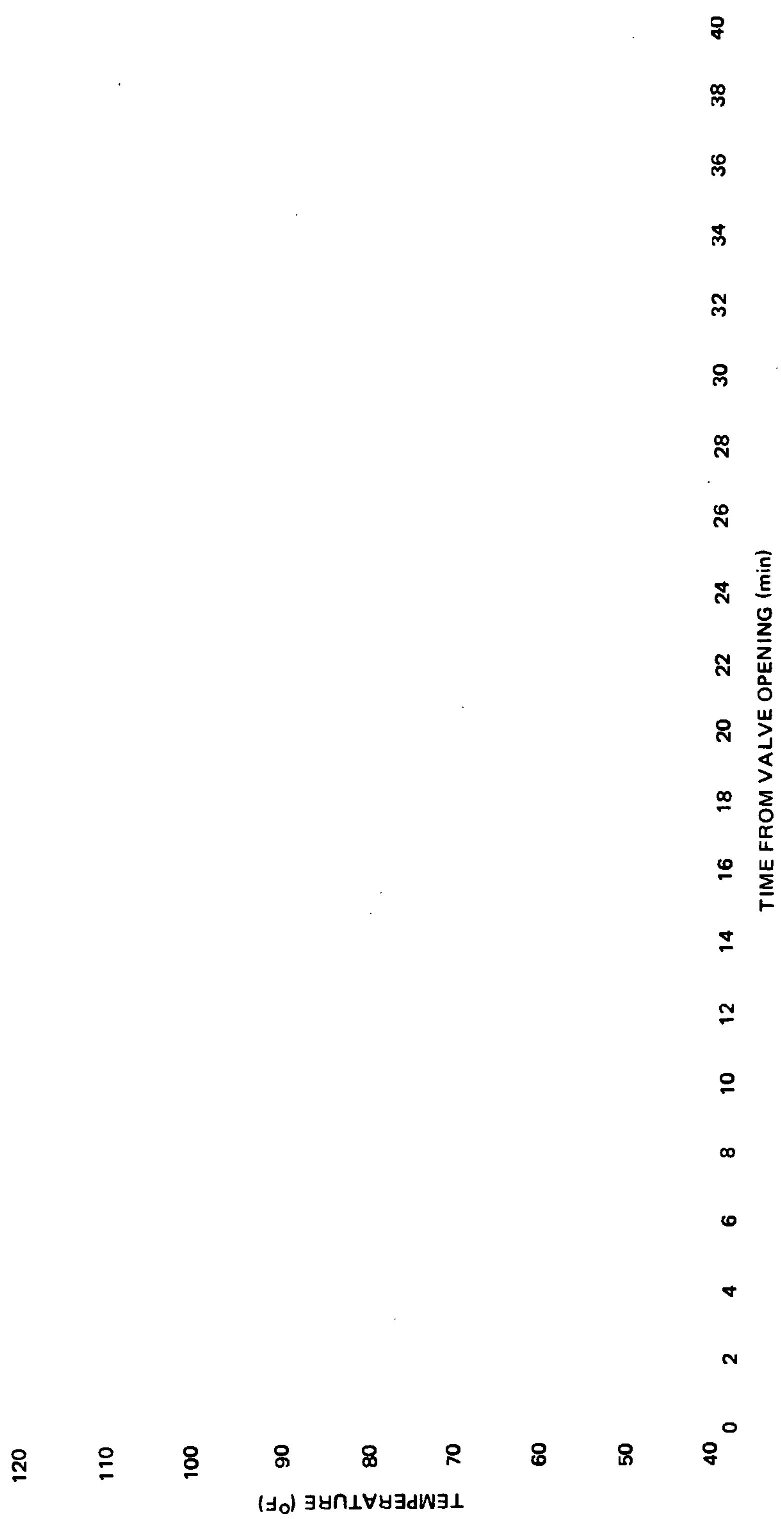

Figure E.4-15. Temperature Histories of RTD Sensors at Azimuth 101 for Test with RHR (2/24/78)

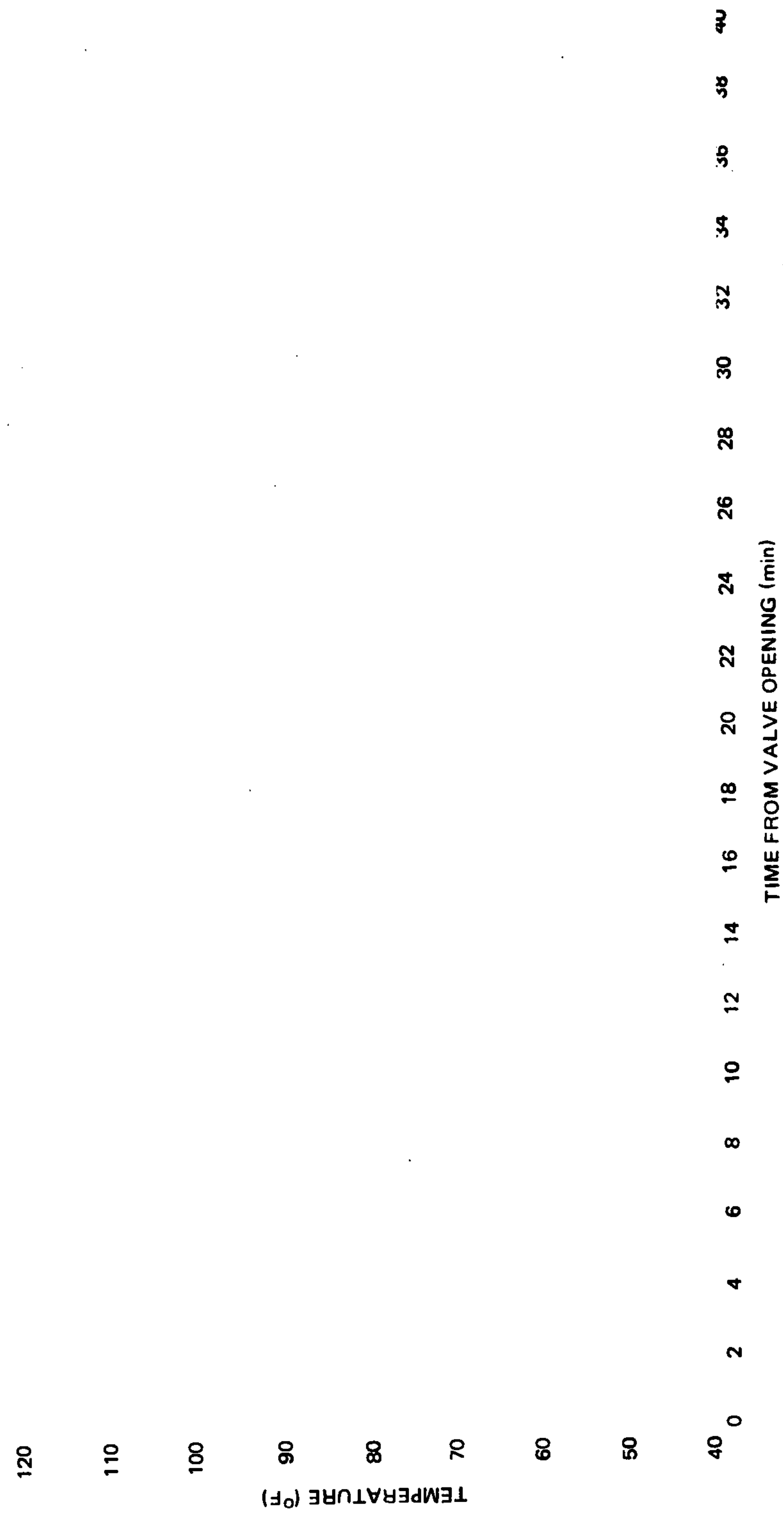

Figure E.4-16. Temperature Histories of RTD Sensors at Azimuth 124° for Test with RHR (2/24/78)

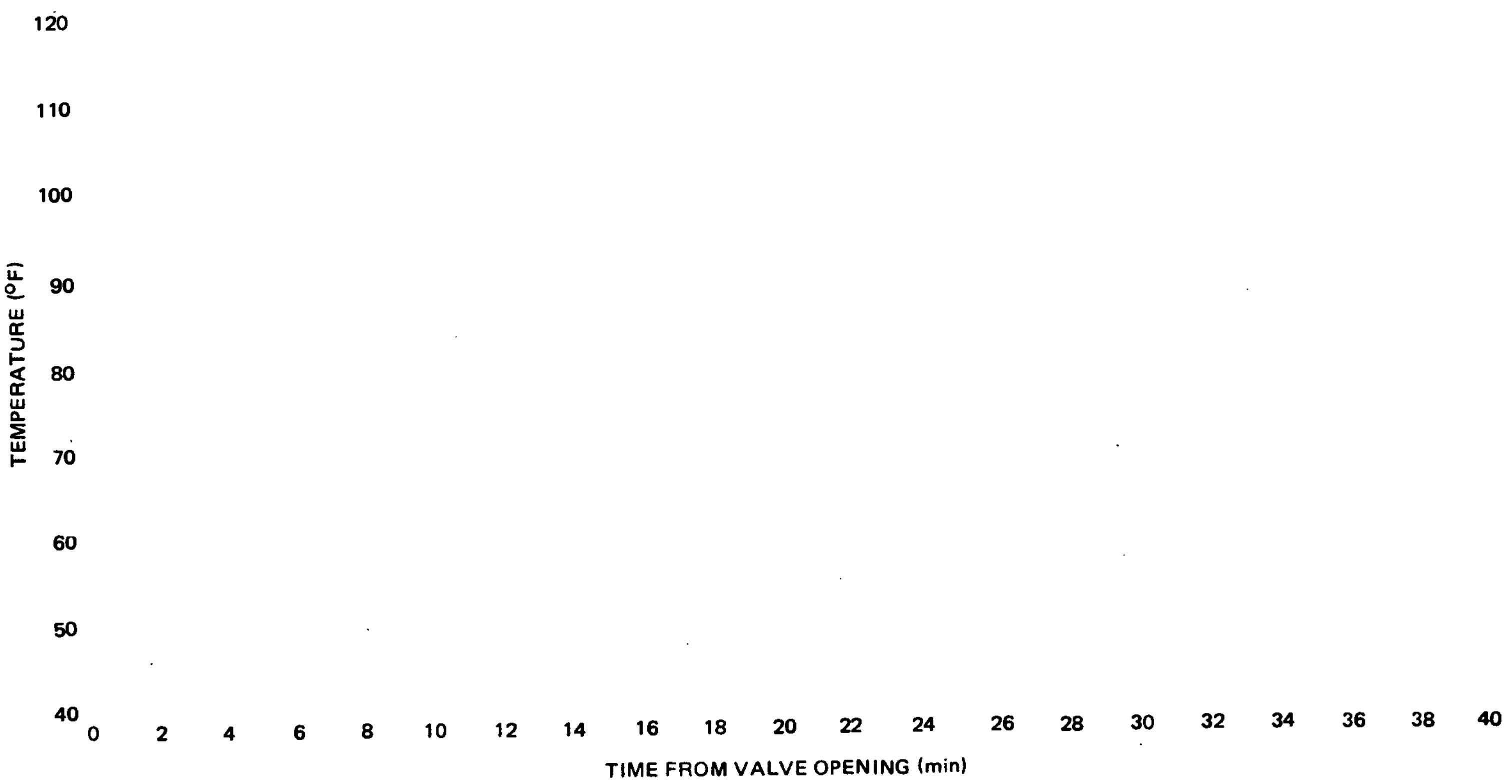

Figure E.4-17. Temperature Histories of RTD Sensors at Azimuth 146° for Test with RHR (2/24/78)

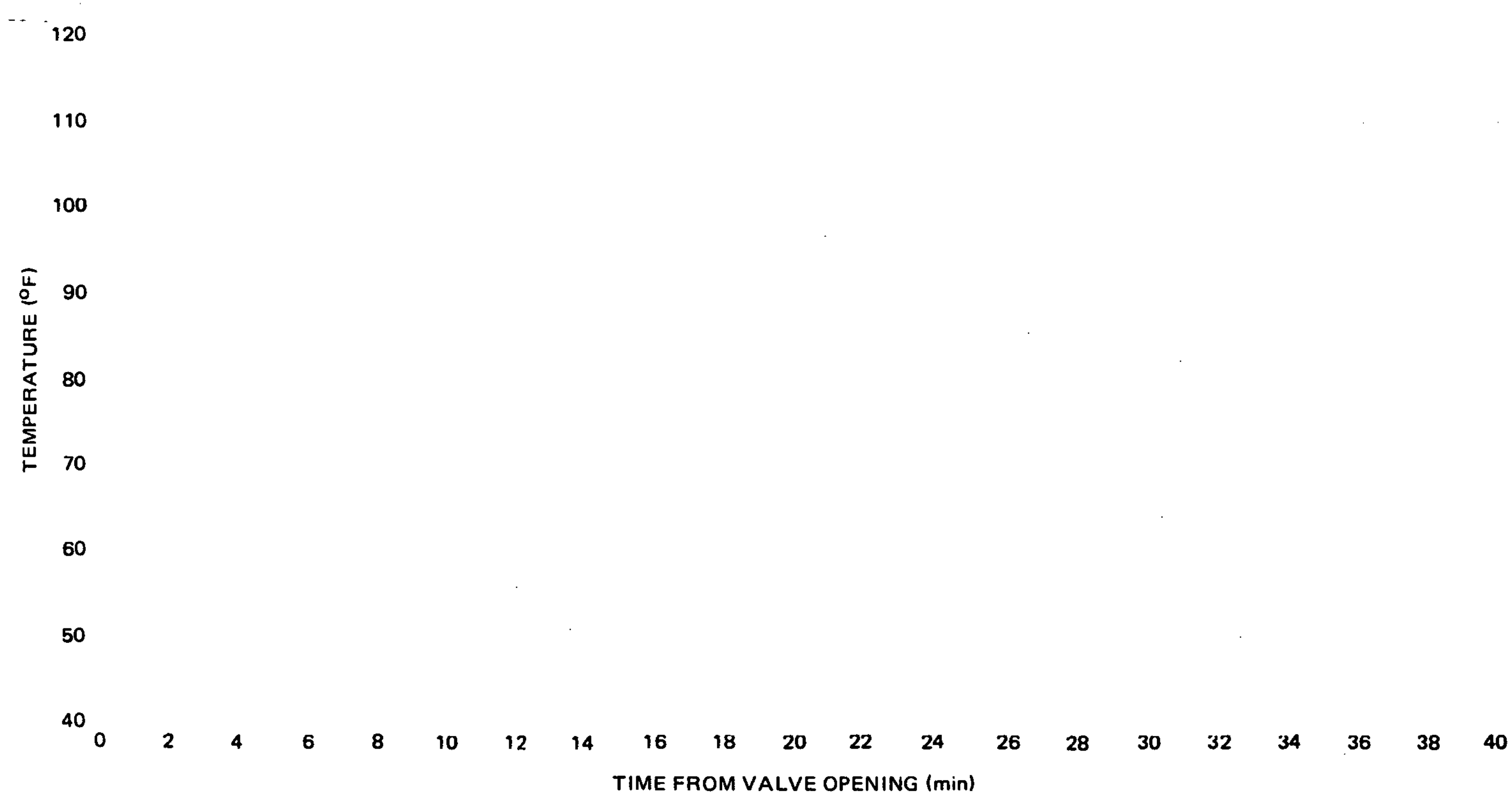

Figure E.4-18. Temperature Histories of RTD Sensors at Azimuth 259° for Test with RHR (2/24/78)

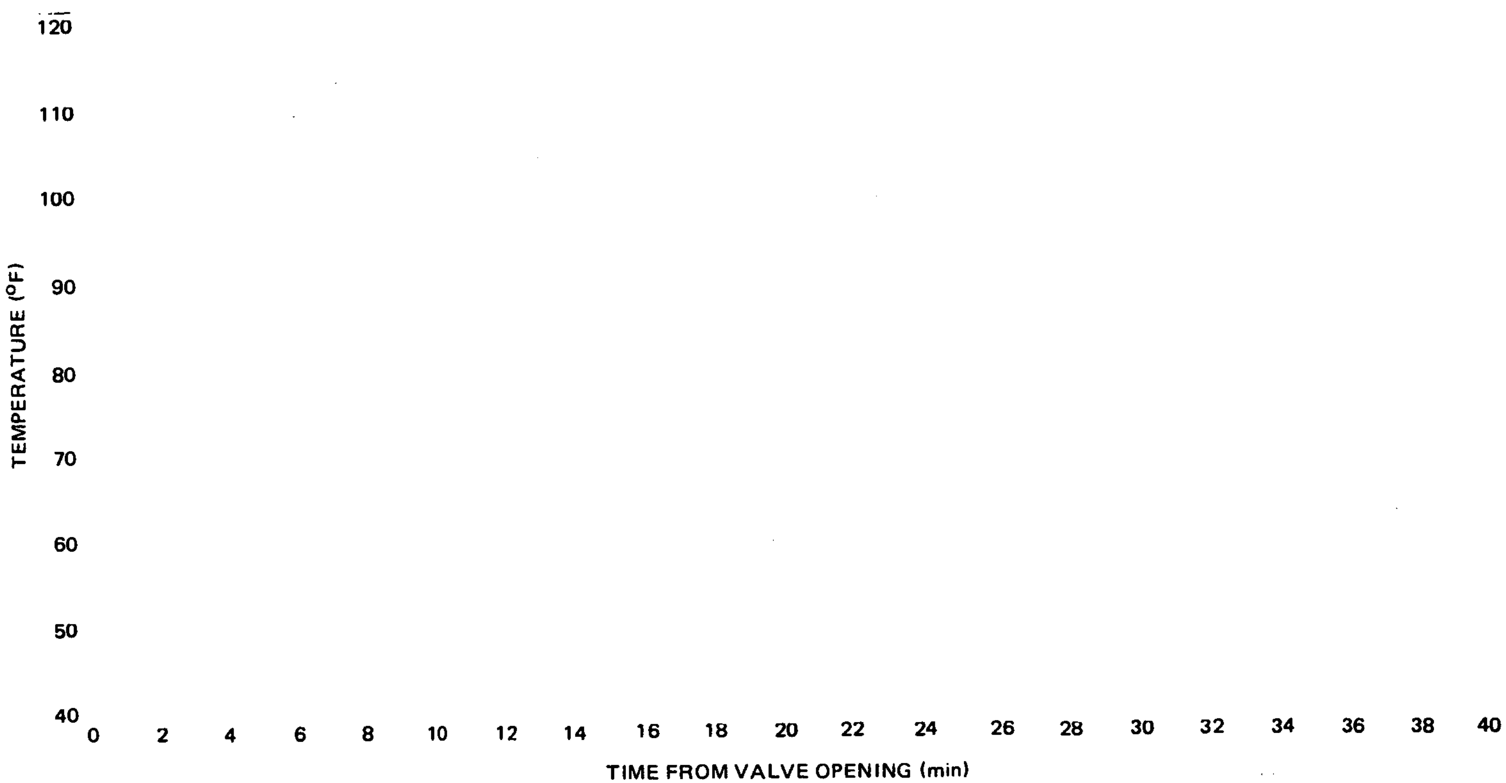

Figure E.4-19. Temperature Histories of RTD Sensors at Azimuth 349° for Test with RHR (2/24/78)

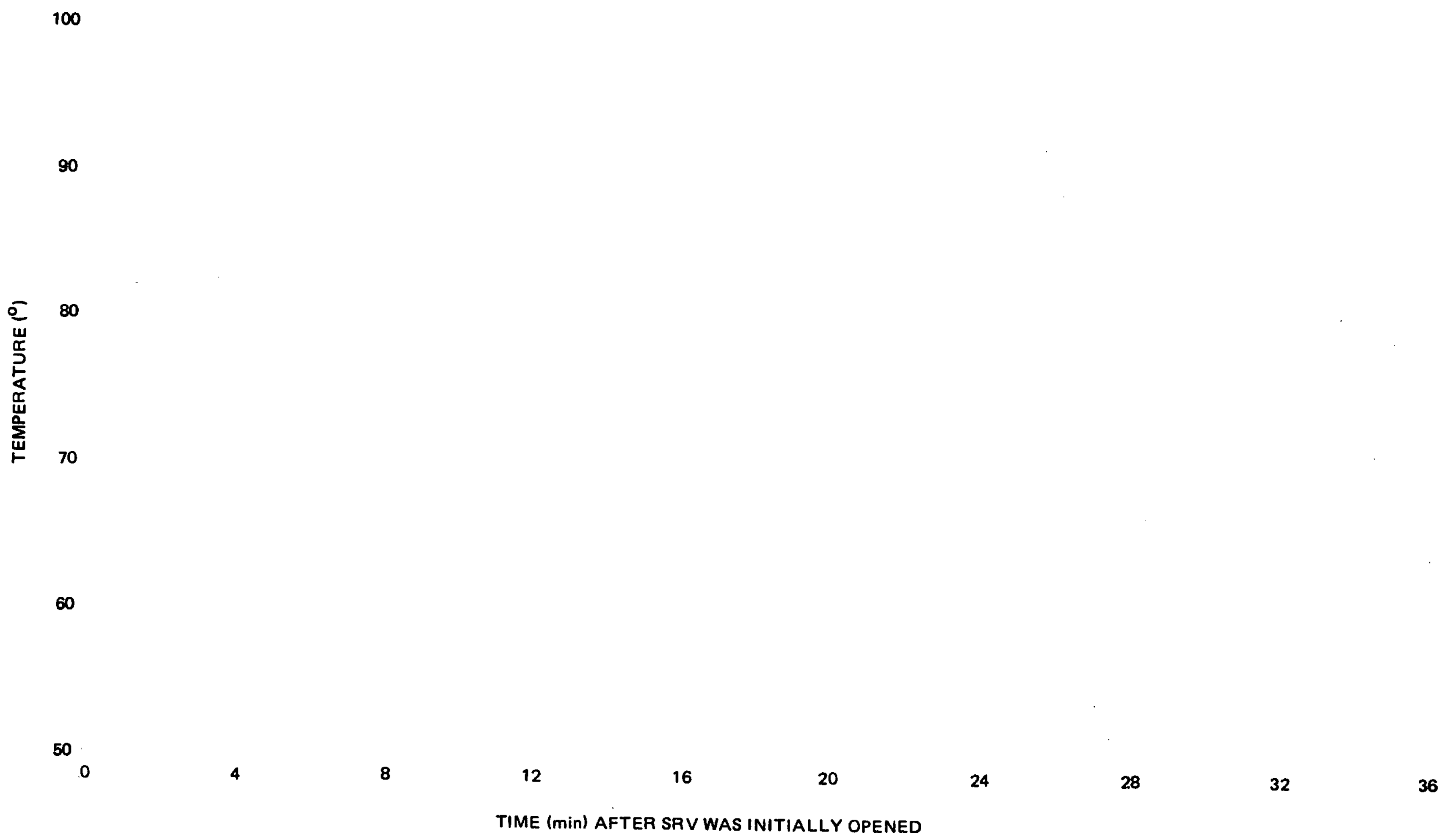

Figure E.4-20 Temperature Histories of Plant Temperature Sensors in Bays E/F and G/H for Test with RHR (2/24/78)

APPENDIX F

SUMMARY OF STRUCTURAL TEST DATA

TEST NO. 2

Gage	STRESS INTENSITY (KSI) - ROSETTE GAGES				
	Outside/Inside Rosettes			Outside Rosettes	
	Outside	Inside	Memb.	Gage	Outside
1				3	
2				11	
4				16	
6				17	
8				18	
10				19	
12				20	
13				21	
14				22	
15				24	
23				25	
32				26	
33				31	
				W1	
				W2	
				W3	
				W4	
				W5	
				W6	
				W7	

Gage	SINGLE GAGE OUTSIDE/INSIDE (KSI)					
	Outside		Inside		Memb.	
	Max	Min	Max	Min	Max	Min
7						

Gage	ROSETTE OUTSIDE/SINGLE INSIDE (KSI)				
	Stress Intensity Out	Stress in Single Direction			
		Inside		Memb.	
		Max	Min	Max	Min
9					

Gage	SINGLE GAGES (KSI)	
	Outside	
	Max	Min
34		
35		
131		
132		
133		
134		
135		
W8		

MAX. COLUMN LOADS (KIPS OR INCH-KIPS)						
Column	Up	Down	Column	Up	Down	Moment
A1			D1			
A2			D2			
B1			D3			
B2			D4			

TEST NO. 501

Gage	STRESS INTENSITY (KSI) - ROSETTE GAGES: Outside/Inside Rosettes - Outside	Inside	Memb.	Outside Rosettes - Gage	Outside
1				3	
2				11	
4				16	
6				17	
8				18	
10				19	
12				20	
13				21	
14				22	
15				24	
23				25	
32				26	
33				31	
				W1	
				W2	
				W3	
				W4	
				W5	
				W6	
				W7	

SINGLE GAGE OUTSIDE/INSIDE (KSI)

Gage	Outside		Inside		Memb.	
	Max	Min	Max	Min	Max	Min
7						

ROSETTE OUTSIDE/SINGLE INSIDE (KSI)

Gage	Stress Intensity Out	Stress in Single Direction: Inside		Memb.	
		Max	Min	Max	Min
9					

SINGLE GAGES (KSI)

Gage	Outside	
	Max	Min
34		
35		
131		
132		
133		
134		
135		
W8		

MAX. COLUMN LOADS (KIPS OR INCH-KIPS)

Column	Up	Down	Column	Up	Down	Moment
A1			D1			
A2			D2			
B1			D3			
B2			D4			

TEST NO. 502

Gage	STRESS INTENSITY (KSI) - ROSETTE GAGES — Outside/Inside Rosettes: Outside	Inside	Memb.	Outside Rosettes: Gage	Outside
1				3	
2				11	
4				16	
6				17	
8				18	
10				19	
12				20	
13				21	
14				22	
15				24	
23				25	
32				26	
33				31	
				W1	
				W2	
				W3	
				W4	
				W5	
				W6	
				W7	

SINGLE GAGE OUTSIDE/INSIDE (KSI)

Gage	Outside		Inside		Memb.	
	Max	Min	Max	Min	Max	Min
7						

ROSETTE OUTSIDE/SINGLE INSIDE (KSI)

Gage	Stress Intensity Out	Stress in Single Direction: Inside		Memb.	
		Max	Min	Max	Min
9					

SINGLE GAGES (KSI)

Gage	Outside	
	Max	Min
34		
35		
131		
132		
133		
134		
135		
W8		

MAX. COLUMN LOADS (KIPS OR INCH-KIPS)

Column	Up	Down	Column	Up	Down	Moment
A1			D1			
A2			D2			
B1			D3			
B2			D4			

TEST NO. 801

Gage	STRESS INTENSITY (KSI) - ROSETTE GAGES				
	Outside/Inside Rosettes			Outside Rosettes	
	Outside	Inside	Memb.	Gage	Outside
1				3	
2				11	
4				16	
6				17	
8				18	
10				19	
12				20	
13				21	
14				22	
15				24	
23				25	
32				26	
33				31	
				W1	
				W2	
				W3	
				W4	
				W5	
				W6	
				W7	

SINGLE GAGE OUTSIDE/INSIDE (KSI)						
Gage	Outside		Inside		Memb.	
	Max	Min	Max	Min	Max	Min
7						

Gage	ROSETTE OUTSIDE/SINGLE INSIDE (KSI)				
	Stress Intensity Out	Stress in Single Direction			
		Inside		Memb.	
		Max	Min	Max	Min
9					

SINGLE GAGES (KSI)		
Gage	Outside	
	Max	Min
34		
35		
131		
132		
133		
134		
135		
W8		

MAX. COLUMN LOADS (KIPS OR INCH-KIPS)						
Column	Up	Down	Column	Up	Down	Moment
A1			D1			
A2			D2			
B1			D3			
B2			D4			

TEST NO. 802

Gage	STRESS INTENSITY (KSI) - ROSETTE GAGES				
	Outside/Inside Rosettes			Outside Rosettes	
	Outside	Inside	Memb.	Gage	Outside
1				3	
2				11	
4				16	
6				17	
8				18	
10				19	
12				20	
13				21	
14				22	
15				24	
23				25	
32				26	
33				31	
				W1	
				W2	
				W3	
				W4	
				W5	
				W6	
				W7	

SINGLE GAGE OUTSIDE/INSIDE (KSI)

Gage	Outside		Inside		Memb.	
	Max	Min	Max	Min	Max	Min
7						

SINGLE GAGES (KSI)

Gage	Outside	
	Max	Min
34		
35		
131		
132		
133		
134		
135		
W8		

ROSETTE OUTSIDE/SINGLE INSIDE (KSI)

Gage	Stress Intensity Out	Stress in Single Direction			
		Inside		Memb.	
		Max	Min	Max	Min
9					

MAX. COLUMN LOADS (KIPS OR INCH-KIPS)

Column	Up	Down	Column	Up	Down	Moment
A1			D1			
A2			D2			
B1			D3			
B2			D4			

TEST NO. 901

Gage	STRESS INTENSITY (KSI) - ROSETTE GAGES: Outside/Inside Rosettes			Outside Rosettes	
	Outside	Inside	Memb.	Gage	Outside
1				3	
2				11	
4				16	
6				17	
8				18	
10				19	
12				20	
13				21	
14				22	
15				24	
23				25	
32				26	
33				31	
				W1	
				W2	
				W3	
				W4	
				W5	
				W6	
				W7	

SINGLE GAGE OUTSIDE/INSIDE (KSI)

Gage	Outside		Inside		Memb.	
	Max	Min	Max	Min	Max	Min
7						

ROSETTE OUTSIDE/SINGLE INSIDE (KSI)

Gage	Stress Intensity Out	Stress in Single Direction: Inside		Memb.	
		Max	Min	Max	Min
9					

SINGLE GAGES (KSI)

Gage	Outside	
	Max	Min
34		
35		
131		
132		
133		
134		
135		
W8		

MAX. COLUMN LOADS (KIPS OR INCH-KIPS)

Column	Up	Down	Column	Up	Down	Moment
A1			D1			
A2			D2			
B1			D3			
B2			D4			

TEST NO. 902

Gage	STRESS INTENSITY (KSI) - ROSETTE GAGES: Outside/Inside Rosettes – Outside	Inside	Memb.	Outside Rosettes – Gage	Outside
1				3	
2				11	
4				16	
6				17	
8				18	
10				19	
12				20	
13				21	
14				22	
15				24	
23				25	
32				26	
33				31	
				W1	
				W2	
				W3	
				W4	
				W5	
				W6	
				W7	

SINGLE GAGE OUTSIDE/INSIDE (KSI)

Gage	Outside		Inside		Memb.	
	Max	Min	Max	Min	Max	Min
7						

ROSETTE OUTSIDE/SINGLE INSIDE (KSI)

Gage	Stress Intensity Out	Stress in Single Direction: Inside		Memb.	
		Max	Min	Max	Min
9					

SINGLE GAGES (KSI)

Gage	Outside	
	Max	Min
34		
35		
131		
132		
133		
134		
135		
W8		

MAX. COLUMN LOADS (KIPS OR INCH-KIPS)

Column	Up	Down	Column	Up	Down	Moment
A1			D1			
A2			D2			
B1			D3			
B2			D4			

TEST NO. 903

Gage	STRESS INTENSITY (KSI) - ROSETTE GAGES				
	Outside/Inside Rosettes			Outside Rosettes	
	Outside	Inside	Memb.	Gage	Outside
1				3	
2				11	
4				16	
6				17	
8				18	
10				19	
12				20	
13				21	
14				22	
15				24	
23				25	
32				26	
33				31	
				W1	
				W2	
				W3	
				W4	
				W5	
				W6	
				W7	

SINGLE GAGE OUTSIDE/INSIDE (KSI)						
Gage	Outside		Inside		Memb.	
	Max	Min	Max	Min	Max	Min
7						

Gage	ROSETTE OUTSIDE/SINGLE INSIDE (KSI)				
	Stress Intensity Out	Stress in Single Direction			
		Inside		Memb.	
		Max	Min	Max	Min
9					

SINGLE GAGES (KSI)		
Gage	Outside	
	Max	Min
34		
35		
131		
132		
133		
134		
135		
W8		

MAX. COLUMN LOADS (KIPS OR INCH-KIPS)						
Column	Up	Down	Column	Up	Down	Moment
A1			D1			
A2			D2			
B1			D3			
B2			D4			

TEST NO. 904

Gage	STRESS INTENSITY (KSI) - ROSETTE GAGES: Outside/Inside Rosettes — Outside	Inside	Memb.	Outside Rosettes — Gage	Outside
1				3	
2				11	
4				16	
6				17	
8				18	
10				19	
12				20	
13				21	
14				22	
15				24	
23				25	
32				26	
33				31	
				W1	
				W2	
				W3	
				W4	
				W5	
				W6	
				W7	

SINGLE GAGE OUTSIDE/INSIDE (KSI)

Gage	Outside		Inside		Memb.	
	Max	Min	Max	Min	Max	Min
7						

ROSETTE OUTSIDE/SINGLE INSIDE (KSI)

Gage	Stress Intensity Out	Stress in Single Direction — Inside		Memb.	
		Max	Min	Max	Min
9					

SINGLE GAGES (KSI)

Gage	Outside	
	Max	Min
34		
35		
131		
132		
133		
134		
135		
W8		

MAX. COLUMN LOADS (KIPS OR INCH-KIPS)

Column	Up	Down	Column	Up	Down	Moment
A1			D1			
A2			D2			
B1			D3			
B2			D4			

TEST NO. 905

Gage	STRESS INTENSITY (KSI) - ROSETTE GAGES				
	Outside/Inside Rosettes			Outside Rosettes	
Gage	Outside	Inside	Memb.	Gage	Outside
1				3	
2				11	
4				16	
6				17	
8				18	
10				19	
12				20	
13				21	
14				22	
15				24	
23				25	
32				26	
33				31	
				W1	
				W2	
				W3	
				W4	
				W5	
				W6	
				W7	

SINGLE GAGE OUTSIDE/INSIDE (KSI)						
Gage	Outside		Inside		Memb.	
	Max	Min	Max	Min	Max	Min
7						

Gage	ROSETTE OUTSIDE/SINGLE INSIDE (KSI)				
	Stress Intensity Out	Stress in Single Direction			
		Inside		Memb.	
		Max	Min	Max	Min
9					

SINGLE GAGES (KSI)		
Gage	Outside	
	Max	Min
34		
35		
131		
132		
133		
134		
135		
W8		

MAX. COLUMN LOADS (KIPS OR INCH-KIPS)						
Column	Up	Down	Column	Up	Down	Moment
A1			D1			
A2			D2			
B1			D3			
B2			D4			

TEST NO. 1101

Gage	STRESS INTENSITY (KSI) - ROSETTE GAGES				
	Outside/Inside Rosettes			Outside Rosettes	
	Outside	Inside	Memb.	Gage	Outside
1				3	
2				11	
4				16	
6				17	
8				18	
10				19	
12				20	
13				21	
14				22	
15				24	
23				25	
32				26	
33				31	
				W1	
				W2	
				W3	
				W4	
				W5	
				W6	
				W7	

Gage	SINGLE GAGE OUTSIDE/INSIDE (KSI)					
	Outside		Inside		Memb.	
	Max	Min	Max	Min	Max	Min
7						

Gage	ROSETTE OUTSIDE/SINGLE INSIDE (KSI)				
	Stress Intensity Out	Stress in Single Direction			
		Inside		Memb.	
		Max	Min	Max	Min
9					

Gage	SINGLE GAGES (KSI)	
	Outside	
	Max	Min
34		
35		
131		
132		
133		
134		
135		
W8		

MAX. COLUMN LOADS (KIPS OR INCH-KIPS)						
Column	Up	Down	Column	Up	Down	Moment
A1			D1			
A2			D2			
B1			D3			
B2			D4			

TEST NO. 1102

Gage	STRESS INTENSITY (KSI) - ROSETTE GAGES				
	Outside/Inside Rosettes			Outside Rosettes	
	Outside	Inside	Memb.	Gage	Outside
1				3	
2				11	
4				16	
6				17	
8				18	
10				19	
12				20	
13				21	
14				22	
15				24	
23				25	
32				26	
33				31	
				W1	
				W2	
				W3	
				W4	
				W5	
				W6	
				W7	

SINGLE GAGE OUTSIDE/INSIDE (KSI)						
Gage	Outside		Inside		Memb.	
	Max	Min	Max	Min	Max	Min
7						

Gage	ROSETTE OUTSIDE/SINGLE INSIDE (KSI)				
	Stress Intensity Out	Stress in Single Direction			
		Inside		Memb.	
		Max	Min	Max	Min
9					

SINGLE GAGES (KSI)		
Gage	Outside	
	Max	Min
34		
35		
131		
132		
133		
134		
135		
W8		

MAX. COLUMN LOADS (KIPS OR INCH-KIPS)						
Column	Up	Down	Column	Up	Down	Moment
A1			D1			
A2			D2			
B1			D3			
B2			D4			

TEST NO. 1103

Gage	STRESS INTENSITY (KSI) - ROSETTE GAGES				
	Outside/Inside Rosettes			Outside Rosettes	
	Outside	Inside	Memb.	Gage	Outside
1				3	
2				11	
4				16	
6				17	
8				18	
10				19	
12				20	
13				21	
14				22	
15				24	
23				25	
32				26	
33				31	
				W1	
				W2	
				W3	
				W4	
				W5	
				W6	
				W7	

SINGLE GAGE OUTSIDE/INSIDE (KSI)						
Gage	Outside		Inside		Memb.	
	Max	Min	Max	Min	Max	Min
7						

Gage	ROSETTE OUTSIDE/SINGLE INSIDE (KSI)				
	Stress Intensity Out	Stress in Single Direction			
		Inside		Memb.	
		Max	Min	Max	Min
9					

SINGLE GAGES (KSI)		
Gage	Outside	
	Max	Min
34		
35		
131		
132		
133		
134		
135		
W8		

MAX. COLUMN LOADS (KIPS OR INCH-KIPS)						
Column	Up	Down	Column	Up	Down	Moment
A1			D1			
A2			D2			
B1			D3			
B2			D4			

TEST NO. 1104

Gage	STRESS INTENSITY (KSI) - ROSETTE GAGES				
	Outside/Inside Rosettes			Outside Rosettes	
	Outside	Inside	Memb.	Gage	Outside
1				3	
2				11	
4				16	
6				17	
8				18	
10				19	
12				20	
13				21	
14				22	
15				24	
23				25	
32				26	
33				31	
				W1	
				W2	
				W3	
				W4	
				W5	
				W6	
				W7	

Gage	SINGLE GAGE OUTSIDE/INSIDE (KSI)					
	Outside		Inside		Memb.	
	Max	Min	Max	Min	Max	Min
7						

Gage	ROSETTE OUTSIDE/SINGLE INSIDE (KSI)				
	Stress Intensity Out	Stress in Single Direction			
		Inside		Memb.	
		Max	Min	Max	Min
9					

Gage	SINGLE GAGES (KSI) Outside	
	Max	Min
34		
35		
131		
132		
133		
134		
135		
W8		

MAX. COLUMN LOADS (KIPS OR INCH-KIPS)						
Column	Up	Down	Column	Up	Down	Moment
A1			D1			
A2			D2			
B1			D3			
B2			D4			

TEST NO. 1105

Gage	STRESS INTENSITY (KSI) - ROSETTE GAGES				
	Outside/Inside Rosettes			Outside Rosettes	
Gage	Outside	Inside	Memb.	Gage	Outside
1				3	
2				11	
4				16	
6				17	
8				18	
10				19	
12				20	
13				21	
14				22	
15				24	
23				25	
32				26	
33				31	
				W1	
				W2	
				W3	
				W4	
				W5	
				W6	
				W7	

SINGLE GAGE OUTSIDE/INSIDE (KSI)						
Gage	Outside		Inside		Memb.	
	Max	Min	Max	Min	Max	Min
7						

Gage	ROSETTE OUTSIDE/SINGLE INSIDE (KSI)				
	Stress Intensity Out	Stress in Single Direction			
		Inside		Memb.	
		Max	Min	Max	Min
9					

SINGLE GAGES (KSI)		
Gage	Outside	
	Max	Min
34		
35		
131		
132		
133		
134		
135		
W8		

MAX. COLUMN LOADS (KIPS OR INCH-KIPS)						
Column	Up	Down	Column	Up	Down	Moment
A1			D1			
A2			D2			
B1			D3			
B2			D4			

TEST NO. 1201

Gage	STRESS INTENSITY (KSI) - ROSETTE GAGES				
	Outside/Inside Rosettes			Outside Rosettes	
	Outside	Inside	Memb.	Gage	Outside
1				3	
2				11	
4				16	
6				17	
8				18	
10				19	
12				20	
13				21	
14				22	
15				24	
23				25	
32				26	
33				31	
				W1	
				W2	
				W3	
				W4	
				W5	
				W6	
				W7	

SINGLE GAGE OUTSIDE/INSIDE (KSI)						
Gage	Outside		Inside		Memb.	
	Max	Min	Max	Min	Max	Min
7						

Gage	ROSETTE OUTSIDE/SINGLE INSIDE (KSI)				
	Stress Intensity Out	Stress in Single Direction			
		Inside		Memb.	
		Max	Min	Max	Min
9					

SINGLE GAGES (KSI)		
Gage	Outside	
	Max	Min
34		
35		
131		
132		
133		
134		
135		
W8		

MAX. COLUMN LOADS (KIPS OR INCH-KIPS)						
Column	Up	Down	Column	Up	Down	Moment
A1			D1			
A2			D2			
B1			D3			
B2			D4			

TEST NO. 1301

Gage	STRESS INTENSITY (KSI) - ROSETTE GAGES				
	Outside/Inside Rosettes			Outside Rosettes	
	Outside	Inside	Memb.	Gage	Outside
1				3	
2				11	
4				16	
6				17	
8				18	
10				19	
12				20	
13				21	
14				22	
15				24	
23				25	
32				26	
33				31	
				W1	
				W2	
				W3	
				W4	
				W5	
				W6	
				W7	

Gage	SINGLE GAGE OUTSIDE/INSIDE (KSI)					
	Outside		Inside		Memb.	
	Max	Min	Max	Min	Max	Min
7						

Gage	ROSETTE OUTSIDE/SINGLE INSIDE (KSI)				
	Stress Intensity Out	Stress in Single Direction			
		Inside		Memb.	
		Max	Min	Max	Min
9					

Gage	SINGLE GAGES (KSI)	
	Outside	
	Max	Min
34		
35		
131		
132		
133		
134		
135		
W8		

MAX. COLUMN LOADS (KIPS OR INCH-KIPS)						
Column	Up	Down	Column	Up	Down	Moment
A1			D1			
A2			D2			
B1			D3			
B2			D4			

TEST NO. 1302

Gage	STRESS INTENSITY (KSI) - ROSETTE GAGES				
	Outside/Inside Rosettes			Outside Rosettes	
	Outside	Inside	Memb.	Gage	Outside
1				3	
2				11	
4				16	
6				17	
8				18	
10				19	
12				20	
13				21	
14				22	
15				24	
23				25	
32				26	
33				31	
				W1	
				W2	
				W3	
				W4	
				W5	
				W6	
				W7	

SINGLE GAGE OUTSIDE/INSIDE (KSI)						
Gage	Outside		Inside		Memb.	
	Max	Min	Max	Min	Max	Min
7						

Gage	ROSETTE OUTSIDE/SINGLE INSIDE (KSI)				
	Stress Intensity Out	Stress in Single Direction			
		Inside		Memb.	
		Max	Min	Max	Min
9					

SINGLE GAGES (KSI)		
Gage	Outside	
	Max	Min
34		
35		
131		
132		
133		
134		
135		
W8		

MAX. COLUMN LOADS (KIPS OR INCH-KIPS)						
Column	Up	Down	Column	Up	Down	Moment
A1			D1			
A2			D2			
B1			D3			
B2			D4			

TEST NO. 1303

Gage	STRESS INTENSITY (KSI) - ROSETTE GAGES: Outside/Inside Rosettes – Outside	Inside	Memb.	Outside Rosettes – Gage	Outside
1				3	
2				11	
4				16	
6				17	
8				18	
10				19	
12				20	
13				21	
14				22	
15				24	
23				25	
32				26	
33				31	
				W1	
				W2	
				W3	
				W4	
				W5	
				W6	
				W7	

SINGLE GAGE OUTSIDE/INSIDE (KSI)

Gage	Outside		Inside		Memb.	
	Max	Min	Max	Min	Max	Min
7						

ROSETTE OUTSIDE/SINGLE INSIDE (KSI)

Gage	Stress Intensity Out	Stress in Single Direction			
		Inside		Memb.	
		Max	Min	Max	Min
9					

SINGLE GAGES (KSI)

Gage	Outside	
	Max	Min
34		
35		
131		
132		
133		
134		
135		
W8		

MAX. COLUMN LOADS (KIPS OR INCH-KIPS)

Column	Up	Down	Column	Up	Down	Moment
A1			D1			
A2			D2			
B1			D3			
B2			D4			

TEST NO. 14

Gage	STRESS INTENSITY (KSI) - ROSETTE GAGES				
	Outside/Inside Rosettes			Outside Rosettes	
	Outside	Inside	Memb.	Gage	Outside
1				3	
2				11	
4				16	
6				17	
8				18	
10				19	
12				20	
13				21	
14				22	
15				24	
23				25	
32				26	
33				31	
				W1	
				W2	
				W3	
				W4	
				W5	
				W6	
				W7	

SINGLE GAGE OUTSIDE/INSIDE (KSI)						
Gage	Outside		Inside		Memb.	
	Max	Min	Max	Min	Max	Min
7						

Gage	ROSETTE OUTSIDE/SINGLE INSIDE (KSI)				
	Stress Intensity Out	Stress in Single Direction			
		Inside		Memb.	
		Max	Min	Max	Min
9					

SINGLE GAGES (KSI)		
Gage	Outside	
	Max	Min
34		
35		
131		
132		
133		
134		
135		
W8		

MAX. COLUMN LOADS (KIPS OR INCH-KIPS)						
Column	Up	Down	Column	Up	Down	Moment
A1			D1			
A2			D2			
B1			D3			
B2			D4			

TEST NO. 15

Gage	STRESS INTENSITY (KSI) - ROSETTE GAGES				
	Outside/Inside Rosettes			Outside Rosettes	
	Outside	Inside	Memb.	Gage	Outside
1				3	
2				11	
4				16	
6				17	
8				18	
10				19	
12				20	
13				21	
14				22	
15				24	
23				25	
32				26	
33				31	
				W1	
				W2	
				W3	
				W4	
				W5	
				W6	
				W7	

SINGLE GAGE OUTSIDE/INSIDE (KSI)						
Gage	Outside		Inside		Memb.	
	Max	Min	Max	Min	Max	Min
7						

ROSETTE OUTSIDE/SINGLE INSIDE (KSI)					
Gage	Stress Intensity Out	Stress in Single Direction			
		Inside		Memb.	
		Max	Min	Max	Min
9					

SINGLE GAGES (KSI)		
Gage	Outside	
	Max	Min
34		
35		
131		
132		
133		
134		
135		
W8		

MAX. COLUMN LOADS (KIPS OR INCH-KIPS)						
Column	Up	Down	Column	Up	Down	Moment
A1			D1			
A2			D2			
B1			D3			
B2			D4			

TEST NO. 1601

Gage	STRESS INTENSITY (KSI) - ROSETTE GAGES				
	Outside/Inside Rosettes			Outside Rosettes	
	Outside	Inside	Memb.	Gage	Outside
1				3	
2				11	
4				16	
6				17	
8				18	
10				19	
12				20	
13				21	
14				22	
15				24	
23				25	
32				26	
33				31	
				W1	
				W2	
				W3	
				W4	
				W5	
				W6	
				W7	

Gage	SINGLE GAGE OUTSIDE/INSIDE (KSI)					
	Outside		Inside		Memb.	
	Max	Min	Max	Min	Max	Min
7						

Gage	ROSETTE OUTSIDE/SINGLE INSIDE (KSI)				
	Stress Intensity Out	Stress in Single Direction			
		Inside		Memb.	
		Max	Min	Max	Min
9					

Gage	SINGLE GAGES (KSI)	
	Outside	
	Max	Min
34		
35		
131		
132		
133		
134		
135		
W8		

MAX. COLUMN LOADS (KIPS OR INCH-KIPS)						
Column	Up	Down	Column	Up	Down	Moment
A1			D1			
A2			D2			
B1			D3			
B2			D4			

TEST NO. 1602

Gage	STRESS INTENSITY (KSI) - ROSETTE GAGES				
	Outside/Inside Rosettes			Outside Rosettes	
	Outside	Inside	Memb.	Gage	Outside
1				3	
2				11	
4				16	
6				17	
8				18	
10				19	
12				20	
13				21	
14				22	
15				24	
23				25	
32				26	
33				31	
				W1	
				W2	
				W3	
				W4	
				W5	
				W6	
				W7	

SINGLE GAGE OUTSIDE/INSIDE (KSI)

Gage	Outside		Inside		Memb.	
	Max	Min	Max	Min	Max	Min
7						

ROSETTE OUTSIDE/SINGLE INSIDE (KSI)

Gage	Stress Intensity Out	Stress in Single Direction			
		Inside		Memb.	
		Max	Min	Max	Min
9					

SINGLE GAGES (KSI)

Gage	Outside	
	Max	Min
34		
35		
131		
132		
133		
134		
135		
W8		

MAX. COLUMN LOADS (KIPS OR INCH-KIPS)

Column	Up	Down	Column	Up	Down	Moment
A1			D1			
A2			D2			
B1			D3			
B2			D4			

TEST NO. 1603

Gage	STRESS INTENSITY (KSI) - ROSETTE GAGES				
	Outside/Inside Rosettes			Outside Rosettes	
	Outside	Inside	Memb.	Gage	Outside
1				3	
2				11	
4				16	
6				17	
8				18	
10				19	
12				20	
13				21	
14				22	
15				24	
23				25	
32				26	
33				31	
				W1	
				W2	
				W3	
				W4	
				W5	
				W6	
				W7	

SINGLE GAGE OUTSIDE/INSIDE (KSI)						
Gage	Outside		Inside		Memb.	
	Max	Min	Max	Min	Max	Min
7						

Gage	ROSETTE OUTSIDE/SINGLE INSIDE (KSI)				
	Stress Intensity Out	Stress in Single Direction			
		Inside		Memb.	
		Max	Min	Max	Min
9					

SINGLE GAGES (KSI)		
Gage	Outside	
	Max	Min
34		
35		
131		
132		
133		
134		
135		
W8		

MAX. COLUMN LOADS (KIPS OR INCH-KIPS)						
Column	Up	Down	Column	Up	Down	Moment
A1			D1			
A2			D2			
B1			D3			
B2			D4			

TEST NO. 1604

Gage	STRESS INTENSITY (KSI) - ROSETTE GAGES				
	Outside/Inside Rosettes			Outside Rosettes	
	Outside	Inside	Memb.	Gage	Outside
1				3	
2				11	
4				16	
6				17	
8				18	
10				19	
12				20	
13				21	
14				22	
15				24	
23				25	
32				26	
33				31	
				W1	
				W2	
				W3	
				W4	
				W5	
				W6	
				W7	

SINGLE GAGE OUTSIDE/INSIDE (KSI)						
Gage	Outside		Inside		Memb.	
	Max	Min	Max	Min	Max	Min
7						

Gage	ROSETTE OUTSIDE/SINGLE INSIDE (KSI)				
	Stress Intensity Out	Stress in Single Direction			
		Inside		Memb.	
		Max	Min	Max	Min
9					

SINGLE GAGES (KSI)		
Gage	Outside	
	Max	Min
34		
35		
131		
132		
133		
134		
135		
W8		

MAX. COLUMN LOADS (KIPS OR INCH-KIPS)						
Column	Up	Down	Column	Up	Down	Moment
A1			D1			
A2			D2			
B1			D3			
B2			D4			

TEST NO. 1605

Gage	STRESS INTENSITY (KSI) - ROSETTE GAGES				
	Outside/Inside Rosettes			Outside Rosettes	
	Outside	Inside	Memb.	Gage	Outside
1				3	
2				11	
4				16	
6				17	
8				18	
10				19	
12				20	
13				21	
14				22	
15				24	
23				25	
32				26	
33				31	
				W1	
				W2	
				W3	
				W4	
				W5	
				W6	
				W7	

SINGLE GAGE OUTSIDE/INSIDE (KSI)						
Gage	Outside		Inside		Memb.	
	Max	Min	Max	Min	Max	Min
7						

Gage	ROSETTE OUTSIDE/SINGLE INSIDE (KSI)				
	Stress Intensity Out	Stress in Single Direction			
		Inside		Memb.	
		Max	Min	Max	Min
9					

SINGLE GAGES (KSI)		
Gage	Outside	
	Max	Min
34		
35		
131		
132		
133		
134		
135		
W8		

MAX. COLUMN LOADS (KIPS OR INCH-KIPS)						
Column	Up	Down	Column	Up	Down	Moment
A1			D1			
A2			D2			
B1			D3			
B2			D4			

TEST NO. 18

Gage	STRESS INTENSITY (KSI) - ROSETTE GAGES				
	Outside/Inside Rosettes			Outside Rosettes	
	Outside	Inside	Memb.	Gage	Outside
1				3	
2				11	
4				16	
6				17	
8				18	
10				19	
12				20	
13				21	
14				22	
15				24	
23				25	
32				26	
33				31	
				W1	
				W2	
				W3	
				W4	
				W5	
				W6	
				W7	

Gage	SINGLE GAGE OUTSIDE/INSIDE (KSI)					
	Outside		Inside		Memb.	
	Max	Min	Max	Min	Max	Min
7						

Gage	ROSETTE OUTSIDE/SINGLE INSIDE (KSI)				
	Stress Intensity Out	Stress in Single Direction			
		Inside		Memb.	
		Max	Min	Max	Min
9					

Gage	SINGLE GAGES (KSI)	
	Outside	
	Max	Min
34		
35		
131		
132		
133		
134		
135		
W8		

MAX. COLUMN LOADS (KIPS OR INCH-KIPS)						
Column	Up	Down	Column	Up	Down	Moment
A1			D1			
A2			D2			
B1			D3			
B2			D4			

TEST NO. 19

Gage	STRESS INTENSITY (KSI) - ROSETTE GAGES				
	Outside/Inside Rosettes			Outside Rosettes	
	Outside	Inside	Memb.	Gage	Outside
1				3	
2				11	
4				16	
6				17	
8				18	
10				19	
12				20	
13				21	
14				22	
15				24	
23				25	
32				26	
33				31	
				W1	
				W2	
				W3	
				W4	
				W5	
				W6	
				W7	

Gage	SINGLE GAGE OUTSIDE/INSIDE (KSI)					
	Outside		Inside		Memb.	
	Max	Min	Max	Min	Max	Min
7						

Gage	ROSETTE OUTSIDE/SINGLE INSIDE (KSI)				
	Stress Intensity Out	Stress in Single Direction			
		Inside		Memb.	
		Max	Min	Max	Min
9					

Gage	SINGLE GAGES (KSI)	
	Outside	
	Max	Min
34		
35		
131		
132		
133		
134		
135		
W8		

MAX. COLUMN LOADS (KIPS OR INCH-KIPS)						
Column	Up	Down	Column	Up	Down	Moment
A1			D1			
A2			D2			
B1			D3			
B2			D4			

TEST NO. 21

Gage	STRESS INTENSITY (KSI) - ROSETTE GAGES: Outside/Inside Rosettes: Outside	Inside	Memb.	Outside Rosettes: Gage	Outside
1				3	
2				11	
4				16	
6				17	
8				18	
10				19	
12				20	
13				21	
14				22	
15				24	
23				25	
32				26	
33				31	
				W1	
				W2	
				W3	
				W4	
				W5	
				W6	
				W7	

SINGLE GAGE OUTSIDE/INSIDE (KSI)

Gage	Outside		Inside		Memb.	
	Max	Min	Max	Min	Max	Min
7						

ROSETTE OUTSIDE/SINGLE INSIDE (KSI)

Gage	Stress Intensity Out	Stress in Single Direction: Inside		Memb.	
		Max	Min	Max	Min
9					

SINGLE GAGES (KSI)

Gage	Outside	
	Max	Min
34		
35		
131		
132		
133		
134		
135		
W8		

MAX. COLUMN LOADS (KIPS OR INCH-KIPS)

Column	Up	Down	Column	Up	Down	Moment
A1			D1			
A2			D2			
B1			D3			
B2			D4			

TEST NO. 22

Gage	STRESS INTENSITY (KSI) - ROSETTE GAGES				
	Outside/Inside Rosettes			Outside Rosettes	
	Outside	Inside	Memb.	Gage	Outside
1				3	
2				11	
4				16	
6				17	
8				18	
10				19	
12				20	
13				21	
14				22	
15				24	
23				25	
32				26	
33				31	
				W1	
				W2	
				W3	
				W4	
				W5	
				W6	
				W7	

SINGLE GAGE OUTSIDE/INSIDE (KSI)						
Gage	Outside		Inside		Memb.	
	Max	Min	Max	Min	Max	Min
7						

Gage	ROSETTE OUTSIDE/SINGLE INSIDE (KSI)				
	Stress Intensity Out	Stress in Single Direction			
		Inside		Memb.	
		Max	Min	Max	Min
9					

SINGLE GAGES (KSI)		
Gage	Outside	
	Max	Min
34		
35		
131		
132		
133		
134		
135		
W8		

MAX. COLUMN LOADS (KIPS OR INCH-KIPS)						
Column	Up	Down	Column	Up	Down	Moment
A1			D1			
A2			D2			
B1			D3			
B2			D4			

TEST NO. 2301

Gage	STRESS INTENSITY (KSI) - ROSETTE GAGES: Outside/Inside Rosettes: Outside	Inside	Memb.	Outside Rosettes: Gage	Outside
1				3	
2				11	
4				16	
6				17	
8				18	
10				19	
12				20	
13				21	
14				22	
15				24	
23				25	
32				26	
33				31	
				W1	
				W2	
				W3	
				W4	
				W5	
				W6	
				W7	

SINGLE GAGE OUTSIDE/INSIDE (KSI)

Gage	Outside		Inside		Memb.	
	Max	Min	Max	Min	Max	Min
7						

ROSETTE OUTSIDE/SINGLE INSIDE (KSI)

Gage	Stress Intensity Out	Stress in Single Direction: Inside Max	Inside Min	Memb. Max	Memb. Min
9					

SINGLE GAGES (KSI)

Gage	Outside Max	Outside Min
34		
35		
131		
132		
133		
134		
135		
W8		

MAX. COLUMN LOADS (KIPS OR INCH-KIPS)

Column	Up	Down	Column	Up	Down	Moment
A1			D1			
A2			D2			
B1			D3			
B2			D4			

TEST NO. 2302

Gage	STRESS INTENSITY (KSI) - ROSETTE GAGES				
	Outside/Inside Rosettes			Outside Rosettes	
	Outside	Inside	Memb.	Gage	Outside
1 2 4 6 8 10 12 13 14 15 23 32 33				3 11 16 17 18 19 20 21 22 24 25 26 31 W1 W2 W3 W4 W5 W6 W7	

SINGLE GAGE OUTSIDE/INSIDE (KSI)						
Gage	Outside		Inside		Memb.	
	Max	Min	Max	Min	Max	Min
7						

Gage	ROSETTE OUTSIDE/SINGLE INSIDE (KSI)				
	Stress Intensity Out	Stress in Single Direction			
		Inside		Memb.	
		Max	Min	Max	Min
9					

SINGLE GAGES (KSI)		
Gage	Outside	
	Max	Min
34 35 131 132 133 134 135 W8		

MAX. COLUMN LOADS (KIPS OR INCH-KIPS)						
Column	Up	Down	Column	Up	Down	Moment
A1 A2 B1 B2			D1 D2 D3 D4			

TEST NO. 2303

Gage	STRESS INTENSITY (KSI) - ROSETTE GAGES				
	Outside/Inside Rosettes			Outside Rosettes	
	Outside	Inside	Memb.	Gage	Outside
1				3	
2				11	
4				16	
6				17	
8				18	
10				19	
12				20	
13				21	
14				22	
15				24	
23				25	
32				26	
33				31	
				W1	
				W2	
				W3	
				W4	
				W5	
				W6	
				W7	

Gage	SINGLE GAGE OUTSIDE/INSIDE (KSI)					
	Outside		Inside		Memb.	
	Max	Min	Max	Min	Max	Min
7						

Gage	ROSETTE OUTSIDE/SINGLE INSIDE (KSI)				
	Stress Intensity Out	Stress in Single Direction			
		Inside		Memb.	
		Max	Min	Max	Min
9					

Gage	SINGLE GAGES (KSI)	
	Outside	
	Max	Min
34		
35		
131		
132		
133		
134		
135		
W8		

MAX. COLUMN LOADS (KIPS OR INCH-KIPS)						
Column	Up	Down	Column	Up	Down	Moment
A1			D1			
A2			D2			
B1			D3			
B2			D4			

TEST NO. 2304

Gage	STRESS INTENSITY (KSI) - ROSETTE GAGES				
	Outside/Inside Rosettes			Outside Rosettes	
	Outside	Inside	Memb.	Gage	Outside
1				3	
2				11	
4				16	
6				17	
8				18	
10				19	
12				20	
13				21	
14				22	
15				24	
23				25	
32				26	
33				31	
				W1	
				W2	
				W3	
				W4	
				W5	
				W6	
				W7	

Gage	SINGLE GAGE OUTSIDE/INSIDE (KSI)					
	Outside		Inside		Memb.	
	Max	Min	Max	Min	Max	Min
7						

Gage	ROSETTE OUTSIDE/SINGLE INSIDE (KSI)				
	Stress Intensity Out	Stress in Single Direction			
		Inside		Memb.	
		Max	Min	Max	Min
9					

Gage	SINGLE GAGES (KSI)	
	Outside	
	Max	Min
34		
35		
131		
132		
133		
134		
135		
W8		

MAX. COLUMN LOADS (KIPS OR INCH-KIPS)						
Column	Up	Down	Column	Up	Down	Moment
A1			D1			
A2			D2			
B1			D3			
B2			D4			

TEST NO. 2305

Gage	STRESS INTENSITY (KSI) - ROSETTE GAGES: Outside/Inside Rosettes			Outside Rosettes	
	Outside	Inside	Memb.	Gage	Outside
1				3	
2				11	
4				16	
6				17	
8				18	
10				19	
12				20	
13				21	
14				22	
15				24	
23				25	
32				26	
33				31	
				W1	
				W2	
				W3	
				W4	
				W5	
				W6	
				W7	

SINGLE GAGE OUTSIDE/INSIDE (KSI)						
Gage	Outside		Inside		Memb.	
	Max	Min	Max	Min	Max	Min
7						

Gage	ROSETTE OUTSIDE/SINGLE INSIDE (KSI)				
	Stress Intensity Out	Stress in Single Direction			
		Inside		Memb.	
		Max	Min	Max	Min
9					

SINGLE GAGES (KSI)		
Gage	Outside	
	Max	Min
34		
35		
131		
132		
133		
134		
135		
W8		

MAX. COLUMN LOADS (KIPS OR INCH-KIPS)						
Column	Up	Down	Column	Up	Down	Moment
A1			D1			
A2			D2			
B1			D3			
B2			D4			

TEST NO. 2306

Gage	STRESS INTENSITY (KSI) - ROSETTE GAGES: Outside/Inside Rosettes: Outside	Inside	Memb.	Outside Rosettes: Gage	Outside
1				3	
2				11	
4				16	
6				17	
8				18	
10				19	
12				20	
13				21	
14				22	
15				24	
23				25	
32				26	
33				31	
				W1	
				W2	
				W3	
				W4	
				W5	
				W6	
				W7	

SINGLE GAGE OUTSIDE/INSIDE (KSI)

Gage	Outside		Inside		Memb.	
	Max	Min	Max	Min	Max	Min
7						

ROSETTE OUTSIDE/SINGLE INSIDE (KSI)

Gage	Stress Intensity Out	Stress in Single Direction: Inside		Memb.	
		Max	Min	Max	Min
9					

SINGLE GAGES (KSI)

Gage	Outside	
	Max	Min
34		
35		
131		
132		
133		
134		
135		
W8		

MAX. COLUMN LOADS (KIPS OR INCH-KIPS)

Column	Up	Down	Column	Up	Down	Moment
A1			D1			
A2			D2			
B1			D3			
B2			D4			

TEST NO. 2307

Gage	STRESS INTENSITY (KSI) - ROSETTE GAGES				
	Outside/Inside Rosettes			Outside Rosettes	
	Outside	Inside	Memb.	Gage	Outside
1				3	
2				11	
4				16	
6				17	
8				18	
10				19	
12				20	
13				21	
14				22	
15				24	
23				25	
32				26	
33				31	
				W1	
				W2	
				W3	
				W4	
				W5	
				W6	
				W7	

SINGLE GAGE OUTSIDE/INSIDE (KSI)						
Gage	Outside		Inside		Memb.	
	Max	Min	Max	Min	Max	Min
7						

Gage	ROSETTE OUTSIDE/SINGLE INSIDE (KSI)				
	Stress Intensity Out	Stress in Single Direction			
		Inside		Memb.	
		Max	Min	Max	Min
9					

SINGLE GAGES (KSI)		
Gage	Outside	
	Max	Min
34		
35		
131		
132		
133		
134		
135		
W8		

MAX. COLUMN LOADS (KIPS OR INCH-KIPS)						
Column	Up	Down	Column	Up	Down	Moment
A1			D1			
A2			D2			
B1			D3			
B2			D4			

TEST NO. 24

Gage	STRESS INTENSITY (KSI) - ROSETTE GAGES				
	Outside/Inside Rosettes			Outside Rosettes	
	Outside	Inside	Memb.	Gage	Outside
1				3	
2				11	
4				16	
6				17	
8				18	
10				19	
12				20	
13				21	
14				22	
15				24	
23				25	
32				26	
33				31	
				W1	
				W2	
				W3	
				W4	
				W5	
				W6	
				W7	

SINGLE GAGE OUTSIDE/INSIDE (KSI)						
Gage	Outside		Inside		Memb.	
	Max	Min	Max	Min	Max	Min
7						

Gage	ROSETTE OUTSIDE/SINGLE INSIDE (KSI)				
	Stress Intensity Out	Stress in Single Direction			
		Inside		Memb.	
		Max	Min	Max	Min
9					

SINGLE GAGES (KSI)		
Gage	Outside	
	Max	Min
34		
35		
131		
132		
133		
134		
135		
W8		

MAX. COLUMN LOADS (KIPS OR INCH-KIPS)						
Column	Up	Down	Column	Up	Down	Moment
A1			D1			
A2			D2			
B1			D3			
B2			D4			

APPENDIX G

SAMPLE OF STRUCTURAL TEST DATA
(TEST 2)

DO12U 042878 0755.8 MONTICELLO T-QUENCHER CRNCH02 PRODUCTION VERSION 02-03-78

MONTICELLO DATA REDUCTION - STRUCTURAL

RAW TIME HISTORY PLOTS

REF. TIME 8:46: 3:998 TEST- 2 RUN- 2 GRP 37 SAMPLE RATE- 10 RASTER- 4 0: 0: 4: 0 - 0: 0: 7: 0

	A1	A2	A3	A4
SCF 1 IN. =	3.000E 00 G	3.000E 00 G	3.000E 00 G	3.000E 00 G
BASELINE =	2.439E-02 G	-2.466E-03 G	-1.272E-02 G	1.072E-02 G

4000. MS

4500. MS

5000. MS

5500. MS

6000. MS

6500. MS

7000. MS

UPLOT COMPLETED TAPE# 1228
DATE: 042878 TIME: 0755.8

DO12U 042878 0755.8 MONTICELLO DATA REDUCTION - MONTICELLO T-QUENCHER STRUCTURAL CRNCH02 PRODUCTION VERSION 02-03-78

RAW TIME HISTORY PLOTS

REF. TIME 8:46: 3:998 TEST- 2 RUN- 2 GRP 38 SAMPLE RATE- 10 RASTER- 4 0: 0: 4: 0 - 0: 0: 7: 0

	A5	A6	A7	SWITCH
SCF 1 IN. •	3.000E 00 G	3.000E 00 G	3.000E 00 G	1.000E 01 DIG
BASELINE •	1.609E-02 G	2.341E-02 G	1.755E-02 G	-5.131E-04 DIG

4000. MS

4500. MS

5000. MS

5500. MS

6000. MS

6500. MS

7000. MS

UPLOT COMPLETED TAPE# 1228
DATE: 042878 TIME: 0755.8

MONTICELLO DATA REDUCTION - STRUCTURAL

BACK-TO-BACK ROSETTES: (3-ELEMENT OUTSIDE/INSIDE)
1. OSG1A 2. OSG1B 3. OSG1C 4. ISG1A 5. ISG1B 6. ISG1C
REF. TIME 0:46: 3:998 TEST- 2 RUN- 2 GRP 1 SAMPLE RATE- 10 RASTER- 4 0: 0: 4: 0 - 0: 0: 7: 0

	SGA OUT(1)	SGB OUT(2)	SGC OUT(3)	SIGMA-A OUT	SIGMA-C OUT	SHEAR AC OUT
	7.168E 02	7.168E 02	7.168E 02	2.000E 01	2.000E 01	2.000E 01
SCF 1 IN. =	MICRO-IN/IN	MICRO-IN/IN	MICRO-IN/IN	KSI	KSI	KSI
4000. MS						
4500. MS						
5000. MS						
5500. MS						
6000. MS						
6500. MS						
7000. MS						

UPLOT COMPLETED TAPE# 1228
DATE: 042878 TIME: 0755.8

DO12U 042878 0755.8 MONTICELLO T-QUENCHER CRNCH02 PRODUCTION VERSION 02-03-78

MONTICELLO DATA REDUCTION - STRUCTURAL

BACK-TO-BACK ROSETTES: (3-ELEMENT OUTSIDE/INSIDE)

1. OSG1A 2. OSG1B 3. OSG1C 4. ISG1A 5. ISG1B 6. ISG1C

REF. TIME 8:46: 3:998 TEST- 2 RUN- 2 GRP 1 SAMPLE RATE- 10 RASTER- 4 0: 0: 4: 0 - 0: 0: 7: 0

	SGA IN(4)	SGB IN(5)	SGC IN(6)	SIGMA-A IN	SIGMA-C IN	SHEAR AC IN
	7.168E 02	7.168E 02	7.168E 02	2.000E 01	2.000E 01	2.000E 01
SCF 1 IN. =	MICRO-IN/IN	MICRO-IN/IN	MICRO-IN/IN	KSI	KSI	KSI

4000. MS

4500. MS

5000. MS

5500. MS

6000. MS

6500. MS

7000. MS

UPLOT COMPLETED TAPE# 1228
DATE: 042878 TIME: 0755.8

0012U 042878 0755.8 MONTICELLO T-QUENCHER CRMCH02 PRODUCTION VERSION 02-03-78
MONTICELLO DATA REDUCTION - STRUCTURAL

BACK-TO-BACK ROSETTES: (3-ELEMENT OUTSIDE/INSIDE)

1. OSG2A 2. OSG2B 3. OSG2C 4. ISG2A 5. ISG2B 6. ISG2C

REF. TIME 8:46: 3:998 TEST- 2 RUN- 2 GRP 2 SAMPLE RATE- 10 RASTER- 4 0: 0: 4: 0 - 0: 0: 7: 0

	SGA OUT(1)	SGB OUT(2)	SGC OUT(3)	SIGMA-A OUT	SIGMA-C OUT	SHEAR AC OUT
	7.168E 02	7.168E 02	7.168E 02	2.000E 01	2.000E 01	2.000E 01
SCF 1 IN. =	MICRO-IN/IN	MICRO-IN/IN	MICRO-IN/IN	KSI	KSI	KSI

4000. MS

4500. MS

5000. MS

5500. MS

6000. MS

6500. MS

7000. MS

UPLOT COMPLETED TAPE# 1228
DATE: 042878 TIME: 0755.8

0012U 042878 0755.8 MONTICELLO T-QUENCHER CRNCN02 PRODUCTION VERSION 02-03-78

MONTICELLO DATA REDUCTION - STRUCTURAL

BACK-TO-BACK ROSETTES: (3-ELEMENT OUTSIDE/INSIDE)

1. OSG2A 2. OSG2B 3. OSG2C 4. ISG2A 5. ISG2B 6. ISG2C

REF. TIME 8:46: 3:998 TEST- 2 RUN- 2 GRP 2 SAMPLE RATE- 10 RASTER- 4 0: 0: 4: 0 - 0: 0: 7: 0

	SGA IN(4)	SGB IN(5)	SGC IN(6)	SIGMA-A IN	SIGMA-C IN	SHEAR AC IN
	7.168E 02	7.168E 02	7.168E 02	2.000E 01	2.000E 01	2.000E 01
SCF 1 IN. =	MICRO-IN/IN	MICRO-IN/IN	MICRO-IN/IN	KSI	KSI	KSI

4000. MS

4500. MS

5000. MS

5500. MS

6000. MS

6500. MS

7000. MS

UPLOT COMPLETED TAPE# 1228
DATE: 042878 TIME: 0755.8

MONTICELLO DATA REDUCTION - STRUCTURAL

BACK-TO-BACK ROSETTES: (3-ELEMENT OUTSIDE/INSIDE)

1. OSG4A 2. OSG4B 3. OSG4C 4. ISG4A 5. ISG4B 6. ISG4C

REF. TIME 8:46: 3:998 TEST- 2 RUN- 2 GRP 3 SAMPLE RATE- 10 RASTER- 4 0: 0: 4: 0 - 0: 0: 7: 0

SCF 1 IN. =	SGA OUT(1)	SGB OUT(2)	SGC OUT(3)	SIGMA-A OUT	SIGMA-C OUT	SHEAR AC OUT
	7.168E 02	7.168E 02	7.168E 02	2.000E 01	2.000E 01	2.000E 01
	MICRO-IN/IN	MICRO-IN/IN	MICRO-IN/IN	KSI	KSI	KSI
4000. MS						
4500. MS						
5000. MS						
5500. MS						
6000. MS						
6500. MS						
7000. MS						

UPLOT COMPLETED TAPE# 1228
DATE: 042878 TIME: 0755.8

DD12U 042878 0755.8 MONTICELLO T-QUENCHER CRNCH02 PRODUCTION VERSION 02-03-78
MONTICELLO DATA REDUCTION - STRUCTURAL

BACK-TO-BACK ROSETTES: (3-ELEMENT OUTSIDE/INSIDE)
1. DSG4A 2. DSG4B 3. DSG4C 4. ISG4A 5. ISG4B 6. ISG4C
REF. TIME 8:46: 3:998 TEST- 2 RUN- 2 GRP 3 SAMPLE RATE- 10 RASTER- 4 0: 0: 4: 0 - 0: 0: 7: 0

	SGA IN(4)	SGB IN(5)	SGC IN(6)	SIGMA-A IN	SIGMA-C IN	SHEAR AC IN
SCF 1 IN. =	7.168E 02 MICRO-IN/IN	7.168E 02 MICRO-IN/IN	7.168E 02 MICRO-IN/IN	2.000E 01 KSI	2.000E 01 KSI	2.000E 01 KSI

4000. MS
4500. MS
5000. MS
5500. MS
6000. MS
6500. MS
7000. MS

VPLOT COMPLETED TAPE# 1228
DATE: 042878 TIME: 0755.8

00120 042878 0755.8 MONTICELLO T-QUENCHER CRNCH02 PRODUCTION VERSION 02-03-78
MONTICELLO DATA REDUCTION - STRUCTURAL

BACK-TO-BACK ROSETTES: (3-ELEMENT OUTSIDE/INSIDE)
1. DSG6A 2. DSG6B 3. DSG6C 4. ISG6A 5. ISG6B 6. ISG6C
REF. TIME 8:46: 3:998 TEST- 2 RUN- 2 GRP 4 SAMPLE RATE- 10 RASTER- 4 0: 0: 4: 0 - 0: 0: 7: 0

	SGA OUT(1)	SGB OUT(2)	SGC OUT(3)	SIGMA-A OUT	SIGMA-C OUT	SHEAR AC OUT
	7.168E 02	7.168E 02	7.168E 02	2.000E 01	2.000E 01	2.000E 01
SCF 1 IN. =	MICRO-IN/IN	MICRO-IN/IN	MICRO-IN/IN	KSI	KSI	KSI

4000. MS

4500. MS

5000. MS

5500. MS

6000. MS

6500. MS

7000. MS

UPLOT COMPLETED TAPE# 1228
DATE: 042878 TIME: 0755.8

OD12U 042878 0755.8 MONTICELLO T-QUENCHER CRNCH02 PRODUCTION VERSION 02-03-78
MONTICELLO DATA REDUCTION - STRUCTURAL

BACK-TO-BACK ROSETTES: (3-ELEMENT OUTSIDE/INSIDE)
1. OSG6A 2. OSG6B 3. OSG6C 4. ISG6A 5. ISG6B 6. ISG6C
REF. TIME 8:46: 3:998 TEST- 2 RUN- 2 GRP 4 SAMPLE RATE- 10 RASTER- 4 0: 0: 4: 0 - 0: 0: 7: 0

	SGA IN(4)	SGB IN(5)	SGC IN(6)	SIGMA-A IN	SIGMA-C IN	SHEAR AC IN
	7.168E 02	7.168E 02	7.168E 02	2.000E 01	2.000E 01	2.000E 01
SCF 1 IN. =	MICRO-IN/IN	MICRO-IN/IN	MICRO-IN/IN	KSI	KSI	KSI

4000. MS

4500. MS

5000. MS

5500. MS

6000. MS

6500. MS

7000. MS

UPLOT COMPLETED TAPE# 1228
DATE: 042878 TIME: 0755.8

DD12U 042878 0755.8 MONTICELLO DATA REDUCTION - STRUCTURAL MONTICELLO T-QUENCHER CRNCH02 PRODUCTION VERSION 02-03-78

BACK-TO-BACK ROSETTES: (3-ELEMENT OUTSIDE/INSIDE)

1. OSG8A 2. OSG8B 3. OSG8C 4. ISG8A 5. ISG8B 6. ISG8C

REF. TIME 0:46: 3:998 TEST- 2 RUN- 2 GRP 5 SAMPLE RATE- 10 RASTER- 4 0: 0: 4: 0 - 0: 0: 7: 0

SCF 1 IN. =	SGA OUT(1) 7.168E 02 MICRO-IN/IN	SGB OUT(2) 7.168E 02 MICRO-IN/IN	SGC OUT(3) 7.168E 02 MICRO-IN/IN	SIGMA-A OUT 2.000E 01 KSI	SIGMA-C OUT 2.000E 01 KSI	SHEAR AC OUT 2.000E 01 KSI
4000. MS						
4500. MS						
5000. MS						
5500. MS						
6000. MS						
6500. MS						
7000. MS						

VPLOT COMPLETED TAPE# 1228
DATE: 042878 TIME: 0755.8

OD12U 042878 0755.8 MONTICELLO T-QUENCHER CRNCH02 PRODUCTION VERSION 02-03-78

MONTICELLO DATA REDUCTION - STRUCTURAL

BACK-TO-BACK ROSETTES: (3-ELEMENT OUTSIDE/INSIDE)

1. OSGBA 2. OSGBB 3. OSGBC 4. ISGBA 5. ISGBB 6. ISGBC

REF. TIME 8:46: 3:998 TEST- 2 RUN- 2 GRP 5 SAMPLE RATE- 10 RASTER- 4 0: 0: 4: 0 - 0: 0: 7: 0

	SGA INC4)	SGB INC5)	SGC INC6)	SIGMA-A IN	SIGMA-C IN	SHEAR AC IN
	7.168E 02	7.168E 02	7.168E 02	2.000E 01	2.000E 01	2.000E 01
SCF 1 IN. =	MICRO-IN/IN	MICRO-IN/IN	MICRO-IN/IN	KSI	KSI	KSI

4000. MS

4500. MS

5000. MS

5500. MS

6000. MS

6500. MS

7000. MS

UPLOT COMPLETED TAPE# 1228
DATE: 042878 TIME: 0755.8

DO12U 042878 0755.8 MONTICELLO T-QUENCHER CANCH02 PRODUCTION VERSION 02-03-78
MONTICELLO DATA REDUCTION - STRUCTURAL

BACK-TO-BACK ROSETTES: (3-ELEMENT OUTSIDE/INSIDE)
1. OSG10A 2. OSG10B 3. OSG10C 4. ISG10A 5. ISG10B 6. ISG10C
REF. TIME 8:46: 3:998 TEST- 2 RUN- 2 GRP 6 SAMPLE RATE- 10 RASTER- 4 0: 0: 4: 0 - 0: 0: 7: 0

SCP 1 IN.	SGA OUT(1)	SGB OUT(2)	SGC OUT(3)	SIGMA-A OUT	SIGMA-C OUT	SHEAR AC OUT
	7.168E 02	7.168E 02	7.168E 02	2.000E 01	2.000E 01	2.000E 01
	MICRO-IN/IN	MICRO-IN/IN	MICRO-IN/IN	KSI	KSI	KSI
4000. MS						
4500. MS						
5000. MS						
5500. MS						
6000. MS						
6500. MS						
7000. MS						

UPLOT COMPLETED TAPE# 1228
DATE: 042878 TIME: 0755.8

OD12U 042878 0755.8 MONTICELLO T-QUENCHER CRNCH02 PRODUCTION VERSION 02-03-78

MONTICELLO DATA REDUCTION - STRUCTURAL

BACK-TO-BACK ROSETTES: (3-ELEMENT OUTSIDE/INSIDE)

1. DSG10A 2. DSG10B 3. DSG10C 4. ISG10A 5. ISG10B 6. ISG10C

REP. TIME 8:46: 3:998 TEST- 2 RUN- 2 GRP 6 SAMPLE RATE- 10 RASTER- 4 0: 0: 4: 0 - 0: 0: 7: 0

	SGA INC4)	SGB INC5)	SGC INC6)	SIGMA-A IN	SIGMA-C IN	SHEAR AC IN
	7.168E 02	7.168E 02	7.168E 02	2.000E 01	2.000E 01	2.000E 01
SCF 1 IN. =	MICRO-IN/IN	MICRO-IN/IN	MICRO-IN/IN	KSI	KSI	KSI

4000. MS

4500. MS

5000. MS

5500. MS

6000. MS

6500. MS

7000. MS

UPLOT COMPLETED TAPE# 1228
DATE: 042878 TIME: 0755.8

DD12U 042878 0755.8 MONTICELLO T-QUENCHER CANCH02 PRODUCTION VERSION 02-03-78
MONTICELLO DATA REDUCTION - STRUCTURAL

BACK-TO-BACK ROSETTES: (3-ELEMENT OUTSIDE/INSIDE)
1. OSG12A 2. OSG12B 3. OSG12C 4. ISG12A 5. ISG12B 6. ISG12C
REF. TIME 8:46: 3:998 TEST- 2 RUN- 2 GRP 7 SAMPLE RATE- 10 RASTER- 4 0: 0: 4: 0 - 0: 0: 7: 0

	SGA OUT(1)	SGB OUT(2)	SGC OUT(3)	SIGMA-A OUT	SIGMA-C OUT	SHEAR AC OUT
	7.168E 02	7.168E 02	7.168E 02	2.000E 01	2.000E 01	2.000E 01
SCF 1 IN. -	MICRO-IN/IN	MICRO-IN/IN	MICRO-IN/IN	KSI	KSI	KSI

4000. MS

4500. MS

5000. MS

5500. MS

6000. MS

6500. MS

7000. MS

UPLOT COMPLETED TAPE# 1228
DATE: 042878 TIME: 0755.8

DD12U 042878 0755.8 MONTICELLO T-QUENCHER CRNCH02 PRODUCTION VERSION 02-03-78
MONTICELLO DATA REDUCTION - STRUCTURAL

BACK-TO-BACK ROSETTES: (3-ELEMENT OUTSIDE/INSIDE)
1. DSG12A 2. DSG12B 3. DSG12C 4. ISG12A 5. ISG12B 6. ISG12C
REF. TIME 8:46: 3:998 TEST- 2 RUN- 2 GRP 7 SAMPLE RATE- 10 RASTER- 4 0: 0: 4: 0 - 0: 0: 7: 0

	SGA IN(4)	SGB IN(5)	SGC IN(6)	SIGMA-A IN	SIGMA-C IN	SHEAR AC IN
	7.168E 02	7.168E 02	7.168E 02	2.000E 01	2.000E 01	2.000E 01
SCF 1 IN. =	MICRO-IN/IN	MICRO-IN/IN	MICRO-IN/IN	KSI	KSI	KSI

4000. MS

4500. MS

5000. MS

5500. MS

6000. MS

6500. MS

7000. MS

UPLOT COMPLETED TAPE# 1228
DATE: 042878 TIME: 0755.8

DD12U 042878 0755.8 MONTICELLO T-QUENCHER CRNCH02 PRODUCTION VERSION 02-03-78
MONTICELLO DATA REDUCTION - STRUCTURAL

BACK-TO-BACK ROSETTES: (3-ELEMENT OUTSIDE/INSIDE)
1. OSG13A 2. OSG13B 3. OSG13C 4. ISG13A 5. ISG13B 6. ISG13C
REF. TIME 8:46: 3:998 TEST- 2 RUN- 2 GRP 8 SAMPLE RATE- 10 RASTER- 4 0: 0: 4: 0 - 0: 0: 7: 0

	SGA OUT(1)	SGB OUT(2)	SGC OUT(3)	SIGMA-A OUT	SIGMA-C OUT	SHEAR AC OUT
	7.168E 02	7.168E 02	7.168E 02	2.000E 01	2.000E 01	2.000E 01
SCF 1 IN. =	MICRO-IN/IN	MICRO-IN/IN	MICRO-IN/IN	KSI	KSI	KSI

4000. MS

4500. MS

5000. MS

5500. MS

6000. MS

6500. MS

7000. MS

UPLOT COMPLETED TAPE# 1228
DATE: 042878 TIME: 0755.8

DD12U 042878 0755.8 MONTICELLO T-QUENCHER CRNCH02 PRODUCTION VERSION 02-03-78
MONTICELLO DATA REDUCTION - STRUCTURAL

BACK-TO-BACK ROSETTES: (3-ELEMENT OUTSIDE/INSIDE)
1. OSG13A 2. OSG13B 3. OSG13C 4. ISG13A 5. ISG13B 6. ISG13C
REF. TIME 8:46: 3:998 TEST- 2 RUN- 2 GRP 8 SAMPLE RATE- 10 RASTER- 4 0: 0: 4: 0 - 0: 0: 7: 0

SCF 1 IN. -	SGA IN(4) 7.168E 02 MICRO-IN/IN	SGB IN(5) 7.168E 02 MICRO-IN/IN	SGC IN(6) 7.168E 02 MICRO-IN/IN	SIGMA-A IN 2.000E 01 KSI	SIGMA-C IN 2.000E 01 KSI	SHEAR AC IN 2.000E 01 KSI
4000. MS						
4500. MS						
5000. MS						
5500. MS						
6000. MS						
6500. MS						
7000. MS						

UPLOT COMPLETED TAPE# 1228
DATE: 042878 TIME: 0755.8

OD12U 042878 0755.8 MONTICELLO DATA REDUCTION - STRUCTURAL MONTICELLO T-QUENCHER CRNCH02 PRODUCTION VERSION 02-03-78

BACK-TO-BACK ROSETTES: (3-ELEMENT OUTSIDE/INSIDE)

1. OSG14A 2. OSG14B 3. OSG14C 4. ISG14A 5. ISG14B 6. ISG14C

REF. TIME 8:46: 3:998 TEST- 2 RUN- 2 GRP 9 SAMPLE RATE- 10 RASTER- 4 0: 0: 4: 0 - 0: 0: 7: 0

SCF 1 IN. =	SGA OUT(1)	SGB OUT(2)	SGC OUT(3)	SIGMA-A OUT	SIGMA-C OUT	SHEAR AC OUT
	7.168E 02	7.168E 02	7.168E 02	2.000E 01	2.000E 01	2.000E 01
	MICRO-IN/IN	MICRO-IN/IN	MICRO-IN/IN	KSI	KSI	KSI

4000. MS

4500. MS

5000. MS

5500. MS

6000. MS

6500. MS

7000. MS

UPLOT COMPLETED TAPE# 1228

DATE: 042878 TIME: 0755.8

0012U 042878 0755.8 MONTICELLO T-QUENCHER CANCH02 PRODUCTION VERSION 02-03-78
MONTICELLO DATA REDUCTION - STRUCTURAL

BACK-TO-BACK ROSETTES: (3-ELEMENT OUTSIDE/INSIDE)

1. OSG14A 2. OSG14B 3. OSG14C 4. ISG14A 5. ISG14B 6. ISG14C

REF. TIME 8:46: 3:998 TEST- 2 RUN- 2 GRF 9 SAMPLE RATE- 10 RASTER- 4 0: 0: 4: 0 - 0: 0: 7: 0

SCF 1 IN. =	SGA IN(4)	SGB IN(5)	SGC IN(6)	SIGMA-A IN	SIGMA-C IN	SHEAR AC IN
	7.168E 02	7.168E 02	7.168E 02	2.000E 01	2.000E 01	2.000E 01
	MICRO-IN/IN	MICRO-IN/IN	MICRO-IN/IN	KSI	KSI	KSI

4000. MS

4500. MS

5000. MS

5500. MS

6000. MS

6500. MS

7000. MS

VPLOT COMPLETED TAPE# 1228
DATE: 042878 TIME: 0755.8

DD12U 042878 0755.8 MONTICELLO T-QUENCHER CRNCH02 PRODUCTION VERSION 02-03-78
MONTICELLO DATA REDUCTION - STRUCTURAL

RECTANGULAR STRAIN GAGE ROSETTE

1. OSG15A 2. OSG15B 3. OSG15C
REF. TIME 8:46: 3:998 TEST- 2 RUN- 2 GRP 10 SAMPLE RATE- 10 RASTER- 4 0: 0: 4: 0 - 0: 0: 7: 0

	GAGE-A (1)	GAGE-B (2)	GAGE-C (3)	SIGMA-A	SIGMA-C	SHEAR A-C
	7.168E 02	7.168E 02	7.168E 02	2.000E 01	2.000E 01	2.000E 01
SCF 1 IN. =	MICRO-IN/IN	MICRO-IN/IN	MICRO-IN/IN	KSI	KSI	KSI

4000. MS

4500. MS

5000. MS

5500. MS

6000. MS

6500. MS

7000. MS

UPLOT COMPLETED TAPE# 1228
DATE: 042878 TIME: 0755.8

DO12U 042878 0755.8 MONTICELLO T-QUENCHER CRNCH02 PRODUCTION VERSION 02-03-78

MONTICELLO DATA REDUCTION - STRUCTURAL

RECTANGULAR STRAIN GAGE ROSETTE

1. ISG23A 2. ISG23B 3. ISG23C

REF. TIME 8:46: 3:998 TEST- 2 RUN- 2 GRP 11 SAMPLE RATE- 10 RASTER- 4 0: 0: 4: 0 - 0: 0: 7: 0

SCF 1 IN. =	GAGE-A (1)	GAGE-B (2)	GAGE-C (3)	SIGMA-A	SIGMA-C	SHEAR A-C
	7.168E 02	7.168E 02	7.168E 02	2.000E 01	2.000E 01	2.000E 01
	MICRO-IN/IN	MICRO-IN/IN	MICRO-IN/IN	KSI	KSI	KSI

4000. MS

4500. MS

5000. MS

5500. MS

6000. MS

6500. MS

7000. MS

UPLOT COMPLETED TAPE# 1228
DATE: 042878 TIME: 0755.8

DD12U 042878 0755.8 MONTICELLO T-QUENCHER CRNCH02 PRODUCTION VERSION 02-03-78

MONTICELLO DATA REDUCTION - STRUCTURAL

BACK-TO-BACK ROSETTES: (3-ELEMENT OUTSIDE/INSIDE)

1. OSG32B 2. OSG32A 3. OSG32C 4. ISG32C 5. ISG32B 6. ISG32A

REF. TIME 8:46: 3:998 TEST- 2 RUN- 2 GRP 12 SAMPLE RATE- 10 RASTER- 4 0: 0: 4: 0 - 0: 0: 7: 0

	SGA OUT(1)	SGB OUT(2)	SGC OUT(3)	SIGMA-A OUT	SIGMA-C OUT	SHEAR AC OUT
	7.168E 02	7.168E 02	7.168E 02	2.000E 01	2.000E 01	2.000E 01
SCP 1 IN. =	MICRO-IN/IN	MICRO-IN/IN	MICRO-IN/IN	KSI	KSI	KSI

4000. MS

4500. MS

5000. MS

5500. MS

6000. MS

6500. MS

7000. MS

UPLOT COMPLETED TAPE# 1228
DATE: 042878 TIME: 0755.8

DD12U 042878 0755.8 MONTICELLO T-QUENCHER CRNCH02 PRODUCTION VERSION 02-03-78
MONTICELLO DATA REDUCTION - STRUCTURAL

BACK-TO-BACK ROSETTES: (3-ELEMENT OUTSIDE/INSIDE)
1. OSG32B 2. OSG32A 3. OSG32C 4. ISG32C 5. ISG32B 6. ISG32A
REF. TIME 8:46: 3:998 TEST- 2 RUN- 2 GRP 12 SAMPLE RATE- 10 RASTER- 4 0: 0: 4: 0 - 0: 0: 7: 0

	SGA IN(4)	SGB IN(5)	SGC IN(6)	SIGMA-A IN	SIGMA-C IN	SHEAR AC IN
	7.168E 02	7.168E 02	7.168E 02	2.000E 01	2.000E 01	2.000E 01
SCF 1 IN. =	MICRO-IN/IN	MICRO-IN/IN	MICRO-IN/IN	KSI	KSI	KSI
4000. MS						
4500. MS						
5000. MS						
5500. MS						
6000. MS						
6500. MS						
7000. MS						

UPLOT COMPLETED TAPE# 1228
DATE: 042878 TIME: 0755.8

0012U 042878 0755.8 MONTICELLO T-QUENCHER CRNCH02 PRODUCTION VERSION 02-03-78
MONTICELLO DATA REDUCTION - STRUCTURAL

UNIAXIAL (SINGLE GAGE)

1. OSG33A 2. OSG33B
REF. TIME 8:46: 3:998 TEST- 2 RUN- 2 GRP 13 SAMPLE RATE- 10 RASTER- 4 0: 0: 4: 0 - 0: 0: 7: 0

	SG (1)	SIGMA (1)	SG (2)	SIGMA (2)
	7.168E 02	2.000E 01	7.168E 02	2.000E 01
SCF 1 IN. =	MICRO-IN/IN	KSI	MICRO-IN/IN	KSI

4000. MS

4500. MS

5000. MS

5500. MS

6000. MS

6500. MS

7000. MS

VPLOT COMPLETED TAPE# 1228
DATE: 042878 TIME: 0755.8

DD12U 042878 0755.8 MONTICELLO DATA REDUCTION - STRUCTURAL MONTICELLO T-QUENCHER CRNCH02 PRODUCTION VERSION 02-03-78

RECTANGULAR STRAIN GAGE ROSETTE

1. DSG3A 2. DSG3B 3. DSG3C
REF. TIME 0:46: 3:998 TEST- 2 RUN- 2 GRP 14 SAMPLE RATE- 10 RASTER- 4 0: 0: 4: 0 - 0: 0: 7: 0

	GAGE-A (1)	GAGE-B (2)	GAGE-C (3)	SIGMA-A	SIGMA-C	SHEAR A-C
SCF 1 IN. =	7.168E 02 MICRO-IN/IN	7.168E 02 MICRO-IN/IN	7.168E 02 MICRO-IN/IN	2.000E 01 KSI	2.000E 01 KSI	2.000E 01 KSI

4000. MS

4500. MS

5000. MS

5500. MS

6000. MS

6500. MS

7000. MS

VPLOT COMPLETED TAPE# 1228
DATE: 042878 TIME: 0755.8

0012U 042878 0755.8 MONTICELLO T-QUENCHER CRNCH02 PRODUCTION VERSION 02-03-78

MONTICELLO DATA REDUCTION - STRUCTURAL

RECTANGULAR STRAIN GAGE ROSETTE

1. DSG11A 2. DSG11B 3. DSG11C

REF. TIME 8:46: 3:998 TEST- 2 RUN- 2 GRP 15 SAMPLE RATE- 10 RASTER- 4 0: 0: 4: 0 - 0: 3: 7: 0

SCF 1 IN. =	GAGE-A (1)	GAGE-B (2)	GAGE-C (3)	SIGMA-A	SIGMA-C	SHEAR A-C
	7.168E 02	7.168E 02	7.168E 02	2.000E 01	2.000E 01	2.000E 01
	MICRO-IN/IN	MICRO-IN/IN	MICRO-IN/IN	KSI	KSI	KSI

4000. MS

4500. MS

5000. MS

5500. MS

6000. MS

6500. MS

7000. MS

UPLOT COMPLETED TAPE# 1228
DATE: 042878 TIME: 0755.8

DD12U 042878 0755.8 MONTICELLO DATA REDUCTION - STRUCTURAL MONTICELLO T-QUENCHER CRNCH02 PRODUCTION VERSION 02-03-78

RECTANGULAR STRAIN GAGE ROSETTE

1. DSG16A 2. DSG16B 3. DSG16C
REF. TIME 8:46: 3:998 TEST- 2 RUN- 2 GRP 16 SAMPLE RATE- 10 RASTER- 4 0: 0: 4: 0 - 0: 0: 7: 0

SCF 1 IN. =	GAGE-A (1) 7.168E 02 MICRO-IN/IN	GAGE-B (2) 7.168E 02 MICRO-IN/IN	GAGE-C (3) 7.168E 02 MICRO-IN/IN	SIGMA-A 2.000E 01 KSI	SIGMA-C 2.000E 01 KSI	SHEAR A-C 2.000E 01 KSI
4000. MS						
4500. MS						
5000. MS						
5500. MS						
6000. MS						
6500. MS						
7000. MS						

VPLOT COMPLETED TAPE# 1228
DATE: 042878 TIME: 0755.8

D012U 042878 0755.8 MONTICELLO DATA REDUCTION - MONTICELLO T-QUENCHER STRUCTURAL CRMCH02 PRODUCTION VERSION 02-03-78

RECTANGULAR STRAIN GAGE ROSETTE

1. OSG17A 2. OSG17B 3. OSG17C
REF. TIME 8:46: 3:998 TEST- 2 RUN- 2 GRP 17 SAMPLE RATE- 10 RASTER- 4 0: 0: 4: 0 - 0: 0: 7: 0

SCF 1 IN.	GAGE-A (1)	GAGE-B (2)	GAGE-C (3)	SIGMA-A	SIGMA-C	SHEAR A-C
	7.168E 02	7.168E 02	7.168E 02	2.000E 01	2.000E 01	2.000E 01
	MICRO-IN/IN	MICRO-IN/IN	MICRO-IN/IN	KSI	KSI	KSI
4000. MS						
4500. MS						
5000. MS						
5500. MS						
6000. MS						
6500. MS						
7000. MS						

VPLOT COMPLETED TAPE# 1228
DATE: 042878 TIME: 0755.8

DD12U 042878 0755.8 MONTICELLO T-QUENCHER CRNCH02 PRODUCTION VERSION 02-03-78
MONTICELLO DATA REDUCTION - STRUCTURAL

RECTANGULAR STRAIN GAGE ROSETTE

1. OSG18A 2. OSG18B 3. OSG18C
REF. TIME 8:46: 3:998 TEST- 2 RUN- 2 GRP 18 SAMPLE RATE- 10 RASTER- 4 0: 0: 4: 0 - 0: 0: 7: 0

	GAGE-A (1)	GAGE-B (2)	GAGE-C (3)	SIGMA-A	SIGMA-C	SHEAR A-C
	7.168E 02	7.168E 02	7.168E 02	2.000E 01	2.000E 01	2.000E 01
SCF 1 IN. =	MICRO-IN/IN	MICRO-IN/IN	MICRO-IN/IN	KSI	KSI	KSI

4000. MS

4500. MS

5000. MS

5500. MS

6000. MS

6500. MS

7000. MS

UPLOT COMPLETED TAPE# 1228
DATE: 042878 TIME: 0755.8

0012U 042878 0755.8 MONTICELLO T-QUENCHER CRMCH02 PRODUCTION VERSION 02-03-78
MONTICELLO DATA REDUCTION - STRUCTURAL

RECTANGULAR STRAIN GAGE ROSETTE

1. OSG19A 2. OSG19B 3. OSG19C
REF. TIME 8:46: 3:998 TEST- 2 RUN- 2 GRP 19 SAMPLE RATE- 10 RASTER- 4 0: 0: 4: 0 - 0: 0: 7: 0

	GAGE-A (1)	GAGE-B (2)	GAGE-C (3)	SIGMA-A	SIGMA-C	SHEAR A-C
	7.168E 02	7.168E 02	7.168E 02	2.000E 01	2.000E 01	2.000E 01
SCF 1 IN. =	MICRO-IN/IN	MICRO-IN/IN	MICRO-IN/IN	KSI	KSI	KSI

4000. MS

4500. MS

5000. MS

5500. MS

6000. MS

6500. MS

7000. MS

UPLOT COMPLETED TAPE# 1228
DATE: 042878 TIME: 0755.8

MONTICELLO DATA REDUCTION - STRUCTURAL

RECTANGULAR STRAIN GAGE ROSETTE

1. OSG20A 2. OSG20B 3. OSG20C
REF. TIME 8:46: 3:998 TEST- 2 RUN- 2 GRP 20 SAMPLE RATE- 10 RASTER- 4 0: 0: 4: 0 - 0: 0: 7: 0

	GAGE-A (1)	GAGE-B (2)	GAGE-C (3)	SIGMA-A	SIGMA-C	SHEAR A-C
	7.168E 02	7.168E 02	7.168E 02	2.000E 01	2.000E 01	2.000E 01
SCF 1 IN. =	MICRO-IN/IN	MICRO-IN/IN	MICRO-IN/IN	KSI	KSI	KSI

4000. MS

4500. MS

5000. MS

5500. MS

6000. MS

6500. MS

7000. MS

VPLOT COMPLETED TAPE# 1228
DATE: 042878 TIME: 0755.8

D012U 042878 0755.8 MONTICELLO DATA REDUCTION - STRUCTURAL MONTICELLO T-QUENCHER CRNCH02 PRODUCTION VERSION 02-03-78

RECTANGULAR STRAIN GAGE ROSETTE

1. OSG21A 2. OSG21B 3. OSG21C
REF. TIME 8:46: 3:998 TEST- 2 RUN- 2 GRP 21 SAMPLE RATE- 10 RASTER- 4 0: 0: 4: 0 - 0: 0: 7: 0

SCF 1 IN. =	GAGE-A (1)	GAGE-B (2)	GAGE-C (3)	SIGMA-A	SIGMA-C	SHEAR A-C
	7.168E 02	7.168E 02	7.168E 02	2.000E 01	2.000E 01	2.000E 01
	MICRO-IN/IN	MICRO-IN/IN	MICRO-IN/IN	KSI	KSI	KSI

4000. MS

4500. MS

5000. MS

5500. MS

6000. MS

6500. MS

7000. MS

UPLOT COMPLETED TAPE# 1228
DATE: 042878 TIME: 0755.8

DD12U 042878 0755.8 MONTICELLO DATA REDUCTION - STRUCTURAL MONTICELLO T-QUENCHER CRNCH02 PRODUCTION VERSION 02-03-78

RECTANGULAR STRAIN GAGE ROSETTE

1. OSG22A 2. OSG22B 3. OSG22C

REF. TIME 8:46: 3:998 TEST- 2 RUN- 2 GRP 22 SAMPLE RATE- 10 RASTER- 4 0: 0: 4: 0 - 0: 0: 7: 0

	GAGE-A (1)	GAGE-B (2)	GAGE-C (3)	SIGMA-A	SIGMA-C	SHEAR A-C
	7.168E 02	7.168E 02	7.168E 02	2.000E 01	2.000E 01	2.000E 01
SCF 1 IN. =	MICRO-IN/IN	MICRO-IN/IN	MICRO-IN/IN	KSI	KSI	KSI

4000. MS

4500. MS

5000. MS

5500. MS

6000. MS

6500. MS

7000. MS

UPLOT COMPLETED TAPE# 1228
DATE: 042878 TIME: 0755.8

0012U 042878 0755.8 MONTICELLO T-QUENCHER CRNCH02 PRODUCTION VERSION 02-03-78
MONTICELLO DATA REDUCTION - STRUCTURAL

RECTANGULAR STRAIN GAGE ROSETTE

1. FSG24A 2. FSG24B 3. FSG24C
REF. TIME 8:46: 3:998 TEST- 2 RUN- 2 GRP 23 SAMPLE RATE- 10 RASTER- 4 0: 0: 4: 0 - 0: 0: 7: 0

	GAGE-A (1)	GAGE-B (2)	GAGE-C (3)	SIGMA-A	SIGMA-C	SHEAR A-C
	7.168E 02	7.168E 02	7.168E 02	2.000E 01	2.000E 01	2.000E 01
SCF 1 IN. -	MICRO-IN/IN	MICRO-IN/IN	MICRO-IN/IN	KSI	KSI	KSI

4000. MS

4500. MS

5000. MS

5500. MS

6000. MS

6500. M

7000. M

UPLOT COMPLETED TAPE# 1228
DATE: 042878 TIME: 0755.8

OD12U 042878 0755.8 MONTICELLO T-QUENCHER CRNCH02 PRODUCTION VERSION 02-03-78
MONTICELLO DATA REDUCTION - STRUCTURAL

RECTANGULAR STRAIN GAGE ROSETTE

1. FSG25A 2. FSG25B 3. FSG25C
REF. TIME 8:46: 3:998 TEST- 2 RUN- 2 GRP 24 SAMPLE RATE- 10 RASTER- 4 0: 0: 4: 0 - 0: 0: 7: 0

	GAGE-A (1)	GAGE-B (2)	GAGE-C (3)	SIGMA-A	SIGMA-C	SHEAR A-C
	7.168E 02	7.168E 02	7.168E 02	2.000E 01	2.000E 01	2.000E 01
SCF 1 IN. =	MICRO-IN/IN	MICRO-IN/IN	MICRO-IN/IN	KSI	KSI	KSI

4000. MS

4500. MS

5000. MS

5500. MS

6000. MS

6500. MS

7000. MS

UPLOT COMPLETED TAPE# 1228
DATE: 042878 TIME: 0755.8

DD12U 042878 0755.8 MONTICELLO T-QUENCHER CRNCH02 PRODUCTION VERSION 02-03-78

MONTICELLO DATA REDUCTION - STRUCTURAL

RECTANGULAR STRAIN GAGE ROSETTE

1. FSG26A 2. FSG26B 3. FSG26C

REF. TIME 8:46: 3:998 TEST- 2 RUN- 2 GRP 25 SAMPLE RATE- 10 RASTER- 4 0: 0: 4: 0 - 0: 0: 7: 0

SCF 1 IN. =	GAGE-A (1)	GAGE-B (2)	GAGE-C (3)	SIGMA-A	SIGMA-C	SHEAR A-C
	7.168E 02	7.168E 02	7.168E 02	2.000E 01	2.000E 01	2.000E 01
	MICRO-IN/IN	MICRO-IN/IN	MICRO-IN/IN	KSI	KSI	KSI

4000. MS

4500. MS

5000. MS

5500. MS

6000. MS

6500. MS

7000. MS

UPLOT COMPLETED TAPE# 1228
DATE: 042878 TIME: 0755.8

DD12U 042878 0755.8 MONTICELLO T-QUENCHER CRNCH02 PRODUCTION VERSION 02-03-78
MONTICELLO DATA REDUCTION - STRUCTURAL

RECTANGULAR STRAIN GAGE ROSETTE

1. FSG31A 2. FSG31B 3. FSG31C
REF. TIME 8:46: 3:998 TEST- 2 RUN- 2 GRP 26 SAMPLE RATE- 10 RASTER- 4 0: 0: 4: 0 - 0: 0: 7: 0

SCF 1 IN. =	GAGE-A (1)	GAGE-B (2)	GAGE-C (3)	SIGMA-A	SIGMA-C	SHEAR A-C
	7.168E 02	7.168E 02	7.168E 02	2.000E 01	2.000E 01	2.000E 01
	MICRO-IN/IN	MICRO-IN/IN	MICRO-IN/IN	KSI	KSI	KSI

4000. MS

4500. MS

5000. MS

5500. MS

6000. MS

6500. MS

7000. MS

UPLOT COMPLETED TAPE# 1228
DATE: 042878 TIME: 0755.8

OD12U 042878 0755.8 MONTICELLO T-QUENCHER CRNCH02 PRODUCTION VERSION 02-03-78

MONTICELLO DATA REDUCTION - STRUCTURAL

ROSETTE OUTSIDE/UNIAXIAL INSIDE

1. OSG9A 2. OSG9B 3. OSG9C 4. ISG9

REF. TIME 8:46: 3:998 TEST- 2 RUN- 2 GRP 27 SAMPLE RATE- 10 RASTER- 4 0: 0: 4: 0 - 0: 0: 7: 0

SCF 1 IN. =	SGA OUT(1)	SGB OUT(2)	SGC OUT(3)	SG IN(4)	SIGMA-A IN	SIGMA-A BEND
	7.168E 02	7.168E 02	7.168E 02	7.168E 02	2.000E 01	2.000E 01
	MICRO-IN/IN	MICRO-IN/IN	MICRO-IN/IN	MICRO-IN/IN	KSI	KSI

4000. MS

4500. MS

5000. MS

5500. MS

6000. MS

6500. MS

7000. MS

UPLOT COMPLETED TAPE# 1228

DATE: 042878 TIME: 0755.8

0012U 042878 0755.8 MONTICELLO DATA REDUCTION - STRUCTURAL MONTICELLO T-QUENCHER CANCH02 PRODUCTION VERSION 02-03-78

ROSETTE OUTSIDE/UNIAXIAL INSIDE

1. OSG9A 2. OSG9B 3. OSG9C 4. ISG9

REF. TIME 8:46: 3:998 TEST- 2 RUN- 2 GRP 27 SAMPLE RATE- 10 RASTER- 4 0: 0: 4: 0 - 0: 0: 7: 0

	SIGMAMAX-OUT	SIGMAMIN-OUT	SHEARMAX-OUT	SIGMA-A MEM
SCF 1 IN. =	2.000E 01 KSI	2.000E 01 KSI	2.000E 01 KSI	2.000E 01 KSI

4000. MS

4500. MS

5000. MS

5500. MS

6000. MS

6500. MS

7000. MS

UPLOT COMPLETED TAPE# 1228
DATE: 042878 TIME: 0755.8

0012U 042878 0755.8 MONTICELLO T-QUENCHER CRNCH02 PRODUCTION VERSION 02-03-78
MONTICELLO DATA REDUCTION - STRUCTURAL

UNIAXIAL OUTSIDE/INSIDE

1. OSG7 2. ISG7
REF. TIME 8:46: 3:998 TEST- 2 RUN- 2 GRP 28 SAMPLE RATE- 10 RASTER- 4 0: 0: 4: 0 - 0: 0: 7: 0

	SG OUT(1)	SG IN(2)	SIGMA-OUT	SIGMA-IN	SIGMA-MEM	SIGMA-BEND
	7.168E 02	7.168E 02	2.000E 01	2.000E 01	2.000E 01	2.000E 01
SCF 1 IN. =	MICRO-IN/IN	MICRO-IN/IN	KSI	KSI	KSI	KSI

4000. MS

4500. MS

5000. MS

5500. MS

6000. MS

6500. MS

7000. MS

UPLOT COMPLET
DATE: 042878 TIME: 0755.8

DD12U 042878 0755.8 MONTICELLO DATA REDUCTION - STRUCTURAL MONTICELLO T-QUENCHER CRNCH02 PRODUCTION VERSION 02-03-78

UNIAXIAL (SINGLE GAGE)

1. SG34 2. SG34

REF. TIME 8:46: 3:998 TEST- 2 RUN- 2 GRP 29 SAMPLE RATE- 10 RASTER- 4 0: 0: 4: 0 - 0: 0: 7: 0

SCF 1 IN. -	SG (1) 7.168E 02 MICRO-IN/IN	SIGMA (1) 2.000E 01 KSI	SG (2) 7.168E 02 MICRO-IN/IN	SIGMA (2) 2.000E 01 KSI
4000. MS				
4500. MS				
5000. MS				
5500. MS				
6000. MS				
6500. MS				
7000. MS				

UPLOT COMPLETED TAPE# 1228
DATE: 042878 TIME: 0755.8

OO12U 042878 0755.8 MONTICELLO T-QUENCHER CRNCH02 PRODUCTION VERSION 02-03-78
MONTICELLO DATA REDUCTION - STRUCTURAL

UNIAXIAL (SINGLE GAGE)

1. SG131 2. SG132
REF. TIME 8:46: 3:998 TEST- 2 RUN- 2 GRP 30 SAMPLE RATE- 10 RASTER- 4 0: 0: 4: 0 - 0: 0: 7: 0

SCP 1 IN. =	SG (1) 7.168E 02 MICRO-IN/IN	SIGMA (1) 2.000E 01 KSI	SG (2) 7.168E 02 MICRO-IN/IN	SIGMA (2) 2.000E 01 KSI
4000. MS				
4500. MS				
5000. MS				
5500. MS				
6000. MS				
6500. MS				
7000. MS				

UPLOT COMPLETED TAPE# 1228
DATE: 042878 TIME: 0755.8

OO12U 042878 0755.8 MONTICELLO DATA REDUCTION - MONTICELLO T-QUENCHER STRUCTURAL CRNCH02 PRODUCTION VERSION 02-03-78

UNIAXIAL (SINGLE GAGE)

1. SG133 2. SG134
REF. TIME 8:46: 3:998 TEST- 2 RUN- 2 GRP 31 SAMPLE RATE- 10 RASTER- 4 0: 0: 4: 0 - 0: 0: 7: 0

	SG (1)	SIGMA (1)	SG (2)	SIGMA (2)
SCF 1 IN. =	7.168E 02 MICRO-IN/IN	2.000E 01 KSI	7.168E 02 MICRO-IN/IN	2.000E 01 KSI

4000. MS

4500. MS

5000. MS

5500. MS

6000. MS

6500. MS

7000. MS

UPLOT COMPLETED TAPE# 1228
DATE: 042878 TIME: 0755.8

D012U   042878   0755.8 MONTICELLO DATA REDUCTION - MONTICELLO T-QUENCHER STRUCTURAL   CRNCH02 PRODUCTION VERSION 02-03-78

UNIAXIAL (SINGLE GAGE)

1. SG135 2. SG135
REF. TIME 8:46: 3:998 TEST- 2 RUN- 2 GRP 32 SAMPLE RATE- 10 RASTER- 4 0: 0: 4: 0 - 0: 0: 7: 0

SCF 1 IN. =	SG (1) 7.168E 02 MICRO-IN/IN	SIGMA (1) 2.000E 01 KSI	SG (2) 7.168E 02 MICRO-IN/IN	SIGMA (2) 2.000E 01 KSI

4000. MS

4500. MS

5000. MS

5500. MS

6000. MS

6500. MS

7000. MS

UPLOT COMPLETED TAPE# 1228
DATE: 042878 TIME: 0755.8

0012U 042878 0755.8 MONTICELLO T-QUENCHER CRNCH02 PRODUCTION VERSION 02-03-78
MONTICELLO DATA REDUCTION - STRUCTURAL

COLUMN AXIAL AND MOMENTS

1. AB-01 2. BB1-01 3. BB2-01
REF. TIME 8:46: 3:998 TEST- 2 RUN- 2 GRP 33 SAMPLE RATE- 10 RASTER- 4 0: 0: 4: 0 - 0: 0: 7: 0

	SG AXIAL (1)	SG BEND1 (2)	SG BEND2 (3)	AXIAL LOAD	M-RADIAL	M-CIRCUMFR
	7.168E 02	7.168E 02	7.168E 02	1.000E 02	2.000E 02	2.000E 02
SCF 1 IN. =	MICRO-IN/IN	MICRO-IN/IN	MICRO-IN/IN	KIPS	IN-KIPS	IN-KIPS

4000. MS

4500. MS

5000. MS

5500. MS

6000. MS

6500. MS

7000. MS

UPLOT COMPLETED TAPE# 1228
DATE: 042878 TIME: 0755.8

D012U 042878 0755.8 MONTICELLO T-QUENCHER CRNCH02 PRODUCTION VERSION 02-03-78
MONTICELLO DATA REDUCTION - STRUCTURAL

COLUMN AXIAL AND MOMENTS

1. AB-02 2. BB1-02 3. BB2-02
REF. TIME 8:46: 3:998 TEST- 2 RUN- 2 GRP 34 SAMPLE RATE- 10 RASTER- 4 0: 0: 4: 0 - 0: 0: 7: 0

	SG AXIAL (1)	SG BEND1 (2)	SG BEND2 (3)	AXIAL LOAD	M-RADIAL	M-CIRCUMFR
	7.168E 02	7.168E 02	7.168E 02	1.000E 02	2.000E 02	2.000E 02
SCP 1 IN. =	MICRO-IN/IN	MICRO-IN/IN	MICRO-IN/IN	KIPS	IN-KIPS	IN-KIPS

4000. MS

4500. MS

5000. MS

5500. MS

6000. MS

6500. MS

7000. MS

UPLOT COMPLETED TAPE# 1228
DATE: 042878 TIME: 0755.8

DO12U 042878 0755.8 MONTICELLO T-QUENCHER CRNCH02 PRODUCTION VERSION 02-03-78
MONTICELLO DATA REDUCTION - STRUCTURAL

COLUMN AXIAL AND MOMENTS

1. AB-D3 2. BB1-D3 3. BB2-D3
REF. TIME 8:46: 3:998 TEST- 2 RUN- 2 GRP 35 SAMPLE RATE- 10 RASTER- 4 0: 0: 4: 0 - 0: 0: 7: 0

SCF 1 IN. =	SG AXIAL (1)	SG BEND1 (2)	SG BEND2 (3)	AXIAL LOAD	M-RADIAL	M-CIRCUMFR
	7.168E 02	7.168E 02	7.168E 02	1.000E 02	2.000E 02	2.000E 02
	MICRO-IN/IN	MICRO-IN/IN	MICRO-IN/IN	KIPS	IN-KIPS	IN-KIPS
4000. MS						
4500. MS						
5000. MS						
5500. MS						
6000. MS						
6500. MS						
7000. MS						

UPLOT COMPLETED TAPE# 1228
DATE: 042878 TIME: 0755.8

DD12U 042878 0755.8 MONTICELLO DATA REDUCTION - MONTICELLO T-QUENCHER - STRUCTURAL CRNCH02 PRODUCTION VERSION 02-03-78

COLUMN AXIAL AND MOMENTS

1. AB-04 2. BB1-04 3. BB2-04
REF. TIME 8:46: 3:998 TEST- 2 RUN- 2 GRP 36 SAMPLE RATE- 10 RASTER- 4 0: 0: 4: 0 - 0: 0: 7: 0

	SG AXIAL (1)	SG BEND1 (2)	SG BEND2 (3)	AXIAL LOAD	M-RADIAL	M-CIRCUMFR
	7.168E 02	7.168E 02	7.168E 02	1.000E 02	2.000E 02	2.000E 02
SCF 1 IN. =	MICRO-IN/IN	MICRO-IN/IN	MICRO-IN/IN	KIPS	IN-KIPS	IN-KIPS

4000. MS

4500. MS

5000. MS

5500. MS

6000. MS

6500. MS

7000. MS

UPLOT COMPLETED TAPE# 1228
DATE: 042878 TIME: 0755.8

D012U 042878 0755.8 MONTICELLO DATA REDUCTION - STRUCTURAL MONTICELLO T-QUENCHER CRNCH02 PRODUCTION VERSION 02-03-78

UNIAXIAL (SINGLE GAGE)

1. ISG15A 2. ISG15C

REF. TIME 8:46: 3:998 TEST- 2 RUN- 2 GRP 39 SAMPLE RATE- 10 RASTER- 4 0: 0: 4: 0 - 0: 0: 7: 0

	SG (1)	SIGMA (1)	SG (2)	SIGMA (2)
SCF 1 IN. =	7.168E 02 MICRO-IN/IN	2.000E 01 KSI	7.168E 02 MICRO-IN/IN	2.000E 01 KSI

4000. MS

4500. MS

5000. MS

5500. MS

6000. MS

6500. MS

7000. MS

UPLOT COMPLETED TAPE# 1228
DATE: 042878 TIME: 0755.8

OD12U 042878 0755.8 MONTICELLO T-QUENCHER CANCH02 PRODUCTION VERSION 02-03-78

MONTICELLO DATA REDUCTION - STRUCTURAL

RECTANGULAR STRAIN GAGE ROSETTE

1. ISG33A 2. ISG33B 3. ISG33C

REF. TIME 8:46: 3:998 TEST- 2 RUN- 2 GAP 40 SAMPLE RATE- 10 RASTER- 4 0: 0: 4: 0 - 0: 0: 7: 0

	GAGE-A (1)	GAGE-B (2)	GAGE-C (3)	SIGMA-A	SIGMA-C	SHEAR A-C
	7.168E 02	7.168E 02	7.168E 02	2.000E 01	2.000E 01	2.000E 01
SCF 1 IN. =	MICRO-IN/IN	MICRO-IN/IN	MICRO-IN/IN	KSI	KSI	KSI

4000. MS

4500. MS

5000. MS

5500. MS

6000. MS

6500. MS

7000. MS

UPLOT COMPLETED TAPE# 1228
DATE: 042878 TIME: 0755.8

APPENDIX H

MAXIMUM STRESSES - T-QUENCHER AND SRV PIPING

Table H-1

SUMMARY OF SRV STRESS DATA*

Test	Cond**	Sensors 39	40	41	42	43	44	45	46	47A	47B	47C	48A	48B	48C	49A	49B	49C	51A	51B	51C
2	1	4200	1400	5600	4480	2520	2520	2380	2800	2800	1120	840	2380	980	1120	2800	1400	700	2520	1540	1120
501	1	4760	1960	5320	4760	4200	3640	3640	3920	3080	1400	1680	3080	1400	1120	4200	2240	700	2520	1960	1680
801	1	4760	1960	5320	4760	3640	3920	2520	3360	3360	1120	980	2800	1120	1120	2800	1680	560	3360	1960	1680
901	1	5600	1820	3640	3640	2800	1400	1680	1960	1680	1120	980	1960	1120	560	2800	1680	560	1960	1400	840
1301	1	4480	1960	4200	4200	3080	2520	2240	2240	2800	420	420	2800	1120	560	3080	1680	420	2520	1400	700
1601	1	4200	1820	3360	3220	2800	1540	1820	1820	1680	700	840	1400	1120	840	3360	1680	560	1680	1120	840
24	1	4620	1820	3080	3640	2520	2520	2240	2800	3220	1120	1120	2240	1680	980	2800	1960	560	2800	1680	0
802	2	4760	1400	4200	3080	3360	1680	3080	2800	2240	980	840	2520	840	700	2800	1400	560	2520	1400	700
902	2	4200	1400	4200	4760	3080	1680	2800	2800	1960	840	560	2100	1400	840	3080	1400	840	2800	1400	980
903	2	4340	1680	4760	3640	4480	3500	3220	3080	1960	840	700	2240	700	560	2240	1120	700	2240	1120	1120
904	2	4340	1960	5320	4480	3920	2240	3640	2800	1680	560	560	2520	1120	1120	2800	1400	420	2800	1680	1120
905	2	4340	1680	5320	3920	3640	1960	1680	2520	1680	840	840	2240	1120	560	2520	1400	840	2520	1120	1120
2305	3	4200	1960	5320	3640	560	2520	2800	3500	2240	1120	1120	1680	1680	1960	2240	1680	1120	1680	1120	840
2306	3	5040	1960	4760	4480	6160	3360	0	3080	1680	840	840	1680	840	1120	2800	1400	980	2240	1120	840
1303	4	4200	1540	4620	3920	4200	1820	0	3080	1960	1400	1120	2800	1120	840	3920	1960	560	3640	2240	1680
1602	4	4480	1400	3920	3360	3220	1680	0	2240	1400	560	700	1960	840	700	2240	1120	560	2520	840	560
1603	4	4340	1680	4480	3920	3920	1680	0	3080	2520	840	700	1680	1120	700	3640	1400	1120	2240	1680	840
1604	4	4480	1540	4760	3640	4200	1820	0	2800	1960	1820	840	2380	1400	840	3360	1680	840	2800	1680	1400
1605	4	4480	1400	4060	3080	3360	1680	0	2240	1960	1540	840	1960	1120	840	2800	1400	840	2520	1960	1120
2301	5	4200	1680	3640	3640	2240	2520	1400	1960	2800	840	1120	2800	840	840	2520	1400	560	1680	840	0
2302	5	3920	1960	3780	3080	2520	1540	2240	1960	1960	700	1120	2520	840	560	1960	1680	560	2380	980	0
2303	5	5180	1680	3640	3360	2520	1540	1400	1960	2240	840	700	2380	1120	840	3080	1540	560	1960	1120	0
2304	5	4480	1680	4760	4480	3220	1960	2520	2800	3360	1400	840	2800	840	840	3080	2240	560	1960	1260	1120
14	6	1120	420	840	840	840	280	840	560	980	280	280	1120	560	140	560	560	140	560	140	420
18	6	1400	280	840	700	1120	700	0	560	1120	560	140	840	420	280	420	280	140	560	420	140
21	6	1120	140	420	560	840	560	280	560	560	280	140	420	280	140	280	280	0	280	0	0
1101	6	1400	280	840	560	980	420	560	420	840	280	280	840	420	280	420	280	280	840	280	140
1102	7	1820	140	560	560	700	700	420	560	700	280	280	840	280	140	280	140	140	560	140	140
1103	7	1820	140	280	280	700	700	280	280	420	140	140	560	280	280	420	140	140	560	140	140
1104	7	1260	140	420	560	840	560	280	280	560	140	140	140	280	140	280	140	140	280	140	280
1105	7	1120	140	280	420	840	420	280	420	280	140	280	280	140	140	280	140	140	280	140	140
15	8	560	280	700	560	840	560	560	700	840	560	560	840	560	560	560	560	140	560	280	0
19	8	140	140	280	420	700	280	420	560	700	280	280	840	420	280	140	140	140	420	140	140
22	8	280	280	700	560	1120	420	420	700	1120	560	420	1120	420	280	420	280	140	560	280	0
1201	8	280	280	560	560	840	560	420	560	840	560	280	700	280	140	140	140	140	560	280	140

*1) Tabulated stresses (in psi) are from strain gages.

**2) Test conditions:

1 = SVA, CP, NWL
2 = CVA, HP, NWL
3 = CVA, HP, EWL
4 = CVA, HP, DWL
5 = MVA, CP, NWL
6 = Bay C, CP
7 = Bay C, HP
8 = Bay E, CP

Table H-2

SUMMARY OF SRV STRESS DATA*

Test	Cond**	52A	52B	52C	53A	53B	53C	54	55A	55B	55C	56A	56B	56C	60	61A	61B	61C	62A	62B	62C	A9H
		Sensors																				
2	1	2520	1960	840	1120	1120	1120	3640	2240	3360	3080	3080	2240	2240	5040	1960	1820	560	3360	1680	1120	10.8
501	1	2520	1960	1120	1680	1120	1960	3920	3920	4480	4200	2800	2520	2800	5320	2660	1820	700	2300	1400	840	26.6
801	1	2240	1680	1680	1960	1400	1400	3220	2240	4200	2520	2800	3080	2240	5600	1960	1400	560	1960	980	700	14.2
901	1	2240	1680	840	1120	700	1400	3360	1820	3640	3360	3360	1680	2240	4480	1680	840	560	1680	700	560	10.1
1301	1	2800	2240	1120	1680	1120	1120	3920	1960	3080	3080	2520	2100	2240	4760	2800	980	840	2800	1120	840	19.0
1601	1	2100	1400	840	1260	840	1120	2800	1120	2800	2240	2800	1400	1680	4200	2520	1260	700	2520	1120	840	12.0
24	1	2520	1120	1680	2520	1400	1120	2800	2240	2800	2240	1680	2240	1960	4200	3360	1960	560	3080	1680	1120	8.2
802	2	1960	1120	1960	1120	1120	980	2660	1960	3360	2520	2800	1400	2520	5320	1540	840	420	1680	700	700	11.2
902	2	2240	1540	1680	1680	1120	840	3360	1400	3920	3360	2240	1680	2520	5040	2100	840	420	2240	840	700	11.5
903	2	1960	1400	1540	1540	1120	840	3080	1400	3360	3080	2240	1680	1960	5600	2660	1400	420	1960	1120	1120	23.7
904	2	3080	1680	1680	2240	1400	1120	3360	1400	3080	2800	2240	1400	3080	5320	1820	840	560	1680	840	560	13.0
905	2	2240	1400	1960	1400	1120	1680	2520	1960	2300	3080	2520	1960	1960	4760	1960	1120	700	1820	840	840	11.6
2305	3	2520	1120	1960	1400	840	1120	3220	1960	2240	1680	2240	1120	1960	4760	2800	1400	700	2800	1400	840	39.2
2306	3	1400	1680	1400	2240	1120	1120	2800	1680	3080	2800	1960	1960	1120	4760	5600	1960	1400	4200	1680	1260	99.0
1303	4	3080	1660	1400	2520	1540	840	3360	1680	4200	3640	2800	1960	3640	4340	1960	840	560	2240	560	840	14.5
1602	4	1960	840	1680	1960	1260	980	1680	1400	3080	2240	1540	1120	1960	4480	1260	840	700	1260	840	560	10.4
1603	4	2520	1400	2240	1960	1400	1120	2660	1680	2800	2800	2520	1960	2800	5320	1540	700	420	1400	560	700	38.
1604	4	2520	1680	1960	840	840	840	2800	1960	3500	3080	2800	1680	2800	5040	1680	1120	560	1680	840	840	17.7
1605	4	1680	1680	1960	1680	1120	840	2520	1680	3080	2520	1680	1960	1960	4760	2240	1120	560	1960	840	840	10.6
2301	5	2520	980	1400	1960	1120	840	2800	1960	3080	2520	2520	2800	2520	4760	3220	1820	420	2940	1400	1400	8.9
2302	5	1960	1400	1960	1400	840	980	3360	1400	2800	2520	2240	2240	1960	4200	2800	1400	560	2520	1260	840	28.0
2303	5	2800	1120	1120	1400	840	1260	2800	1960	2800	2800	2520	1260	1960	4200	1960	1120	560	1960	980	980	7.6
2304	5	3360	1820	1400	1960	1400	1120	3360	2520	3080	2520	3080	2520	2940	5460	3080	1540	700	3080	1400	1260	28.8
14	6	280	140	140	560	280	280	280	560	840	840	420	560	280	560	840	420	140	700	280	280	7.0
18	6	280	140	140	560	280	280	420	560	560	560	280	560	420	560	560	420	140	560	280	280	6.6
21	6	140	0	0	280	140	0	280	140	280	280	280	280	140	560	700	280	140	420	140	280	5.3
1101	6	140	140	140	420	140	140	280	280	840	560	280	560	280	700	560	420	140	560	280	140	5.6
1102	7	140	140	140	420	140	140	280	420	700	700	280	560	280	560	840	560	140	420	280	140	5.4
1103	7	280	140	140	280	140	140	280	280	140	140	280	140	140	700	560	140	140	560	140	140	4.7
1104	7	280	140	0	280	140	0	560	560	560	420	280	280	140	700	560	140	140	560	280	0	4.9
1105	7	140	140	0	280	140	140	280	280	280	140	280	140	140	560	560	280	0	560	140	140	4.8
15	8	280	420	280	560	420	280	560	560	840	560	280	420	560	560	840	420	420	840	420	420	5.5
19	8	140	140	140	280	140	140	840	420	560	420	140	280	280	280	1120	280	280	700	140	140	5.0
22	8	280	280	140	280	280	280	840	840	840	560	280	280	560	420	1400	420	140	980	280	420	4.7
1201	8	280	280	140	420	140	140	560	560	700	0	280	280	280	420	840	280	280	840	280	280	5.3

*1) Tabulated stresses (in psi) are from strain gages except A9H which measured the acceleration (in g) of the quencher support.

**2) Test conditions:

1 = SVA, CP, NWL	5 = MVA, CP, NWL
2 = CVA, HP, NWL	6 = Bay C, CP
3 = CVA, HP, EWL	7 = Bay C, HP
4 = CVA, HP, DWL	8 = Bay E, CP

Table H-3

SUMMARY OF SRV STRESS DATA (PRINCIPAL STRESSES)*

Test	Cond**	Sensors 47	48	49	51	52	53	55	56	61	62
2	1	-2100	-2100	2700	-2700	-2700	-1800	3000	-2400	3600	-3300
501	1	-3300	2400	2400	-3000	-2400	-2100	4800	-2100	3000	-2700
801	1	2100	-2700	3000	-3000	-2700	1800	3600	-3000	-2400	2400
901	1	2100	2100	2400	-2100	-3000	1800	2400	-1800	-2100	-1950
1301	1	-3300	2400	2700	2700	-3000	2100	3600	2400	3000	-2700
1601	1	-1500	2100	2700	1500	-3000	1800	2700	1500	-2700	2550
24	1	-1800	2100	2400	2400	1800	2400	2400	2400	3600	3300
802	2	-1800	2850	-2400	-2250	-2400	-1800	-3300	1800	-2100	-1800
902	2	1500	1800	2400	3000	2700	2700	-3300	2250	-2400	-2100
903	2	-2100	2400	2100	2100	-2100	1800	3300	2400	-2850	-2550
904	2	-1200	1500	2100	2400	-2400	2400	-3300	2700	-2250	2400
905	2	-1800	2700	2100	2100	2100	1200	-3600	2100	-2100	-2100
2305	3	1050	1200	1800	1500	-2400	2400	2100	-1500	3000	-2700
2306	3	2400	1050	-2100	2100	-2700	2400	2400	2400	-4800	-4200
1303	4	-1200	2550	3900	3000	2700	3000	3900	2400	-2100	1800
1602	4	-1800	2100	-2400	2100	-2100	1650	-2400	-2100	1500	1200
1603	4	1350	1650	-2100	2100	-2250	1800	2400	2100	-2400	-1650
1604	4	-1200	1800	-2550	-2550	2100	1800	-3000	-1500	-1800	1800
1605	4	-1500	1650	2400	1950	-1500	1500	-2700	-1800	-2400	-2400
2301	5	-2700	2700	2700	2700	-2400	1800	-3900	3000	-3600	-3000
2302	5	-2100	2400	2400	2100	-2400	1200	-2400	2100	-3000	-2700
2303	5	2400	2100	4500	2250	-2400	1800	3000	1500	-2400	-2100
2304	5	-2700	2400	3000	2400	-2400	1800	2700	-2100	-3300	3000
14	6	-1200	1350	900	900	450	900	1050	-600	-1050	900
18	6	-1500	1200	600	750	-600	900	1050	-900	-1200	-900
21	6	-600	600	450	450	-300	-600	-600	-450	-3600	-600
1101	6	-1050	1050	600	900	-300	-600	900	-750	-750	-750
1102	7	900	900	450	750	300	750	-900	-750	-900	750
1103	7	-600	-750	450	-750	-600	-450	450	0	0	0
1104	7	-600	-600	600	-600	-450	600	900	-600	-600	-600
1105	7	-600	750	-450	600	-450	-450	-600	-600	-750	-600
15	8	1200	1200	600	900	-900	900	1200	750	1650	1350
19	8	-600	900	450	-1200	-600	-600	-900	-450	1500	900
22	8	-1200	1350	600	-750	750	600	1050	750	-1500	1200
1201	8	-900	-900	600	-750	300	600	900	-600	-1200	900

*1) Tabulated stresses (in psi) are from strain gages.

**2) Test conditions:

1 = SVA, CP, NWL
2 = CVA, HP, NWL
3 = CVA, HP, EWL
4 = CVA, HP, DWL
5 = MVA, CP, NWL
6 = Bay C, CP
7 = Bay C, HP
8 = Bay E, CP

APPENDIX I

METHODS USED TO EVALUATE TEST INITIAL CONDITIONS

This appendix describes the basis for test initial conditions presented in Tables 3-2 and 3-3. These initial conditions are provided to aid in the verification of the SRV discharge analytical models.

1.0 Basis For Initial Conditions Presented in Table 3-2

Table 3-2 presents a summary of test initial conditions just before prepressurization.(1) The values reported in this table correspond in time to the arrival of the initial pressure wave (due to SRV steam bleed) at the air/water interface.

1.1 Average Pipe Temperature

Values for the average pipe temperature were calculated based on the pipe length weighted average of the pipe wall axial temperatures. The pipe wall temperatures were measured by T11 through T15. Figure I-1 provides the locations of these temperature sensors along the pipe.

1.2 Air Mass

Values for the air mass inside the pipe were obtained in one of two ways:

1.2.1 Use of measured data

1.2.2 Use of the ideal gas law equation (PV = m RT) and Dalton's partial pressure law ($P_{total} = P_{air} + P_{steam}$).

For the first method, the air mass was obtained from the flowrate of air through the vacuum breaker (VB). This flowrate was obtained by evaluation of data recorded by an annubar device which was installed on the drywell side of the SRVDL vacuum breaker. A typical plot of the VB flowrate vs. time is presented in Figure I-2. The area under the curve of this figure represents the air mass that entered the pipe in pounds mass. The first method is

(1) See section 8.3 for a discussion of the discharge line prepressurization phenomena.

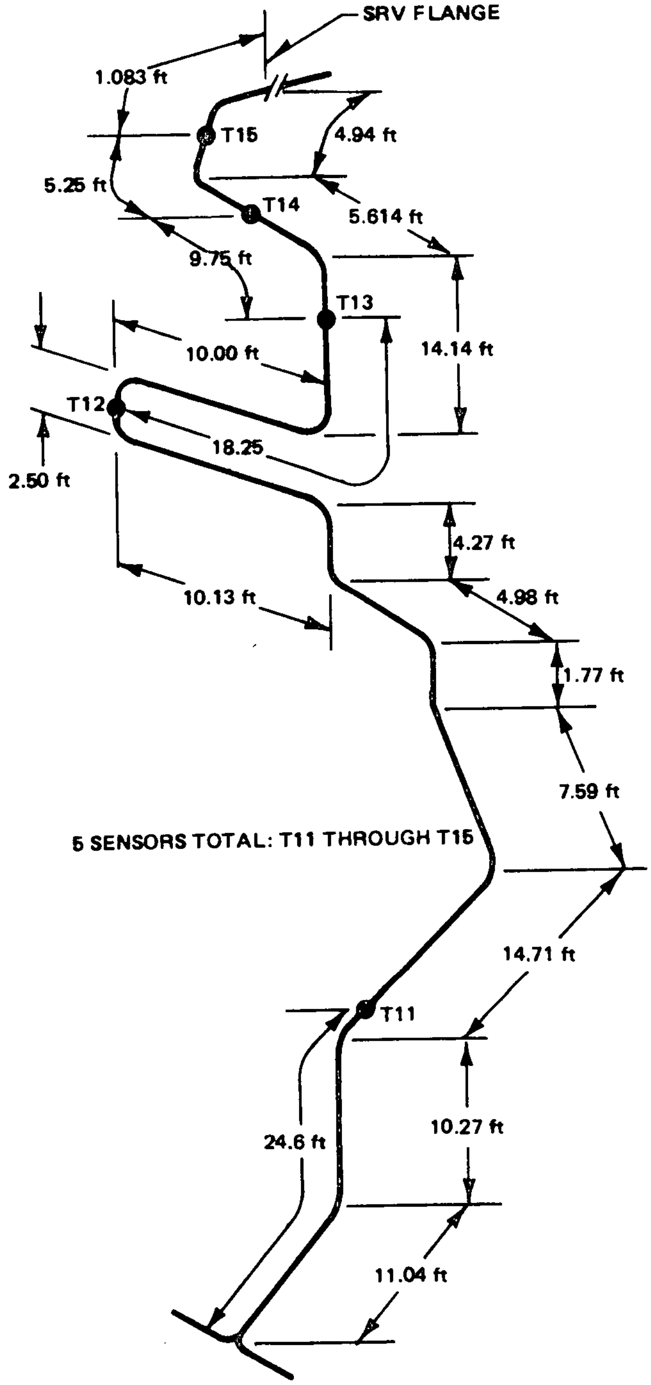

Figure I-1. Temperature Sensor Locations - Strap-On SRV Pipe for Skin Temperature Measurement

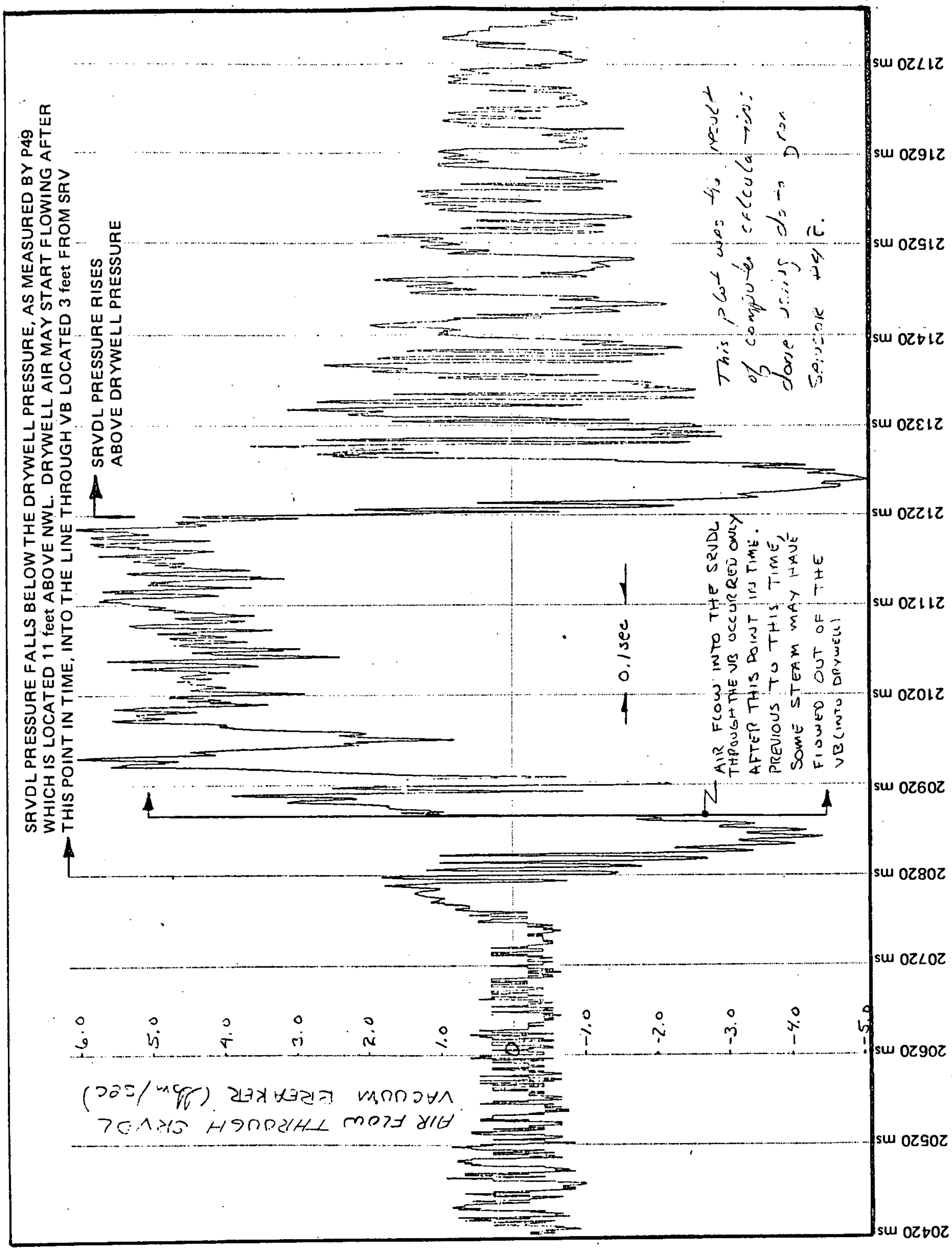

Figure I-2. Air Flow Through SRVDL Vacuum Breaker applicable to all tests in which the bleed valve between the discharge line and the drywell was not opened following the previous test. Tests for which this method is applicable are 1302, 1303, 1602-1605, and 2305-2307. Note that the air mass values for each of these tests were obtained by measuring the amount of air that entered through the VB at the end of the test that preceded the test in question. For example, air that entered at the end of test 1301 was used as the initial air mass in the pipe for test 1302, and so on.

The second method is applicable to all cold pipe tests when the bleed valve was opened following the previous test. Since sufficient time was allowed (2 - 2-1/2 hours) for pipe cooling between tests, gas in the discharge line for all cold pipe tests was assumed to be air at 100% relative humidity (at the measured temperature of the pipe). The gas would attain this conditions as the pipe cooled, since the pressure inside the line would drop (due to condensation of steam on the cooling pipe wall) allowing additional air to enter to the line both through the SRV discharge line VB and the SRVDL bleed valve when it was open.

The second method is applicable to tests 2, 501, 801, 901, 1101, 12, 1301, 14, 15, 1601, 18, 19, 21, 22, 2301-2304, and 24.

1.3 Steam Partial Pressure

Values for the steam partial pressure were obtained in one of two ways:

1.3.1 For CP, NWL tests, the steam partial pressure was set equal to the steam saturation pressure evaluated from the Steam Tables at the Average Pipe Temperature and assuming 100% relative humidity.

1.3.2 For HP, DWL, and HP, EWL tests, the steam partial pressure was obtained using the ideal gas law equation to get the air pressure (since mass of air, temperature of air (assumed same as pipe), and the volume of air were known) and then using Dalton's partial pressure law (since the total pipe pressure was measured).

1.3.3 Before HP, NWL tests, the bleed valve was opened. Therefore, the air mass could not be accurately determined using the VB flow data. An extensive analytical evaluation would be required before an accurate estimate of the air and steam masses could be made for these tests. No values are provided at this time.

1.4 Water Leg Length

Values for the water leg length were obtained from test data based on readings at sensor P49, which measured the pressure difference between the SRVDL and the drywell. This pressure difference was then converted to a static head and was either added or subtracted from the normal water leg, depending on the value of the pressure difference (i.e., whether ΔP was negative or positive, respectively).

1.5 Pool Temperature at T-Quencher Elevation

Values for the pool temperature at T-Quencher elevation were obtained in the bay of discharge from measurements made by the temperature sensor closest to the T-Quencher. For Bay D (valve A), Bay C (valve E) and Bay E (valve G) the data read from temperature sensor T25, T49 and T40 were used, respectively. Note that for the HP, DWL (tests 1303, 1602 - 1605), the pool temperature for test 1303 was assumed to be the same as that for test 1301, and the pool temperatures for 1602 - 1605 were assumed to be the same as that for test 1601 because the hot water near the T-Quencher (due to the SRV discharge) will rise quickly to the pool surface causing the pool temperature at the T-Quencher to drop back close to the original value before SRV discharge. The local bay bulk pool temperature rise during 18 seconds of SRV discharge did not exceed 1°F. (The increase in pool temperature at T-Quencher elevation is expected to be bounded by 1°F.) For HP, EWL, the pool temperature at the T-Quencher elevation was evaluated by determining the temperature increase during the SRV discharge of the previous test. Note that the time between SRV on and off for EWL and previous test was approximately 1 sec.

1.6 Drywell Pressure

Values for the drywell pressure were obtained from plant instrumentation.

1.7 Drywell/Wetwell Pressure Difference

Values for the drywell/wetwell pressure difference were obtained from plant instrumentation.

1.8 Total Pipe Pressure

Values for the total pipe pressure were obtained from measured test data by addition of the drywell pressure to the pressure difference recorded at the pressure transducer P49 (P49 measures the pressure difference between the SRVDL and drywell).

1.9 Estimated Water Leg Velocity

Values for the estimated water leg velocity were zero except for the HP, EWL tests (i.e., tests 1302, and 2305 - 2307). For these tests, the time it took the water slug to travel from water leg sensor W3 to W4 was determined. Knowing the distance between W3 and W4, the average velocity was calculated and reported in Table 3-2 as the estimated water leg velocity.

2.0 Basis For Initial Conditions Presented in Table 3-3

Table 3-3 presents test initial conditions just before the arrival of the primary pressure wave (due to the SRV main disk motion) at the air/water interface. Except for the steam partial pressure, the parameters not shown in Table 3-3 are assumed to be the same as those reported in Table 3-2.

The parameters presented in Table 3-3 were obtained from measured test data in combination with the analytical model for SRVDL clearing transient.*

*This model is documented in the General Electric Company report NEDE-23739.

2.1 Estimated Water Leg Velocity/Length

The water leg velocity/length were estimated as follows. The tests were categorized into two groups:

2.1.1 Hot Pipe, Elevated Water Level Tests (i.e., 1302, 2305-2307).

2.1.2 All Other Tests

For the first group, the values for the water leg velocity presented in Table 3-3 were the same as those presented in Table 3-2. The values for the water leg length were estimated by the following method:

From test data recorded by the water leg probes (i.e., W1, W3, W4 and W5), an approximate location of the water leg was estimated by knowing the last probe that sensed the water, the time difference between the arrival of the water leg at the last water leg probe contacted (during the water rise transient) and the arrival of the primary pressure wave at the air/water interface was determined from water leg probe and P3 data. The additional rise above the last water leg probe contacted was calculated from the product of this time difference and the estimated water leg velocity.

For the second group, a typical pressure transient recorded by sensor P3 (near the air/water interface), was chosen for each of the following test conditions:

1) Cold pipe, normal water leg
2) Hot pipe, depressed water leg
3) Hot pipe, normal water leg

These measured pressure transients were then used as input to the analytical model for the SRVDL clearing transient, to determine the displacement and velocity of the water slug during the period of prepressurization for each of these test conditions.

2.3 Total Pipe Pressure

Values for the total pipe pressure were obtained from the measured test data (sensor P49) at the time the primary pressure wave arrived at the air/water interface. This pressure differential (P49) is then added to the drywell pressure.

APPENDIX J

METHOD USED TO EVALUATE THE SRV FLOWRATE

Three methods were used to calculate S/RV flow ($\dot{M}$). The methods and results are summarized below

Method I: Change in pool temperature for extended discharge test with RHR.

Results: $\dot{M}$ = 200 lbm/sec $^{+27\ \text{lbm/sec}}_{-11\ \text{lbm/sec}}$

Method II: Mass flow balance on feedmat flow, steam flow and S/RV flow (based on plant data taken during the test).

Result: $\dot{M}$ = 219 lbm/sec (error of approximately ± 10%)

Method III: Monticello Start-up Test Data

Result: $\dot{M}$ = 226 lbm/sec (error of approximately ± 5%)

Methods Used to Determine SRV Flowrate

Method I - Bulk Pool Temperature Increase

Temperature sensors in the torus pool permit a reasonably accurate calculation of bulk pool temperature before and after the SRV discharges. With these data, a knowledge of the enthalpy of the steam passing into the pool, and initial pool water mass, the steam flow rate can be calculated by applying mass and energy conservation.

$$M_f e_f = M_o e_o + h_g \Delta M \quad (1)$$

$$M_f = M_o + \Delta M \quad (2)$$

Then (1) becomes

$$(M_o + \Delta M)e_f = M_o e_o + h_g \Delta M$$

then

$$\Delta M(e_f - h_g) = M_o(e_o - e_f)$$

$$\Delta M = M_o \left(\frac{e_f - e_o}{h_g - e_f} \right) \qquad (3)$$

$$\dot{M} = \frac{\Delta M}{\Delta t} = \frac{M_o}{\Delta t} \left(\frac{e_f - e_o}{h_g - e_f} \right) \qquad (4)$$

Final bulk pool temperature is known with greatest accuracy for the extended discharge test with RHR, since within 30 minutes following SRV closure the operation of the RHR system (recirculation mode only, no cooling) resulted in a nearly uniform pool temperature distribution. Using equation (4) on this test, the following values are appropriate:

M_f = final mass of water in pool (lbm)

M_o = initial mass of water in pool (lbm) = 4.3×10^6 lbm

ΔM = mass of water added to pool (lbm)

e_f = final fluid internal energy (Btu/lbm) = 42.7 Btu/lbm at pool temp = 74.7°F

e_o = initial fluid internal energy (Btu/lbm) = 17.5 Btu/lbm at pool temp = 49.5°F

h_g = enthalpy of steam of 1000 psia (Btu/lbm) = 1193 Btu/lbm

Δt = time that SRV was discharging (sec) = 475 sec (6 min 55 sec)

$$\dot{M} = \frac{4.3 \times 10^6}{475} \left[\frac{42.7 - 17.5}{1193 - 42.7}\right] \text{lbm/sec}$$

$$\dot{M} = 200 \text{ lbm/sec} + 27, -11 \text{ lbm/sec}$$

The calculation of the final bulk pool temperature was based on a weighted average of the pool temperature sensor measurements. The upper half of the pool was relatively well instrumented and a good estimate for average temperature of this region was possible. The lower half of the pool was instrumented only in Bay D. Pool temperature data indicated that the upper region of the pool had reached a near uniform temperature (following several minutes of RHR operation). The data recorded in the lower regime of the test bay indicated that there was a linear decrease in temperature from the middle of the bottom of the pool. The calculation of bulk pool temperature was based on the assumption that this linear decrease in pool temperature observed in the test bay (Bay D) existed throughout the pool. This assumption is considered the major source of error in the calculation. Estimates of this error were made by assuming first that there was no decrease in temperature from the middle to the bottom of the pool and then by assuming that the lower portion of the pool was at the temperature recorded on the pool bottom. The range of possible SRV flows determined using this procedure was 189 to 227 lbm/sec.

Method II - Mass/Flow balance involving steam flowing to the turbine (STF), steam flowing through the safety/relief valve (SRVF), and feedwater flow (FWF) to the RPV

At the time of the extended discharge test, plant instrumentation recorded steam flow (STF) and feedwater flow (FWF). A mass balance can be written.

(Inputs to RPV) = (Outputs) + (Storage)

If measurements are taken when water level change and transients in FWF and STF had stabilized the storage term is removed.

$$\therefore \quad FWF = STF + SRVF$$

Likewise:

$$\Delta FWF = \Delta STF + \Delta SRVF$$

where

$\Delta \equiv$ (Flow before SRV is opened) minus (flow after SRV has been opened long enough for transients to stabilize)

since

$$SRVF_{initial} = 0,$$

$$SRVF_{final} = \Delta STF - \Delta FWF$$

Using transient data for $\Delta FWF < \Delta STF$

$$SRVF_{final} = (0.82 - 0.03) \times 10^6 \text{ lbm/hr}$$

$$SRVF_{final} = 219 \text{ lbm/sec}$$

Method Three - Monticello Startup Test Results

On April 21, 22, and 23, 1971 Startup tests were run on SRV capacity. This information is available from the Monticello Unit I Startup Test Results (Test 22 - Relief Valves, NEDE-10488 71NED42). For an RPV pressure of 1080 psig, the SRV capacity for RV2-71A was 890,000 lb/hr. For sonic flow, capacity is directly proportional to RPV pressure. Thus the flowrate ($\dot{m}$) which occurred during the test was determined using the following equation:

$$\dot{m} = \frac{890{,}000}{36000} \frac{(987^* \text{ psig} + 14.7)}{(1080 \text{ psig} + 14.7)} = 226 \text{ lbm/sec}$$

*Test was performed at an RPV pressure of 987 psig.

Range of m by this method is about ±10%. Range of $\dot{m}$ by Method II is thought to exceed ±10%.

NUCLEAR ENERGY DIVISIONS • GENERAL ELECTRIC COMPANY
SAN JOSE, CALIFORNIA 95125

GENERAL ELECTRIC

TECHNICAL INFORMATION EXCHANGE

TITLE PAGE

AUTHOR	SUBJECT	TIE NUMBER / DATE
R. A. Asai, et al.	730	TIE NUMBER: 79NED73 DATE: June 1979
TITLE: Mark I Containment Program Final Report - Monticello T-Quencher Test		GE CLASS: I GOVERNMENT CLASS:
REPRODUCIBLE COPY FILED AT TECHNICAL SUPPORT SERVICES, R&UO, SAN JOSE, CALIFORNIA 95125 (Mail Code 211)		NUMBER OF PAGES: 455

SUMMARY

The overall objective of the Monticello T-Quencher test was to obtain containment loads resulting from discharges through a T-Quencher device in support of Mark I Containment Load Definition Report.

By cutting out this rectangle and folding in half, the above information can be fitted into a standard card file.

DOCUMENT NUMBER NEDO-21864

INFORMATION PREPARED FOR Nuclear Energy Projects Division

SECTION Containment Improvement Programs

BUILDING AND ROOM NUMBER PYD 402 MAIL CODE 904

— NOTICE —

THE ATTACHED FILES ARE OFFICIAL RECORDS OF THE DIVISION OF DOCUMENT CONTROL. THEY HAVE BEEN CHARGED TO YOU FOR A LIMITED TIME PERIOD AND MUST BE RETURNED TO THE RECORDS FACILITY BRANCH 016. PLEASE DO NOT SEND DOCUMENTS CHARGED OUT THROUGH THE MAIL. REMOVAL OF ANY PAGE(S) FROM DOCUMENT FOR REPRODUCTION MUST BE REFERRED TO FILE PERSONNEL.

50-263

DEADLINE RETURN DATE ____________

~~RETURN TO REACTOR DOCKET FILES~~

Lh 8-13-79

7908310441

RECORDS FACILITY BRANCH

GENERAL ELECTRIC